PALEOENVIRONMENT, PALEOECOLOGY, AND STRATIGRAPHY OF THE UPPERMOST ORDOVICIAN SECTION, NORTH OF GRAND RAPIDS, MANITOBA

by

Lori A. Stewart

A Thesis submitted to the Faculty of Graduate Studies
The University of Manitoba
in partial fulfillment of the requirements for the degree of

MASTER OF SCIENCE

Department of Geological Sciences
Clayton H. Riddell Faculty of Environment, Earth, and Resources
University of Manitoba
Winnipeg, Manitoba

ABSTRACT

North of Grand Rapids, Manitoba, new exposures of a carbonate succession prompted study of the lithology and paleontology of the uppermost Ordovician along the northern edge of the Williston Basin in Manitoba. Modern concepts and approaches were applied in examining the sedimentary rocks and fossils, including X-ray diffraction, stable carbon and oxygen isotope analysis, and statistical algorithms. Nine lithofacies, representing a series of shallowing events, and environmentally significant subaerial exposure surfaces, were identified. The distribution and relative abundance of identified fossils were used to delineate faunal associations, which were examined in the context of the impending end-Ordovician mass extinction. Historically, the stratigraphy of the latest Ordovician has been problematic. Therefore, detailed examination of this succession aided in clarifying unit boundaries in the Stony Mountain and Stonewall formations. Study of this new succession contributed a wealth of information to the understanding of the uppermost Ordovician of Manitoba.

ACKNOWLEDGEMENTS

I am exceedingly grateful to my thesis advisors Dr. Robert Elias and Dr. Graham Young for their invaluable insight and guidance during this project. It was a privilege to work under these distinguished researchers who have provided a wealth of knowledge not only in the geology field, but moreover in life. I am also highly thankful to Dr. Nancy Chow and Dr. Brenda Hann for examining my thesis. I would like to thank my assistants Ryus St. Pierre, Matt Demski, and Brett Duncan for their hard work and good company in the field and laboratory. A special thanks to the resilient Ed Dobrzanski for his help in the field with GPS mapping and with the dissolution analysis. I would also like to thank the Manitoba Geological Survey for access to the drill core and facilities. I would like to express appreciation to Dr. Godfrey Nowlan of the Geological Survey of Canada for execution of the conodont analysis, as well to Neil Ball of the University of Manitoba for assistance with the X-ray diffraction (XRD), and additionally to Dr. Paul Middlestead of the G.G. Hatch Stable Isotope Laboratory at the University of Ottawa for resolving the stable isotope analysis.

My graduate program and thesis research was supported by grants to both Dr. Robert Elias and Dr. Graham Young as well as a Postgraduate Research Scholarship from the Natural Sciences and Engineering Research Council of Canada (NSERC), and donations from Robert McAuley to the University of Manitoba in support of Dr. Robert Elias's research program. I am also appreciative of the financial support from the following sources: the University of Manitoba Faculty of Graduate Studies Top-up Program, the William J. Hill Memorial Award, and the Rita Wadien Memorial Scholarship.

I would like to thank the staff and students from the Department of Geological Sciences for providing a foundation of knowledge, direction, and personal relations on which to build my future. I owe a debt of gratitude to my family and friends, who have supported me through this endeavor.

TABLE OF CONTENTS

LIST OF TABLES

LIST OF FIGURES

LIST OF COPYRIGHTED MATERIAL FOR WHICH PERMISSION WAS OBTAINED

CHAPTER 1 - INTRODUCTION

1.1 INTRODUCTION AND OBJECTIVES

The Ordovician Period was a time of great transition that encompassed some of the most significant events of Earth's history. The Ordovician radiation was one of the greatest periods of diversification and biotic change including the establishment of the Paleozoic Evolutionary Fauna (Harper, 2006; Servais et al., 2009). This increase in biodiversity involved innovation of morphologic complexity, development of megaguilds and ecologic evolutionary units, and expansion into more environments, including tiering above and below the sediment-water interface as well as extension into offshore areas (Droser and Finnegan, 2003). The latest Ordovician represents the initiation of deteriorating environmental conditions, culminating in the first mass extinction of the Phanerozoic (Sheehan, 2001). Based on literature reviews, a suggested 26% of families and 49% of genera became extinct (Sepkoski, 1996).

The identification of the position of the Ordovician-Silurian boundary within the Williston Basin of Manitoba has been problematic. Previously, workers placed the boundary at the top or base of the Stonewall Formation (Stearn, 1956; Kindle, 1914; respectively); recently it was placed in the vicinity of an argillaceous "*t*-marker" interval within the upper portion of the Stonewall Formation (Norford et al., 1998). Work is currently being undertaken to gain understanding of the Upper Ordovician interval in an attempt to constrain the position of the Ordovician-Silurian boundary within Manitoba (Demski et al., 2011).

An area north of Grand Rapids, Manitoba, along the northern flank of the Williston Basin, provides an exposure of latest Ordovician carbonate strata containing a

rich succession of fossilized tropical shallow marine biotic assemblages. This succession has not been studied comprehensively since the work of Stearn (1956); there is much to be gained from the application of modern concepts and approaches. The many weathered surface exposures and a newly exposed road cut section provide an excellent opportunity to study the uppermost Ordovician strata along the edge of the Williston Basin of Manitoba. Within this succession is the exposure of a unique argillaceous marker interval allowing clarification of the ambiguous marker intervals of the Stonewall Formation.

The primary objective of this study is to describe in detail the exposed portion of the carbonate succession in the William Lake area north of Grand Rapids, in order to interpret the strata and biotic relations in terms of paleoenvironment and paleoecology that existed at this location during the latest Ordovician. Recognition of lithologic relations facilitates interpretation of environmental conditions impacting on the fauna. Examination of the relations between different groups of fossils and their distribution through the interval allows for recognition of faunal associations. Exploration of these associations can provide valuable information on the paleoecological succession within the Williston Basin.

The latest Ordovician mass extinction negatively impacted marine communities and their environments. This study will provide critical information about the ecologic and environmental changes leading up to this global event. The present study will be related to the regional context of the Williston Basin and to the global changes associated with the end-Ordovician mass extinction.

1.2 PREVIOUS WORK

Over the past century, numerous individuals have studied and analyzed Upper Ordovician and Lower Silurian strata from the Williston Basin area within Manitoba. Tyrrell (1892) was the first to examine the physical geography and geology of southern Manitoba and Saskatchewan, and Whiteaves (1897) completed the first detailed paleontologic study of the Paleozoic fossils. These works provided the foundation of study on the Early Paleozoic and have since been expanded upon by many authors.

Dowling (1900) was the first to name the Stony Mountain Formation while Okulitch (1943) named most of the members therein. The exception is the Williams Member, which was named and described by Smith (1963). Baillie (1952) was the first to name the Interlake Group, which included the Stonewall Formation as the basal unit. Stearn (1956) produced the most comprehensive and detailed stratigraphic and paleontologic study to date of the Interlake Group and Stonewall Formation, which he separated from the group and first suggested was Ordovician in age. After this, stratigraphic work based on subsurface data was completed by Porter and Fuller (1959) and Andrichuk (1959), and expanded upon with more detailed descriptions from drill core from the Interlake area by Cowan (1971). Brindle (1960) was the first to hypothesize that the Ordovician-Silurian boundary occurs at the "*t*-marker" interval identified by Porter and Fuller (1959).

Many paleontologic studies have been completed, most focusing on particular groups: corals (Elias, 1983; Young and Elias, 1999B), bryozoans (Lobdell, 1992), conodonts (Norford et al., 1998), brachiopods (Jin and Zhan, 2001), and, most recently, exceptionally preserved lagerstätte biota (Young et al., 2007).

CHAPTER 2 - GEOLOGIC SETTING

2.1 CONDITIONS DURING THE ORDOVICIAN

The paleogeography of continents during the Ordovician differs strikingly from the arrangement of land masses around the world we know today (Figure 2.1). A large supercontinent, Gondwana (which included areas now known as Africa, South America, Antarctica, Australia, and India), was by far the largest land mass, extending from the South Pole to the equator; Siberia, Baltica, and Laurentia were moderate-sized masses situated at intermediate to equatorial latitudes; and several smaller areas were dispersed around these larger land masses (Servais et al., 2010). After the breakup of the supercontinent of Rodinia in the Late Proterozoic, the Ordovician was a time of maximum dispersal of continents before amalgamation into Pangaea in the Late Paleozoic (Servais et al., 2010). The Ordovician Period was characterized by rapid plate movement resultant from intense magmatic and tectonic activity, resulting in abundant young oceanic crust (Servais et al., 2009). It was also characterized by an extremely high sea level, which contributed to the extensive epicontinental seas with restricted land areas (Servais et al., 2010), and distinct biogeographical differentiation (Harper, 2006).

The Ordovician is considered to have been mostly a greenhouse phase in the geologic record. Expansive epicontinental seas covered much of the large land masses, and estimates of the atmospheric pCO_2 are about 16 times present atmospheric level (PAL) (Sheehan, 2001). An enormous shift to glaciation conditions is recognized from extensive glacial deposits preserved on what was Gondwana, initiating at the start of the latest Ordovician Hirnantian Stage and continuing to the later part of the stage.

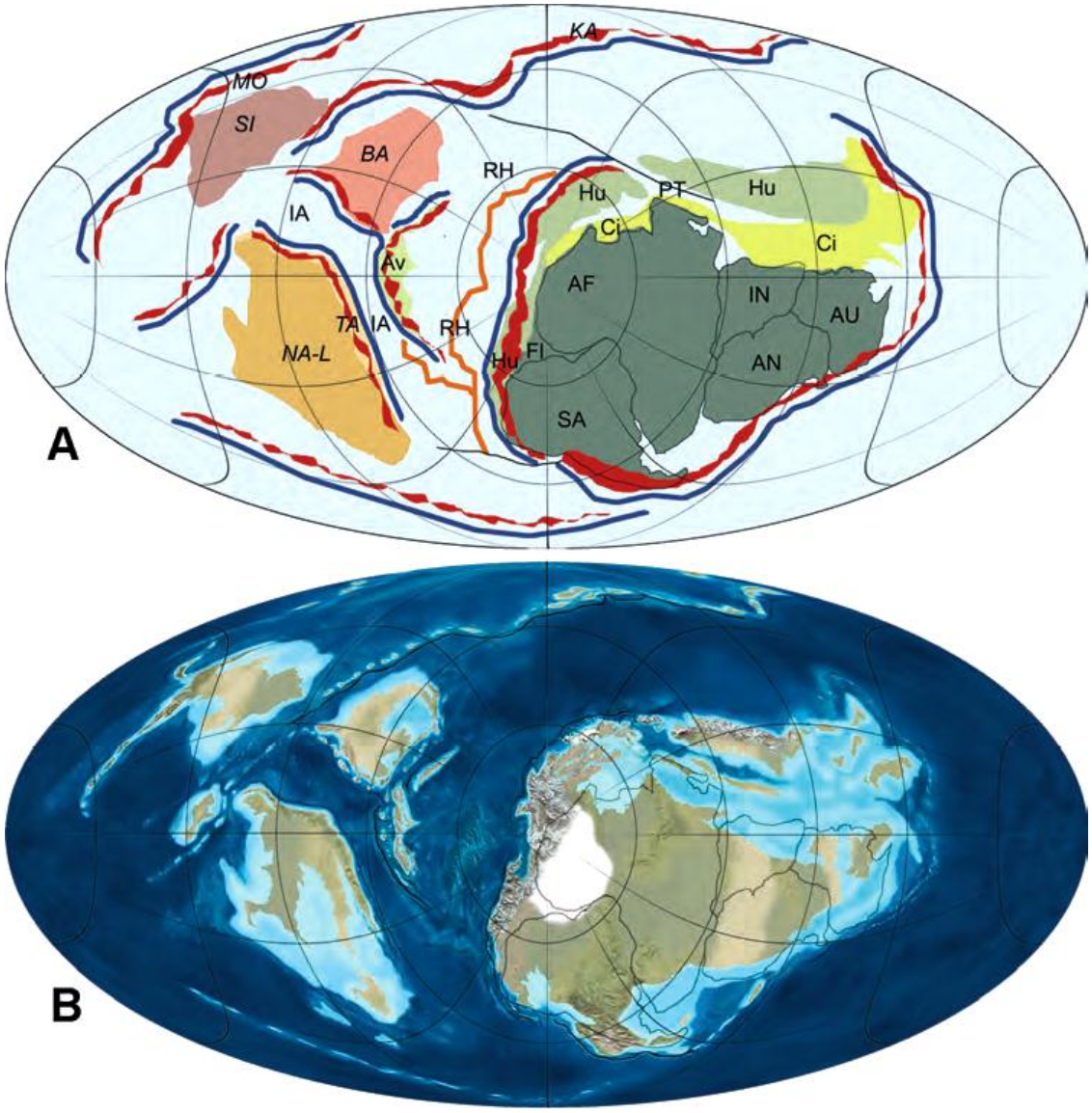

Figure 2.1: Paleotectonic (A) and paleogeographic (B) maps of the Late Ordovician (450 Ma). Maps are South Pole Molleweide projections. Red lines = active arcs; blue lines = subduction zones; and orange lines = spreading centres. MO = Mongolia, SI = Siberia, BA = Baltica, IA = Iapetus, NA-L = North America/Laurentia, TA = Taconic/Taconia, AV = Avalonia, RH = Rheic, KA = Kalahari, HU = Hun (Hunic), PT = Paleo-Tethys, CI = Cimmerian, AF = Africa, FL = Florida, SA = South America, IN = India, AN = Antarctica, AU = Australia. (After Blakey, 2008, fig. 6)

The Ordovician chronicles a major diversification event, known as the Great Ordovician Biodiversification Event, which resulted in the establishment of the Paleozoic Evolutionary Fauna (Droser and Finnegan, 2003). The Ordovician radiation was one of the greatest periods of diversification and biotic change, registering significant changes in taxonomic diversity, morphologic disparity, and ecologic change (Harper, 2006). During this diversification, organisms progressed into more varied environments than had commonly been occupied through the Cambrian. One of the most notable changes was the advancement of some communities from onshore to offshore locations (Droser and Sheehan, 1997).

This period of diversification was followed by the end-Ordovician mass extinction, which resulted in one of the largest decreases in biodiversity in the history of life, and in a reorganization of faunas (Sheehan, 2001). It was the first of the "big five" extinction events of the Phanerozoic Eon, and resulted in the extinction of an estimated 85% of marine species (Sepkoski, 1996). It is hypothesized that the intense greenhouse conditions were interrupted by the brief glaciation in the Hirnantian, thus creating great stress within greenhouse-adapted communities. Due to water sequestration in the ice cap, epicontinental seaways drained, resulting in the elimination of habitats for endemic communities (Sheehan, 2001).

2.2 THE LATE ORDOVICIAN OF MANITOBA

In the early Paleozoic, Manitoba was located within the interior of Laurentia, the ancestral paleocontinent of most of North America. During the later part of the

Ordovician, Manitoba was situated within the tropical equatorial belt near the paleoequator and was inundated by a shallow sea.

The Ordovician sedimentary outcrop belt of central Manitoba is intermittently exposed along the northeastern flank of the Williston Basin, one of the largest North American intracratonic basins (Figure 2.2). This linear belt extends from a northern limit just north of The Pas to a southern limit just north of Winnipeg (Baillie, 1952) (Figure 2.3). It is bounded to the north by the Precambrian Shield, to the east by Lake Winnipeg, and to the southwest by the overlying Silurian strata.

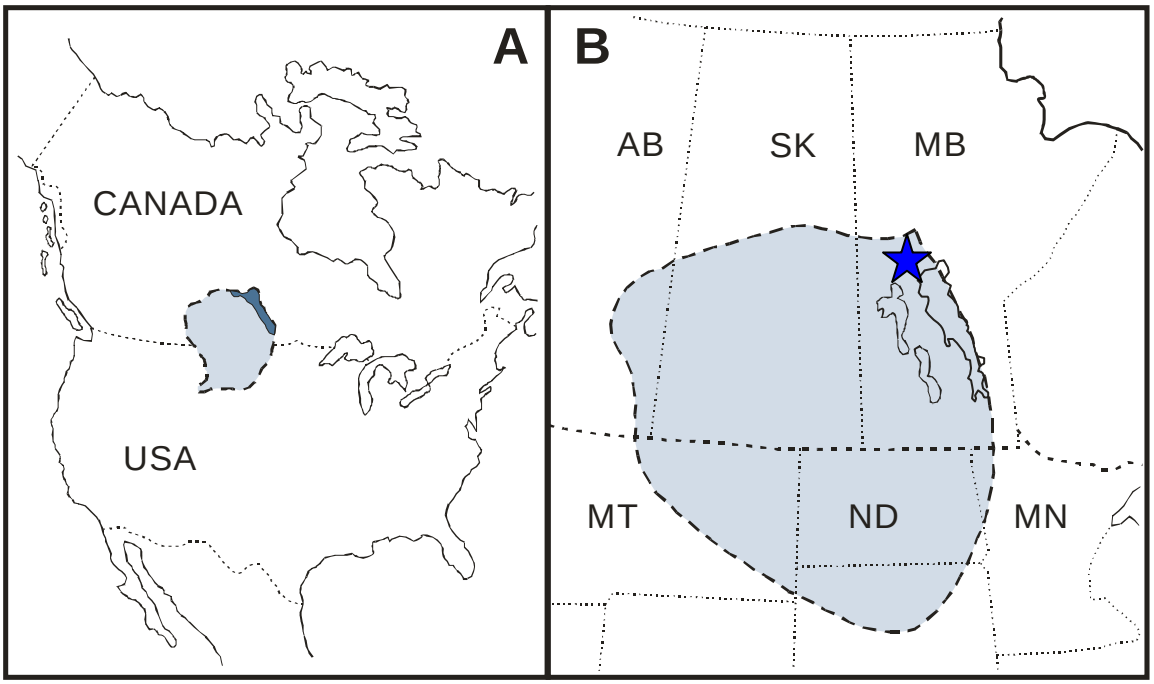

Figure 2.2: The Williston Basin. A) Position of the Williston Basin within North America. Darker area represents the Ordovician outcrop belt in southwestern Manitoba, while the lighter area represents the subsurface. B) Extent of Williston Basin across the international border. Blue star indicates approximate position of the Grand Rapids study area. (Modified from Johnson and Lescinsky, 1986 (A), fig 1A; and Elias, 1991 (B), fig. 1)

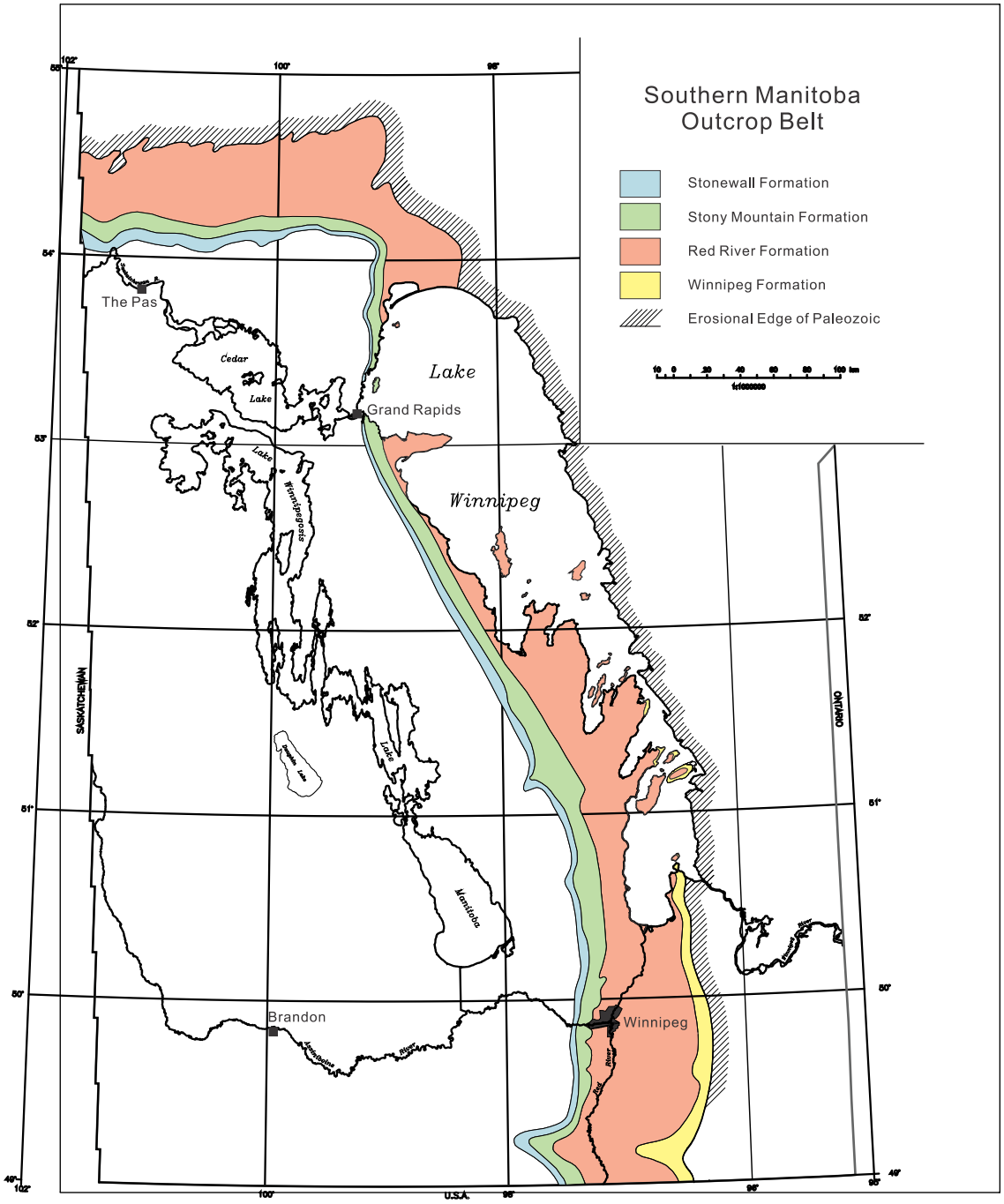

Figure 2.3: Ordovician outcrop belt of southern Manitoba. (Modified from Bezys, 1998, map P-1)

The Ordovician rock units gently dip about 2.8 m per kilometre and generally become thicker towards the centre of the basin in northwestern North Dakota (Bezys and McCabe, 1996). This reflects the subsidence of the basin, which is considered the primary control on sedimentary deposition in southern Manitoba. The Ordovician of southern Manitoba consists of four formations: the Upper Ordovician Winnipeg, Red River, and Stony Mountain formations, and the Upper Ordovician to Lower Silurian Stonewall Formation (Figure 2.4).

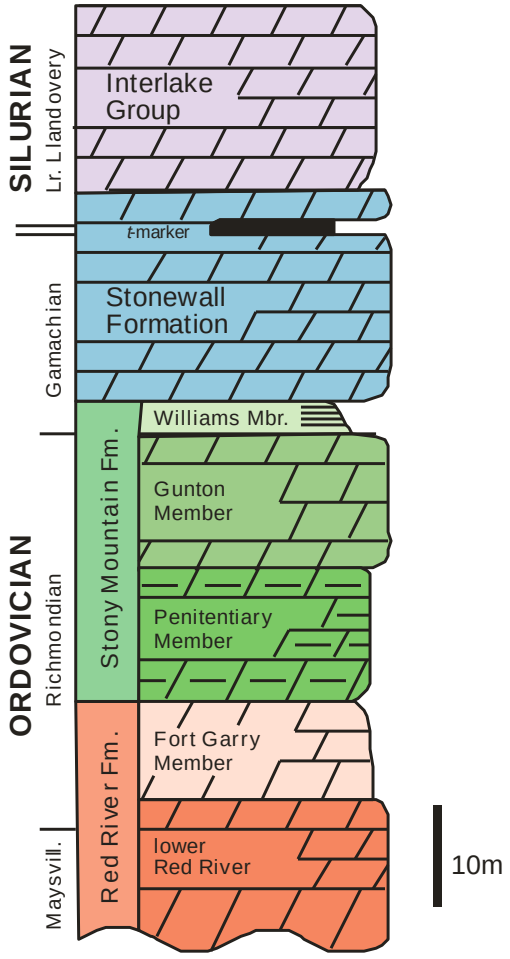

Figure 2.4: Stratigraphy of the Ordovician and Silurian of southern Manitoba. The Winnipeg Formation is not shown, but is located below the Red River Formation. (Modified from Young et al., 2007, fig. 1)

2.2.1 Winnipeg Formation

In many parts of the Williston Basin, the Winnipeg Formation unconformably lies on a weathered Precambrian surface (McCabe, 1971). This formation is composed of a lower, relatively mature, poorly cemented, white to buff quartzose sandstone unit and an upper, green to brown, non-calcareous shale to siltstone unit (Andrichuk, 1959). Macrofossils are rare but include receptaculitids, corals, brachiopods, bivalves, gastropods, and cephalopods (Baillie, 1952); abundant conodonts have been reported from the subsurface (Sweet, 1982). This formation is thought to represent the first Ordovician transgression recorded in the Williston Basin and is of Chatfieldian age based on conodonts (Sweet, 1982).

2.2.2 Red River Formation

The Red River Formation, which overlies the Winnipeg Formation, represents the initiation of carbonate deposition. The formation is composed of mottled dolomitic bioclastic limestones, and to a lesser extent, sublithographic dolostones (Cowan, 1971). The biota is diverse, including sponges, corals, echinoderms, bryozoans, brachiopods, bivalves, gastropods, cephalopods, trilobites, ostracodes, and trace fossils (Baillie, 1952), as well as conodonts (Elias, Nowlan et al., 1988). This formation comprises four members: the Dog Head, Cat Head, Selkirk, and Fort Garry in ascending order.

The Dog Head Member is composed of yellowish to mottled brownish-gray dolomitic limestone, and contains a diverse biota (Cowan, 1971). It was likely deposited during deepening conditions of the transgressive phase of the Red River Cycle and is considered Edenian in age (Elias, 1991).

The conformably overlying Cat Head Member is composed of bedded, yellowish-grey, fine-grained, cherty dolostones. Macrofossils are generally rare, but include some unusual groups in addition to the more typical open shelf elements (Young et al., 2008). This member likely represents the deepest water conditions of the Red River Cycle and is considered early Maysvillian in age (Elias, 1991).

The Selkirk Member is composed of mottled dolomitic limestone, in which dolomitized burrow mottles are surrounded by limestone. This unit exhibits an increase in biodiversity, containing an abundant, well preserved fauna representing warm, normal, shallow-marine conditions (Wong, 2002). This member was deposited in an open setting during the start of marine regression and is considered to be Maysvillian to Richmondian in age (Elias, 1991).

The Fort Garry Member is composed of dense, relatively structureless, sublithographic dolostones (Cowan, 1971). The member contains abundant conodonts as well as macrofossils within the upper portion (Elias, Nowlan et al., 1988). This member was deposited under generally restricted conditions during the later part of the regressive phase (Elias, 1991). It is considered mid-Richmondian in age based on a conodont assemblage representing the *Aphelognathus divergens* Zone (Elias, Nowlan et al., 1988).

2.2.3 Stony Mountain Formation

The Stony Mountain Formation was first named by Dowling (1900) to describe the rocks of a rounded hill in the vicinity of Stony Mountain. A mountain only by prairie standards, the 25 m hill of bedded limestone has been quarried extensively for use in construction (Young et al., 2008). This formation represents the beginning of the next

large cycle of sedimentation within the Williston Basin, and shows similarities in depositional pattern to the Red River Cycle. The nomenclature of the Stony Mountain Formation has evolved over time with increased study of the strata. Currently, the formation comprises four members: the Gunn, Penitentiary, Gunton, and Williams in ascending order.

Gunn and Penitentiary members

The Gunn Member was originally called the Stony Mountain Shale Member (Okulitch, 1943), but this was changed to the Gunn Member to avoid dual usage of the term (Sinclair and Leith, 1958). It is named for Mr. Gunn, for his quarry and well exposure at Stony Mountain (Dowling, 1900). Overall it is composed of interbedded argillaceous fossiliferous biomicrite, calcareous shale, and fossiliferous biosparite, and thins laterally to the north (Porter and Fuller, 1959). The member is defined by a sharp lower contact, marked by an abrupt increase in insoluble residue, and an upper gradational contact into the Penitentiary Member (Cowan, 1971).

The name Penitentiary Member was first used by Okulitch (1943) to describe a well and quarry near Stony Mountain Penitentiary correctional facility. Overall it is composed of massive burrow-mottled argillaceous sublithographic limestones and dolostones, and thickens to the north coincident with thinning of the Gunn Member (Cowan, 1971). Northward, within the transition zone of thinning Gunn, the micrite matrix in the lower Penitentiary Member is dolomitized and remaining fossils are composed of calcite; above this interval fossils have been selectively dissolved producing

vuggy dolostone (Cowan, 1977). The upper contact is defined by a decrease in soluble residue (Cowan, 1977).

Both the Gunn and Penitentiary members are extensively bioturbated and have similar biotas including solitary rugose corals, tabulate corals, brachiopods, bryozoans, gastropods, cephalopods, and trilobites (Young et al., 2008). These members were likely deposited under similar environmental conditions during a transgressive phase. Northward of the exposures near Stony Mountain, drilling has shown that the diagnostic Gunn-like lithology thins rapidly and is replaced by dolostones similar to those of the Penitentiary Member (Bezys and Bamburak, 2004). Beyond about 60 km from the Stony Mountain area, these members are similarly composed of an argillaceous dolostone and cannot be distinguished in drill core or outcrop (McCabe and Barchyn, 1982). The strata have been either assigned to the Penitentiary Member or called "Gunn/Penitentiary Equivalent" (Young et al., 2008). For this study, the Gunn/Penitentiary Equivalent designation is utilized.

Gunton Member

The name Gunton Member was first used by Okulitch (1943) to describe exposures near the town of Gunton. Okulitch (1943) also named a member above the Gunton for the Birse quarry, but subsequent authors have not accepted the Birse Member and have included those strata within the Gunton Member (Porter and Fuller, 1959; Andrichuk, 1959; Cowan, 1971). Overall it is composed of mainly dense, massive sublithographic dolostone with laminar to nodular bedding (Cowan, 1971), and the upper contact is defined by an increase in soluble residue (Cowan, 1977).

In southern Manitoba, poorly preserved corals and stromatoporoid fossils are rare, and the occurrences of halite crystal molds indicate restricted hypersaline conditions (Young et al., 2008). Northward, in the Grand Rapids Uplands area, the Gunton Member is locally heavily mottled by dense *Thalassinoides* burrowing, and brachiopods, cephalopods, and gastropods can be found (Young et al., 2008).

Williams Member

The Williams Member was introduced by Smith (1963) to describe the strata observed in the lowest portion of the Stonewall Quarry, and was named for a station north of the Stonewall quarries along the Winnipeg-Arborg line of the Canadian Pacific Railway. There have been some inconsistencies in assignment of the Williams Member; some authors place it within the Stonewall Formation (Bezys, 1995), while others have placed it within the Stony Mountain Formation (Cowan, 1971; Young et al., 2008). Overall it is composed of interbedded arenaceous, argillaceous, sublithographic dolomudstone and shale, and the upper contact is sharply defined as a lithologic change (Cowan, 1977).

This member was originally thought to be unfossiliferous, but recent work has revealed an excellently preserved restricted marine biota, including linguloids, jellyfish, eurypterids, and large problematic tubes (Young et al., 2007). The conodont assemblage (*Rhipidognathus* assemblage) represents the shallowest conditions of the Williston Basin, and the presence of halite lattices indicates hypersaline conditions consistent with the interpretation that this member represents shallow, restricted tidal flat to lagoonal deposition (Young et al., 2007).

2.2.4 STONEWALL FORMATION

The Stonewall Formation was named by Kindle (1914) for the town near which the type section was first described. Thereafter, determination of the age of the Stonewall Formation has been problematic. The formation was initially considered by Kindle (1914) to include all rocks in the area of Silurian age. Baillie (1951) agreed, but restricted it to the Early Silurian. Other authors have suggested that the formation is entirely Late Ordovician (Stearn, 1956; Porter and Fuller, 1959), or both Ordovician and Silurian (Brindle, 1960; Cowan, 1971).

The Stonewall Formation is composed of dolostones divided by an argillaceous interval named the "*t*-marker" by Porter and Fuller (1959). This marker was subsequently identified as two successive markers by Kendall (1976) within the subsurface of Saskatchewan, consequently termed the "lower *t*-marker" and "upper *t*-marker". Based upon paleontological evidence from Saskatchewan drill core, Brindle (1960) hypothesized that the likely position of the Ordovician-Silurian boundary was at the *t*-marker horizon. Conodont stratigraphy has identified a turnover of fauna, further supporting placement of the boundary in the vicinity of the upper *t*-marker interval (Norford et al., 1998).

Recent re-examination of the upper Stonewall Formation within the Cormorant and Grand Rapids Uplands areas of Manitoba has integrated stable isotope data with biostratigraphic data, suggesting the possible presence of the HICE (Hirnantian isotopic carbon excursion) (Demski et al., 2011). Analysis of road cut and drill core material from the uppermost portion of the Stonewall Formation reveals a positive $\delta^{13}C_{carb}$ excursion, recognized in association with a conodont turnover, within the vicinity of the *t*-marker

(Demski et al., 2011). Recognition of Hirnantian age strata would support a position of the Ordovician-Silurian boundary at a higher stratigraphic position than previously accepted.

The type section of the Stonewall Formation (including the lower Stonewall above the uppermost portion of the Williams Member of the Stony Mountain Formation) is located at Stonewall Quarry Park in the town of Stonewall, 25 km northwest of Winnipeg (Young et al., 2008). Overall the entire Stonewall Formation is composed of dolostones interbedded with thin argillaceous, sandy dolostone units, most notably the *t*-marker (Stearn, 1956). The formation is generally accepted to be composed of three portions: below the *t*-marker (lower Stonewall), the *t*-marker itself, and above the *t*-marker (upper Stonewall).

The portion of the Stonewall Formation below the *t*-marker is composed of light yellowish-grey, slightly mottled, fossiliferous, finely crystalline dolostone (Cowan, 1971). The general appearance is similar to that of the Gunton Member, complicating the correlation of small isolated exposures. Macrofossils are rare to locally abundant but poorly preserved, including stromatoporoids, solitary and colonial corals, brachiopods, gastropods, and cephalopods (Stearn, 1956).

Porter and Fuller (1959) originally described the *t*-marker interval as coarse-grained quartz-sand lenses interspersed through shale and argillaceous dolomite. Within the subsurface in Saskatchewan, the "lower *t*-marker" is composed of argillaceous dolomudstone to dolomitic shale and the "upper *t*-marker" is composed of dolomudstone (Young et al., 2008), but only one marker is observed in outcrop in Manitoba. Within the

subsurface of Manitoba the *t*-marker interval contains well-rounded quartz sand grains suspended within a fine crystalline dolomite matrix (Cowan, 1977).

The portion of the Stonewall Formation above the *t*-marker is composed of a dense, massive, mostly structureless fine-crystalline to sublithographic dolostone (Cowan, 1971). Some horizons may be vuggy; others may be conglomeratic to brecciated (Young et al., 2008). This portion of the formation generally lacks macrofossils, but contains conodonts typical of the Early Silurian (Norford et al., 1998).

The Stonewall Formation represents deposition of a series of small transgressive-regressive cycles. The marker intervals are interpreted to have been deposited during a regression within the Williston Basin, in a supratidal environment based on recognition of pitted, frosted quartz (Cowan, 1971), either as lag deposits at the start of transgression (Kendall, 1977) or the result of subaerial exposure at the end of regressive phases (Johnson and Lescinsky, 1986).

Within the present study, an argillaceous marker interval is identified in the Stonewall Formation. Additional work within the proximal area has identified the *t*-marker portion at a higher stratigraphic position in the Stonewall (Demski et al., 2011). Confusion presents itself in distinguishing nomenclature of multiple marker intervals within the proximal study region. Clarification of the nomenclature is presented in Table 2.1. The upper Stonewall and *t*-marker interval will retain their designation. The lower Stonewall will be divided into “below LS-marker lower Stonewall”, “lower Stonewall marker (LS-marker)”, and “above LS-marker lower Stonewall”.

Table 2.1. Stratigraphic nomenclature of the Stonewall Formation.

Previous	**New**
upper Stonewall	upper Stonewall
t-marker	*t*-marker
lower Stonewall	above LS-marker lower Stonewall
	lower Stonewall marker (LS-marker)
	below LS-marker lower Stonewall

CHAPTER 3 - METHODOLOGY

This chapter includes a description of all methodology and scientific techniques utilized for this study. Field and laboratory analyses were conducted on rocks and fossils collected from the study site, including instrumental analyses on select samples.

3.1 FIELD METHODS

Field work for this project was conducted in central Manitoba near William Lake, approximately 100 km north of the town of Grand Rapids along Provincial Trunk Highway #6 (Figure 3.1). Necessary access permissions were obtained from the Provincial Highways Department to work along the highway and transmission lines, and a Manitoba Heritage Permit allowed for the collection of material. This study site comprises two suites of exposures: a sequence of weathered surface exposures, collectively designated as "surface exposures" (Figure 3.2A), and a newly exposed road cut displaying a stratigraphic section, designated as "road cut succession" (Figure 3.2B). Work was originally initiated in the summer of 2005 by Brandy Chapman under the supervision of Dr. Robert Elias and Dr. Graham Young, resulting in preliminary collection of material and data. In the summer of 2007, the project was resumed by Lori Stewart and developed into the present study.

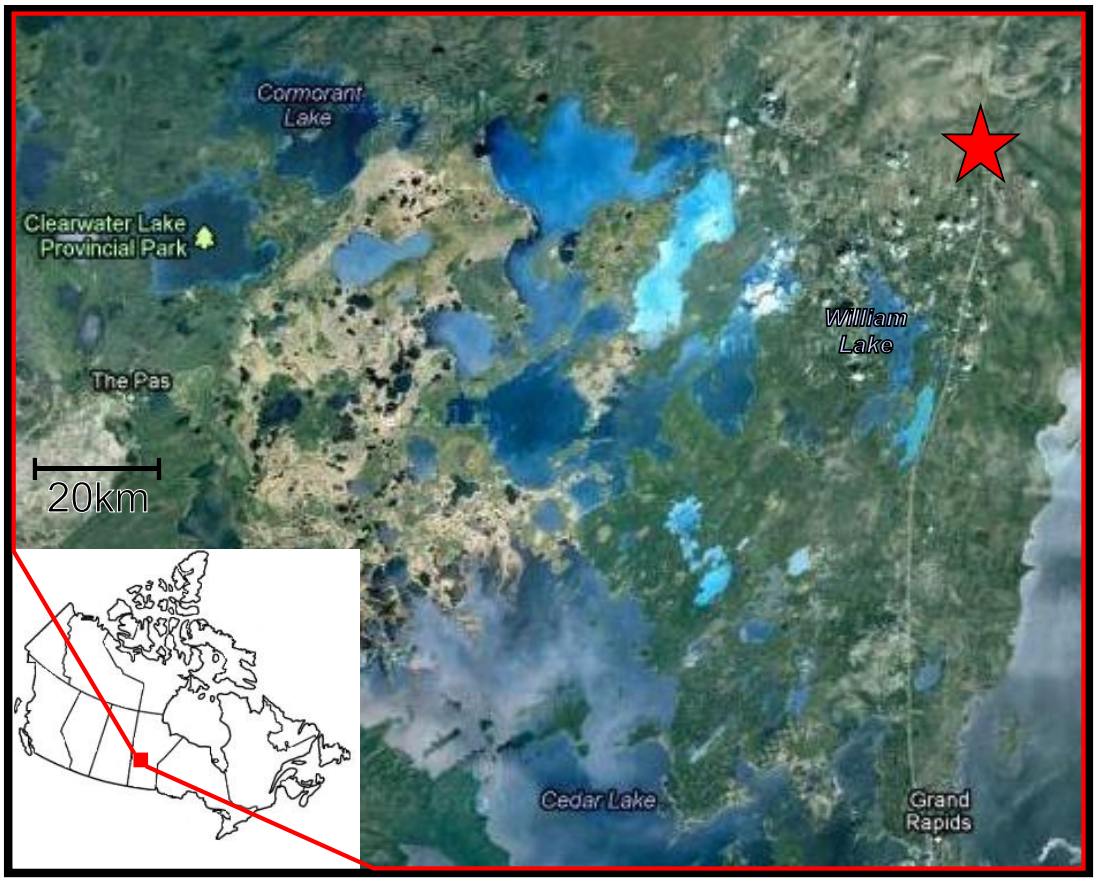

Figure 3.1. Satellite image of west-central Manitoba showing the location of the Grand Rapids study area (red star). (Modified from Google, 2012)

Figure 3.2: Photographs of examples of the field work suites of exposures. A**)** Stitched panoramic photograph of surface exposure site BC-1; spanning north to south from left to right. B) Photograph of road cut succession, east side (LS-1) looking south.

3.1.1 SURFACE EXPOSURES

The surface exposures of essentially horizontal strata are intermittently located over a distance of approximately 5 km, immediately adjacent to Provincial Highway #6, and between the highway and the hydro transmission line (Figure 3.3). The transmission line includes two parallel transmission lines that generally follow alongside the highway; the surface exposure localities are adjacent to the west line, as well as between the two lines. A hand-held global positioning system unit (GPS) was utilized to obtain accurate positions of the study localities (using map datum NAD 27) (Appendix A) (Figure 3.4). Measurement of elevation changes between localities involved laser-aided surveying techniques, spanning a vertical equivalent of approximately 35 m (Figure 3.5). The succession encompasses the upper portion of the Gunn/Penitentiary Equivalent, the entire Gunton and Williams members, and the lower portion of the Stonewall Formation.

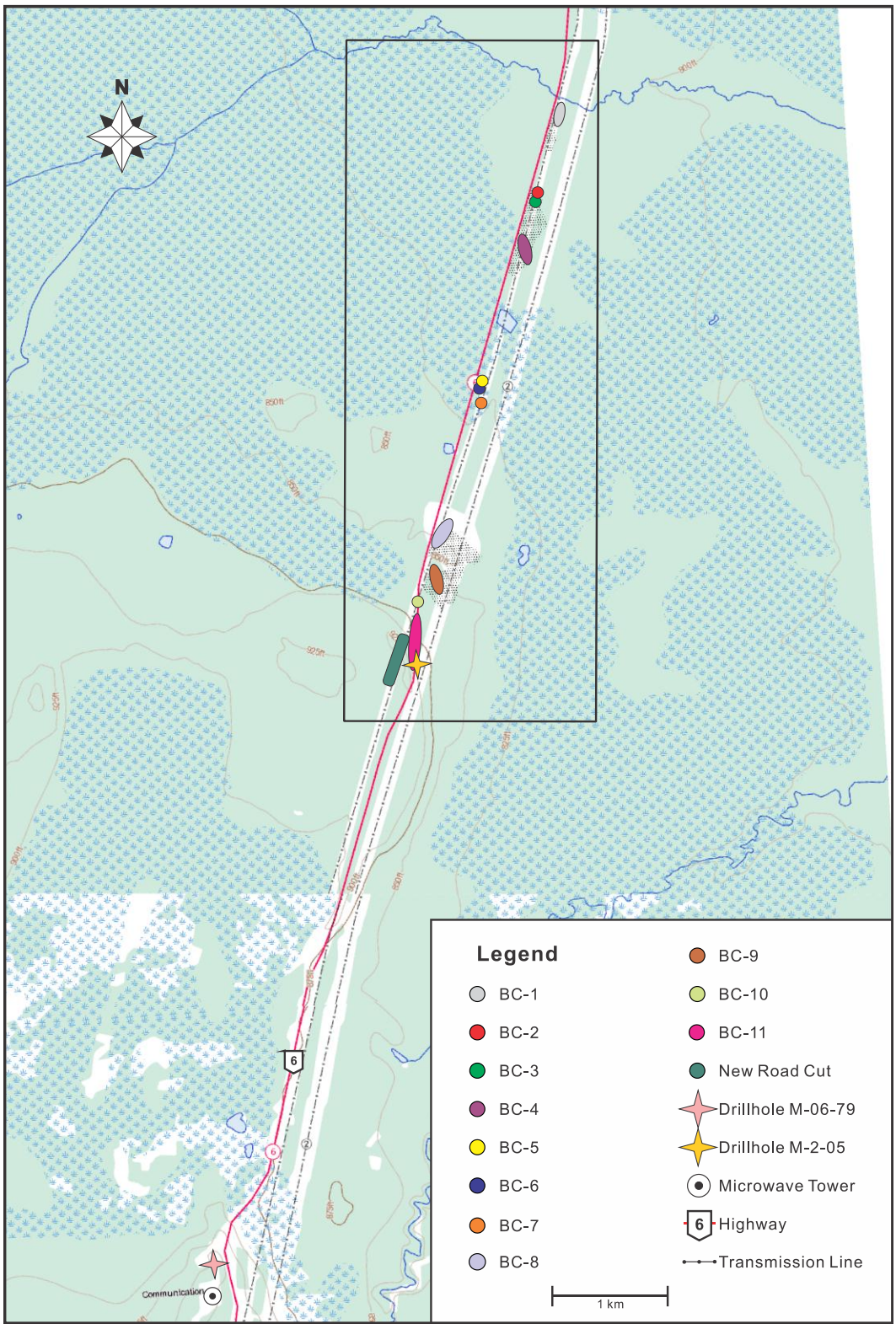

Figure 3.3: Topographic map showing the locations of the surface exposure sites, new road cut succession, and drill holes. Outlined box is magnified in Figure 3.4. (Modified from Natural Resources Canada, 2012)

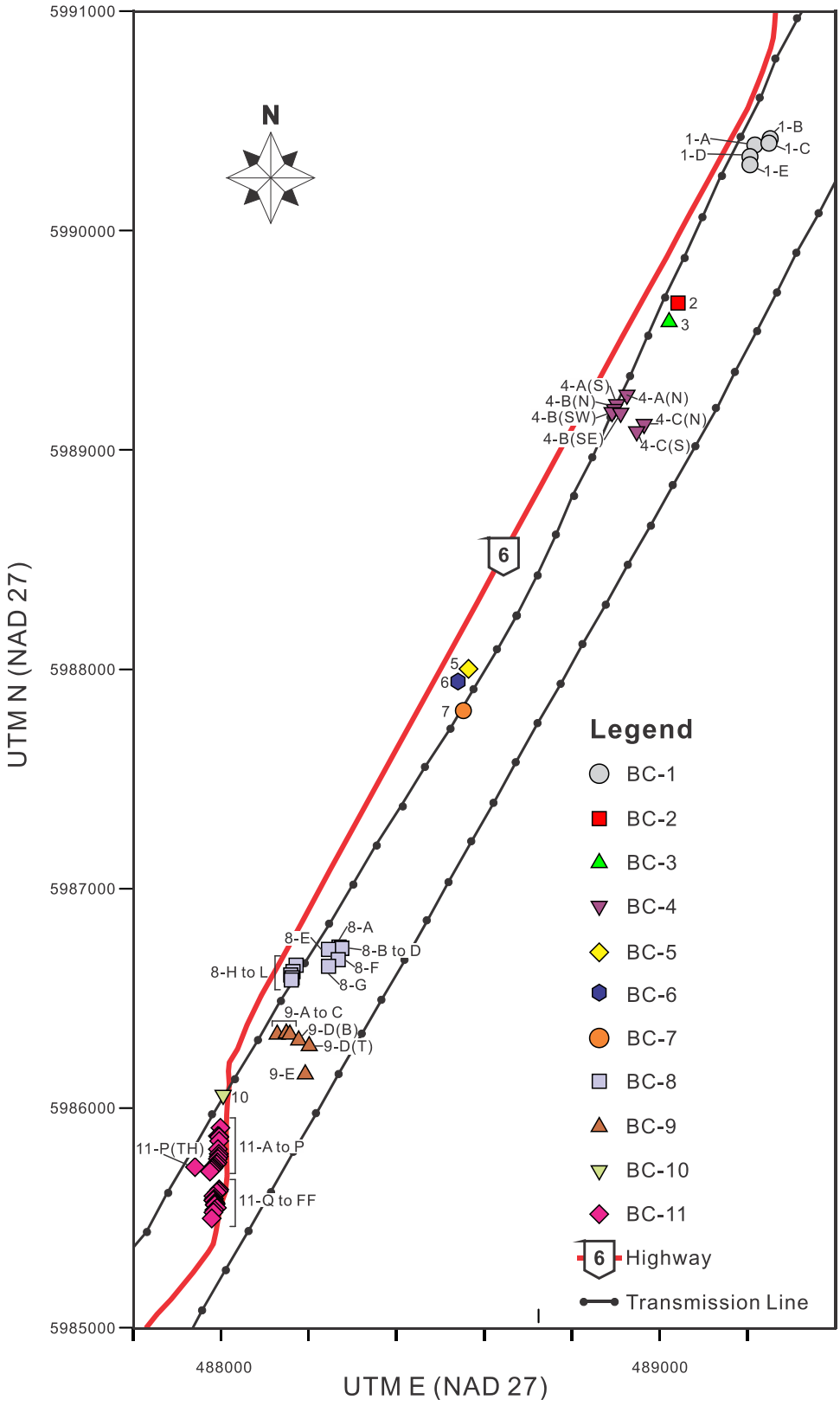

3.4. Map of surface exposure sites showing the distribution of individual localities.

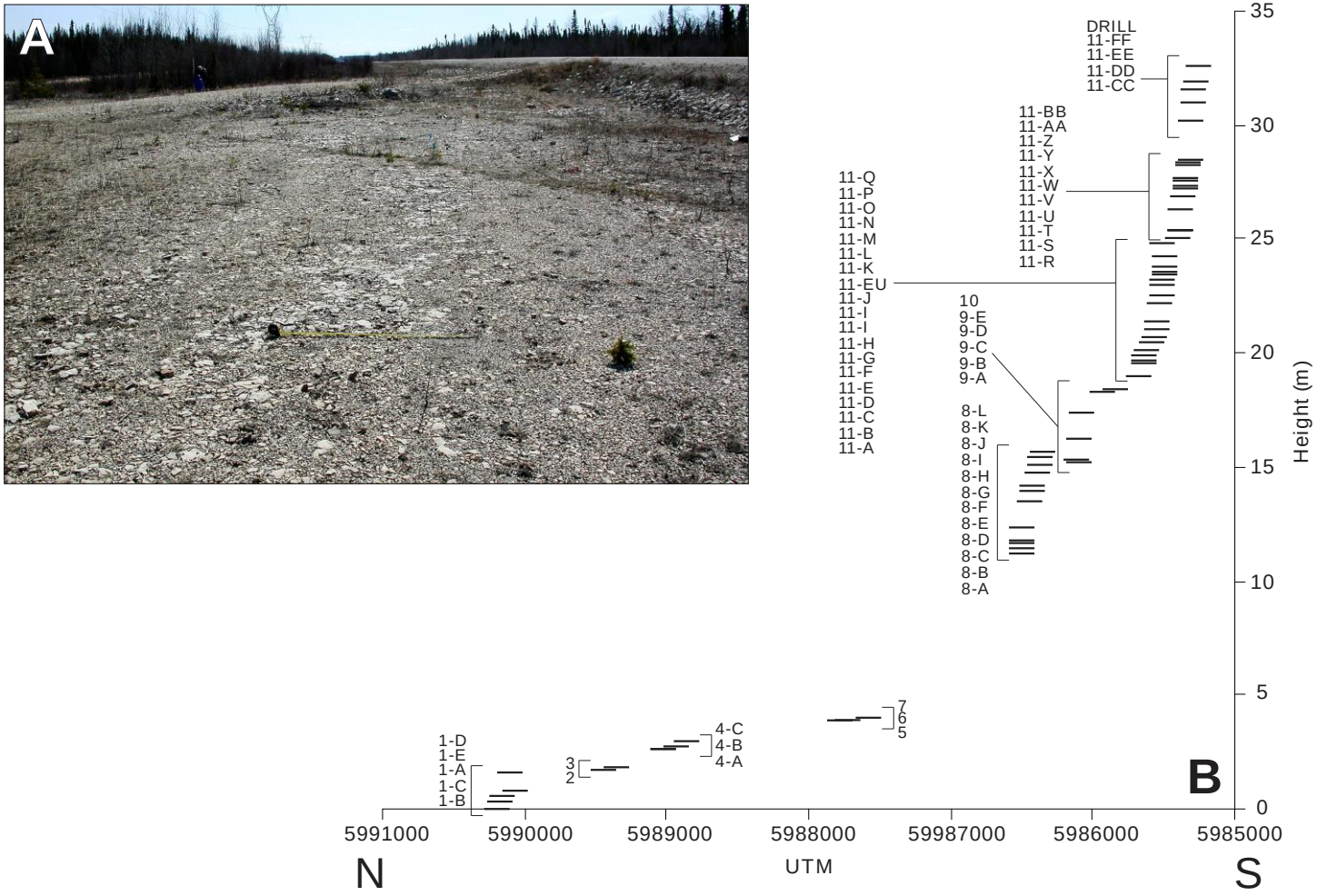

Figure 3.5: Surface exposure study material. A) Photograph of surface exposure (looking south) at locality BC-1-D. Tape measure shown in the lower middle portion of the photograph is extended to 1m length. B) Figure relating north-south geographic separation of BC exposures (measured by GPS) to stratigraphic height above lowest BC exposure (measured by laser-aided surveying).

Although the localities are extensively weathered, all *in situ* exposed surfaces were examined for fossil content and general features including bedding, textures, lithology, and areal extent. A total of 63 localities were identified, which are grouped together into sites based on spatial proximity and stratigraphic continuity. All areas were described and photographed to document general appearance and condition. Samples were collected from representative points at each locality for lithologic identification and where macrofossils were present, many were collected. A stratigraphic orientation label was drawn on each individual sample to maintain context from the field collection to the laboratory. A total of 275 samples were collected to be used in analyses. Samples and data relating to the surface exposures are identified in this study with numbers prefixed by BC (eg: BC-11-E-7). Exposure surface samples were numbered using the following scheme:

BC	=	surface exposure
11	=	site identification
E	=	locality of collection
7	=	sample number

3.1.2 ROAD CUT SUCCESSION

In the summer of 2006, maintenance and improvement were conducted on Provincial Trunk Highway #6 near the southern portion of the surface exposures. The route of this portion of the highway was modified, consequently exposing a new road cut section (Figure 3.6). The north-south trending stratigraphic section is exposed for approximately 420 m along both sides of the new portion of the highway. The stratigraphic succession of essentially horizontal strata was mapped utilizing a hand-held GPS (using map datum NAD 27) (Appendix A). The exposures on the east and west sides

of the highway are separated 28 m. The succession attains a maximum thickness of about 6 m near the middle of the roadcut section but thins toward the northern and southern extents. Along the section, a total of nearly 12 m of stratigraphic thickness is exposed, encompassing the top of the Williams Member and lower portion of the Stonewall Formation.

The new road cut section succession provided a complement to the weathered surface exposures. The new road cut succession is proximal to the surface exposures along the highway, allowing for correlation between the field materials.

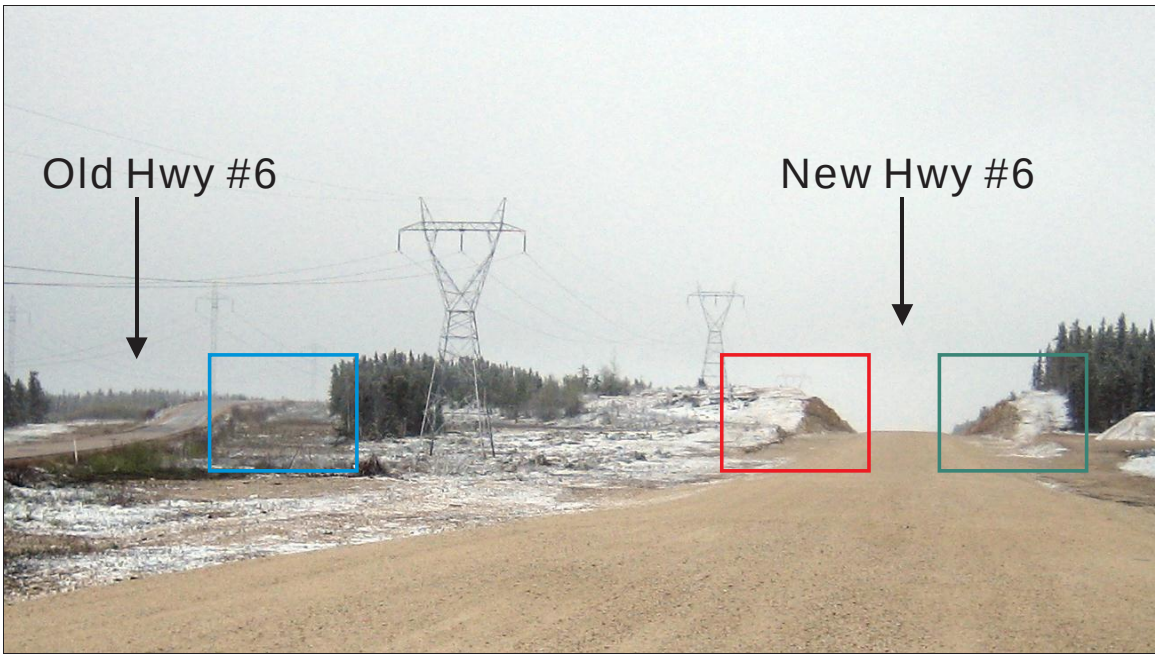

Figure 3.6: Photo of the southern portion of the William Lake study area (looking south) showing the proximity of the new Highway #6 to the old Highway #6. The east and west sites of the road cut succession (red and green boxes respectively) are shown in relation to the surface exposures (blue box).

Both the east and west sides of the section were examined for fossil content and general features, including bedding, lithology, and contact relationships, which were then compared for areal continuity. Fifteen stratigraphic units were delineated through the succession and the east side section was utilized for detailed measurements (Figure 3.7). Representative hand samples were collected from each unit for lithologic identification and where macrofossils were present, many were collected. A stratigraphic orientation label was drawn on each individual sample to maintain context from the field collection to the laboratory. A total of 135 hand samples were collected from the road cut section exposure to be used in analyses. In addition, 24 large samples were collected for microfossil extraction. Samples and data relating to the road cut succession are identified in this study with sample numbers prefixed by LS (eg: LS-1-A2-17 (+45cm)). Road cut succession samples were numbered using the following scheme:

LS	=	road cut succession
1	=	site identification (1=east; 2=west)
A2	=	stratigraphic unit
17	=	sample number
(+45cm)	=	stratigraphic position above base of unit

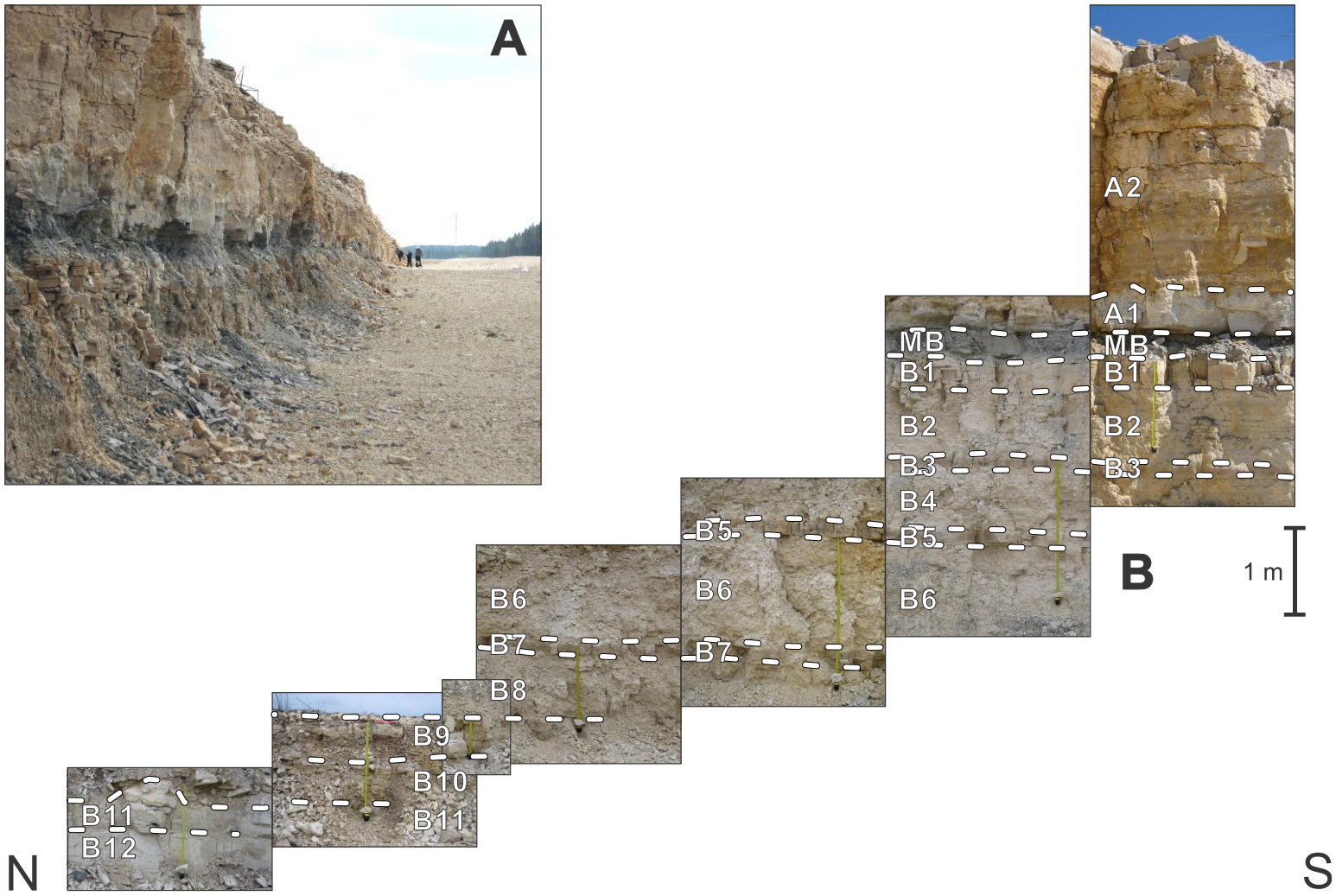

Figure 3.7: Road cut succession. A) Photograph of road cut succession exposure (looking south) at LS-1 (east side of highway). B) Stitched composite of photographs displaying the relation of stratigraphic units.

3.2 LITHOLOGIC ANALYSIS

The collected hand samples were brought back to the laboratory, where they were cleaned and prepared for analyses. Hand sample analysis involved detailed descriptions of each sample to determine the sedimentologic and paleontologic characteristics.

Samples to be used for lithologic identification were cut perpendicular to the exposure surface for the surface exposure samples (BC) or parallel to the face of the rock for road cut section samples (LS). Cut surfaces were polished, and subsequently scanned for digital images. Each lithologic sample was examined for sedimentological characteristics to delineate lithofacies (Appendix B).

A total of 148 thin sections were prepared to supplement hand sample analysis, which included representatives from each stratigraphic interval, as well as for interesting or otherwise unidentifiable features. All thin sections were examined with a stereoscopic microscope and with a petrographic microscope under plane-polarized and cross-polarized light at low magnification to identify micro-scale textures and structures. The lithological thin sections were treated with Alizarin red-S and potassium ferricyanide staining techniques to determine the carbonate phases. The identification of various phases of carbonate minerals and their proportion can be used in evaluating the extent of dolomitization through the study area (Dickson, 1966). This technique yielded ambiguous results, as could be expected given the fine-grained nature of the lithologies (Gensmer and Weiss, 1980).

3.3 DRILL CORE

Two drill cores from the vicinity of William Lake were examined for this study (Appendix C). In response to the preliminary work conducted on the study site in the summer of 2005, a hole was drilled at William Tower (M-2-05, adjacent to study site) to provide stratigraphic control for future work in the area. This core was examined in order to compare the surface exposures and road cut section to the subsurface geology. A second core was examined from the nearby Minago River Microwave Tower (M-6-79) to document the lateral extent of the units and describe the nature of stratigraphic contacts.

The slabbed drill cores were examined at the Government of Manitoba, Department of Innovation, Energy, and Mines Core Storage Facility in Winnipeg, Manitoba. Core examination included description of lithology, sedimentary structures, fauna, and stratigraphic contacts for the study interval. Portions of the core relevant to the study were photographed and representative samples were taken for preparation into polished sections and thin sections, and for geochemical analysis.

3.4 SUPPLEMENTARY ANALYSES

3.4.1 X-RAY DIFFRACTION

X-ray diffraction (XRD) is a commonly used technique for qualitative identification of minerals in geological samples. Quantification may be obtained for some mineral phases based on relating the peak intensity of a mineral phase to the proportional content of that phase in the sample. Measurement of the peak intensities, therefore, can provide information regarding the relative proportion of a mineral phase within a sample (Gensmer and Weiss, 1980). This technique was used to determine the compositions of

the lithologies, due to the ambiguous results obtained from the staining technique. This X-ray diffraction method is preferred over the point-counting staining method for determining calcite-dolomite ratios in fine grained material, as the staining method is less accurate for smaller grain sizes (Gensmer and Weiss, 1980).

Eight intervals of the road cut section were selected for analysis using the XRD technique. Samples were extracted and powdered from hand samples using a vibrograver and adhered as smear mounts onto glass slides with acetone. Measurements were carried out on a Philips PW1710 automated powder diffractometer using Cu radiation powered at 40 kV and 40 mA; the diffractogram was collected with scintillation. The diffraction pattern was recorded for 2θ from 3° to 65° and a 2θ step scan of 0.05° was used, counting for 1 second at every step. The generated XRD pattern was then compared using the analysis software MDI Jade-XRD Processing Software with PDF-4 database to identify bulk mineral phases present within the samples. The results are presented in Chapter 6.

3.4.2 DISSOLUTION

Dolomite is easily dissolved within a mild acid solution. Based on the results of the initial XRD analysis, three samples were selected for more detailed research to determine the composition of the minor mineral phases. Attempts were made to isolate the minor components for quantitative identification by dissolving out the dominant dolomitic component.

Samples to be dissolved were selected from intervals that showed an indication of minor minerals in the previously analyzed XRD samples. Samples ranged between 144.75 g and 178.96 g and were allowed to completely digest in 5% hydrochloric acid.

Samples were dried and measured for residual mass. The resultant residue was examined under a microscope to isolate grains and subsequently re-analyzed by XRD. X-ray analysis was conducted with the same parameters as previously described, but carried out on a Siemens D5000 automated powder diffractometer. The results are presented in Chapter 6.

3.4.3 GEOCHEMISTRY

Isotope analysis has become widely applicable to study of Earth sciences. Whole rock samples of dolomitic mudstones were selected as material for stable carbon ($\delta^{13}C$) and oxygen ($\delta^{18}O$) isotopic analysis. A total of 38 samples were analyzed; 26 from hand samples collected from the road cut succession, and 12 samples from the Minago River Microwave Tower core (M-06-79).

Samples were extracted and powdered using a vibrograver and massed on an analytical scale. Care was taken to select areas of carbonate mud and to avoid areas with vug-filled cement and fossil material. Samples averaging 0.03 g were packaged in 1 gram glass vials and labeled accordingly. Analyses were conducted at G.G. Hatch Stable Isotope Laboratory at the University of Ottawa under the supervision of Dr. Paul Middlestead.

At the laboratory, the samples were weighed into exetainers and 0.1 mL H_3PO_4 (S.P. 1.91) was added to the side of the container. Samples were capped and helium-flushed while horizontal. The samples were allowed to react at 50.0°C and continued for 48 hours. The resultant gas was extracted by continuous flow technique and measured using Delta XP and Gas Bench II mass spectrometers, both manufactured by Thermo

Finnigan. Results are reported in standard δ notation, as per mil deviation from VPDB. Conversion to the VPDB scale was performed using international standards NBS-18, NBS-19, and LSVEC. The analytical precision (2 sigma) was +/-0.1 per mil. Results are presented in Chapter 6.

3.5 FOSSIL ANALYSES

Taxonomic identification of macrofossils was based on examination of hand samples for morphological and internal characteristics diagnostic of particular taxa (Appendix D). Thin sections were prepared for some types of fossils to determine macro- and microstructures for taxonomic assignment.

In addition to the samples collected for lithologic and paleontologic analyses, samples were collected from the road cut section for microfossil analysis. Twenty-four samples of dolostone were submitted to Geological Survey of Canada Calgary Conodont Laboratory and processed under supervision of chief paleontologist Dr. Godfrey Nowlan. Samples were collected from the new road cut section and ranged from 1.146 to 3.485 kg. The samples digested well (87-100% breakdown), yielding mostly moderately well preserved conodonts and numerous fragmentary elements as well as fragments of macrofossils.

3.6 STATISTICAL METHODS

3.6.1 SERIATION

Due to limitations of the sampling that was executed, typical quantitative statistical methods commonly used for evaluating diversity, ecology, and distribution are

unsuitable. Seriation is a qualitative statistical method that is useful in describing data of this nature. It is an algorithm operated on a presence-absence matrix that reorganizes the rows and columns so that presences are concentrated along a diagonal (Brower and Kile, 1988). The resultant ordination may be used to recognize trends and patterns, permitting interpretation of unconventional data.

The seriation method was employed over the grouped distribution of macrofossils, trace fossils, and biosedimentary structures. Tables describing these features were converted to presence-absence matrices, and an unconstrained seriation algorithm was run using PAST (PAlaeontological STatistics) data analysis package (Hammer, 2002). The resulting ordinated matrices were examined for patterns and trends. Results of this statistical algorithm are presented in Chapter 9.

3.6.2 Paleocurrent Analysis

Paleocurrent analysis was conducted on nine localities of the weathered exposure surfaces. Localities were chosen where there was sufficient abundance of measurable fossil specimens. The surface exposure localities were essentially horizontal bedding surfaces, thus the data for each represent the same time interval and therefore environment (Appendix F). The vertical displacement between localities was measured by laser aided surveying techniques.

The attitudinal orientation of solitary rugose corals was documented from the surface exposure surfaces; horizontal, upright, and upside down. For corals deposited with the axis horizontal, directional orientations of elongate solitary rugose corals were measured with a compass to the nearest degree. Unidirectional orientations were

measured from the apex toward the calice of individual corals in which the direction of corallum expansion or the position of calice could be determined.

Data measured from the surface exposure localities is detailed in Appendix F. A few data sets met the required criteria to perform the chi-square test for preferred orientation (Appendix F.2). The results of the paleocurrent analysis are presented in Chapter 10.

CHAPTER 4 - LITHOFACIES

Sedimentological characteristics were utilized to delineate facies within the William Lake study area, which encompasses strata ranging from the lower Stony Mountain Formation through the middle Stonewall Formation. Colour descriptions are derived from the "Geological Society of America Rock-Color Chart" (Goddard et al., 1970). Classification of carbonate rocks follows Dunham (1962) as modified by Embry and Klovan (1972), and porosity classification follows Choquette and Pray (1970). Data were compiled from field description, examination of hand samples and thin sections, as well as comparison with the two drill cores.

Eight lithofacies were distinguished using a suite of lithologic characteristics and sedimentary features incorporating a range of variability. A general description of the lithofacies is summarized in Table 4.1, and details are tabulated in Appendix B. Some lithofacies occur in multiple intervals. The stratigraphic distribution of lithofacies is illustrated in Figure 5.8.

Table 4.1. Lithofacies summary.

Lithofacies	General Description	Occurrence			
		BC	LS	M-2-05	M-06-79
1	Highly fossiliferous bioturbated dolomitic mudstone	BC-1 to BC-7		27.10 - 40.80 m	51.90 - 65.70 m
2	Highly bioturbated dolomitic mudstone with localized wackestone	BC-8-A to BC-8-E		21.22 - 27.10 m	43.94 - 51.90 m
3	Mildly bioturbated dolomitic mudstone grading into nodular bedding	BC-8-F to BC-11 (A-H)		12.40 - 21.22 m	37.80 - 43.94 m
4	Sublithographic dolomitic mudstone	BC-11-I to BC-11-O	LS-B12	9.24 - 12.40 m	34.39 - 37.80 m
5	Thrombolitic dolomitic mudstone	BC-P	LS-B11	9.10 - 9.24 m	34.30 - 34.39 m
			LS-A1	3.02 - 3.31 m	28.15 - 28.50 m
6	Massive bedded mudstone; thick nodular mudstone to wackestone and thin sublithographic mudstone	BC-11-Q to BC-11-BB	LS-B10 to LS-B2	4.30 - 9.10 m	29.66 - 34.30 m
7	Brecciated dolomitic mudstone		LS-B1	3.52 - 4.30 m	28.65 - 29.66 m
8	Argillaceous fissile dolomitic mudstone		LS-MB	3.31 - 3.52 m	28.50 - 28.65 m
9	Highly bioturbated dolomitic wackestone to packstone	BC-11-CC to BC-11-FF	LS-A2	0.00 - 3.02 m	25.03 - 28.15 m

4.1 LITHOFACIES 1

Lithofacies 1 is a highly fossiliferous bioturbated dolomitic mudstone (Figure 4.1A). It ranges in colour from very pale orange to yellowish brown with darkened areas locally associated with greater bioturbation and bioclastic material, where the lithology approaches a wackestone. Within this facies, macrofossil fragments account for 5-20% of rock volume, and micritic matrix accounts for 75-90%. Porosity is vuggy and interparticle, limited to 5-15% of total volume. Microfossil fragments comprise mainly unidentifiable bioclasts; identifiable forms are dominated by echinoderm fragments, but solitary and colonial coral and shell fragments can be identified. Some fossils and fragments are replaced by silica, and localized areas are permeated with cherty material. Bioturbation is pervasive, with areas identifiable as *Thalassinoides*. The degree of bioturbation decreases slightly upward within this lithofacies in the drill core. Evaporite

molds were identified; generally small, measuring 1-3 mm. Pale red iron oxides occur in small clusters, concentrating near weathered edges.

Lithofacies 1 comprises the Gunn/Penitentiary Equivalent of the Stony Mountain Formation in the study area, and is recognized in the surface exposures and present in drill cores (Figure 4.1B). It is intermittently exposed through an estimated 4.0-m-thick interval of strata encompassing the upper portion of the member, comprising sites BC-1 to BC-7. In drill core it occurs through 13.70 m in M-2-05 and 13.80 m in M-06-79. The lower contact of this facies is defined by a gradational loss of shaly interbeds of the underlying Red River Formation and can be observed in drill core. The upper contact is defined by a gradational increase in the pervasiveness and change in character of bioturbation mottling accompanied by decrease in abundance of macrofossils and can be observed in drill core.

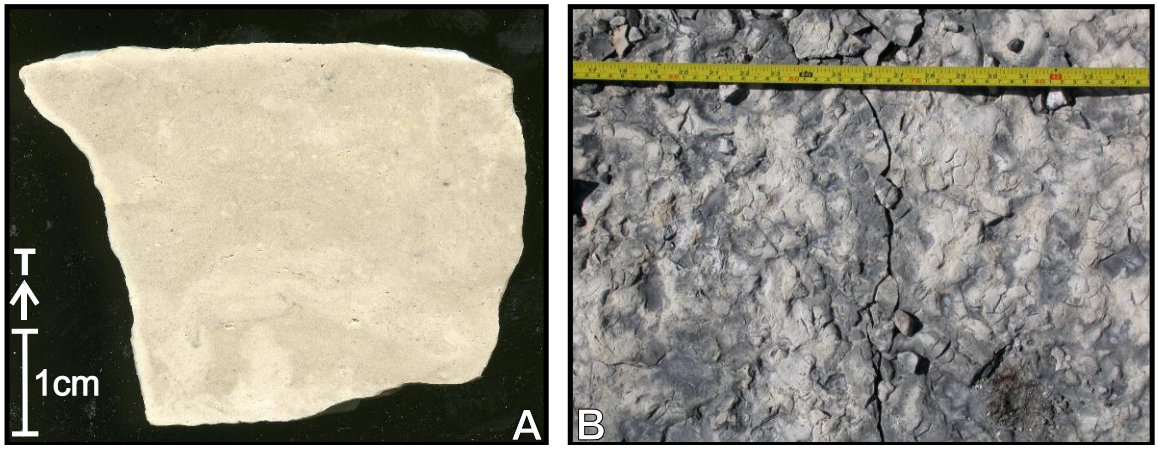

Figure 4.1: Lithofacies 1. A) Digital scan of polished surface of sample collected from BC-4-B. B) Photograph of bedding surface at site BC-1-E. Stratigraphic orientation indicating top surface is shown by the arrow with “T”.

4.2 LITHOFACIES 2

Lithofacies 2 is a highly bioturbated dolomitic mudstone with localized areas of wackestone (Figure 4.2A). It generally is coloured very pale orange but is darkened to yellowish brown within burrow mottles. Within this facies, macrofossil fragments account for about 5-10% of rock volume, and micritic matrix accounts for 95%. Porosity is mostly interparticle, with higher concentrations in fractures and molds, but limited to <5% of total volume. Most macrofossil fragments generally are <1 mm and are mainly unidentifiable forms. Bioturbation is pervasive, identifiable as *Thalassinoides*. Differential weathering of the burrow and surrounding matrix produces distinct patterns (Figure 4.2B).

Lithofacies 2 is identified within the Gunton Member of the Stony Mountain Formation in the study area, and is exposed in the surface exposures and present in drill cores. It is intermittently exposed through an estimated 1.1-m-thick interval of strata, comprising sites BC-8-A to BC-8-E. In drill core it occurs through 5.88 m in M-2-05 and 7.96 m in M-06-79. The upper contact is defined by the gradational decrease of distinctive *Thalassinoides* bioturbation grading into nodular bedding and can be observed in drill core.

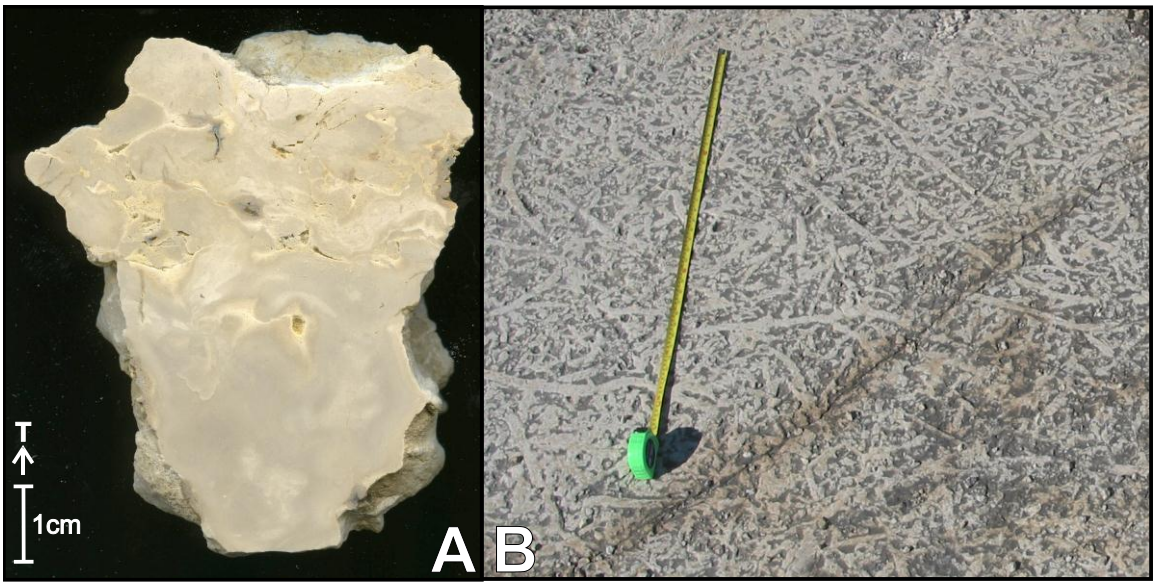

Figure 4.2: Lithofacies 2. A) Digital scan of polished surface of sample collected from BC-8-D. B) Photograph of bedding surface at site BC-8-E. Stratigraphic orientation indicating top surface is shown by the arrow with "T".

4.3 LITHOFACIES 3

Lithofacies 3 is a mildly bioturbated dolomitic mudstone grading gradually upward into nodular bedding (Figure 4.3A). It ranges in colour from very pale orange to light gray, with darkened areas associated with greater incidence of bioturbation. Within this facies, macrofossil fragments account for <5% of rock volume, and micritic matrix accounts for about 95%. Porosity is vuggy, moldic, and interparticle, limited to <5% of total volume. Most macrofossil fragments generally measure <1 mm and are mainly unidentifiable bioclasts; identifiable forms include echinoderm and brachiopod fragments. Bioturbation decreases upward into nodular bedding. Evaporite molds resembling halite crystals are common near the top portion of the lithofacies, measuring 1-5 mm in diameter, with few attaining 1-2 cm laths.

Lithofacies 3 is identified within the Gunton Member of the Stony Mountain Formation in the study area and is exposed in the surface exposures (Figure 4.3B) and present in drill cores. It is intermittently exposed through an estimated 7.9 m thick interval of strata, comprising sites BC-8-F to BC-11 (A-H). In drill core it occurs through 8.82 m in M-2-05 and 6.14 m in M-06-79. The upper contact is defined by a relatively sharp change in lithology from nodular bedded dolostone to laminated mudstones and can be observed in drill core.

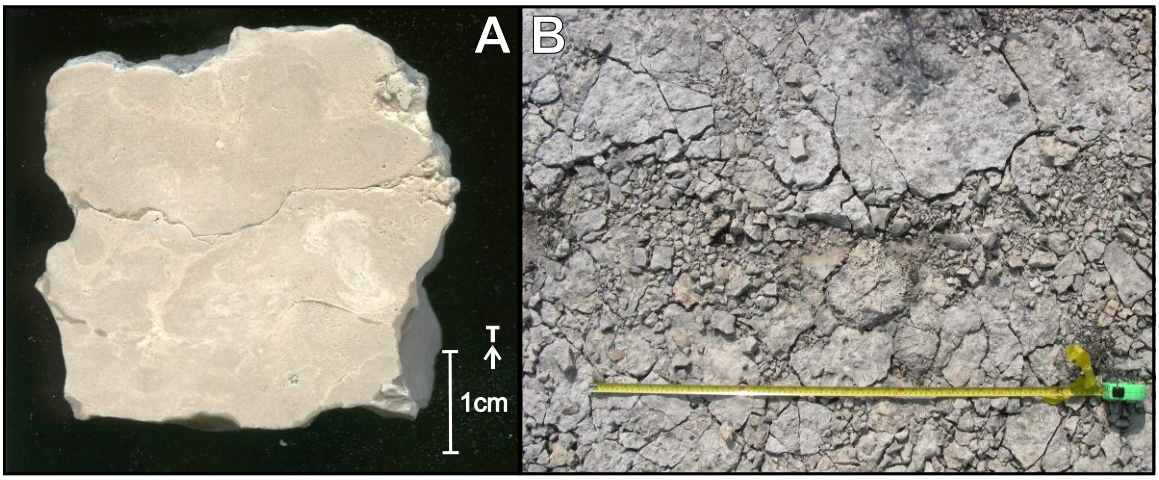

Figure 4.3: Lithofacies 3. A) Digital scan of polished surface of sample collected from BC-9-D. B) Photograph of bedding surface at site BC-11-D. Stratigraphic orientation indicating top surface is shown by the arrow with "T".

4.4 LITHOFACIES 4

Lithofacies 4 is sublithographic dolomitic mudstone, with intervals of thin laminations (Figure 4.4A). It is light gray and overall homogenous, but fine scale variations on discrete horizons provide valuable information on paleoenvironment. Within this facies, macrofossils are rare, and micritic matrix accounts for 95-100% of rock volume. This facies is argillaceous, and fine-grained clay occurs throughout this

facies and fine-grained subrounded sand particles are identified within isolated intervals (BC-11-M). Porosity is not visible. Symmetrical ripples can be observed in the field and some areas are crossbedded and channeled. Dewatering structures such as small flame structures, or dish and pillars, are identified on some horizons. The lower portion of the interval contains dissolution voids of evaporite molds resembling halite crystals. Much of the facies is platy, breaking along laminae into thin beds. The upper portion of the facies contains grayish red purple laminations of 0.5-1 mm thickness that are spaced 1-10 mm apart.

Lithofacies 4 is identified within the Williams Member of the Stony Mountain Formation in the study area and is exposed in the surface exposures and road cut succession and occurs in the drill cores. It is intermittently exposed through an estimated 1.56 m thick interval of strata from the surface exposures, comprising sites BC-11-I to BC-11-O, and continuously through a 0.75 m thick interval of the road cut succession representing the uppermost portion of the member (LS-B12) (Figure 4.4B). In drill core it occurs through 3.16 m in M-2-05 and 3.41 m in M-06-79. The upper contact of the unit is defined by a distinct change to thrombolites, identified by disruption of laminae into small patches forming a clotted texture.

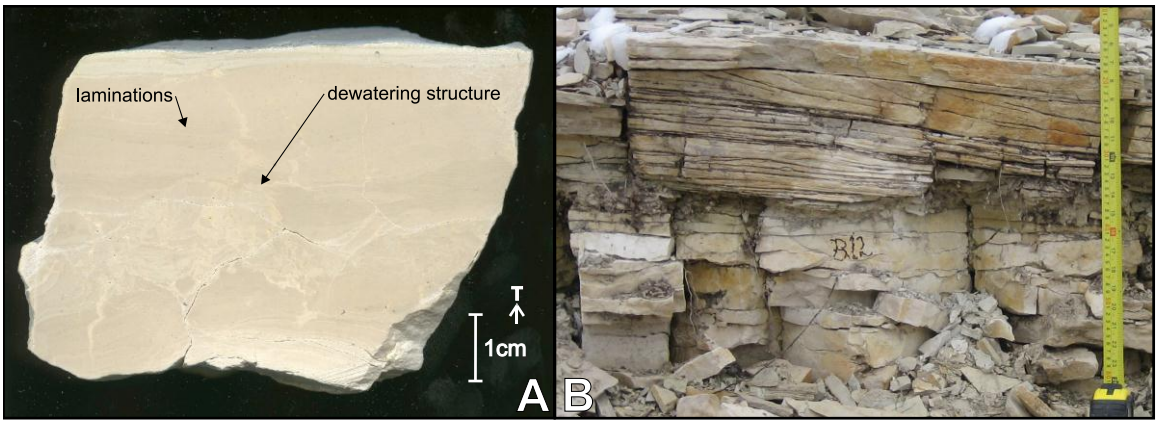

Figure 4.4: Lithofacies 4. A) Digital scan of polished surface of sample collected from BC-11-L showing laminations and dewatering structures. B) Photograph of vertical section through beds at site LS-1-12 showing the platy nature and cross-bedding of the interval. Stratigraphic orientation indicating top surface is shown by the arrow with "T".

4.5 LITHOFACIES 5

Lithofacies 5 is a thrombolitic dolomitic mudstone. It is medium gray to medium bluish gray with a clotted texture (Figure 4.5). The thrombolites occur as mounds up to 30 cm in height formed of patches of microbial build-ups of laminated to clotted mudstone, interspersed with argillaceous to sublithographic mudstone. The patches are highly variable, but most are a few millimetres to centimetres in diameter. Within this facies, macrofossils are extremely rare, with only a single linguloid brachiopod identified, and micritic matrix accounts 95-100% of rock volume. Porosity is vuggy, limited to 5-10% of total volume. Areas of bioturbation disrupt the thrombolitic texture, identified by 1-3 mm diameter, highly irregular, circular burrows occurring as darker matrix.

Lithofacies 5 occurs in two intervals within the study area: the top of the Williams Member of the Stony Mountain Formation, and in the above LS-marker portion of the lower Stonewall Formation. It is exposed in surface exposures and the road cut succession and occurs in drill core.

In the Williams Member, this lithofacies is exposed over an estimated 0.54-m-thick interval of strata in surface exposures (BC-P), and continuously through a 0.5-m-thick interval of the road cut succession (LS-B11). In drill core it occurs through 0.14 m in M-2-05 and 0.09 m in M-06-79. In the Stonewall Formation this lithofacies is exposed continuously through a 0.56-m-thick interval of the road cut succession (LS-A1). In drill core it occurs through 0.29 m in M-2-05 and 0.35 m in M-06-79. The lower contact in both the Williams Member and Stonewall Formation intervals is defined by the sharp emergence of the thrombolitic texture. The upper contact in both intervals is defined by a sharp but highly irregular top of the mounds; up to 30 cm of relief can be measured in places along the contact.

Figure 4.5: Lithofacies 5. A) Digital scan of polished surface of sample collected from LS-1-A1. Stratigraphic orientation indicating top surface is shown by the arrow with “T”. B) Photograph of vertical section at site LS-1-A1. Yellow arrows point to contact with overlying Lithofacies 9.

4.6 LITHOFACIES 6

Lithofacies 6 is massive bedded mudstone, with an alternation between thinner sublithographic mudstone beds (lithofacies subunit 6a) and thick nodular mudstone to wackestone beds (lithofacies subunit 6b) (Figure 4.6). The thinner sublithographic beds (6a) are composed of dense dolomitic mudstone (Figure 4.6A). They are very pale yellowish brown and average 0.21 m in thickness. Within these beds macrofossils are rare, and micritic matrix accounts for 95-100% of rock volume. Porosity is concentrated in fractures, limited to <5% of total volume. Localized areas contain nodules of dense, hard, cherty material that are white with dark brown centres. The thick nodular beds (6b) are composed of chalky dolomitic mudstone to wackestone (Figure 4.6B). They range from white to very pale orange and average 0.89 m in thickness. Within these beds macrofossil fragments are very poorly preserved and mostly unidentifiable, accounting for 5-20% of rock volume, and micritic matrix accounts for 70-80%. Porosity is vuggy and interstitial with few examples of moldic porosity due to dissolution, and is limited to 5-15% of total volume. Bioturbation is irregular and not identifiable to an ichnogenus.

Lithofacies 6 is identified within the below LS-marker portion of the lower Stonewall Formation in the study area and is exposed in the surface exposures and the road cut section, and occurs in drill core. It is intermittently exposed over an estimated 3.71-m-thick interval in strata of surface exposures, comprising sites BC-11-Q to BC-11-BB, and continuously through a 5.31-m-thick interval of the road cut succession (LS-B10 to LS-B2). In drill core it occurs through 4.80 m in M-2-05 and 4.64 m in M-06-79. The upper contact is gradational, defined by loss of bioturbation and emergence of brecciated texture.

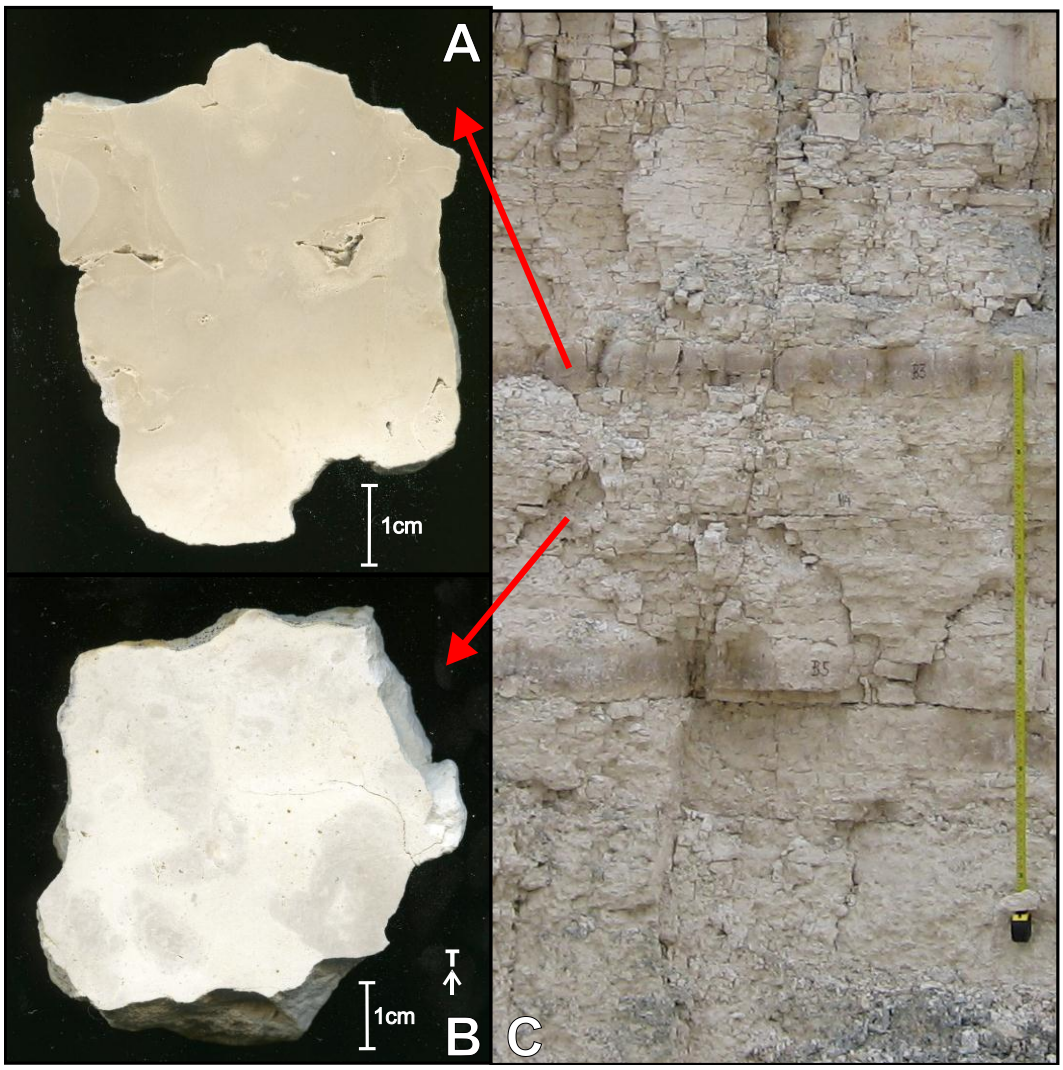

Figure 4.6: Lithofacies 6. A) Digital scan of polished surface of sample collected from LS-1-B7, representing the thinner, sublithographic subunit (6a). B) Digital scan of polished surface of sample collected from BC-11-U, representing the thicker nodular bedded subunit (6b). C) Photograph of vertical section at sites LS-1-B2 to LS-1-B6 showing the alternation of subunits. Stratigraphic orientation indicating top surface is shown by the arrow with "T".

4.7 LITHOFACIES 7

Lithofacies 7 is a brecciated dolomitic mudstone. It is pale yellowish brown and mostly massive with localized areas of brecciation (Figure 4.7). These areas have enveloping darkened bluish gray staining of the matrix material, enabling delineation of

the clasts. The intraclasts are subangular and range from 1-4 mm, accounting for up to 10% of rock volume and are composed of dolomitic mudstone similar to surrounding matrix. Within this facies macrofossils are absent, and micrite accounts for 90-100% of rock volume. Porosity is vuggy and interstitial, limited to <5% of total volume.

Lithofacies 7 is identified within the below LS-marker portion of the lower Stonewall Formation and is exposed within the study area in the road cut section and occurs in drill core. It is continuously exposed through a 0.38-m-thick interval of the road cut section immediately below the LS-marker bed of this study (LS-B1), and in drill core it occurs through 0.78 m in M-2-05 and 1.01 m in M-06-79. The lower contact is gradational, defined by the emergence of the clastic texture. The upper contact is sharp and irregular, defined by distinct change in lithology.

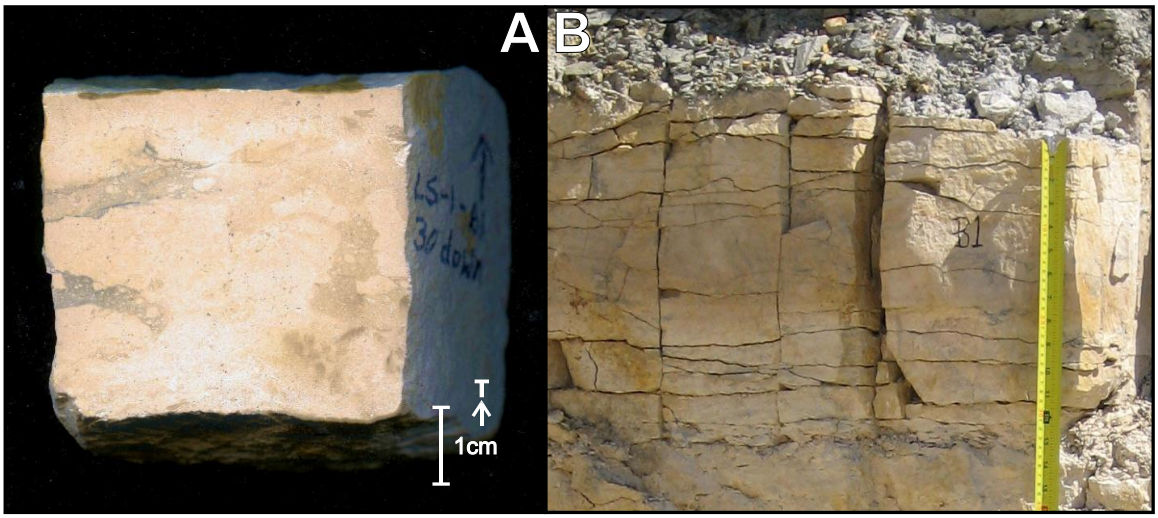

Figure 4.7: Lithofacies 7. A) Digital scan of polished surface of sample collected from LS-1-B1. B) Photograph of vertical section at site LS-1-B1. Stratigraphic orientation indicating top surface is shown by the arrow with “T”.

4.8 LITHOFACIES 8

Lithofacies 8 is a fissile argillaceous dolomitic mudstone (Figure 4.8). It is variably bluish gray, with colour gradation progressing from reddish brown to bluish green to yellowish green to greenish gray. The unit has a friable texture resulting in continual deterioration of the exposure. Within the facies, macrofossils are absent, and micrite accounts for 95-100% of rock volume. Porosity is vuggy, limited to <5% of total volume. Although the exposure of the rock was recent, evidence of weathering was readily evident from muddy degradation. Overall the unit is very soft, and collected samples were taken as a composite across the unit. The base of the lithofacies is sharp. The mudstone shows fine scale changes upward, grading from finely arenaceous and argillaceous, to crumbly and fissile, and into more coherent shaly sublithographic beds.

Lithofacies 8 comprises the LS-marker portion of the Stonewall Formation and is exposed in the study area along the road cut succession and occurs in drill core. It is continuously exposed through a 0.3-m-thick interval of the road cut section (Figure 4.8), and in drill core it occurs through 0.21 m in M-2-05 and 0.15 m in M-06-79. The upper contact is relatively sharp, defined by the emergence of thrombolitic texture within the sublithographic dolomitic mudstone.

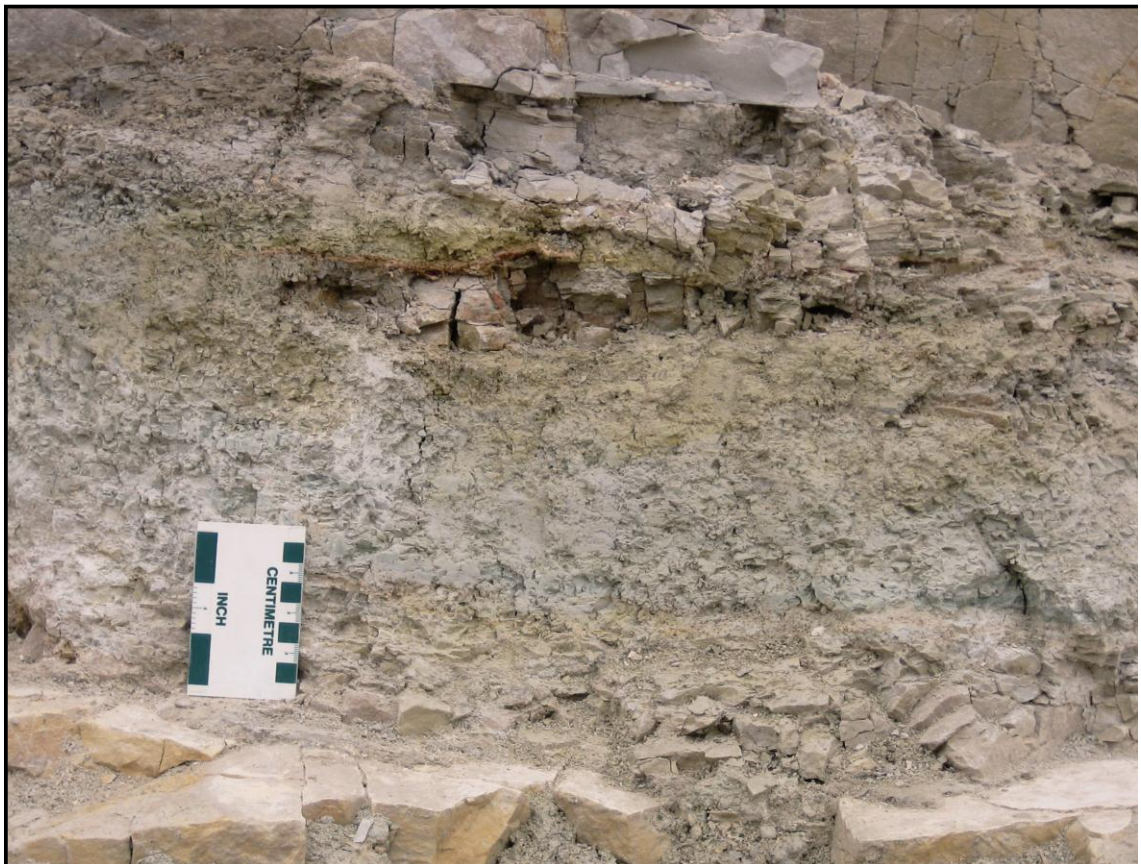

Figure 4.8: Lithofacies 8. Photograph of the LS-marker interval LS-1-MB.

4.9 LITHOFACIES 9

Lithofacies 9 is highly bioturbated dolomitic wackestone (Figure 4.9A) with localized areas of packstone (Figure 4.9B). It is very pale orange to pale yellowish brown. Within this facies, macrofossil fragments account for 5-40% of rock volume, and matrix accounts for 60-90%. Porosity is vuggy and interstitial, limited to <10% of total volume. The facies grades from nearly mudstone at the base to intervals of packstone. Bioturbation emerges quickly and is pervasive throughout, with areas identifiable as *Thalassinoides*. Localized areas associated with greater bioturbation contain nodules of dense, hard, cherty material that are white with dark brown centres. Within the lower

portion of the facies, where it onlaps the thrombolite lithofacies, laminations were identified.

Lithofacies 9 is identified within the above LS-marker portion of the lower Stonewall Formation and in the study area is exposed in the surface exposures and road cut succession, and occurs in drill core. It is intermittently exposed over an estimated 2.4-m-thick interval of surface exposures, comprising sites BC-11-CC to BC-11-FF, and continuously through a 3.8-m-thick interval of road cut succession (LS-A2) (Figure 4.9C). In drill core it occurs through 3.02 m in M-2-05 and 3.12 m in M-06-79. The lower contact is sharp, defined by the top boundary of the thrombolitic mounds. The upper contact for this lithofacies was not observed in the study area.

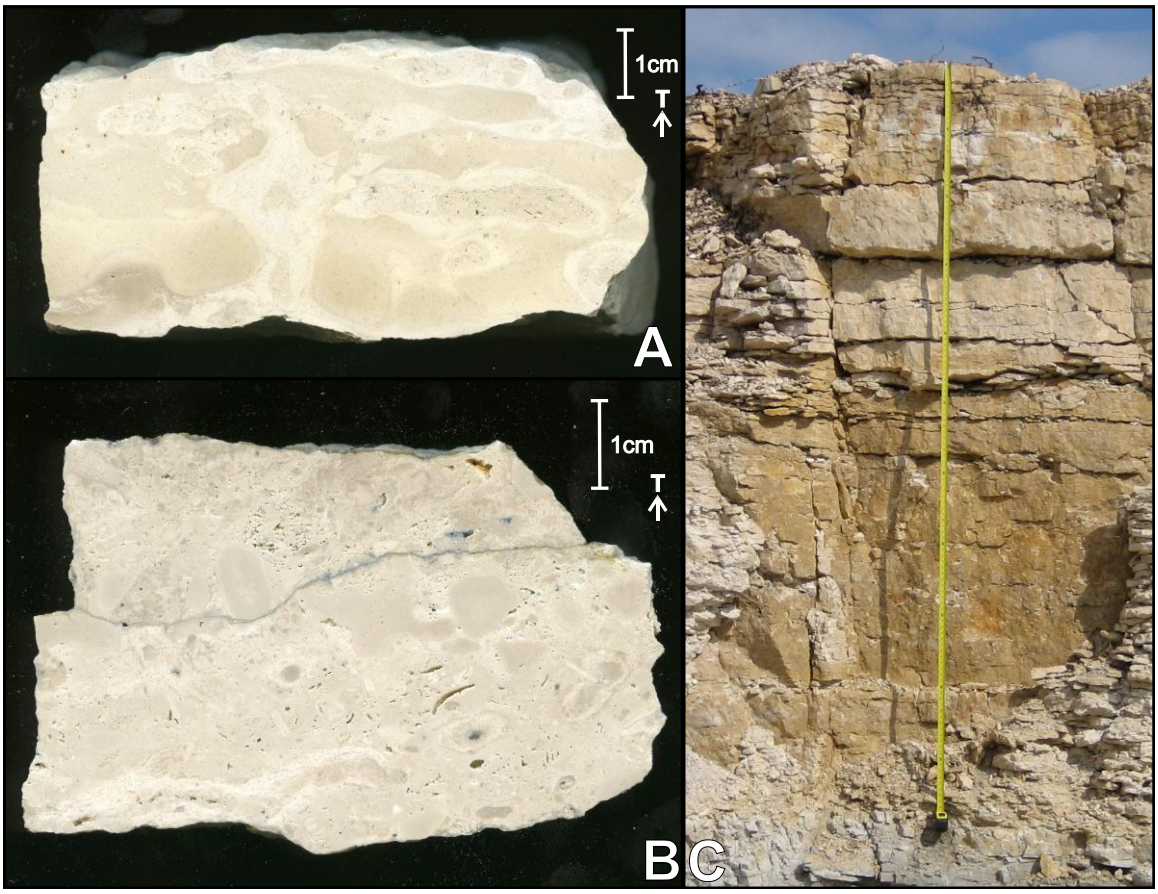

Figure 4.9: Lithofacies 9. A) Digital scan of polished surface of sample collected from BC-11-CC. B) Digital scan of polished surface of sample collected from LS-1-A2 (+40cm). C) Photograph of vertical section at site LS-1-A2. Stratigraphic orientation indicating top surface is shown by the arrow with “T”.

CHAPTER 5 - SUBSURFACE ANALYSIS

An important aspect of the uppermost Ordovician succession is the nature of the contacts between stratigraphic units. Drill core provides a critical uninterrupted record of strata, permitting assessment of these contacts. Two cores obtained from close proximity to the William Lake study site were examined for this study in order to relate the surface exposures and road cut section to the subsurface geology, including lateral extension of units and nature of contacts. Details of the core are presented in Appendix C.

The cores were drilled by the Government of Manitoba Mineral Resource Division and are warehoused at their Core Storage Facility in Winnipeg, Manitoba. The rock quality designation (RQD) of the cores is poor, which is reflected in obscured visibility over some intervals. The recovery of both cores is good.

5.1 M-2-05 (WILLIAM TOWER DRILL CORE)

The M-2-05 core was drilled in 2005 alongside Provincial Highway 6 near William Tower, adjacent to the road cut succession at the top of exposure surface locality BC-11 (Figure 3.3). This location was chosen at the highest extent of the succession of surface exposures to provide a complete stratigraphic control for the surveyed section. The location was mapped with GPS and laser-aided surveying. The 39-mm-diameter core originates in the Stonewall Formation and extends 90.6 m downward into the Winnipeg Formation. Only the upper portion extending down into the Red River Formation was considered in this study. This core was previously logged by R.K. Bezys (Manitoba Geological Survey), whose descriptions were used as a guide for this study (Bezys,

2006). Examination of the William Tower drill core revealed the same lithofacies as those described from outcrop.

Stony Mountain Formation

The lower contact of the Stony Mountain Formation is defined by the loss of shaly interbeds characteristic of the underlying Red River Formation. The Gunn/Penitentiary Equivalent is 13.7 m thick, composed of fossiliferous mottled dolomitic mudstone comparable to lithofacies 1. The contact with the Gunton Member is gradational into the lower 5.88 m composed of intensely *Thalassinoides*-mottled dolomitic mudstone comparable with lithofacies 2. The upper 8.82 m portion of the Gunton Member is composed of nodular bedded, mildly bioturbated, evaporate-hosting mudstone, which is comparable to lithofacies 3. Contact with the overlying Williams Member is relatively sharp (Figure 5.1). The lower 3.16 m of Williams Member is composed of laminated to sublithographic mudstone comparable with lithofacies 4. The interval grades into the remaining 14-cm-thick thrombolitic mudstone, which is comparable to lithofacies 5 (Figure 5.2). The upper contact of the Williams Member of the Stony Mountain Formation is sharp and undulatory, reflecting the variability of the thrombolitic mounds.

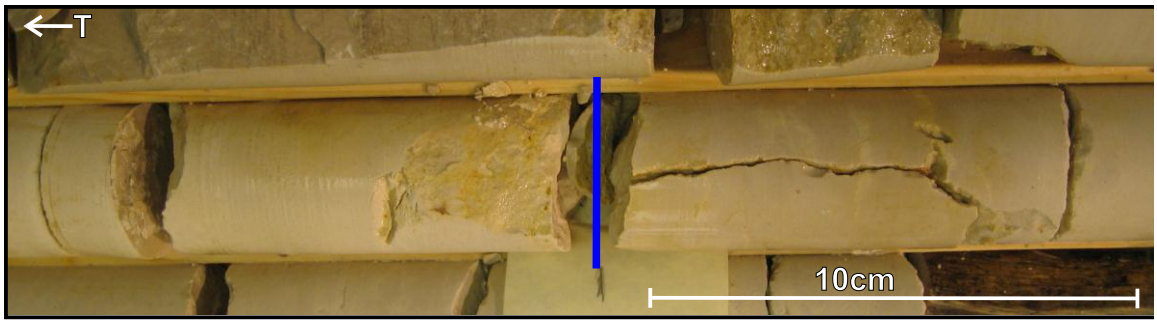

Figure 5.1: Close up photograph of M-2-05 core at about 12.4 m showing the relatively sharp contact between Gunton and Williams members of the Stony Mountain Formation. Blue line shows the change from nodular lithofacies 3 to sublithographic lithofacies 4. Top direction is upper left and core is wetted to enhance colour and texture.

Figure 5.2: Close up photograph of M-2-05 core at about 9.1 m showing the gradational contact between laminated sublithographic lithofacies 4 and thrombolitic lithofacies 5 (in the vicinity of the red arrow). Top direction is upper left and core is wetted to enhance colour and texture.

Stonewall Formation

The Stonewall Formation in core is comparable to the strata measured in the study area. The lower contact of the Stonewall Formation is defined by the sharp boundary between lithofacies 6 and 5. The lower 4.8 m of the formation is composed of interbedded nodular and sublithographic dolomitic mudstone comparable to lithofacies 6, and grades into a 78 cm interval of brecciated dolomitic mudstone comparable to lithofacies 7. Immediately above is a 21-cm-thick LS-marker interval composed of greenish gray, fissile argillaceous dolomitic mudstone with a sharp base, which is

comparable to lithofacies 8. This interval is crumbly and is falling apart in the core box. It grades into 29 cm of thrombolitic mudstone, which is comparable to lithofacies 5. There is a sharp upper contact reflecting the variability of the thrombolitic mounds. The uppermost 3 m is composed of *Thalassinoides*-mottled mudstone to wackestone corresponding to lithofacies 9. This interval contains abundant bioclastic material including coral, brachiopod, and echinoderm fragments.

5.2 M-06-79 (MINAGO RIVER MICROWAVE TOWER DRILL CORE)

The M-06-79 core was drilled in 1979 near the Minago River Microwave Tower, approximately 5 km south of the road cut succession (Figure 3.3). This 28-mm-diameter core originates in the Silurian Interlake Group, within the Atikameg Formation, and extends downward 111.9 m into the Ordovician Winnipeg Formation. Only the interval from within the lower part of the Fisher Branch Formation to the top of the Red River Formation was considered in this study. This core was previously logged by H.R. McCabe (Manitoba Geological Survey), whose descriptions were used as a guide for this study (McCabe, 1979). Examination of the Minago River Microwave Tower drill core revealed the same lithofacies as those described from outcrop.

Stony Mountain Formation

The basal contact of the Stony Mountain Formation is sharp, defined by the loss of characteristic shaly interbeds of the underlying Red River Formation. The Gunn/Penitentiary Equivalent is 13.8 m thick and is composed of fossiliferous mottled dolomitic mudstone assigned to lithofacies 1. The contact with the overlying Gunton

Member is gradual, defined by a change in the nature and pervasiveness of the bioturbation (Figure 5.3). The lower 7.96 m of the member is composed of highly *Thalassinoides*-mottled, dolomitic mudstone comparable to lithofacies 2. The upper 6.14 m of the member is composed of nodular bedded dolomitic mudstone, assigned to lithofacies 3. The contact with the overlying Williams Member is sharp but difficult to distinguish. The lower 3.4 m of the Williams Member is composed of laminated sublithographic mudstone assigned to lithofacies 4. This grades into a 10-cm-thick interval of thrombolitic mudstone, which is comparable to lithofacies 5.

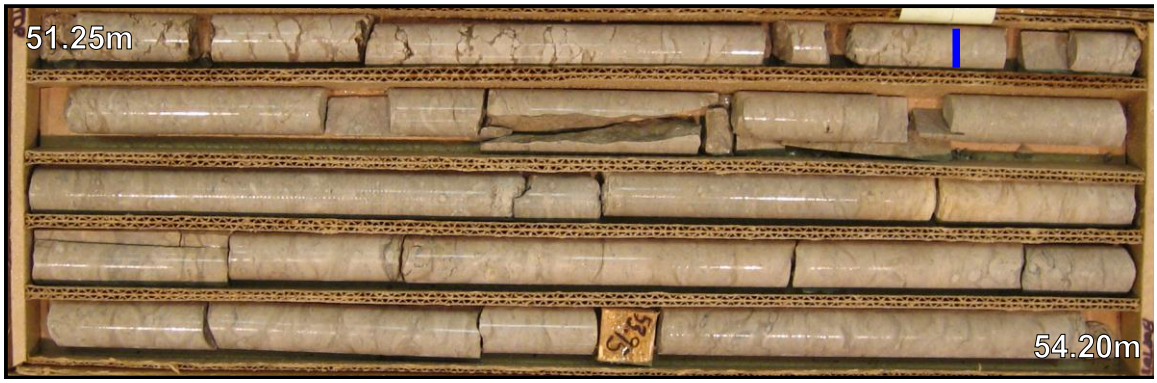

Figure 5.3: Photograph of box of M-06-79 core from 51.25 to 54.20 m showing the contact between the Gunn/Penitentiary Equivalent and Gunton members of the Stony Mountain Formation. Blue line shows the change from mildly bioturbated lithofacies 1 to *Thalassinoides* bioturbated lithofacies 2 at the contact. Top direction is upper left.

Stonewall Formation

The basal contact of the Stonewall Formation is sharp and undulatory, defined by the irregular top of the underlying thrombolitic lithofacies (Figure 5.4). The Stonewall Formation is variably composed of massive to bioturbated dolomitic mudstone interrupted by an argillaceous *t*-marker bed.

Figure 5.4: Photograph of box of M-06-79 core from 33.3 to 36.25 m showing the contact between the Williams Member of the Stony Mountain Formation and the lower Stonewall Formation. Blue line at the formational contact shows the change from thrombolitic lithofacies 5 to interbedded lithofacies 6. Top direction is upper left.

The lower 4.6 m of Stonewall Formation is composed of interbedded nodular and sublithographic dolomitic mudstone, comparable to lithofacies 6. It grades upward into a 1-m-thick interval of brecciated dolomitic mudstone comparable to lithofacies 7. This interval has a sharp upper contact with a 15 cm LS-marker interval of light bluish gray fissile argillaceous mudstone, which is comparable to lithofacies 8 (Figure 5.5). The mudstone grades into an overlying 35 cm of thrombolitic mudstone comparable to lithofacies 5; the upper contact appears sharp but is obscured due to poor RQD. Above this interval almost 6 m of the "lower" Stonewall Formation is composed of variably bioturbated dolomitic mudstone to wackestone. The lower portion of this interval is more highly bioturbated wackestone, which is comparable to lithofacies 9, containing abundant bioclastic material including coral and echinoderm fragments. It grades upward into more massive mudstone, with dendrites occurring as fracture fill. Fossil content is not identifiable above 25.03 m depth.

Figure 5.5: Close up photograph of M-06-79 core showing the fissile argillaceous lithofacies 8. Lower row shows the sharp lower contact with brecciated lithofacies 7 at 28.65 m and the upper contact with thrombolitic lithofacies 5 at 28.5 m. Upper row shows a portion of the wackestone-packstone of lithofacies 9. Top direction is upper left.

The lower contact of the *t*-marker interval is sharp and undulatory. The 80-cm-thick *t*-marker is composed of mostly pale reddish brown argillaceous dolomitic mudstone. The lower- and uppermost portions of this *t*-marker interval do not show the reddish brown staining but are composed of similar argillaceous dolomitic mudstone. The "upper" Stonewall Formation is in sharp contact with the *t*-marker (Figure 5.6). This interval is 3.4 m thick and is composed of vuggy dolomitic mudstone. The upper contact of the Stonewall Formation is sharp, defined by a distinct change in texture (Figure 5.7).

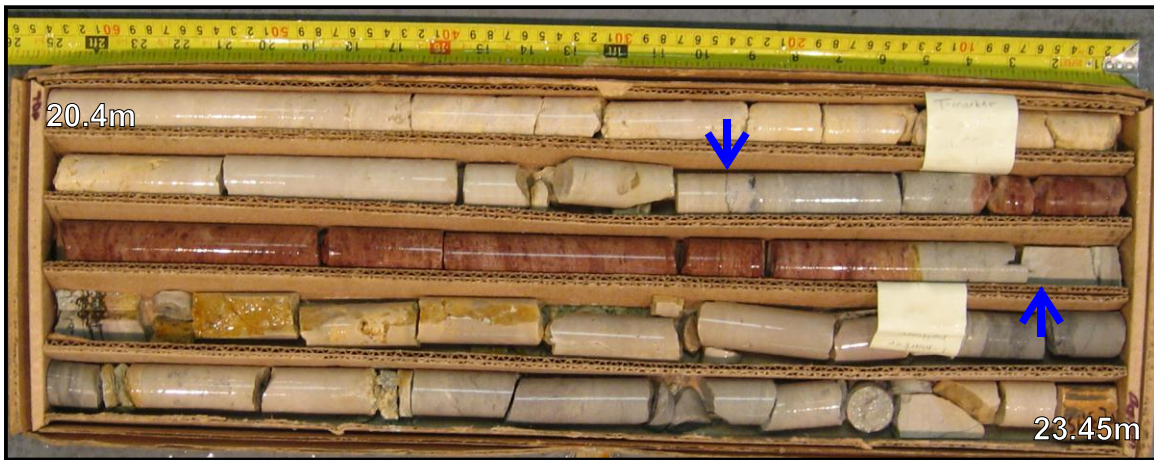

Figure 5.6: Photograph of box of M-06-79 core from 20.4 to 23.45 m showing the *t*-marker bed interval of the Stonewall Formation. Blue arrows show the upper and lower contacts. Top direction is upper left and core is wetted to enhance colour and texture.

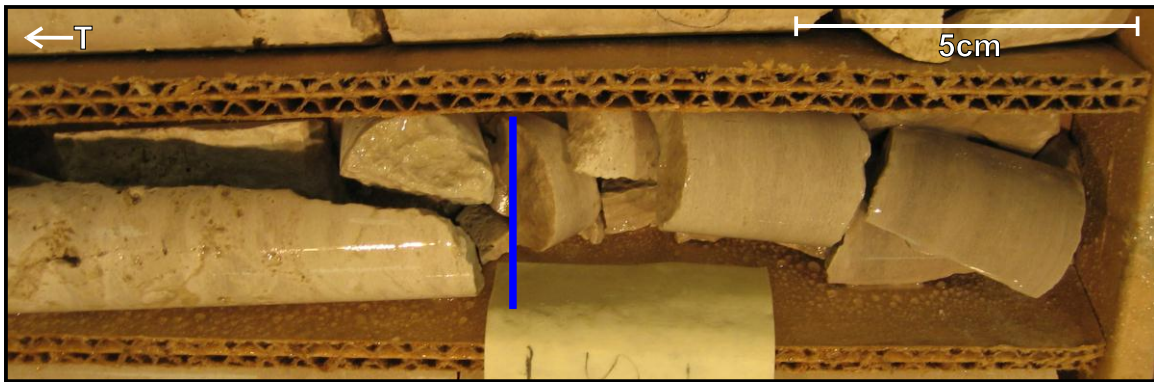

Figure 5.7: Close up photograph of M-06-79 core at about 19.0 m showing the sharp contact between dolomitic mudstone of the Stonewall Formation and the vuggy Fisher Branch Formation (blue line). Top direction is upper left and core is wetted to enhance colour and texture.

Fisher Branch Formation

The base of the Fisher Branch Formation is composed of vuggy dolomitic mudstone, and bioclastic material is mostly unidentifiable. Overall the interval is massive and generally homogenous in core.

5.3 CORRELATIONS AND INTERPRETATIONS

The correlation of the Minago River Microwave Tower drill core (M-06-79), William Tower drill core (M-02-05), surface exposures, and road cut succession is displayed in Figure 5.8. The baseline used for correlation of the two drill cores and the road cut succession is the base of the LS-marker bed interval (lithofacies 8). The elevation of the top of the William Tower drill core was mapped by laser-aided surveying, allowing the surface exposures to be tied to the drill core.

The close proximity of the William Tower drill core to the surface sites permitted stratigraphic control for the outcrop areas. The correlation places the position of the nine

lithofacies described from the surface exposures and road cut succession at approximately the same positions as in the drill core. These lithofacies were extrapolated through the subsurface to the Minago River Microwave Tower drill core. Little appreciable thickness variation was recognized for the identified lithofacies across the correlation, indicating that the stratigraphic successions are comparable.

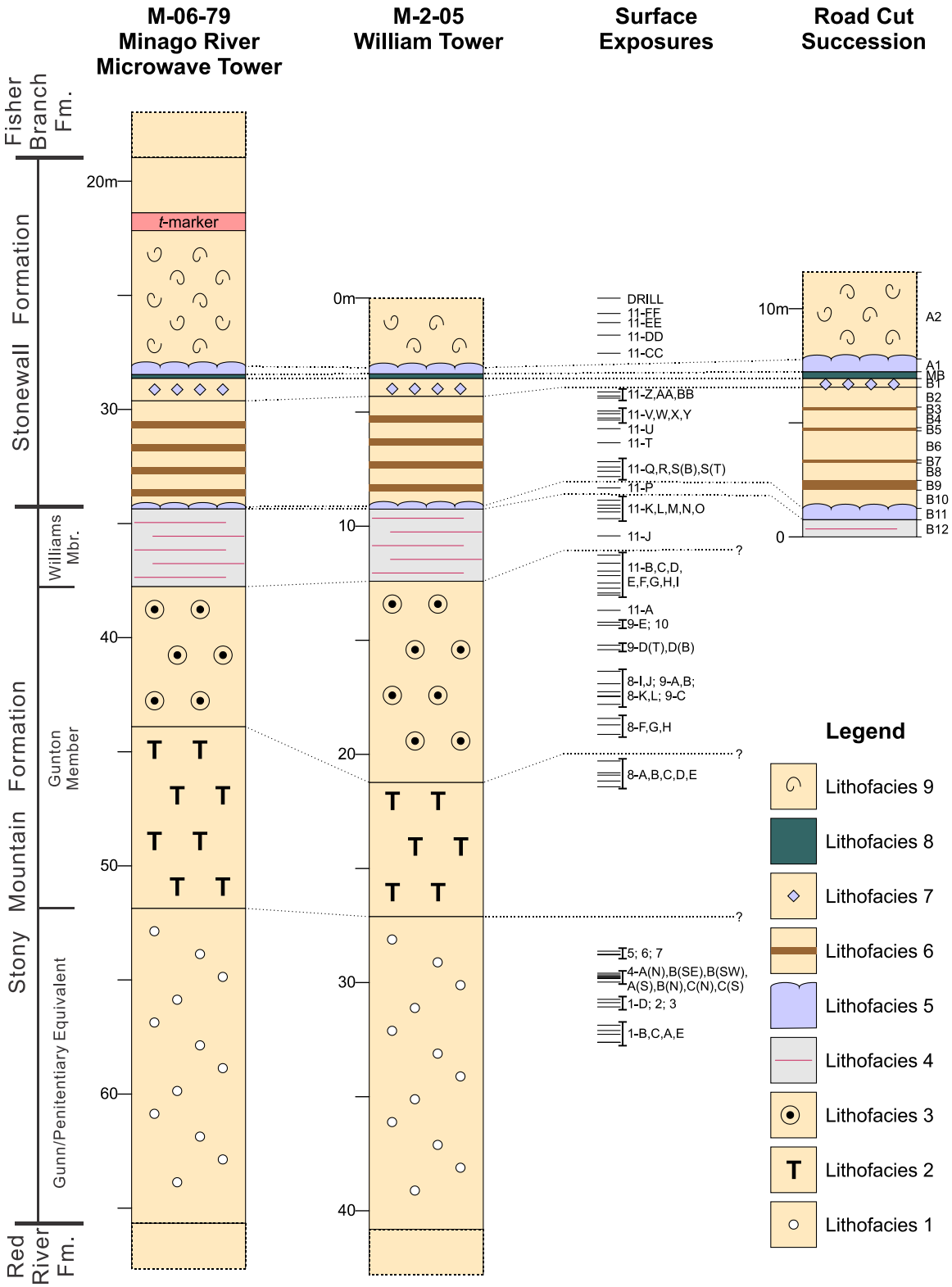

Figure 5.8: Stratigraphic correlation of lithofacies identified from the study area. Locations are shown in Figures 3.3 and 3.4.

.

CHAPTER 6 - SUPPLEMENTAL ANALYSES

The applications of supplementary analyses were used to contribute to understanding of the study area. The road cut succession provided excellent stratigraphic control enabling detailed analysis. Three accompanying techniques were utilized: 1) X-ray diffraction (XRD), 2) dissolution for insoluble residue, and 3) stable carbon and oxygen isotope analysis.

6.1 X-RAY DIFFRACTION

Initial attempts to identify the carbonate mineral phases within samples from the study area employed Alizarin red-S and potassium ferricyanide staining techniques (Dickson, 1966). This method produces differential staining of the various carbonate phases which can then be used to distinguish between carbonate minerals. Use of this method in this study yielded ambiguous results due to the fine-grained nature of the lithologies. X-ray diffraction is a non-destructive method of qualitatively identifying mineral phases present within a sample (Weber and Smith, 1961). Samples from the study area were analyzed with this method in an attempt to verify the mineral phases present.

Eight samples were analyzed by X-ray diffraction technique (Table 6.1). All samples showed a dolomite phase, with a prominent identifying peak at 30.95° 2θ (Figure 6.1), but none showed any trace of calcite. The only other explicitly identifiable mineral was a quartz phase, with an identifying peak at 26.6° 2θ (Figure 6.2). Considerable background was expressed in few samples; attempts were made to identify phases, resulting in possible evidence for potassium aluminum silicate or glauconite (Figure 6.3).

Table 6.1: Stratigraphic order of samples analyzed by XRD, with the identified phases.

Sample	XRD Identified Mineral Phases
LS-1-A2 +230cm	Dolomite
LS-1-A1 top	Dolomite
LS-1-MB top	Dolomite, quartz
LS-1-MB middle	Dolomite, quartz, potassium aluminum silicate?
LS-1-MB lower	Quartz, dolomite, glauconite?, potassium aluminum silicate?
LS-1-B1 top	Dolomite
LS-1-B4 +50cm	Dolomite
LS-1-B7	Dolomite

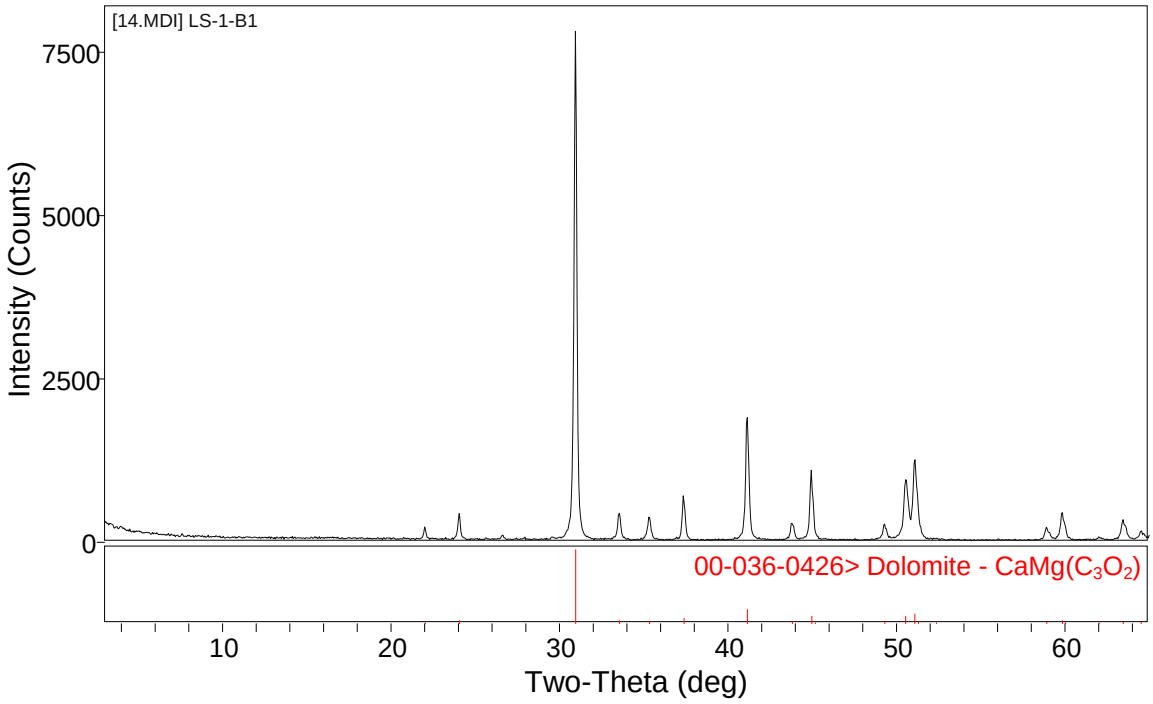

Figure 6.1: XRD plot from site LS-1-B1 showing the characteristic pattern of most of the analyzed samples. There is a large identifying peak for dolomite at 30.95° 2θ.

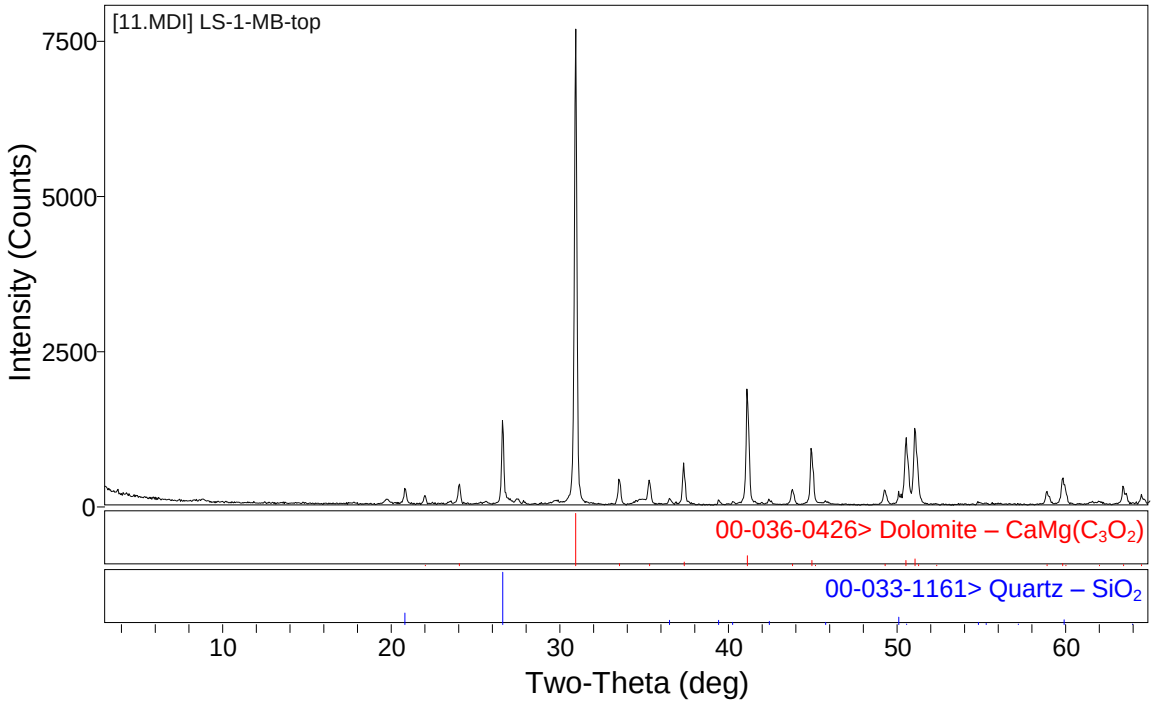

Figure 6.2: XRD plot from site LS-1-MB-top showing a pattern with dolomite and quartz phases. There is a large peak identifying peak for dolomite at 30.95° 2θ (red), and an identifying peak for quartz at 26.6° 2θ (blue).

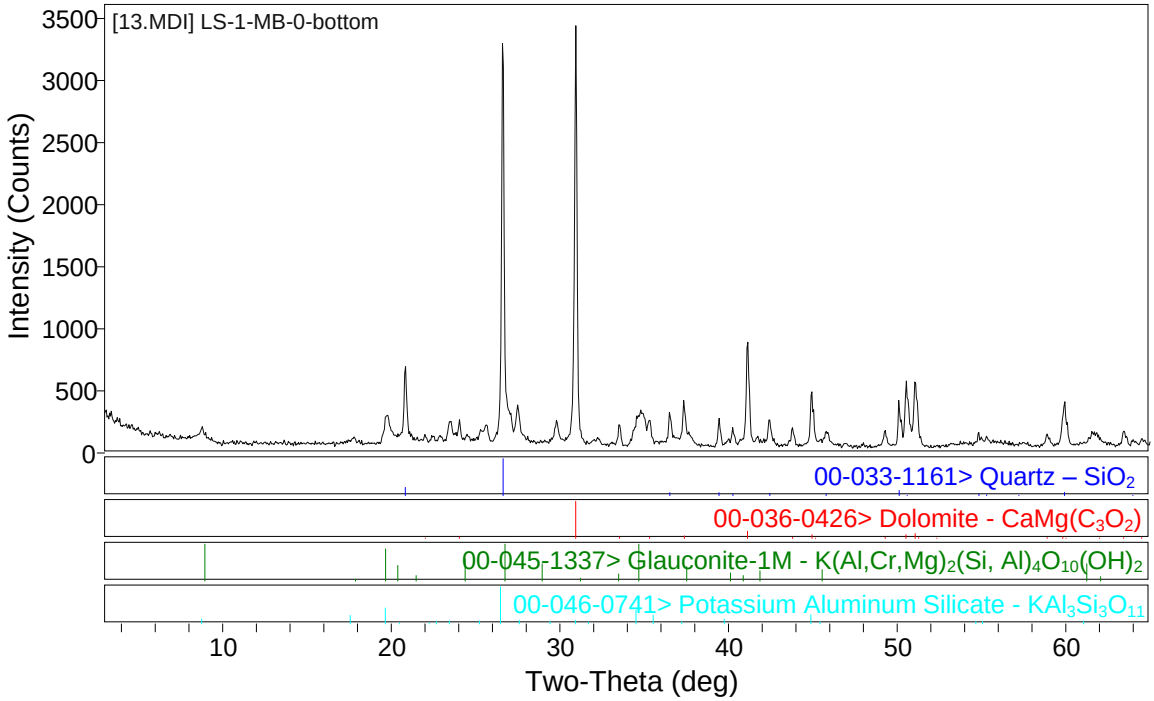

Figure 6.3: XRD plot from site LS-1-MB-bottom showing a pattern with dolomite and quartz phases. There is a large identifying peak for dolomite at 30.95° 2θ (red), a large identifying peak for quartz at 26.6° 2θ (blue), and the possible profiles for glauconite (green) and potassium aluminum silicate (aqua).

In most samples dolomite was the dominant phase; five of the samples produced only the dolomite phase (Figure 6.4). This indicates that the entire section is completely dolomitized, since no expression of calcite was detected.

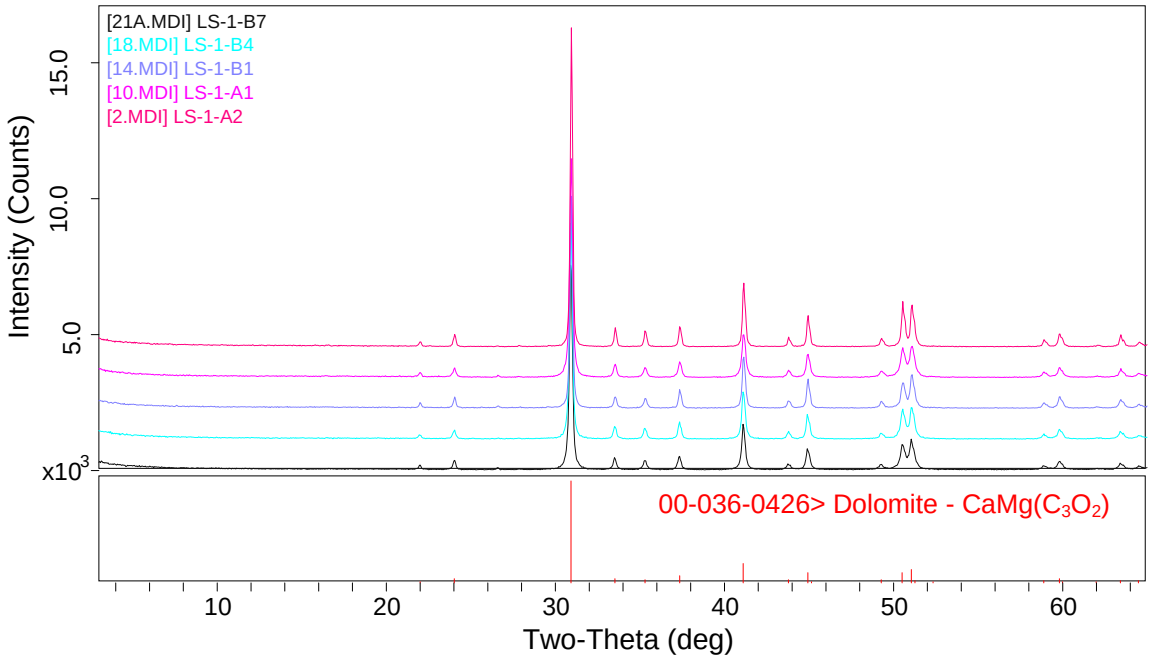

Figure 6.4: Stacked XRD plot of the samples from the road cut exposures showing the characteristic pattern identifying the dolomite phase. The large peak is the identifying peak for dolomite at 30.95° 2θ (red).

Only three samples (LS-1-MB-0-bottom, LS-1-MB-0-middle, and LS-1-MB-0-top) produced the quartz phase in addition to the dolomite phase (Figure 6.5). This quartz phase is expressed within the LS-marker bed interval of the section corresponding to lithofacies 8; it is most prominent within the base and decreases upward. Within sample LS-1-MB-0-bottom the quartz phase is the dominant phase, the dolomite phase is supplementary, and there was additional expression of the considerable background, suggesting possible evidence for potassium aluminum silicate or glauconite. Within

sample LS-1-MB-0-middle the dolomite phase is the dominant phase, the quartz phase is supplementary, and there was expression of the background, suggesting possible evidence for potassium aluminum silicate. Within the sample LS-1-MB-top the dolomite phase is dominant, the quartz phase is supplementary, and there was some expression of the background, but phases could not be distinguished.

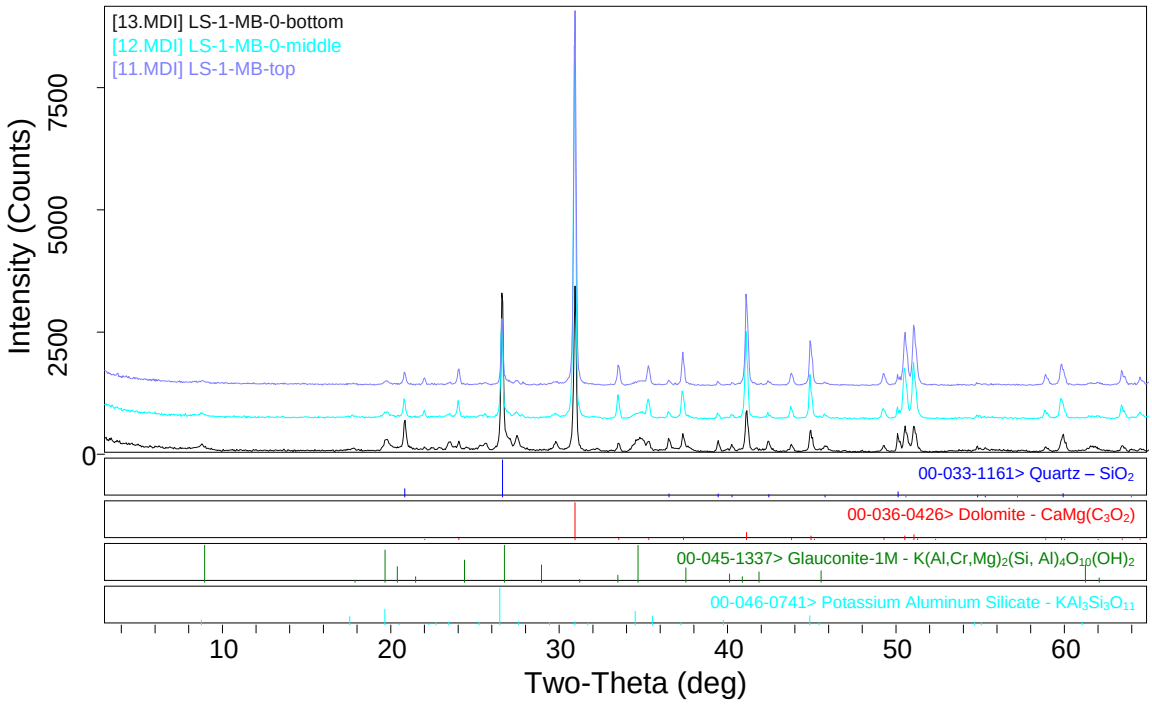

Figure 6.5: Stacked XRD plot showing the characteristic pattern with dolomite phases from within the LS-marker bed interval of the road cut succession. There is a large identifying peak for dolomite at 30.95° 2θ (red), a large identifying peak for quartz at 26.6° 2θ (blue), and the possible profiles for glauconite (green) and potassium aluminum silicate (aqua).

6.2 Dissolution Analyses

Based on the initial XRD results, three samples from the LS-marker bed interval were selected for more detailed research in prospect of identifying possible background phases. These three samples showed possible phases apart from the pronounced dolomite

and quartz phases. The dominant dolomitic component was dissolved out with hydrochloric acid. The mass of insoluble residue resultant from this dissolution was compared with the initial mass to determine the percentage of insoluble material (Table 6.2). The weight percent of residue decreases upward through the LS-marker bed interval.

Table 6.2: Results of Dissolution Analysis

Sample	Initial Mass (g)	Residue Mass (g)	Residue %	Reassessment XRD Identified Mineral Phases
LS-1-MB-top	182.80	39.40	22%	Quartz
LS-1-MB-middle	146.65	58.49	40%	Quartz, potassium aluminum silicate?
LS-1-MB-lower	144.75	68.83	48%	Quartz, potassium aluminum silicate?

The residue material was examined with a petrographic microscope in an attempt to discern mineralogical characteristics of the resultant grains. The residue is poorly consolidated, very fine grained, argillaceous material of unknown composition. Therefore, these samples were analyzed by X-ray diffraction to identify composition.

In the samples of residue material, since the dolomite was dissolved away, the quartz phase was dominant, and considerable background was expressed (Figure 6.6). Within sample LS-1-MB-lower(diss) and LS-1-MB-middle(diss) the quartz phase is dominant and there was additional expression of the considerable background, but in sample LS-1-MB-top(diss) only the quartz phase was identified. Attempts to identify phases within the background were obscured by the diversified background, as few substantial peaks were patterned. Those few peaks suggest a potassium aluminum silicate mineral phase closer to the base of the LS-marker interval.

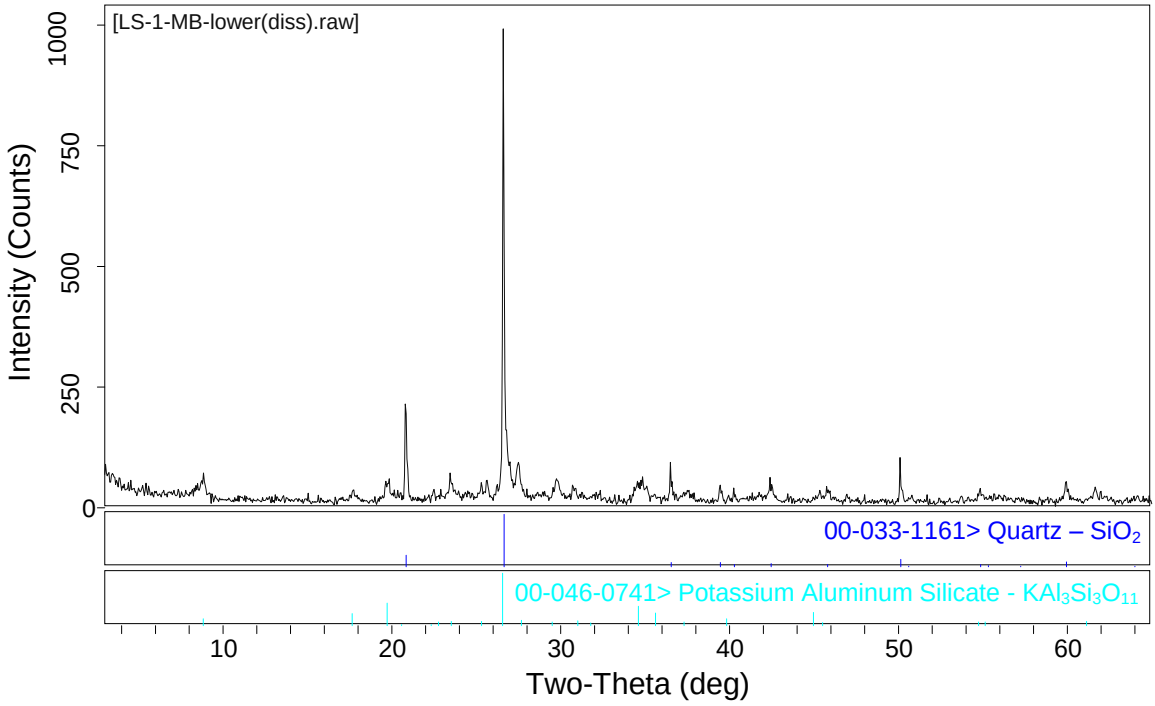

Figure 6.6: XRD plot from the dissolved residue from sample of site LS-1-MB-lower. There is a large identifying peak for quartz at 26.6° 2θ (blue) and the suggested profile for potassium aluminum silicate (aqua).

6.3 STABLE ISOTOPE GEOCHEMISTRY

Analysis for stable carbon and oxygen isotopes was completed on 38 samples (Table 6.3); 26 were obtained from samples collected from the road cut succession and 12 were obtained from samples collected from the Minago River Microwave Tower drill core (M-06-79). Carbon isotope values ($\delta^{13}C$) ranged from -0.3 to +1.3‰ and oxygen isotope values ($\delta^{18}O$) ranged from -5.8 to -3.7‰, and are displayed graphically in Figure 6.7.

Table 6.3: Stable carbon ($\delta^{13}C$) and oxygen ($\delta^{18}O$) isotope results

Road Cut Succession		
Location	$\delta^{13}C$ ‰	$\delta^{18}O$ ‰
LS-1-A2 +330cm	0.93	-5.13
LS-1-A2 +230cm	1.03	-5.35
LS-1-A2 +155cm	1.22	-5.83
LS-1-A2 +90cm	0.95	-5.71
LS-1-A2 +40cm	0.73	-5.25
LS-1-A2 high thrombs	0.78	-5.57
LS-1-A2 low thrombs	0.43	-4.99
LS-1-A1 high thrombs	0.59	-5.72
LS-1-A1 low thrombs	0.44	-5.61
LS-1-A1 top	0.61	-5.79
LS-1-MB-top	0.68	-4.15
LS-1-MB-middle	0.67	-3.72
LS-1-MB-bottom	0.60	-4.11
LS-1-B1 top	1.25	-4.47
LS-1-B1 +10cm	0.97	-5.58
LS-1-B2 +65cm	0.91	-5.29
LS-1-B3	0.89	-5.48
LS-1-B4 +50cm	0.79	-5.27
LS-1-B5	0.80	-5.30
LS-1-B6 +85cm	0.87	-5.26
LS-1-B7	0.70	-5.12
LS-1-B8 +45cm	0.47	-5.07
LS-1-B9	0.53	-5.84
LS-1-B10 +70cm	-0.01	-5.46
LS-1-B-11 middle	-0.33	-4.50
LS-1-B12 +25cm	0.05	-4.76
M-06-79 Minago River Microwave Tower		
Depth (m)	$\delta^{13}C$ ‰	$\delta^{18}O$ ‰
18.00	-0.16	-5.75
18.95	-0.08	-5.23
19.05	-0.19	-5.65
20.00	0.58	-5.43
21.00	0.45	-5.73
21.50	1.80	-4.15
21.85	1.75	-4.32
22.21	0.43	-4.84
23.25	0.70	-4.27
24.10	1.25	-4.57
25.00	0.74	-5.66
25.98	0.62	-5.80

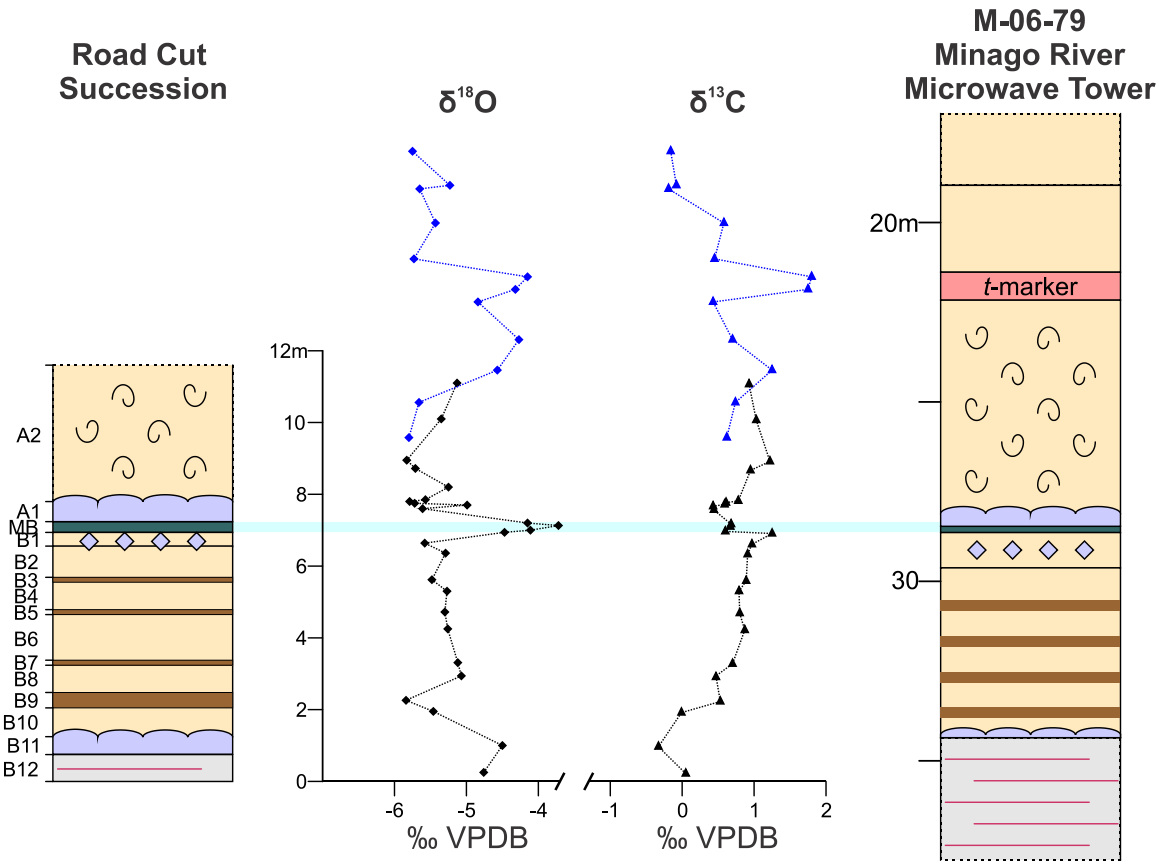

Figure 6.7: Stratigraphic sections with corresponding $\delta^{18}O$ and $\delta^{13}C$ plots from road cut succession (black) and Minago River Microwave Tower drill core (M-06-79) (blue). Light blue shaded line indicates LS-marker bed interval. See Figure 5.8 for lithostratigraphic units and lithologic legend.

The profiles for the road cut succession and the Minago River Microwave Tower core overlap within the Stonewall Formation above the LS-marker bed interval. This allows for the plots to be tied together to examine changes through the succession. Although the proposed excursions are outlined by few points, notable trends can be delinated.

A notable observation regarding the $\delta^{13}C$ profile is a slight negative excursion at both thrombolitic intervals (lithofacies 5). There is a minimum $\delta^{13}C$ value of -0.3‰ in the

lower thrombolitic interval (uppermost Williams Member) which then recovers to a background of ~1.0‰ through the lower portion of Stonewall Formation. There is a minimum $\delta^{13}C$ value of 0.4‰ within the upper thrombolite interval (above the LS-marker bed interval in the Stonewall Formation), which then recovers to background above it. Thus, there is a negative excursion with a magnitude of about -0.5 to -1.3‰ in the vicinity of the thrombolitic intervals.

Another notable observation regarding the $\delta^{13}C$ profiles is the presence of excursions proximate to both the LS-marker bed interval of the study area (lithofacies 8) and the *t*-marker interval of the upper Stonewall Formation. An abrupt positive shift to a peak $\delta^{13}C$ value of 1.3‰ occurs at the top of unit B1, immediately below the LS-marker bed interval (lithofacies 8). Immediately below the *t*-marker, there is a slight negative shift down to 0.4‰, followed by a large positive shift to a peak $\delta^{13}C$ value of 1.8‰ within the *t*-marker interval. Thus, there is a positive excursion with a magnitude of about 0.3 to 0.8‰ in the vicinity of the marker intervals.

Stable oxygen isotopes were also analyzed and results are included in Table 6.3 and Figure 6.7. In general, the profile follows a similar trend to the carbon isotopes. A notable observation regarding the $\delta^{18}O$ profiles is the presence of an excursion proximate to the LS-marker interval (lithofacies 8) and the *t*-marker interval of the upper Stonewall Formation. The background through the section is at ~-5.5‰. An abrupt shift occurs within the LS-marker interval, with a peak $\delta^{18}O$ value of -3.7‰ in the middle. There is another shift to a peak $\delta^{18}O$ value of -4.2‰ within the *t*-marker interval. Thus, there is a positive excursion with a magnitude of about 1.4 to 1.8‰ in the vicinity of the marker

intervals. These results must be regarded with caution, as stable oxygen isotope values are influenced by alteration due to diagenetic effects.

The results identified in this study are consistent with results presented by Demski et al. (2011) from material from the Grand Rapids Uplands. A distinct positive isotopic carbon excursion has been used to suggest that strata of the Stonewall Formation above the base of the *t*-marker interval are Hirnantian age (Demski et al., 2011). This excursion is interpreted to represent an occurrence of HICE, suggesting the placement of the position of the Ordovician-Silurian boundary at the top of the Stonewall Formation.

CHAPTER 7 - FOSSIL IDENTIFICATIONS AND DESCRIPTIONS

The biotas recognized within the William Lake study area consist of a diverse assembly of organisms representing a variety of life modes. Both tabulate and rugose corals dominate through much of the succession along with other normal marine biota such as stromatoporoids, brachiopods, gastropods, cephalopods, and disarticulated echinoderm fragments. Within some stratigraphic units there is the inclusion of some exceptionally preserved fossils that differ strikingly from those in the adjacent units (Young et al., 2007), but these will not be described in detail herein. Microfossils, trace fossil material and biosedimentary structures are also identified. Tabulations of the distribution and abundance of the identified groups are presented in Appendix D. Discussion of the ecologic significance of many groups is presented in Chapter 8.

7.1 MACROFOSSILS

Within the study area, many of the macrofossils that were encountered were collected. The preservation is variable throughout the study area, but in general it is poor, thus making taxonomic identification difficult. Collected fossils range from mere fragments to complete specimens, but only those that could be unequivocally classified to a major group were included in this study. The rocks in this area are extensively dolomitized, obscuring the original mineralogy. Macrofossils are most often preserved as molds and/or dolomitic or siliceous replacements. Taxonomic identification was mainly based upon morphologic and internal characteristics. Many of the fossils identified within this study belong to groups previously documented by Stearn (1956), and his descriptions were used as a guide.

7.1.1 ALGAE

The term “algae” itself has been problematic due to prolonged disagreement among researchers on the systematics of several high-level taxa. Thus, the classification of most groups remains in an uncertain state. Fossils of this problematic group were identified within the study area.

Cyclocrinitids

Cyclocrinitids have often been considered to be allied with receptaculitids as problematic groups commonly linked to either sponges or algae. The present consensus is that cyclocrinitids are a problematic order of algae (Nitecki et al., 2004), whereas receptaculitids are neither sponges nor algae. Both receptaculitids and cyclocrinitids are similarly characterized by a central axis with branches that extend outward, terminating in a calcified plate that produces an external globulose body. These groups may be differentiated because cyclocrinitids are generally smaller than receptaculitids and the shape of their plates is generally hexagonal, whereas receptaculitid plates are rhomboidal (Nitecki et al., 2004).

Pasceolus sp.

(Figure 7.1A)

Specimens of the genus *Pasceolus* were recognized at a single locality within the surface exposures (BC-8) and are preserved as internal molds (Figure 7.1A). This genus is characterized by a globulose body with an approximate thallus diameter of 2-3 cm. The hexagonal lateral heads (plates) are uniform in diameter measuring about 1 mm.

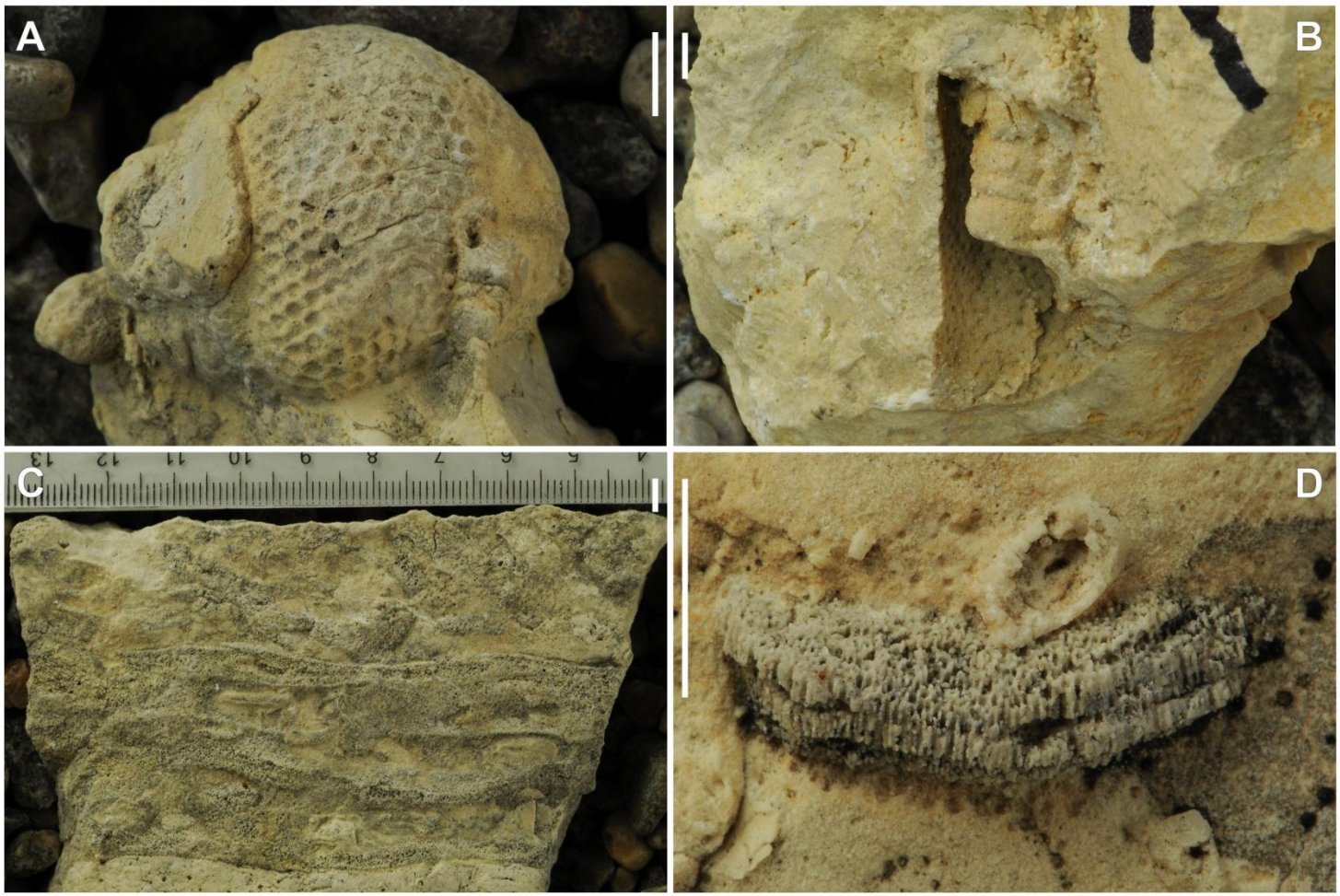

Figure 7.1: Algae and Porifera found within the William Lake study area (scale bar = 5 mm). A) *Pasceolus* sp., lateral view, Gunton Member, Stony Mountain Formation, BC-8-E-*4*. B) *Aulacera* sp., lateral view, Stonewall Formation, LS-2-A2-*38*. C) *Clathrodictyon* sp., longitudinal view, Stonewall Formation, BC-11-EE-*7*. D) chaetetid, lateral view, Gunn/Penn Equivalent, Stony Mountain Formation, BC-1-A-*12*.

In McInnes (1913), *Pasceolus* (*Cyclocrinus*) *spaskii*? was listed within the biota from the Ordovician northern outcrop belt near Cormorant Lake, which includes strata considered to be similar in age to the study area. Baillie (1952) listed this occurrence as *Cyclocrinites spaskii*. At present, the only cyclocrinitid identified globally from Ordovician time slice 6b (late Richmondian) is *Pasceolus* (Nitecki et al., 2004). Therefore the specimens of this study are assigned to *Pasceolus* sp.

7.1.2 Phylum Porifera (Sponges)

Stromatoporoids

Stromatoporoids are a group of sessile, epibenthic animals common in the Paleozoic (Stearn et al., 1999). Historically, these extinct organisms have had a problematic taxonomy. They show poriferan affinities and are presently classified within the phylum Porifera, class Stromatoporidea. They are characterized by a calcareous skeleton consisting of a continuous internal growth network of repetitive horizontal (laminae) and vertical (pillars) support elements (Stearn et al., 1999). Skeletons can be composed of organic fibers, mineral matter called spicules, or layers or plates of calcium carbonate (Rigby et al., 2003).

Specimens that were poorly preserved were difficult to classify to lower taxonomic levels. A few specimens could not be identified beyond the major group, and as such were generally classified as stromatoporoids.

Aulacera sp.

(Figure 7.1B)

Specimens of the genus *Aulacera* are common in the study area and are preserved as molds (Figure 7.1B). This genus is characterized by a columnar skeleton comprising an axial column and lateral zone (Stearn et al., 1999). The axial column is straight and unbranched, arranged from a series of stacked cyst plates. The hemispherical plates measure 4-5 mm in diameter and are aligned in a single column. The lateral zone is made up of smaller cystose structures and there is development of short rounded pillars measuring 0.5-2 mm in diameter. The genus *Beatricea* is currently considered to be a synonym of *Aulacera* (Stearn et al., 1999).

Stearn (1956) recognized two species of *Beatricea*: *B. regularis* from the upper dolomite bed of the Stonewall Formation at Stonewall quarry and *B. undulata* from the Stonewall Formation on a side road ¼ mile west of the Flin Flon highway at Mile 25. The specimens in the present study are inconsistent with the description and illustration of *B. regularis* by Stearn (1956) and do not show affinity with *Aulacera undulata* as described and illustrated from elsewhere in North America by Shimer and Shrock (1944). The specimens possibly resemble *A. nodulosa*, as described and illustrated from elsewhere in North America by Shimer and Shrock (1944). Baillie (1952) listed the species *Beatricea nodulosa* within the Gunton Member of the Stony Mountain Formation. Due to limitations of preservation and quantity of the study material, specimens of this study are not assigned to a species and are identified as *Aulacera* sp.

Clathrodictyon sp.

(Figure 7.1C)

Specimens of the genus *Clathrodictyon* are common through the study area and are preserved as dolomitic replacements (Figure 7.1C). The genus is characterized by an irregular laminar to domical skeleton comprised of undulatory laminae and short pillars (Stearn et al., 1999). Specimens are poorly preserved, therefore details of internal characters were difficult to distinguish.

Although several species of this genus were recognized by Stearn (1956), none were identified within the Stonewall Formation. Specimens identified within the present study are referred to as *Clathrodictyon* sp.

Chaetetids

(Figure 7.1D)

Chaetetids are a group of sessile organisms that previously were considered to be corals but have now been accepted as sponges (Stearn et al., 1999). They are characterized by polygonal tubes (termed calicles) with horizontal tabulae perpendicular to growth (Kershaw and West, 1991). Skeletons can vary in shape from flat laminar and domical to columnar and branching; they can also have a considerable size range (Kershaw and West, 1991).

One chaetetid specimen was recognized within the surface exposures (LS-1-A) and is preserved as a silicified replacement (Figure 7.1D). It is characterized by a low domical skeleton comprised of small rounded polygonal calicles, measuring about 0.2 mm in diameter, and flat tabulae.

Whiteaves (1897) identified *Chaetetes perantiquus* from the Williston Basin outcrop belt of Manitoba. In Young et al. (2008), Chaetetid gen. and sp. undet. was listed from the "Tyndall Stone" quarried from Garson, Manitoba (Selkirk Member of the Red River Formation). Due to the limited quantity of material for comparison, the specimen identified within the present study retains general identification as chaetetid.

Spicules

Sponges may secrete skeletons composed of organic fibers, mineral matter, or plates of calcium carbonate (Rigby et al., 2003). These elements provide support to the body of the sponge. Spicules are the needle-like mineralized structural elements characteristic of sponges (Rigby et al., 2003). Non-calcareous spicules, representing unidentifiable sponges, were documented within the conodont analysis report on samples from the road cut section (Nowlan, 2009). They were reported as being poorly preserved with simple morphology.

In Rigby (1971), sponges with associated spicules were described and illustrated from the Cat Head Member of the Red River Formation.

7.1.3 PHYLUM CNIDARIA

Cnidaria is a diverse phylum of simple-bodied animals common in the Paleozoic (Hill, 1981). The William Lake succession includes several organisms assigned to the phylum Cnidaria. Jellyfish identifiable to the class Hydrozoa, subclass Hydromedusae and possibly the class Scyphomedusae have been recognized within the Williams Member of the Stony Mountain Formation (Young et al., 2007), but the units of the

present study are dominated by corals of the orders Tabulata and Rugosa, representing the class Anthozoa, and subclass Zoantharia.

Cnidarians are diverse organisms representing a variety of morphologies. They are characterized as being composed of tissues not arranged into organs and having a radial symmetry (Hill, 1981). There are two general forms: nektonic medusae and sessile polyps (Bayer et al, 1956). Nektonic medusae are solitary, characterized by a soft, umbrella-shaped body surrounded by tentacles around the rim (Bayer et al., 1956); sessile polyps may be solitary or colonial, and in the case of corals are characterized by a skeleton fixed to the substrate, commonly composed of calcium carbonate (Hill, 1981). As the polyp grows, the skeleton extends upward forming a tube, termed a corallite (Hill, 1981). Colonial forms consist of arrangements of corallites to form a shared structure termed a corallum (Hill, 1981). Within an individual corallite, radial plates (septa) may be inserted parallel to growth and transverse plates (tabulae) may be inserted perpendicular to growth, serving as basal support for the individual polyps (Hill, 1981). It is interpreted that tabulate and rugose colonial corals initiated growth on soft substrates or encrusting on hard surfaces upon which they expanded outward and upward, and their growth reflects a combination of genetic and environmental effects (Scrutton, 1999). Cnidarian specimens are abundant throughout the study area, most often preserved as dolomitic or silica replacements. Young et al. (2007) have also identified medusoid jellyfish from the Williams Member of the Stony Mountain Formation from units within the study area.

Specimens that were poorly preserved were difficult to classify to lower taxonomic levels. A few specimens could not be identified to either Tabulata or Rugosa

and as such were generally classified as colonial corals. Fossils identified within the study area are consistent with those described from the Red River-Stony Mountain Province (Webby et al., 2004).

Tabulata

Tabulate corals were an exclusively colonial subclass of corals having a variety of colony shapes arising from the manner of increase and arrangement and shape of skeletons (Hill, 1981, p. F506). They are characterized by well-developed tabulae and subdued septa that are generally short or absent; septal spines extending inward from the inner walls of corallites are the most common septal elements (Hill, 1981).

Poorly preserved specimens were difficult to classify to lower taxonomic levels. A few specimens could not be identified beyond this subclass and are generally identified as tabulate corals.

Paleofavosites sp.

Specimens of the genus *Paleofavosites* are abundant in some stratigraphic intervals in the study area. They are characterized by cerioid morphology, with corallites that are closely packed and each shares walls with several neighboring corallites. Corallites are prismatic with mural pores along the corners and sometimes the walls. Within corallites, septa may be present, but are commonly short and variably dispersed. Corallites are polygonal, commonly hexagonal in mature corallites (Young and Elias, 1999A). Tabulae are complete, and are numerous.

Specimens that were poorly preserved were difficult to classify beyond the generic level. The differentiation of the two species described below is reliant on examining the size of corallites and the placement of the small mural pores. Specimens that were not readily identifiable as either of the two species were generally classified as *Paleofavosites* sp.

Paleofavosites prolificus (Billings)

(Figure 7.2A, B)

The specimens identified as *Paleofavosites prolificus* are characterized by the small size of corallites and the presence of pores mainly in the corners. Corallites of this species are polygonal and fairly uniform in size, with mature diameters measuring about 2 mm (Figure 7.2A). Walls are thin and straight measuring about 0.3 mm in thickness; few mural pores are present in corners and are rare in walls (Figure 7.2B). Septal spines are subdued to absent within this species. Tabulae are planar and spaced about 16 in 1 cm.

Stearn (1956) recognized *Paleofavosites prolificus* within the Stony Mountain and Stonewall formations. Specimens identified in the present study are consistent with the description. The specimens of this study therefore retain the name *Paleofavosites prolificus*.

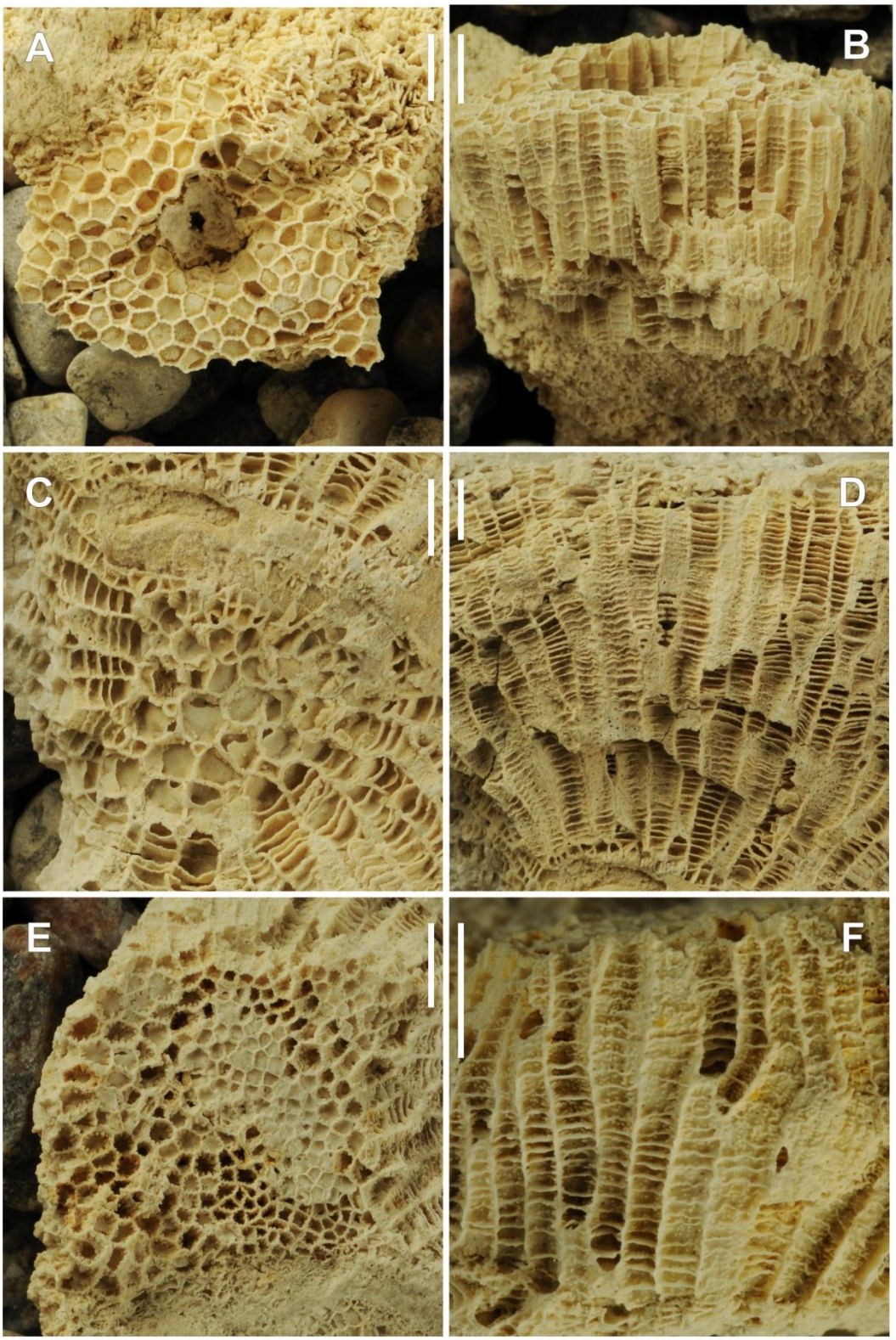

Figure 7.2: Transverse and longitudinal views of tabulate corals found within the William Lake study area (scale bar = 5 mm). A, B) *Paleofavosites prolificus*, Stonewall Formation, LS-2-A2-*37*. C, D) *Paleofavosites okulitchi*, Stonewall Formation, LS-1-A2-*17*. E, F) *Angopora manitobensis*, Stonewall Formation, LS-1-A2-*8*.

Paleofavosites okulitchi Stearn

(Figure 7.2C, D)

The specimens identified as *Paleofavosites okulitchi* are characterized by fairly large corallites and the presence of pores equally distributed within the corners and walls. Corallites of this species are unequal in size, with immature ones interspersed between mature ones; mature corallites are sub-rounded, with mature diameters measuring about 3-4 mm (Figure 7.2C). Walls are thin and straight, measuring 0.3 mm in thickness; mural pores are abundant in corners and walls, generally measuring 0.2 mm in diameter and spaced 15-20 in 1 cm for corners and 10-12 in 1 cm for walls (Figure 7.2D). Septal spines are subdued to absent within this species. Tabulae are planar and spaced 20 in 1 cm.

Stearn (1956) recognized *Paleofavosites okulitchi* in the Stony Mountain and Stonewall formations. Specimens identified in the present study are consistent with his description, and therefore retain the name *Paleofavosites okulitchi*.

Angopora manitobensis Stearn

(Figure 7.2E, F)

The species *Angopora manitobensis* superficially resembles *Paleofavosites* within the study area, but is distinguished by characteristic rows of abundant septal spines. Corallites of this species are unequal in size, with mature diameters ranging from 1.5-2 mm (Figure 7.2E). Walls are straight, but are variable in thickness within coralla, about 0.2 mm in areas having septa and about 0.1 mm in areas where septa are absent (Figure 7.2F). Mural pores are abundant in corners and rare in walls, generally measuring 0.1 mm in diameter and spaced 15 in 1 cm. Septa are locally well developed, projecting 0.3 mm

into corallite, but in areas can be completely absent. Tabulae are planar and spaced about 20 in 1 cm.

This species was recognized by Stearn (1956) within the Stonewall Formation. Though his description indicates corallites of uniform size at 1.89 mm, specimens with coralla containing a range of corallite diameters are present within the study site. The assignment to the genus *Angopora* is regarded as questionable because the poor quality of preservation of the specimens obscures the defining characteristics of the microstructure of this species. The strong development of septal spines differentiates this species from the two *Paleofavosites* species. Specimens of the present study are identified as *Angopora manitobensis* based on similarity to the description by Stearn (1956), but have expanded the range of corallite diameters.

Specimens that are identified as *Angopora* occur only within the Stonewall Formation. Due to the superficial resemblance to *Paleofavosites* and the overall poor quality of preservation, it is possible that some Stonewall specimens identified as *Paleofavosites* sp. may actually be *Angopora*.

Calapoecia sp.

(Figure 7.3A)

Specimens identified as *Calapoecia* sp. are characterized by a coenenchymal colony type, with tabularia separated by common skeletal tissue (Figure 7.3A). This tissue is composed of extensions of the tabulae, and appears vesicular in transverse section. Corallites are round to slightly crenulated, measuring about 3 mm in diameter and centres of corallites are spaced about 3.5 mm apart.

Stearn (1956) recognized the species *Calapoecia canadensis* within the Stony Mountain and Stonewall formations but did not include a description. Due to insufficient data for comparison, the specimens of the present study are identified as *Calapoecia* sp.

Catenipora sp.

(Figure 7.3B)

Specimens identified as *Catenipora* sp. are characterized by cateniform morphology, with corallites aligned in a chain-like network generally one corallite across (Figure 7.3B). Corallites are oval and uniform in size, measuring about 1.5 mm in the long direction. Walls are thick, measuring about 0.5 mm. Septa are absent or perhaps obscured from preservation, but tabulae are complete and planar.

Stearn (1956) recognized *Halysites* sp. in the Stonewall Formation. The genus *Halysites* is now considered to be characterized by corallites separated by coenenchymal tubules, while *Catenipora* does not exhibit such tubules (Hill, 1981). Therefore the specimens of the present study are identified as *Catenipora* sp.

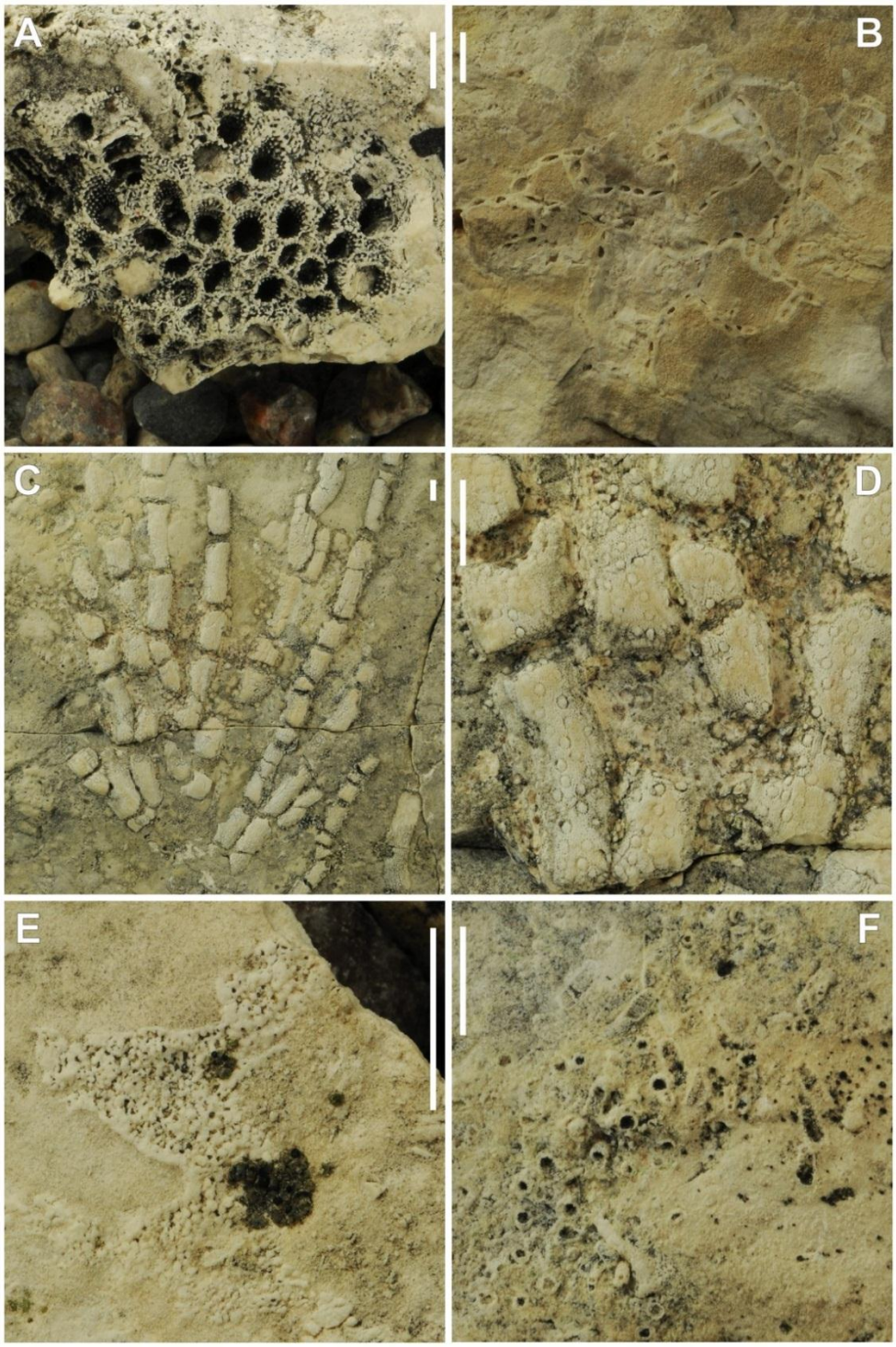

Figure 7.3: Tabulate corals found within the William Lake study area (scale bar = 5 mm). A) *Calapoecia* sp., transverse view, Stonewall Formation, BC-11-CC-*6*. B) *Catenipora* sp., transverse view, Stonewall Formation, LS-1-A2-*loose6*. C, D) *Pragnellia arborescens*, lateral view and close up, Gunn/Penitentiary Equivalent, Stony Mountain Formation, BC-4-C-*MM I-3918*. E) *Ellisites* sp., transverse view, Gunton Member, Stony Mountain Formation, BC-8-E-*1*. F) *Aulopora* sp., transverse view, Stonewall Formation, BC-11-DD-*10*.

Pragnellia arborescens Leith

(Figure 7.3C, D)

Only one specimen of the problematic genus *Pragnellia* was identified within the study area BC-4. *Pragnellia* is characterized by an arborescent corallum, with branches extending from a central axial area (Leith, 1952) (Figure 7.3C). The corallites lack distinct walls, being surrounded by common tissue composed of loosely packed perpendicular rods (Figure 7.3D). The corallites measure about 0.75 mm in diameter and are spaced about 1.25 mm.

Stearn (1956) did not recognize any corals of this genus. The type species, *P. arborescens*, is from the Stony Mountain Formation at Stony Mountain, Manitoba (Leith, 1952). The specimen of the present study is identified as *Pragnellia arborescens* based on the description and illustration by Leith (1952).

Ellisites sp.

(Figure 7.3E)

Specimens identified as *Ellisites* sp. are characterized by an encrusting morphology, indicating that the corallum grew as a laminar sheet reflecting the irregularity of the substrate surface (Figure 7.3E). Corallites are oval and uniform in size, measuring about 0.25 mm.

Stearn (1956) did not describe corals assignable to this genus, but it has been described from the Upper Ordovician Churchill River Group of the Hudson Bay Lowlands (Elias and Young, 2000). Young and Elias (1999B) identified *Ellisites* sp. cf. *E. labechioides* from within the Stony Mountain Formation at Stony Mountain. Due to

insufficient material for examination, the specimens of the present study are identified as *Ellisites* sp.

Aulopora sp.

(Figure 7.3F)

Specimens identified as *Aulopora* sp. are characterized by a loose anastomosing network of small corallites. Corallites are conical and small, with diameters measuring about 0.5 mm (Figure 7.3F). Septal spines are subdued, obscured, or absent. Tabulae are rare, but when present are complete and sub-horizontal.

Aulopora is known from Gamachian strata within the Red River-Stony Mountain Province (Webby et al., 2004, p. 134) and an auloporid identified as fletcheriellid gen. indet. has been identified from the Stony Mountain and Stonewall formations in Manitoba (Webby et al., 2004, p. 135, fig. 15.3). The specimens of the present study are identified as *Aulopora* sp.

Rugosa

Rugosa were a subclass of corals with both solitary and colonial forms and are characterized by the prominent development of radial septal plates (Hill, 1981, p. F96). Septa are serially inserted in a quadrant pattern that produces a bilateral symmetry; minor septa are also present, inserted between major septa (Hill, 1981). There are both solitary and colonial rugose corals identified within the study area.

Solitary Rugosa

Solitary rugose corals are common through the study area and in some areas are locally abundant. Preservation is poor, and specimens are most often fragmentary and preserved as dolomitic replacements. This poor preservation of the material hindered taxonomic identification of the major groups, and as such, many of the specimens were identified only as solitary rugose corals. Where possible, taxonomic identification to the generic and species level was based on shape of the calice and internal characteristics.

Bighornia sp.

Specimens of the genus *Bighornia* are characterized by a flattened convex counter side and a concave cardinal side, which may have a flattened or indented attachment site. Coralla attain a subtriangulate to rounded cross section. Major septa are long and extend to the axis toward a prominent columnella. The cardinal septum is short within a well-defined cardinal fossula.

Poor preservation of some material hindered classification beyond the genus level. The differentiation of the two species described below is based upon the size of corallum and the development of axial structures. Specimens that were not readily assignable to either of the two species were generally identified as *Bighornia* sp.

Bighornia cf. *B. integriseptata* (Parks)

(Figure 7.4A)

Specimens identified as *Bighornia* cf. *B. integriseptata* are characterized by the large size of coralla and the development of an axial structure (Figure 7.4A). The

corallum is more rounded in cross section than that of *Bighornia* cf. *B. patella* and is about 20 mm in diameter. Septa extend toward the centre and the cardinal fossula is well developed.

This species was recognized by Young and Elias (1999B) in the Stony Mountain Formation of southern Manitoba. Within the Stonewall Formation in northern Manitoba, Stearn (1956) recognized the species *Streptelasma* cf. *integriseptatum*, which is now included in *Bighornia* (Duncan, 1957). Specimens in the present study are identified as *Bighornia* cf. *B. integriseptata*.

Bighornia cf. *B. patella* (Wilson)

(Figure 7.4B)

Specimens identified as *Bighornia* cf. *B. patella* are characterized by the small size of coralla. Each corallum is subtriangulate to ovate, ranging from 5 to 15 mm in diameter, with a flattened counter side (Figure 7.4B). Septa extend toward a rounded columnella at the centre.

Elias (1983) recognized *Bighornia* cf. *B. patella* within the Stony Mountain Formation of southern Manitoba. Specimens identified in the present study retain this classification.

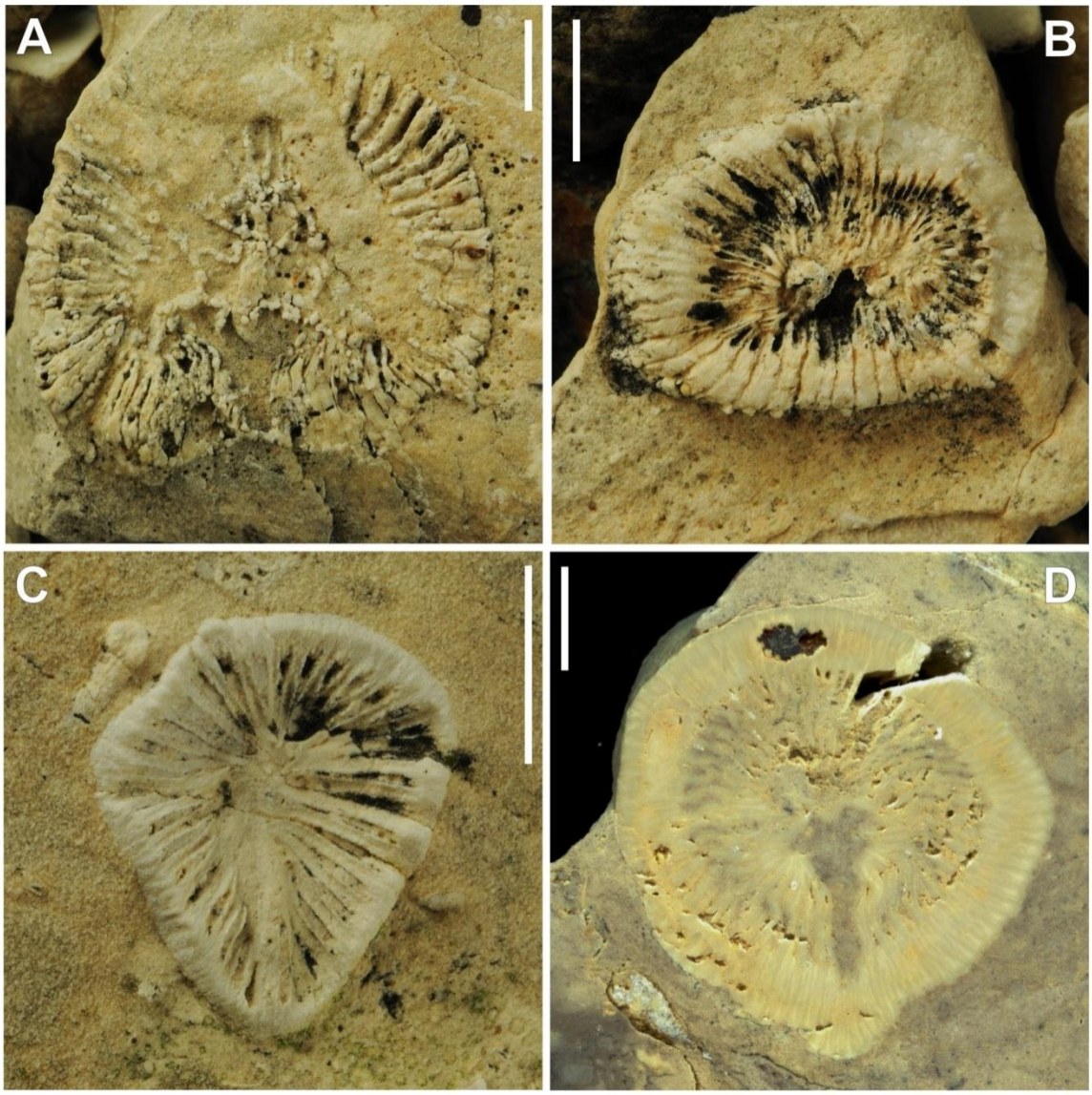

Figure 7.4: Solitary rugose corals found within the William Lake study area (scale bar = 1 mm). All transverse view with cardinal side down. A) *Bighornia* cf. *B. integriseptata*, Gunn/Penitentiary Equivalent, Stony Mountain Formation, BC-4-A-*12*. B) *Bighornia* cf. *B. patella*, Gunn/Penitentiary Equivalent, Stony Mountain Formation, BC-4-*6*. C) *Deiracorallium angulatum*, Stonewall Formation, BC-11-DD-*11*. D) *Salvadorea* sp., Gunn/Penitentiary Equivalent, Stony Mountain Formation, BC-4-B-*5*.

Deiracorallium angulatum (Billings)

(Figure 7.4C)

Specimens identified as *Deiracorallium angulatum* are characterized by a small trochoid corallum with a triangulate to slightly trilobate cross section (Figure 7.4C). Coralla range from 2 to 13 mm in diameter. Major septa are long and extend toward the axis but remain detached. The cardinal septum is short within a narrow cardinal fossula.

The subspecies *Deiracorallium angulatum gunni* was recognized by Elias (1983) within the Stony Mountain Formation of southern Manitoba. The species identification *Deiracorallium angulatum* is used herein because the amount and preservation of material is insufficient for identification to the subspecies level.

Salvadorea sp.

(Figure 7.4D)

Specimens of the genus *Salvadorea* are characterized by a large trochoid corallum with a circular cross section (Figure 7.4D). Coralla range from 7 to 32 mm in diameter. Major septa are long and extend toward axis, developing an axial structure during later ontogenetic stages. The cardinal septum is short within a well-developed cardinal fossula.

The species *Salvadorea selecta* was recognized by Young and Elias (1999B) within the Gunn and Penitentiary members of the Stony Mountain Formation of southern Manitoba. The species *Salvadorea kingae* was recognized by Nelson (1981) within the Hudson Bay Lowlands. Poor preservation of material hindered species identification, but corals show greater affinity to the species described from Hudson Bay than those of the Stony Mountain of southern Manitoba.

Colonial Rugosa

Colonial rugose corals are common in the study area. They exhibit a generally fasciculate morphology, in which the corallites are parallel, but are generally separated from each other. They do not show evidence of connecting processes between corallites. Preservation is poor, and specimens are identified from fragmentary material preserved as dolomitic replacements. A few specimens could not be identified beyond a major group, therefore they are generally classified as colonial rugose corals.

Palaeophyllum sp.

Specimens of the genus *Palaeophyllum* are characterized by a generally fasciculate morphology, but in places corallites are in contact similar to that in cateniform growth. Corallites are circular and do not show evidence of connecting processes. Septa are well developed and extend to the centre of the corallite but are not joined. Tabulae are convex upward and may be numerous.

Young and Elias (1999B) identified *Palaeophyllum* sp. within the Stony Mountain Formation of southern Manitoba. Due to the irregularity of the fasciculate growth of colonies of this genus, complete coralla were not always collected. Some specimens were identified based on a few corallites representing a portion of a colony, in which case the growth form is not known. For those specimens in which the growth form was obscured, or poor preservation hindered identification as either of the identified species described below, a general classification as *Palaeophyllum* sp. was applied.

Palaeophyllum pasense pasense Stearn

(Figure 7.5A)

Specimens identified as *Palaeophyllum pasense pasense* are characterized by their large corallites in a loose cateniform arrangement (Figure 7.5A). Corallites of this subspecies are generally fasciculate, with arrangement ranging from individually separated corallites to groups of corallites connected into loose cateniform chains; centres of corallites are spaced about 4-5 mm apart. Corallites are circular in cross-section and measure 2.5-3.0 mm in diameter. Primary septa are well developed, extending to the centre of each corallite but are not joined. Tabulae are planar to convex upward.

Stearn (1956) identified *Palaeophyllum pasense* within the Stonewall Formation at Mile 24.5, ¼ mile west of Flin Flon highway. Due to identification of a subspecies by Stearn (1956), the specimens of this study are classified as *Palaeophyllum pasense pasense*.

Palaeophyllum pasense parvum Stearn

(Figure 7.5B)

Specimens identified as *Palaeophyllum pasense parvum* are characterized by smaller diameters of corallites, and tighter cateniform growth (Figure 7.5B). Corallites of this species are generally appressed on two or more sides by neighbors. Corallites are circular in cross-section and measure about 2 mm in diameter. Primary septa are well-developed, extending to the centre of each corallite but are not joined, and are about 10 in number. Tabulae are planar to convex upward.

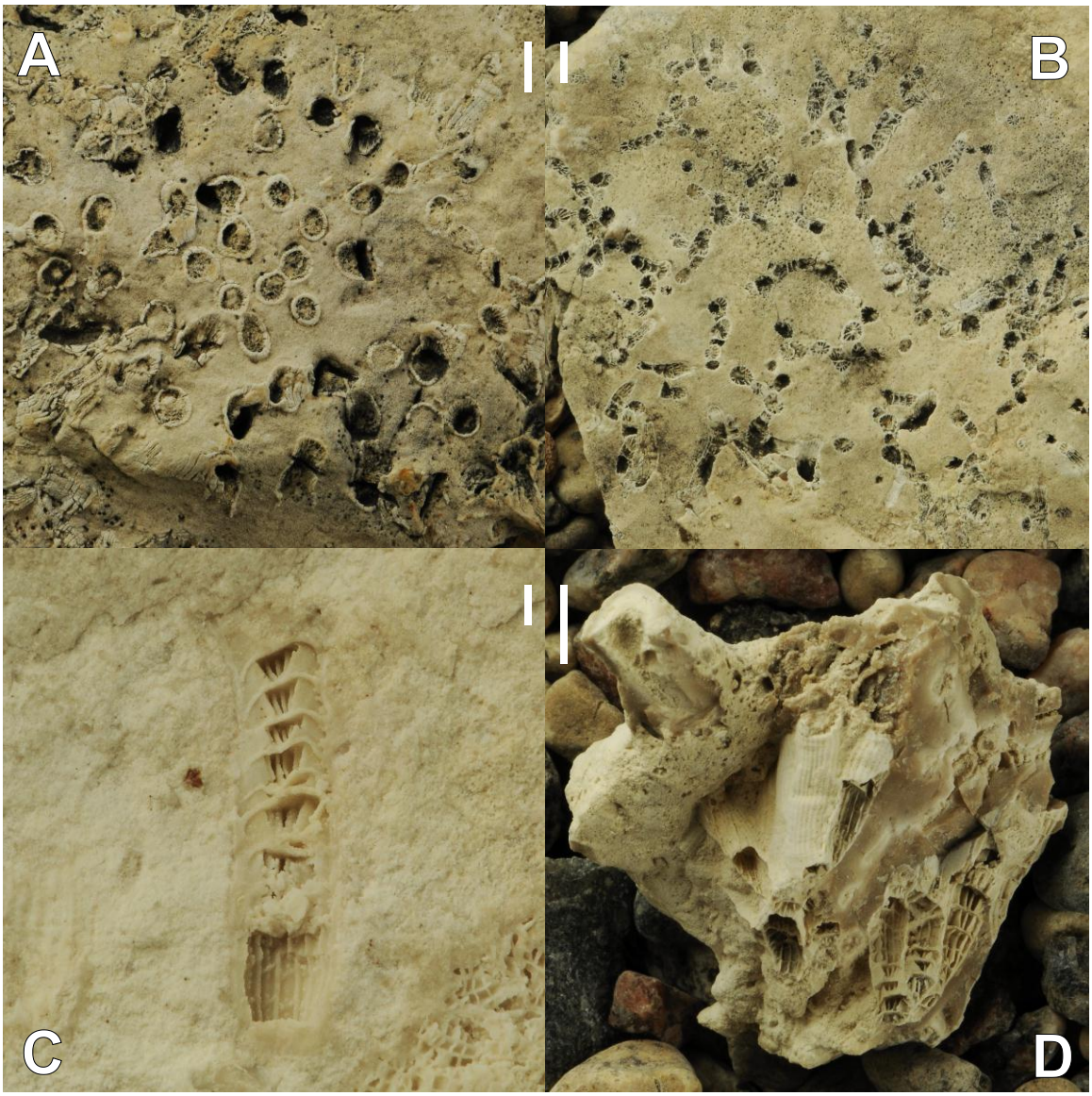

Figure 7.5: Colonial rugose corals found within the William Lake study area (A, B, D scale bar = 5 mm; C scale bar = 1 mm). A) *Palaeophyllum pasense pasense*, transverse view, Gunn/Penitentiary Equivalent, Stony Mountain Formation, BC-4-A-*27*. B) *Palaeophyllum pasense parvum*, transverse view, Stonewall Formation, BC-11-DD-*14*. C, D) *Pycnostylus* sp. (C) lateral view of individual corallite, Stonewall Formation, LS-1-A2-*16*; (D) lateral view of corallum, Stonewall Formation, LS-1-A2-*12*.

This subspecies was identified by Stearn (1956) and agrees in all qualitative characteristics with *P. pasense pasense*, differing only in the size of corallites, number of septa, and juxtaposition of corallites. Stearn (1956) suggested that it is a dwarfed version of *P. pasense pasense*.

Pycnostylus sp.

(Figure 7.5C, D)

Specimens of the genus *Pycnostylus* are characterized by fasciculate morphology, with corallites parallel to each other after branching from the base of the colony; they are not connected by processes (Figure 7.5C, D). Corallites are cylindrical with exterior walls ornamented with septal grooves. Septa are amplexoid, attaining their greatest length on the upper surfaces of tabulae and becoming shorter or absent between tabulae. Tabulae are horizontal.

Stearn (1956) recognized *Pycnostylus guelphensis*, but indicated that it was confined to the Cedar Lake Formation of the Interlake Group. *Pycnostylus* is known from early Rhuddanian? strata within the Edgewood Province (Webby et al., 2004, p. 134). Due to the higher stratigraphic position of previous identified occurrences, specimens of the present study are only identified as *Pycnostylus* sp.

Tryplasma gracilis (Whiteaves)

Specimens identified as *Tryplasma gracilis* are characterized by a fasciculate corallum consisting of cylindrical, radiating corallites that are rarely in contact. Corallites

are circular in cross-section with walls externally ornamented with rugae. Septal spines are arranged in longitudinal rows, about 10 in number. Tabulae are complete and planar.

This species was recognized by Stearn (1956) and is a characteristic fossil of the Stonewall Formation.

7.1.4 PHYLUM MOLLUSCA

Gastropoda

(Figure 7.6A, B, C)

Gastropods are a diverse group of organisms, and fossils of this group are characterized by an unchambered shell that is commonly trochospiral (spiraled along an axis) (Knight et al., 1960). Specimens of this group are rare within the study area and are preserved as internal molds. Some specimens identified within the present study were very poorly preserved and are only classified as gastropods.

Lower classification was based on variations in shell morphology. Most specimens are characterized by small, trochospirally coiled shells, of which three genera are identified: *Liospira* is characterized by a low spired smooth shell (Figure 7.6A); *Hormotoma* is characterized by a high spired smooth shell (Figure 7.6B); and *Trochonema* is characterized by a low spired dorsally ridged shell (Figure 7.6C). A few specimens of the large genus *Maclurina* were identified in the field but were not collected.

Hormotoma sp., *Liospira* sp., and *Trochonema* sp. were recognized by Stearn (1956) within the Stonewall Formation, and are listed in Young et al. (2008) from the Gunn Member of the Stony Mountain Formation. *Maclurina manitobensis* was described

and illustrated by Whiteaves (1897) from the Williston Basin outcrop belt of Manitoba, and listed by Dowling (1900) from the Dog Head, Cat Head, and Selkirk members of the Red River Formation. Due to non-collection of material for re-examination the field identification as *Maclurina* sp. is retained.

Cephalopods

Cephalopods are a diverse group of nektonic organisms, many of them with a characteristic chambered shell of varying morphologies (Knight et al., 1960). Specimens of this group are rare in the study area and are preserved as internal molds. Internal characteristics are important for identification of major groups. Due to the poor preservation of material, internal characteristics were not discernible, therefore classification was based on external shell morphology.

Kinaschukoceras sp.

(Figure 7.6D)

Specimens identified as *Kinaschukoceras* sp. are rare within the study area. They are characterized by a large planispirally coiled shell, and attain a maximum shell diameter of 12 cm across 3 volutions (Figure 7.6D). During growth, the shell maintained a uniform expansion, only gradually widening through ontogeny. The shell bears the genus characteristic of a concave ventral side producing ventrolateral keels.

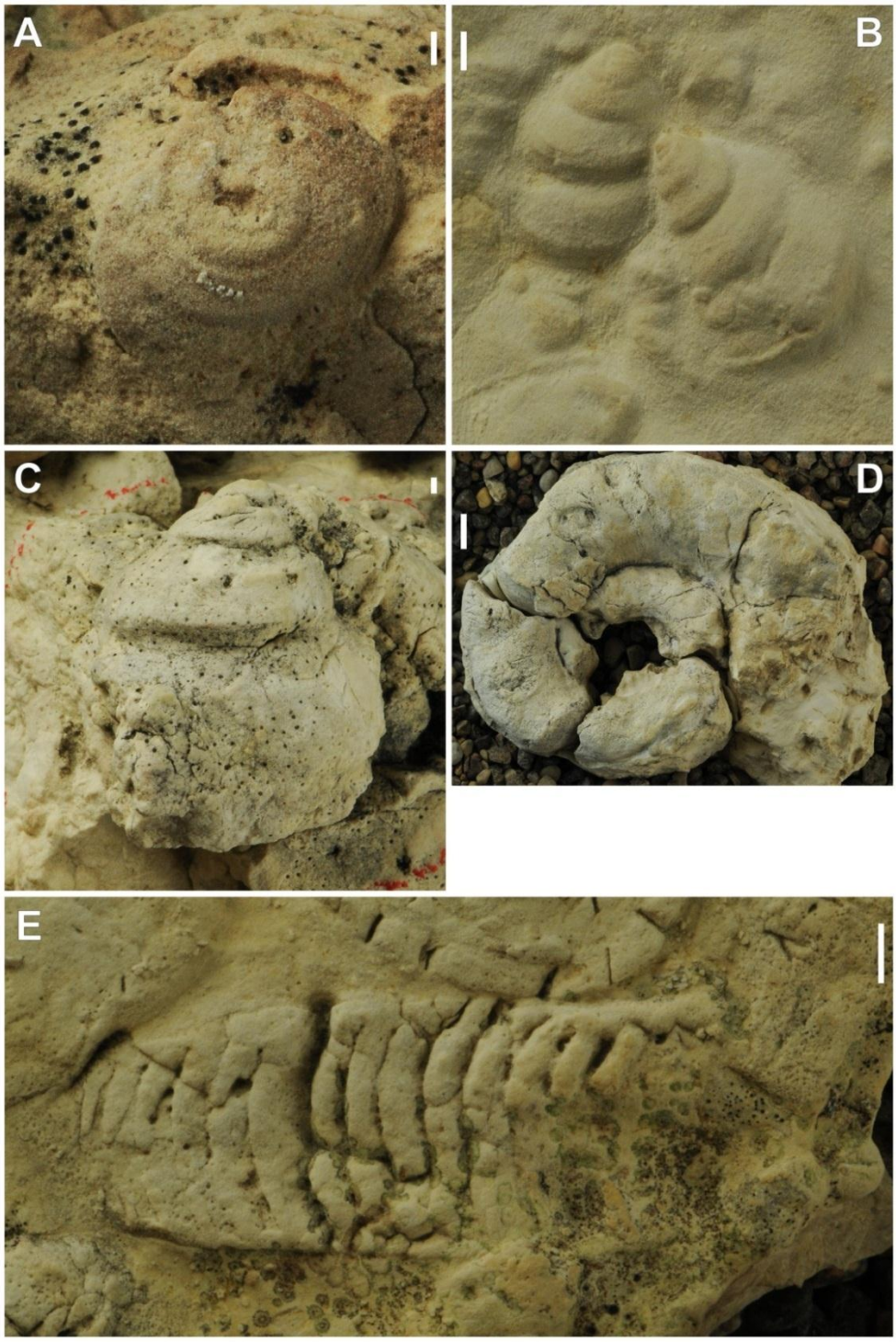

Figure 7.6: Molluscs found within the William Lake study area (A-C scale bar = 1 mm; D, E scale bar = 5 mm). A) *Liospira* sp., Gunn/Penitentiary Equivalent, Stony Mountain Formation, BC-1-E-*3*. B) *Hormotoma* sp., Gunton Member, Stony Mountain Formation, BC-11-H-*1*. C) *Trochonema* sp., Gunton Member, Stony Mountain Formation, BC-8-*4*. D) *Kinaschukoceras* sp., Gunton Member, Stony Mountain Formation, BC-8-*3*. E) orthoconic cephalopod, Gunn/Penitentiary Equivalent, Stony Mountain Formation, BC-1-E-*1*.

Nelson (1963) described and illustrated *Kinaschukoceras churchillense* based on five poorly preserved specimens collected from within Member No.4 of the Chasm Creek Formation from the Upper Ordovician of the Hudson Bay Lowlands. The poor preservation of the type material and of the study material precludes identification to the species level, therefore specimens in the present study are classified as *Kinaschukoceras* sp.

Orthoconic cephalopods

(Figure 7.6E)

Specimens of orthoconic cephalopods are rare within the study area. They are poorly preserved and characterized by a straight, gently widening shell (Figure 7.6E). The lengths of specimens are incomplete and the siphuncle is not preserved.

Stearn (1956) identified several kinds of straight cephalopods from the Stonewall Formation, such as *Ephippiorthoceras minutum* and *Kochoceras* cf. *productum*. The poor preservation of study material inhibits further classification, therefore the specimens are generally classified as orthoconic cephalopods.

7.1.5 PHYLUM BRACHIOPODA

Brachiopods are a diverse group of benthic, sessile, suspension-feeding organisms that were abundant in the Paleozoic (Williams et al., 1997). They are characterized by an upper and lower valve, and can be separated into two basic groups based on the nature of how the valves are joined: inarticulate brachiopods are connected by a complex configuration of muscles, and articulate brachiopods involve a hinge-like configuration to

open and close the valves (Williams et al., 1997). The brachiopod shell is commonly attached to the substrate by a structure called a pedicle, or it may rest directly on the sediment. Molds of both inarticulate and articulate brachiopods are identified within the study sites.

Inarticulate Brachiopods

Linguloid brachiopod

(Figure 7.7A)

Specimens of linguloid brachiopods are generally rare within the study area. The originally organophosphatic shells are preserved on discrete bedding planes and are characterized by a small rounded elongate shell (Figure 7.7A). The average length measures about 7 mm and width measures about 6 mm. The shell is externally ornamented with growth lines.

Specimens are not classified to lower taxonomic level because internal characteristic features could not be observed from the material. This group was recognized by Young et al. (2007) within the Williams Member at the William Lake study area, where they are abundant in certain horizons.

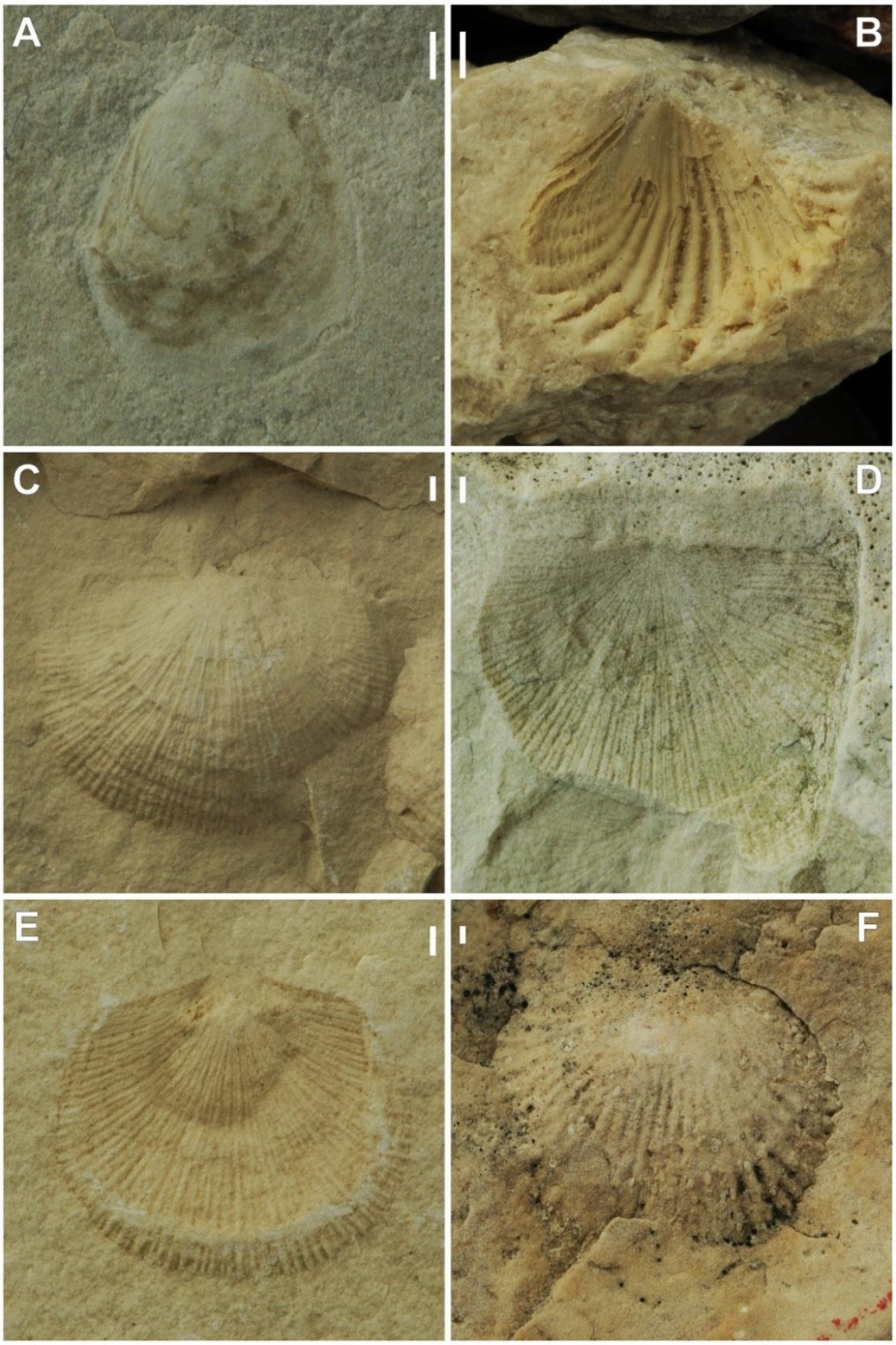

Figure 7.7: Brachiopods found within the William Lake study area (scale bar = 1 mm). A) linguloid brachiopod, Stonewall Formation, LS-1-A1-*1*. B) rhynchonellid brachiopod, Stonewall Formation, LS-2-A2-*29*. C) *Oepikina limbrata*, ventral valve, Gunton Member, Stony Mountain Formation, BC-11-E-*6*. D) *Oepikina limbrata*, dorsal valve, Gunton Member, Stony Mountain Formation, BC-11-E-*9*. E) *Diceromyonia storeya*, Gunton Member, Stony Mountain Formation, BC-11-G-*1*. F) *Dinorthis occidentalis*, Gunn/Penitentiary Equivalent, Stony Mountain Formation, BC-4-A-*36*.

Articulate Brachiopods

Specimens of articulate brachiopods are rare within the study area. Those that were poorly preserved were difficult to classify to a lower taxonomic level. The differentiation of the identified groups of articulate brachiopods is reliant on examining the size of shell and morphologic characteristics. Those that were not readily identifiable into any of the groups described below were generally classified as articulate brachiopods.

Rhynchonellid brachiopod

(Figure 7.7B)

Specimens of this group are characterized by a small subtriangulate outline (Figure 7.7B). The average length is about 6 mm and width about 6 mm. The hingeline is short, extending less than half of the maximum width of the shell. The shell is ornamented with well-developed plications. Concentric growth lamellae are well developed toward the anterior margin, and are spaced about 0.1-0.2 mm.

Jin and Zhan (2001) identified several species of rhynchonellid brachiopods within the Gunn and Penitentiary members of the Stony Mountain Formation of southern Manitoba. The poor preservation of studied material inhibits classification to a lower taxonomic level, so specimens are only identified as rhynchonellid brachiopods.

Oepikina limbrata Wang

(Figure 7.7C, D)

Specimens identified as *Oepikina limbrata* are common only within the BC-11-E locality of the exposure surfaces, and are characterized by a medium-sized semicircular shell. The average length measures about 10 mm and width measures about 15 mm. The ventral valve is strongly convex (Figure 7.7C), and the dorsal valve is flat to slightly concave (Figure 7.7D). The hingeline is long and straight, extending to the maximum shell width. The shell is ornamented with pericostellate costae. Concentric growth lines are developed toward the anterior margin.

This species was recognized by Jin and Zhan (2001) in the Gunn and Penitentiary members of the Stony Mountain Formation of southern Manitoba.

Diceromyonia storeya (Okulitch)

(Figure 7.7E)

Specimens identified as *Diceromyonia storeya* are characterized by small-sized subelliptical shells with prominent costae (Jin and Zhan, 2001). The average length measures about 10 mm and width measures about 12 mm (Figure 7.7E). The hingeline is short, extending less than half of maximum shell width. The shell is ornamented by coarse, simple costae of uniform strength from apex to margin.

This species was recognized by Jin and Zhan (2001) in the Gunn and Penitentiary members of the Stony Mountain Formation of southern Manitoba.

Dinorthis occidentalis (Okulitch)

(Figure 7.7F)

Specimens identified as *Dinorthis occidentalis* are characterized by medium-sized subcircular to subrectangular shells with prominent costae (Jin and Zhan, 2001). The average length measures about 15 mm and width measures about 20 mm (Figure 7.7F). The hingeline is straight, extending almost across the maximum width of the shell. The shell is ornamented by coarse, simple costae of uniform strength from apex to margin. Concentric growth lines are well developed toward the anterior margin.

This species was recognized by Jin and Zhan (2001) in the Gunn and Penitentiary members of the Stony Mountain Formation in southern Manitoba.

7.1.6 PHYLUM BRYOZOA

(Figure 7.8A)

Bryozoans are a group of exclusively colonial organisms that originated within the Cambrian (Landing et al., 2010). They are characterized by an encrusting colony comprised of very small circular tubes called zooecia (Boardman et al., 1983).

Specimens of bryozoans are common within the study area, preserved as dolomitic replacements (Figure 7.8A). They occur as fragments of colonies and are characterized by a network of zooecial openings measuring 0.1 mm in diameter. Within the conodont analysis report on samples from the road cut section, Nowlan (2009) identified fragments of dolomitized(?) bryozoan colonies.

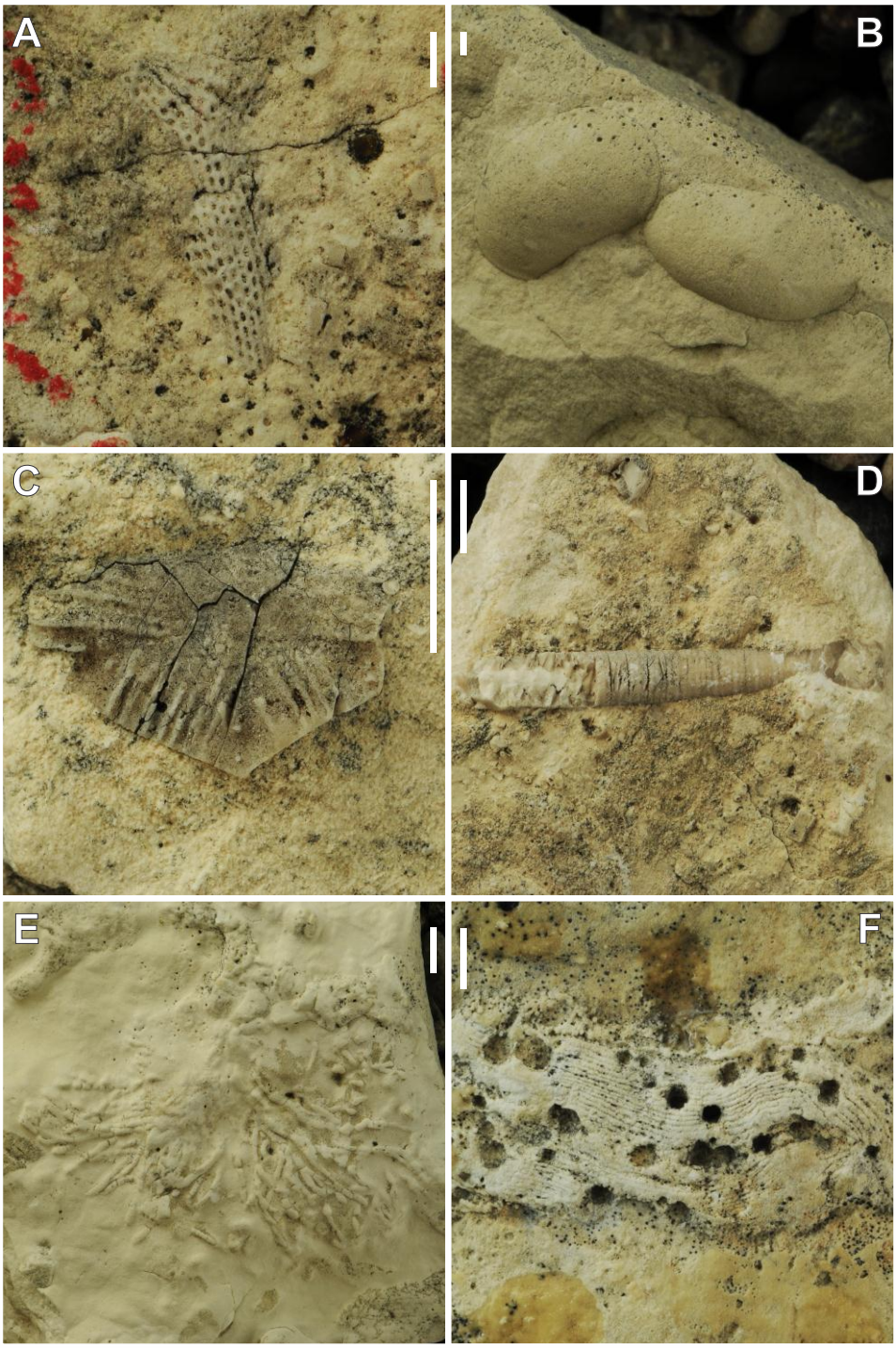

Figure 7.8: Fossils found within the William Lake study area (A, B scale bar = 1 mm; C-F scale bar = 5 mm). A) bryozoan, Stonewall Formation, BC-11-EE-*19*. B) *Leperditia* sp., Gunton Member, Stony Mountain Formation, BC-11-E-*8*. C) rhombiferan cystoid plate, Stonewall Formation, BC-11-EE-*19*. D) portion of echinoderm stem, Stonewall Formation, BC-11-EE-*11*. E) *Chondrites* sp., Gunton Member, Stony Mountain Formation, BC-11-I-*1*. F) *Trypanites* sp. borings within *Clathrodictyon* stromatoporoid, Gunn/Penitentiary Equivalent, Stony Mountain Formation, BC-5-*1*.

Several species of bryozoans were described by Ulrich (1889) from the Stony Mountain Formation. Also, many were described by Lobdell (1992) within the Gunn Member of the Stony Mountain Formation from southern Manitoba. Poor preservation of material in the present study hindered identification to lower taxonomic level, so specimens were only classified as bryozoans.

7.1.7 PHYLUM ARTHROPODA

Arthropods are a diverse group of organisms that were abundant in the Paleozoic (Harrington et al., 1959). They are characterized by an exoskeleton, a segmented body, and jointed appendages. A variety of different arthropod groups are identified within the study area. Specimens of ostracodes and a few fragments of unidentifiable trilobites were found, and exceptionally preserved fossils of eurypterids and xiphosurids have been described from the Williams Member of the Stony Mountain Formation (Young et al., 2007; Rudkin et al., 2008), but only the ostracodes will be described herein. Westrop and Ludvigsen (1983) identified a trilobite assemblage from the Selkirk Member of the Red River Formation, but present study material requires more complete specimens for identification.

Leperditia sp.

(Figure 7.8B)

Ostracodes are a group of very small crustaceans that are characterized by a flattened body that is enclosed within a calcium carbonate, dorsally hinged, bivalved shell (Benson et al., 1961). Ostracodes of the study area are preserved as molds (Figure 7.8B).

Specimens identified as *Leperditia* sp. are characterized by an elongate unornamented shell that measures about 6 mm in width and 9 mm in length with a short hinge line.

Ostracodes were listed by Young et al. (2007) from within the Williams Member of the Stony Mountain Formation at the William Lake study area. Several ostracode species were described and illustrated by Ulrich (1889) from the Stony Mountain Formation, including *Leperditia subcylindrica*. Although several species of *Leperditia* were described and illustrated by Stearn (1956) from the Interlake Group, including the Fisher Branch Formation, none were identified within the Stonewall or Stony Mountain formations. From comparison of descriptions and illustrations of the various species of this genus, specimens of the present study are classified as *Leperditia* sp.

7.1.8 PHYLUM ECHINODERMATA

(Figure 7.8C, D)

Echinoderms are a group of organisms that are characterized by a five-fold radial symmetry, a calcite skeleton composed of plates or ossicles, and a water vascular system (Beaver et al., 1967). Abundant echinoderm fragments, most likely representing crinoids, are scattered within the matrix of most of the fossiliferous strata in the study area. Disarticulated columnals are most common, but a few portions of stems (Figure 7.8D), and one poorly preserved calyx were recovered intact. Though composed of diagenetic dolomite, they retain perfect cleavage of the original calcite.

Within the conodont analysis report on samples from the road cut section, Nowlan (2009) identified dolomitized(?) crinoid ossicles. Taxonomic identification is not possible on the skeletal fragments of the present study. However, one specimen of a rhombiferan

cystoid was identified from surface exposure locality LS-11-EE (Figure 7.8C), based on characteristic arrangement of thecal pores into rhombs shared by adjacent plates (Beaver et al., 1967).

7.2 TRACE FOSSILS

Trace fossils are a collective group of structures that each represent the activity of the organism that produced them (Bromley, 1972). They are diverse, produced from an assortment of activities, and are discriminated into ichnotaxa based on the morphology of the resultant trace. The trace that is produced is reliant on the action of the organism (walking, burrowing, boring, etc.) and the substrate in which it is produced (Ekdale et al., 1984). These features are closely associated with lithology and resultant sedimentary structures.

Burrows

A burrow is an excavation void within a soft substrate, therefore burrowing trace fossils reflects active movement to produce a cavity within the soft sediment (Ekdale et al., 1984). They may be simple excavations or may be coated with a lining. Burrow trace fossils are diverse and classification is generally dependent on the pattern produced.

Thalassinoides sp.

(Figure 4.2B)

Bioturbation mottling is pervasive through sections of the study area, although it is often indistinct. Structures identified as *Thalassinoides* are characterized by a complex,

open network of Y-forked branching, unlined and unornamented, cylindrical burrow mottles (Hass et al., 1962; Myrow, 1995). They are preserved as filled voids and burrows measuring about 10 mm in diameter. Identification of *Thalassinoides* mottling was reliant on differential weathering to enhance texture or variation in colour for distinction.

Thalassinoides mottles are characteristic of the "Tyndall Stone" quarried from the Selkirk Member of the Red River Formation at Garson, Manitoba (Kendall, 1977). In the Grand Rapids Uplands, the Gunton Member of the Stony Mountain Formation is locally heavily mottled with *Thalassinoides* burrows (Young et al., 2008). Mottling that was indistinct and not readily identifiable as *Thalassinoides* was generally identified as bioturbation mottling.

Chondrites sp.

(Figure 7.8E)

Structures identified as *Chondrites* are rare within the study area and are characterized by a radiating network of small burrows, that superficially resemble the roots of a plant (Figure 7.8E). They are preserved as filled voids and burrows measuring about 1 mm in diameter.

Several species of *Chondrites* were described and illustrated by Whiteaves (1897) from the Williston Basin outcrop belt of southern Manitoba. Young et al. (2008) listed cf. *Chondrites* sp. from the Gunn and Penitentiary members of the Stony Mountain Formation. Poor preservation of present study material hindered identification to ichnospecies level, so specimens were classified as *Chondrites* sp.

Borings

A boring is an excavation void produced within a hard substrate, therefore boring trace fossils reflect erosion and penetration of consolidated material (Ekdale et al., 1984). Classification of borings is reliant on the morphology of the trace.

Trypanites sp.

(Figure 7.8F)

Structures identified as *Trypanites* sp. are rare within the study area and are characterized by a simple, cylindrical unbranched boring, that has one opening to the surface (Bromley, 1972). The opening is circular, measuring 0.5-2.5 mm in diameter (Figure 7.8F). The borings are unlined and preserved as voids within dense macrofossils.

Trypanites weisei was described and illustrated by Elias (1980) from the Selkirk Member of the Red River Formation and recognized by Elias (1982) from the Stony Mountain Formation. Poor preservation and a limited amount of study material hindered classification to lower level, so specimens were only identified as *Trypanites* sp.

7.3 BIOSEDIMENTARY STRUCTURES

Thrombolites

(Figure 4.5A, B)

Structures identified as thrombolites occur in isolated intervals of the study area within strata described as lithofacies 5, and are generally characterized by a clotted accretion of sediment. ‘Thrombolite’ is a term originally used by Aitken (1967) to describe “cryptalgal structures related to stromatolites but lacking lamination and

characterized by macroscopic clotted fabric", but 'cryptalgal' has since been modified to 'cryptomicrobial' since sediment-forming microbial communities are dominated by cyanobacteria (Kennard and James, 1986). As such, thrombolites have been described as having similar external form to stromatolites but with distinctive internal structure characterized by darker-coloured microbial clots separated by sediment (Kennard and James, 1986).

The thrombolite mounds identified in the present study have a highly irregular external structure (Figure 4.5B). Thickness ranges from a background of about 30 cm to 54 cm at the peaks of mounds. The surfaces are variegated with discontinuous patches of microbial build-ups interspersed with laminated argillaceous to sublithographic mudstone. The internal structure of these build-ups is similarly highly irregular, consisting of millimetre- to centimetre-sized clots of microbial-like texture, interspaced with sublithographic carbonate (Figure 4.5A). The clots are darker than surrounding mudstone. Thrombolitic structures have not been previously described from the Ordovician of Manitoba.

7.4 MICROFOSSILS

Conodonts are microscopic phosphatic remains of an extinct group of organisms that are common in marine environments from the Cambrian to the Triassic. These problematic organisms are generally assigned to the phylum Chordata based on the presence of a generalized chordate anatomy; bilateral symmetry, a notochord, gill slits, and a tubular nervous system (Sweet, 1988). The understanding of anatomy of the conodont organism is based on the form, composition, and histology of a wide variety of

skeletal elements and a small number of specimens that have preserved features of the soft tissue (Sweet and Donoghue, 2001). The skeletal elements are tooth-like microfossils usually 0.2 to 2 mm in dimension and are composed of calcium phosphate (Briggs, 1992). It is interpreted that conodonts were small, elongate, eel-shaped marine animals that inhabited a variety of environments as mainly nektobenthic predators (Sweet and Donoghue, 2001).

Taxonomic identification of the conodonts for this study was performed by Dr. Godfrey Nowlan at the Geological Survey of Canada Calgary Conodont Laboratory (Nowlan, 2008; Nowlan, 2009). The conodont elements identified represent 22 species of seven genera (Table 7.1). The elements are identified by locality in Appendix E and the identified elements are listed below in Table 7.1.

Table 7.1: List of identified conodont elements.

Identified conodont elements	
Aphelognathus? sp.	*Plegagnathus* sp.
Aphelognathus aff. *A. divergens*	*Plegagnathus nelsoni*
Drepanoistodus sp.	*Pseudobelodina* sp.
Drepanoistodus suberectus	*Pseudobelodina adentata*
Oulodus sp.	*Pseudobelodina inclinata*
Oulodus ulrichi	*Pseudobelodina*? *dispansa*
Panderodus sp.	*Pseudobelodina vulgaris*
Panderodus cf. *P. liratus*	*Pseudobelodina vulgaris ultima*
Panderodus feulneri	*Rhipidognathus*? sp.
Panderodus gibber	*Rhipidognathus symmetricus*
Panderodus gracilis	trichonodelliform element indeterminate
Panderodus panderi	

CHAPTER 8 - FOSSIL ECOLOGY

Fossils provide information on paleoenvironments and can be used to evaluate evolutionary history through the geologic record. The fossils identified within the William Lake study area consist of a diverse assemblage of organisms representing a variety of life modes. The assemblage is dominated by epifaunal suspension feeding organisms consistent with shallow marine environments. The following is an introduction to the general aspects and paleoecologic characteristics of the identified fossils within the study area.

8.1 MACROFOSSILS

8.1.1 ALGAE

Cyclocrinitids are presently accepted as a problematic order of algae, likely a sister group to Dasycladales (Nitecki et al., 2004). Therefore, the dasycladacean algae have been considered as morphologic analogues for cyclocrinitids. They are both characterized by a central axis with extending lateral branches to form a globulous body (Beadle, 1988). Fom this morphologic similarity, it stands to reason that they were ecologically similar as well. Recent dasyclads are not particularly strong or wave resistant, occupying quiet water environments below wave base or restricted pools or lagoons (Beadle, 1988). Silurian cyclocrinitids are most common in quiet water deposits and showed a necessity for light by reduction of growth in increased depths (Beadle and Johnson, 1986).

8.1.2 PHYLUM PORIFERA

The phylum Porifera, more commonly known as sponges, played an important role in building or colonizing reefs in the Phanerozoic (Rigby et al., 2003). These mostly marine, epibenthic, sessile organisms accomplish filter feeding by drawing water from outside the cylindrical body through pores in the skeleton, most often toward the central cavity (Rigby et al., 2003). Fossils of sponges were identified within the study area, represented as non-calcareous spicules documented within the conodont analysis report (Nowlan, 2009), and body fossils of stromatoporoids and a chaetetid.

Ordovician stromatoporoids are interpreted to have occupied clear, warm, shallow, well-circulated waters along reef to bank habitats in a variety of carbonate settings (Webby, 2004). Although it has been assumed that stromatoporoids initiated growth upon a hard substrate, several cases reveal no such surface suggesting growth could have occurred directly on soft substrata (Kershaw, 1998). The growth form has been interpreted to have resulted from a combination of genetic and environmental factors, contributing to the vast variety of skeletal shapes (Kershaw, 1998). The proposed environmental controls on growth include substratum type and stability, sedimentation, nutrient supply, photosensitivity, and competition. Many morphological terms have been introduced to describe the skeletal shapes, resulting in complicated imprecision throughout the literature. A standard classification using the form outline, ornamentation, and internal arrangement of growth has been presented to assist in application in paleoenvironmental analysis (Kershaw, 1998). In general, the form of stromatoporoids has been compared with other organisms that grow by accretion, such as colonial corals, bryozoans, and chaetetids, due to broadly similar lifestyles affected by environmental

changes near the substratum (Kershaw, 1998). Fossils of stromatoporoids were identified within the study area, representing the genera *Aulacera* and *Clathrodictyon*.

Chaetetids are a group of epibenthic sessile organisms identified in the study area. They have been interpreted to have had similar incremental laminar growth form to other organisms from shallow marine habitats, such as stromatoporoids, corals, and bryozoans, but show limited diversity in form (Kershaw and West, 1991). They were likely equally influenced by genetic and environmental factors such as sedimentation, turbulence, and substrate control (Kershaw and West, 1991). A single specimen was identified within the study area.

8.1.3 Phylum Cnidaria

The diverse phylum Cnidaria includes corals, jellyfish and their relatives which have flourished in shallow seas since the Cambrian (Scrutton, 1999). Modern oceans are dominated by the subclass Scleractinia, and have been since the end-Permian extinction of the subclasses Tabulata and Rugosa, which were dominant from the Ordovician through the Permian (Scrutton, 1997).

Tabulate and rugosan corals are characterized by epibenthic sessile polyps with a skeleton fixed to the substrate (Hill, 1981). This skeleton is composed of calcium carbonate, and records the growth of the coral through its ontogeny and, in the case of colonial forms, its astogeny. Because these subclasses are extinct, it is difficult to determine the range of environmental conditions under which they could have lived. Inferences must be made under the assumption that tolerances are likely to have been similar to those of living corals. Generalizations of the conditions are supported by the

sedimentological data from the deposits in which they occur. Tabulate and rugose corals occur in a wide range of carbonate facies, most commonly in those interpreted to have been warm (tropical to warm-temperate), shallow (epicontinental and shelf) waters of normal salinity and oxidation with rich nutrient sources (Hill, 1981). Tabulate corals were exclusively colonial, whereas 64% of rugosan genera were solitary (Scrutton, 1998).

Solitary rugose corals are characterized by a single corallite forming a basic inverted cone shape. They have been interpreted to have been mainly unattached to the substrate, commonly resting on or partially buried in soft substrate, producing the characteristic horn-shaped coralla (Scrutton, 1999). The form and external variation are controlled by the interaction and adaptation with the substrate and strength of water currents (Scrutton, 1998; 1999). The horn shape of the corallum has been interpreted to have resulted from gravitational settling of the heavier mature portion of the corallum. The distinct directional orientation patterns of the solitary corals have been used to interpret current direction (Elias et al., 1987). Less curved to straight coralla are associated with subdued currents, and are interpreted to have sunk into the substrate allowing sediment to build up around them (Scrutton, 1998). During the Late Ordovician, non-circular cross-sections evolved to improve stability when lying on or partially in the substrate (Scrutton, 1998; 1999). Some corals also developed a keeled cardinal side facing into the sediment to counteract the tendency to roll sideways in vigorous currents (Scrutton, 1998). Fossils identified from the study area include the genera *Bighornia*, *Deiracorallium*, and *Salvadorea*. Elias (2010) related adaptations in corallum form for *Deiracorallium* and *Salvadorea* to stability strategies with respect to substrate and current flow. It is interpreted that *Deiracorallium* favored deeper water, more open marine

conditions, while *Salvadorea* and *Bighornia* preferred shallower water and tolerated more restricted conditions (Young and Elias, 1999B).

Colonial tabulate and rugose corals consist of a group of similar corallites forming a compound skeleton. They have been interpreted to have been attached to soft substrates, but some encrusted upon hard surfaces (Scrutton, 1999). The form can vary greatly, dependent on the manner of increase and the arrangement and shape of the skeleton. There are two basic strategies of growth; peripheral growth, where offsets occurred near the edge of the colony promoting lateral expansion of the colony and efficient capture of space, which is suited for low sedimentation environments, and marginal growth, where offsets occurred within the colony between pre-existing corallites promoting rapid upward expansion, which was suited for higher rates of sediment accumulation (Scrutton, 1999). Ultimately, growth form developed from internal structure and was modified by environment controls. In higher energy environments, those that encrusted upon hard substrates had the highest tolerance, and large, massive forms gained stability from their weight (Scrutton, 1998). In general, tabulate coral corallites are about one order of magnitude smaller than those of rugosans; this smaller size of tabulates made them more susceptible to sediment smothering (Scrutton, 1998). But tabulate corals also had a higher degree of integration within colonies, resulting in more flexibility of growth allowing for easier recovery (Scrutton, 1998). Fossils identified in the study area include the tabulate genera *Paleofavosites*, *Angopora*, *Calapoecia*, *Catenipora*, *Pragnellia*, *Ellisites*, and *Aulopora*, and the rugose genera *Palaeophyllum*, *Pycnostylus*, and *Tryplasma*.

A study of *Paleofavosites subelongus* from the latest Ordovician to earliest Silurian of the Edgewood Province of the east-central United States demonstrated that the internal and external morphologic characters were both affected by genetic and environmental factors through growth (Young and Elias, 1999A). The cateniform growth of *Catenipora* and fasciculate form have been interpreted as advantageous in episodes of high sedimentation, due to rapid widespread colonization followed by upward growth with ample medial space for dispersal of sediment (Lee and Elias, 1991; Scrutton, 1999). Leith (1952) compared the similar segmentation of branches in the present-day coral *Isis hippuris* with those of *Pragnellia*, interpreting that the branches could bend freely without breaking, and therefore could tolerate higher energies. The coral *Ellisites* has been interpreted as an encruster that grew in laminar sheets, suggesting a greater tolerance of water flow (Elias and Young, 2000). Most species of the genus *Aulopora* are also interpreted to have been encrusters, attaching to the skeletons of other corals or invertebrates, either living or dead (Scrutton, 1999).

Medusoid cnidarians are commonly called jellyfish and are characterized by a free-swimming umbrella-shaped body. Medusae are extremely rare in the fossil record as they do not possess hard parts, and therefore require specific sedimentologic and taphonomic criteria for recognition (Young and Hagadorn, 2010). The soft body and similar density to water makes them difficult to bury, promoting scavenging and deformation, thus preservation is best within low-energy tidal flats or lagoons (Young and Hagadorn, 2010). Many fossil medusae occur with sedimentary structures or other fossils characteristic of hypersaline, brackish, or emergent conditions (Young and Hagadorn, 2010). The specimens of hydromedusae and possibly scyphomedusae

identified by Young et al. (2007) provide considerable insight into the preservation within the Williams Member.

8.1.4 PHYLUM MOLLUSCA

Modern molluscs are extremely diverse in morphology, behavior, and habitat, with representatives from eight classes adapted to marine to freshwater and terrestrial environments (Knight et al., 1960). They are collectively characterized by an unsegmented body with a muscular extension modified for locomotion or feeding, and highly developed digestive, circulatory, reproductive, nervous, and sensory systems (Knight et al., 1960). Mollusc fossils were identified within the study area, representing the gastropod and cephalopod classes.

Gastropods are the most diverse class of molluscs (Teichert et al., 1964). Although found in marine, freshwater, and terrestrial environments and on nearly all types of substrates, most are benthic marine, of which the majority live in shallow water as grazing herbivores (Knight et al., 1960). Fossils identified herein include the large *Maclurina* sp. and small *Hormotoma* sp., *Liospira* sp., and *Trochonema* sp. It is suggested that the thick and heavy shell of *Maclurina* was adapted to higher energy but would have decreased mobility, restricting it to a sessile lifestyle upon semi-firm substrates with sufficient suspension-feeding conditions of higher energy environments (Linsley, 1977). The smaller species would not have been restricted to this sessile life mode, allowing free movement along the sea floor.

Cephalopods are the most advanced of the molluscs (Knight et al., 1960). These nektonic organisms are exceptionally agile with high metabolic efficiency, making them

successful carnivorous predators (Teichert et al., 1964). The shell of the cephalopod remains buoyant for locomotion by filling various chambers with gas or fluids (Knight et al., 1960). Fossils identified include *Kinaschukoceras* sp. and orthoconic forms. Previous Manitoba occurrences of the coiled *Kinaschukoceras* sp. have been identified within practically unfossiliferous strata from the Hudson Bay Lowlands (Nelson, 1963), and it is also in almost unfossiliferous rocks in the present study area.

8.1.5 PHYLUM BRACHIOPODA

Brachiopods are solitary, sessile, benthic marine suspension feeders (Williams et al., 1997). They require good circulation of water to provide food and oxygen as well as carry away waste (Williams et al., 1997). Although most modern brachiopods live attached to hard substrates, fossil forms adapted their shell and attachment mechanism to suit a range of benthic environments (Williams et al., 1997). Brachiopod fossils were identified within the study area, representing both major groups: inarticulate and articulate brachiopods.

Modern linguloids inhabit shallow water (intertidal to approximately 50 m), in sandy or usually muddy bottoms, and are resistant to osmotic stress (Paine, 1970). Recent linguloids differ little from their ancestors, earning the name “living fossils” (Williams et al., 1997). Therefore, it has been suggested, based on their similar morphologies, that fossil linguloids would have lived in similar conditions.

The identified articulate brachiopods *Dinorthis occidentalis*, *Diceromyonia storeya*, *Oepikina limbrata*, and rhynchonellid brachiopods are characteristic of the *Diceromyonia storeya* Community of the lower Stony Mountain Formation (Jin and

Zhan, 2001). This community has been interpreted as a continuous evolution of the *Kjaerina hartae* Community of the Red River Formation, and occurs mainly within the Gunn and Penitentiary members, but some elements extend into the Stonewall Formation (Jin and Zhan, 2001). The *Diceromyonia storeya* Community is diverse but dominated by a few species. It was suggested that this predominance and their relatively small size compared to the brachiopods of the Selkirk Member is related to increased environmental stress, possibly due to increased clastic sedimentation and associated turbidity on the seafloor (Jin and Zhan, 2001).

8.1.6 PHYLUM BRYOZOA

Bryozoans are a group of very small suspension-feeding organisms. After originating in the Cambrian, they became important contributors to shallow water communities, and were capable of forming sizable mounds (Landing et al., 2010; Taylor and Ernst, 2004). They are characterized by encrusting colonies that superficially resemble corals but the individuals are much smaller (usually less than 1 mm) and lack radial septa (Boardman et al., 1983). Research on Ordovician bryozoans is limited, hindered by the lack of utility in biostratigraphy and the precision required for identification (Taylor and Ernst, 2004). Modern bryozoans are widely distributed in marine environments, common in caves within tropical reefs and under rocks and overhangs (Cuffey, 1972). The growth form of bryozoans has been linked to rate of sedimentation and turbulence, substrate conditions, salinity, and wave energy or currents, and as such has been used for paleoenvironmental reconstruction (Schopf, 1969). Fossils

of bryozoans were identified within the study area, but were fragmentary and not identified beyond the phylum level.

8.1.7 Phylum Arthropoda

Arthropods are by far the most diverse phylum, cumulatively outnumbering members of all other invertebrate phyla combined (Harrington et al., 1959). Arthropoda includes all insects, centipedes, chelicerates, crustaceans, and trilobites. Arthropods can occupy aquatic, terrestrial, and aerial environments. They are characterized by jointed appendages, a segmented body, and a tough exoskeleton which is shed periodically through the process of ecdysis (Harrington et al., 1959). This process allows the organism to assume multiple body plans through ontogeny. The flexible appendages may be differentiated for specialized functions such as walking, swimming, or food handling, therefore enabling a multitude of lifestyles (Harrington et al., 1959). Arthropod fossils were identified within the study area, represented by ostracodes, trilobites, eurypterids, and xiphosurids.

Ostracodes are stratigraphically useful in the fossil record. Their characteristic bivalved shells are small and often ornamented, permitting identification from relatively small amounts of material (Benson et al., 1961). The shell structure, shape, and sculpture vary according to substrate type, salinity, temperature, and depth, allowing ostracodes to be useful paleoenvironmental indicators. Fossils of ostracodes representing only the genus *Leperditia* are identified within the study area.

Trilobites are important fossils in the study of Paleozoic rocks because of their use in correlation and paleoenvironmental studies. All were marine. Most are interpreted

as benthic detritus feeders, although some are interpreted as burrowers, active swimmers, or pelagic forms (Harrington et al., 1959). Variation in morphology allows for interpretation of life habits and rapid diversification through the early Paleozoic permits biostratigraphic correlation (Harrington et al., 1959). Detailed study of trilobites from the Selkirk Member of the Red River Formation in southern Manitoba interpreted them to be benthic, occupying both infaunal and epifaunal positions (Westrop and Ludvigsen, 1983). Present study material is fragmentary, and therefore cannot be identified beyond the major group.

Xiphosurids and eurypterids are chelicerates, characterized by adaptation of the first appendages to claws for grasping food (Harrington et al., 1959). Xiphosurids, commonly known as horseshoe crabs, are recognized from their unmistakable morphology and are regarded as "living fossils" from their limited deviation in body plan since origination in the Ordovician (Rudkin et al., 2008). They have a sparse preservation record, known from few marginal marine, brackish, or possibly freshwater environments (Rudkin et al., 2008). Eurypterids had adaptations to appendages used for swimming or digging (Plotnick, 1985). Fossils of xiphosurids and eurypterids were identified within the Williams Member of the Stony Mountain Formation of the study area (Young et al., 2007).

8.1.8 PHYLUM ECHINODERMATA

First introduced by J.T. Klein in 1734, the name echinoderm originates from two Greek words, *echinos* meaning hedgehog or urchin, and *derma* meaning skin (Beaver et al., 1967). As such, echinoderms are easily distinguished by their skeleton of calcite

plates. Originating in the Cambrian, they have become one of the most highly diversified phyla with representatives presently found in all seas, at all latitudes, on all types of substrates, and at all depths ranging from littoral to deep oceanic abysses (Beaver et al., 1967). While echinoderms are known from a variety of habitats, they are exclusively marine and are generally stenohaline (Beaver et al., 1967).

Echinoderm fossils were identified in the study area representing the subphylum Crinozoa, including a rhombiferan cystoid. These echinoderms produced a globose plated body that had varying numbers of food-gathering appendages, and were typically attached to the substrate by a jointed stalk (Beaver et al., 1967). The rhombiferian cystoids are similar to crinoids except that the skeletal plates are pierced by pores which are interpreted to have been involved with respiratory functions or locomotion and food gathering (Beaver et al., 1967). Crinoids and cystoids are passive suspension feeders and rely on flowing water for food particles (Baumiller, 2008). When exposed to currents, the food-gathering appendages are oriented to maximize surface area, radiating into a fan-like configuration (Baumiller, 2008). Because the skeletal plates are held together by soft tissue, after death these elements can be easily disarticulated. Thus, they were important contributors to bioclastic packstones and grainstones in the Paleozoic (Beaver et al., 1967).

8.2 TRACE FOSSILS

Trace fossils are important biogenic sedimentary structures because they record the activity of the organism that produced the trace. They are most often preserved *in situ*, and therefore can be used as indicators of the sedimentary environment (Ekdale et

al., 1984). They are not without complications, as there is no simple correlation between organism, activity, and trace. It should be advised that the same species may produce different traces with separate activities, the same species may produce different structures from identical behavior but within different substrates, or different species can produce identical traces with similar behaviour (Ekdale et al.,1984). To complicate things, traces may be differentially preserved in different sediments, or modified by environmental conditions (Ekdale et al., 1984). Classification is founded on the inferred behaviour represented by the trace (feeding, dwelling, locomotion, etc.). Trace fossils have been identified within the study area, representing burrowing, boring, and binding activities.

Burrows are diverse traces that reflect movement by infaunal organisms, commonly related to protection or feeding (Ekdale et al., 1984). They are generally characterized by a simple excavation within soft sediment, but may be modified with various types of linings (Ekdale et al., 1984). Fossils of burrows identified within the study area include *Thalassinoides* and *Chondrites*. *Thalassinoides*-like burrows, created by thalassinid shrimp, are common in modern intertidal and shallow subtidal environments (Myrow, 1995). *Thalassinoides* is currently interpreted to have been produced by the dwelling and feeding activities of Ordovician-equivalent thalassinid shrimp (Myrow, 1995). *Chondrites* has been interpreted to be dwelling or feeding burrows, possibly formed by marine worms (Hass et al., 1962).

Borings may be similar in general morphology to some burrows but are differentiated by the nature of the substrate. Borings require that the substrate be hard, whether it is lithified sediment or the skeletons of other organisms. Fossils of borings representing the ichnogenus *Trypanites* are identified within the study area. *Trypanites*

borings in solitary rugose corals from the Tyndall Stone of southern Manitoba were interpreted to have been produced by worms such as polychaete annelids (Elias, 1980). Due to the requirement of hard surfaces, these fossils are indicative of the nature of substrate and have been related to episodes of exposure on seafloor environments (Young et al., 2008).

8.3 BIOSEDIMENTARY STRUCTURES

The trapping and binding activity of microorganisms can result in distinct biosedimentary structures recognizable in the sedimentary record. The term ‘thrombolite’ was proposed by Aitken (1967) to describe stromatolite-related structures with a clotted fabric but lacking lamination. The domical masses are interpreted to have been produced from microbial calcification and agglutination by cyanobacteria within the subtidal environment (Riding, 2000). Fossils of thrombolites are identified within the study area.

8.4 MICROFOSSILS

Conodonts are important to paleontological studies as they are utilized in a variety of ways. They have been used to reveal the thermal histories of sedimentary basins because they undergo a proportional colour change upon heating; they have been used extensively as biostratigraphic indicators for the correlation of sedimentary sequences; and they have been used as paleoenvironmental indicators of conditions of sedimentary basins (Briggs, 1992). It is hypothesized that the majority of conodonts were nektobenthic, and were laterally segregated into well-defined communities controlled by environmental factors (Sweet and Donoghue, 2001). Only those bearing simple cones

with absent to weak symmetry are regarded as pelagic (Barnes and Fåhræus, 1975). Understanding the dynamics of these communities allows for recognition of depositional environments and the associated changes in temperature and salinity conditions with relative depth of basins.

CHAPTER 9 - FOSSIL DISTRIBUTION

Fossil specimens can give considerable insight into the environmental conditions present during the time in which the sediments were deposited. Although the relationships between the different organisms cannot usually be observed, interpretations can be inferred based on the fossil record. Organisms are extremely sensitive to environmental change, which is reflected in the distribution of the various faunal groups. The patterns of distribution, diversity, and abundance of the various faunal elements concurrent with associated lithologies provide the foundation of paleoenvironmental interpretation.

In the following sections some concepts will be discussed that require clarification of terminology. Diversity is an important aspect in evaluating paleoecology. It is generally measured by richness, evenness, or a combination thereof (Stirling and Wilsey, 2001). Richness refers to the number of different species, whereas evenness relates to the relative species abundance (Stirling and Wilsey, 2001). Low evenness is where there is high single-species dominance, and high evenness is an equal balance of all species (Stirling and Wilsey, 2001). There are many calculations of diversity, by providing differing weights to these indices (Hammer, 2002). Diversity can be recognized at different scales: alpha (α) or local diversity, beta (β) or differentiation diversity, and gamma (γ) or regional diversity (Koleff et al., 2003). In the present study, the number of fossil groups identified in each stratigraphic interval will be assessed with their relative abundance through the succession in an attempt to determine the diversity trends in the William Lake study area.

A total of 991 macrofossil specimens was identified in the study area, encompassing members of seven distinct phyla of the kingdom Animalia (Arthropoda, Brachiopoda, Bryozoa, Cnidaria, Echinodermata, Mollusca, and Porifera) and one representative from the kingdom Plantae (Chlorophyta). A few trace fossils and biosedimentary structures are also identifiable (Appendix D-1). In addition, a total of 2346 microfossils was identified, represented by conodont elements, from the animal phylum Chordata (Appendix D-2).

For the following discussion of distribution of fossils, the macrofossils, trace fossils, and biosedimentary structures were grouped together. There was sufficient abundance for microfossil data to be discussed independently.

9.1 MACROFOSSILS, TRACE FOSSILS, AND BIOSEDIMENTARY STRUCTURES

9.1.1 DISTRIBUTION

Macrofossils, trace fossils, and biosedimentary structures of this study were identified from field descriptions, hand sample analysis, and microfossil analysis. These fossil elements were observed through the majority of study area; only about 19% of the localities are barren of fossils. Figures showing the distribution and stratigraphic range of fossils are presented by locality; Figure 9.1 shows the exposure surface material and Figure 9.2 shows the road cut succession material. A complete guide to the fossil distribution is shown in Figure 9.3.

The identified macrofossils represent a wide range of recognizable taxonomic levels, from those merely identifiable to phyla ranging to identification of subspecies. This disparity hinders direct comparison but inferences can be made with regard to the

variation in identifiable groups. The suite of macrofossils is rich, with 50 identifiable types, but is variable through the study site. The suite is consistent with the assemblages previously described from the Stony Mountain and Stonewall formations.

9.1.2 Abundance

Although the quantity of identifiable fossils varies substantially between the individual localities, inferences can be made by the overall abundance of certain groups. Information on the abundances of fossils is presented in Appendix D.3. The study site overall is dominated by echinoderm fragments and corals; the tabulate, solitary rugose, and colonial rugose corals are rich and abundant, representing almost half of the identifiable types and almost 60% of the total of individual fossils. Brachiopods, molluscs, and stromatoporoids are also moderately common through the study area. The diversity through the study area is not consistent, and varies from highly diverse to near barren. This will be discussed further in a subsequent section (9.4.1 Relative Abundance).

Within the study area, there is also the inclusion of a diverse suite of exceptionally preserved fauna that is restricted within the Williams Member. This material is not represented in the data for this study but can be referred to in Young et al. (2007). Material from these localities required more detailed analysis outside the scope of this study. Therefore, a brief discussion of the significance of these fossils will be presented in a subsequent section (9.1.4 Relative Abundance) based on previous work by Young et al. (2007).

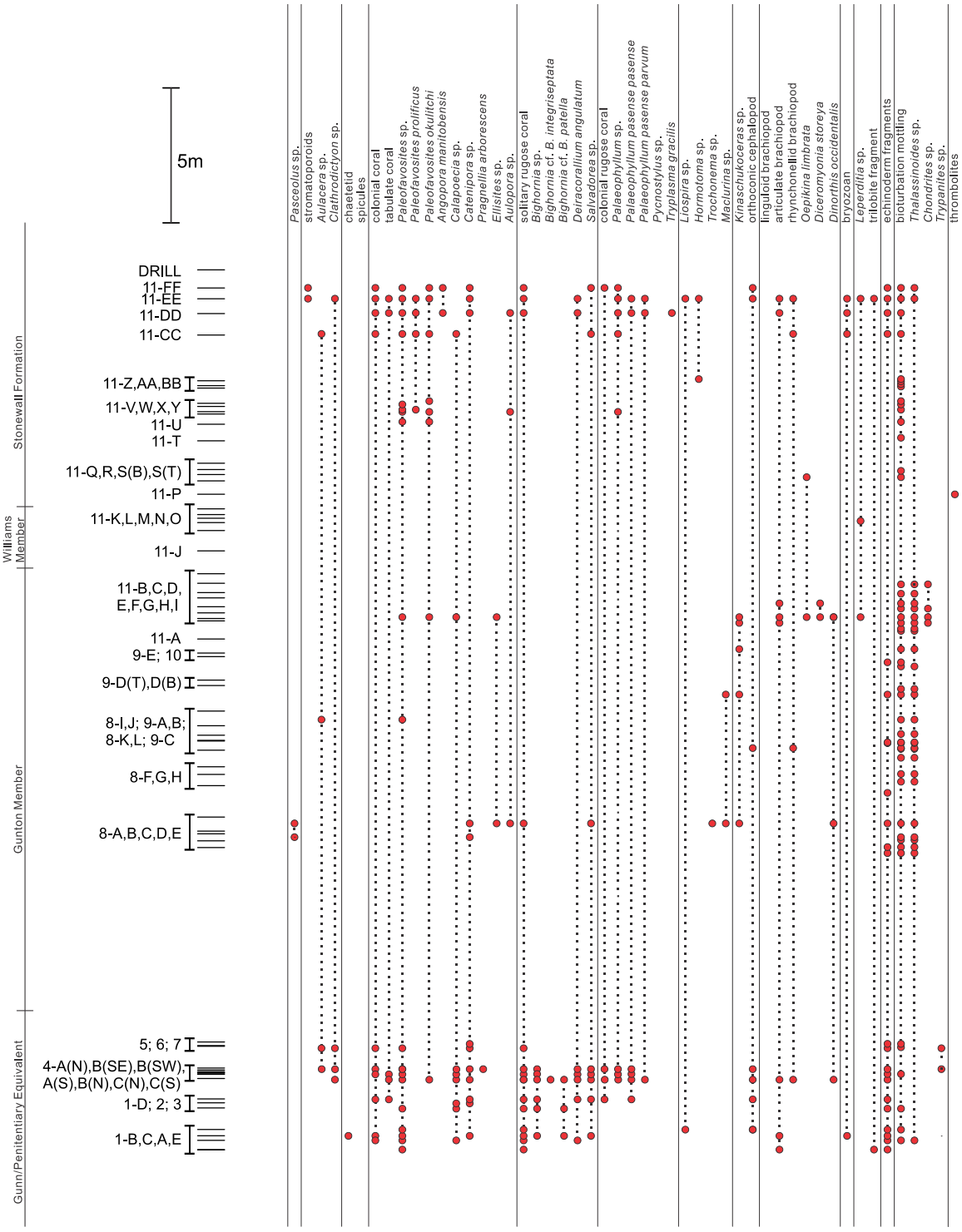

Figure 9.1: Distribution of macrofossils, trace fossils, and biosedimentary structures identified from surface exposure material. Red circles indicate the presence of identified fossil at locality. Dotted lines show the stratigraphic ranges of the identified fossil groups.

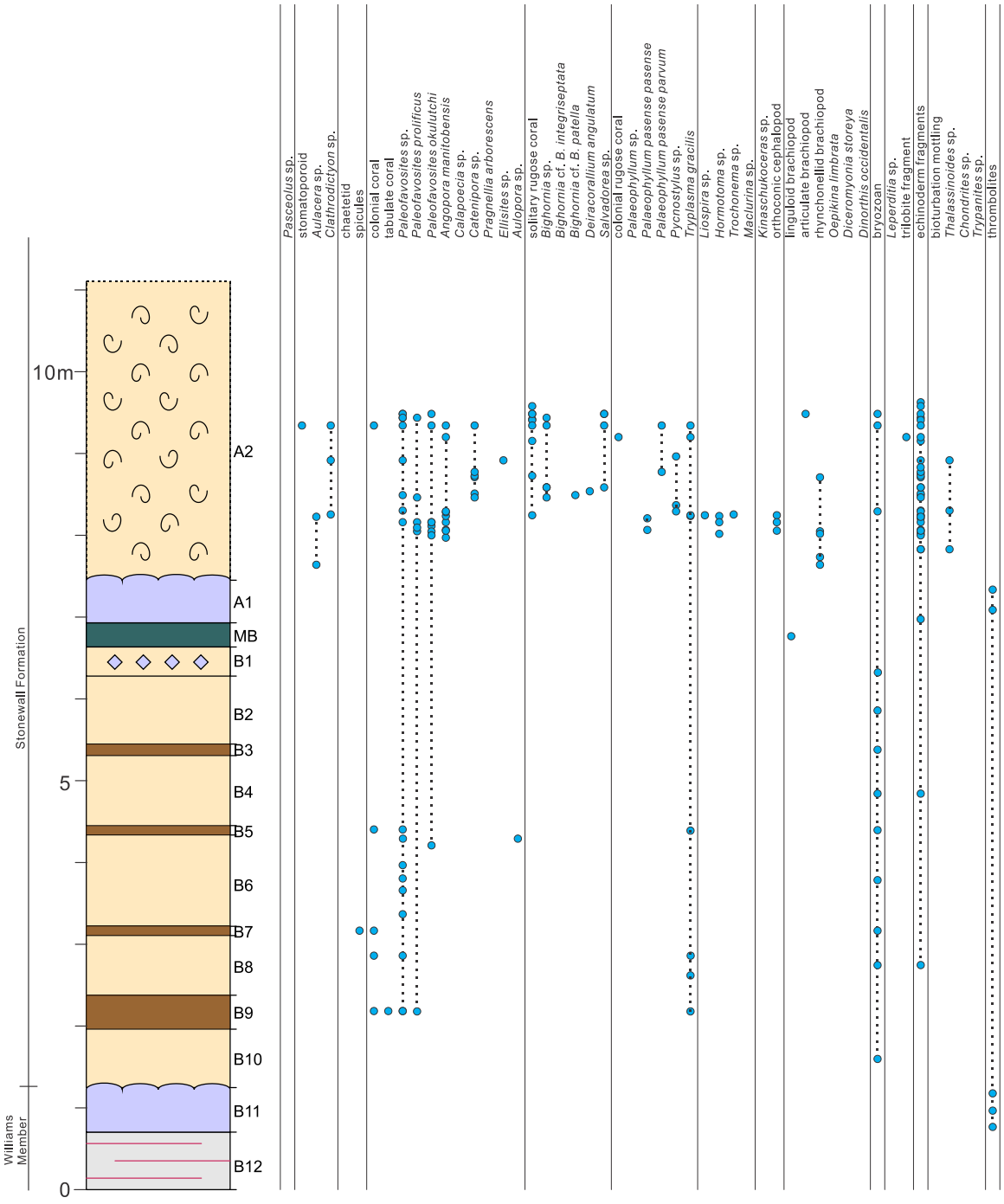

Figure 9.2: Distribution of macrofossils, trace fossils, and biosedimentary structures identified from road cut succession material. Blue circles indicate the presence of identified fossil at locality. Dotted lines show the stratigraphic ranges of the identified fossil groups. For legend see Figure 5.8.

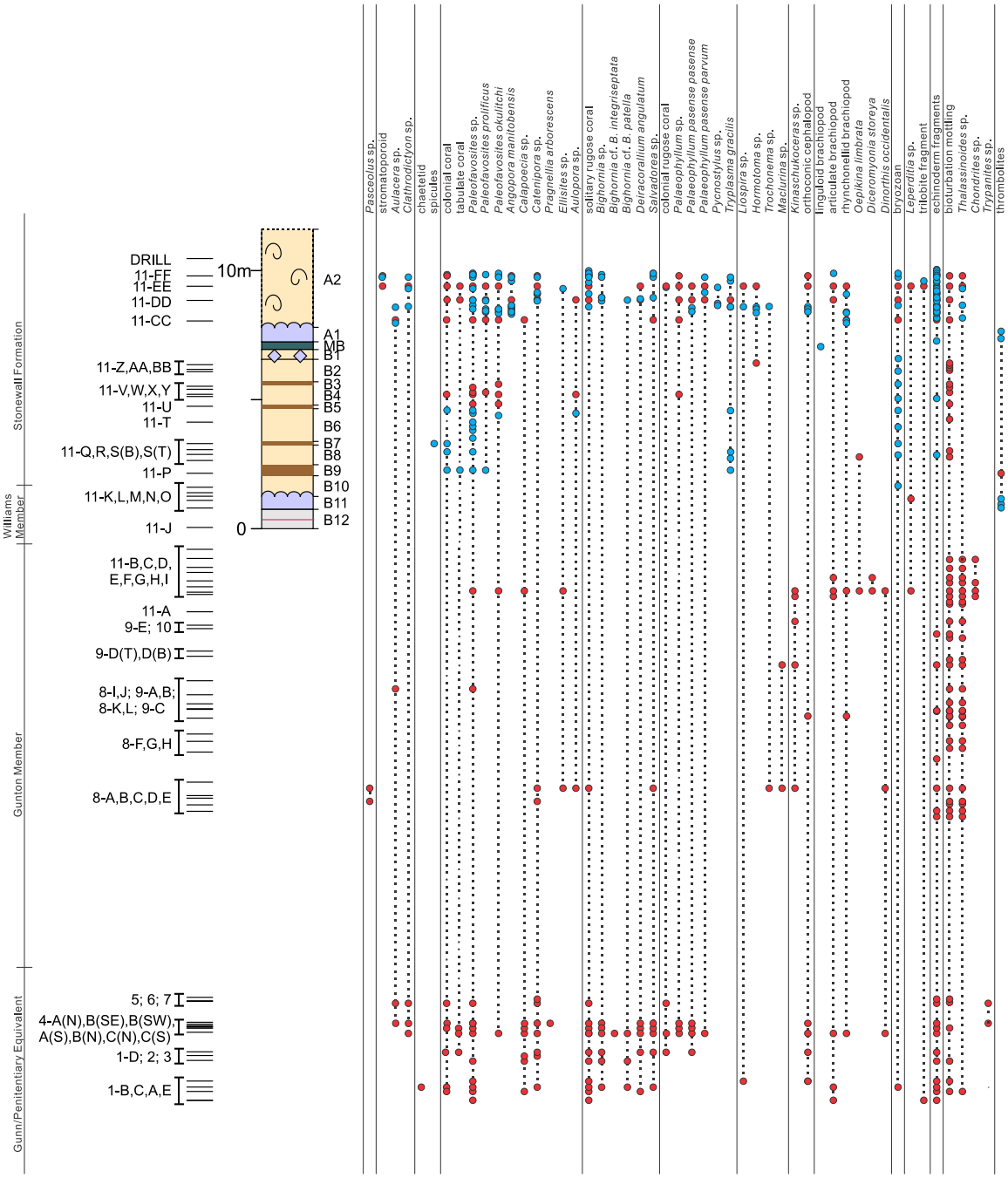

Figure 9.3: Combined distribution of macrofossils, trace fossils, and biosedimentary structures identified from surface exposure material (red) and road cut succession material (blue). Dotted lines show the stratigraphic ranges for the identified fossil groups. For legend see Figure 5.8.

The most abundant and most common macrofossils within the study area are echinoderm fragments, occurring at ~48% of localities and representing ~19% of the total number of fossils. These specimens are most often preserved as disarticulated bioclastic material incorporated within the host lithology, but a few portions of the stem are preserved. Due to identification at the high taxonomic level, they are of limited use beyond measure of the proportion of bioclastic material. The stem segments that are preserved provide information on environmental conditions.

The second most abundant macrofossil group is unidentifiable solitary rugose corals, identified at ~19% of localities and representing ~16% of the total fossils. When included with the remainder of solitary rugose corals that were identifiable to lower taxonomic levels, they collectively represent ~24% of the total fossils. These specimens are preserved in various positions (upright, upside down, and sideways) which can provide considerable insight into the environmental conditions present at the time of burial. A discussion of this aspect is presented in Chapter 10.

The third most abundant macrofossil is *Paleofavosites* sp., identified at ~30% of localities and representing ~12% of the total fossils. When included with the members of this genus identifiable to a lower level, they collectively represent ~16% of the total fossils. This genus is the most common tabulate coral, representing ~64% of all tabulate corals.

The remaining fossil groups are not individually notable for abundance. Additional approaches were employed to investigate the distribution of fossils.

9.1.3 SERIATION

Recognizable variations in the diversity of fauna were observed through the study area. A horizon may be crudely regarded as a snapshot in time in which a particular grouping of fossils represents the preservable portion of a community of organisms living at that location and time. This is a loose assessment, as the snapshot is affected by sediment deposition processes such as mixing, time averaging of the preserved fossils, and transport in and out of the vicinity. Localities and their taxa are often depicted by a presence-absence matrix, where rows correspond to localities and columns correspond to taxa: thus, a one (1) in entry (a,b) indicates that taxon "b" occurs at locality "a". Seriation is an algorithm operated on a presence-absence matrix that reorganizes the matrix so that presences are concentrated along a diagonal (Brower and Kile, 1988). When run in the unconstrained mode, both rows and columns are rearranged to provide a simple ordination. This algorithm was employed in order to relate the various localities according to type of fossils without obstruction by abundance.

A presence-absence matrix was compiled from the summary abundance distribution table (Appendix D.3). An unconstrained seriation algorithm from PAST (PAlaeontological STatistics) was run on this matrix in an attempt to recognize patterns or trends in fossil associations. The results of the seriation are presented in Figure 9.4. The criterion value is a test of the amount of concentration of the presences along the diagonal of the matrix; a perfect seriation yields a test value of 1.0 (Brower and Kile, 1988). The criterion value of the results is -2.09, reflecting the large proportion of unfossiliferous localities. The resulting matrix shows a pattern of diversity changes across the various localities. The presences are arranged along the diagonal, with three distinct

groupings that are readily identifiable: a highly diverse, coral dominated assemblage (green); a lower diversity, brachiopod-gastropod-trace fossil dominated assemblage (yellow); and unfossiliferous strata (white).

Given that these clusters were produced by rearranging the rows and columns, the localities were returned to the stratigraphic order retaining the cluster information in an attempt to identify any patterns resultant of the seriation. A diagram showing the stratigraphic sections of the localities with the cluster information is shown in Figure 9.5. A distinct organization of the clustered localities emerges, revealing similarities between stratigraphic intervals.

Through examination of the organization of the clusters, some general trends of groupings could be identified. The Gunn/Penitentiary Equivalent includes mostly the highly diverse assemblage. The Gunton Member includes mostly the lower diversity assemblage with isolated exposures of higher diversity. The Williams Member includes some occurrence of the low diversity assemblage but is mostly unfossiliferous with respect to the fossils identified in this study. The interval below the LS-marker in the lower Stonewall Formation includes a basal lower diversity assemblage, a middle higher diversity portion, and an upper lower diversity portion. The interval above the LS-marker bed in the lower Stonewall Formation includes mostly the higher diversity assemblage.

Figure 9.4 (next page): Seriation matrix showing the groupings of fossils and localities. Green indicates highly diverse cluster, yellow indicates lower diversity cluster, and white indicates barren cluster.

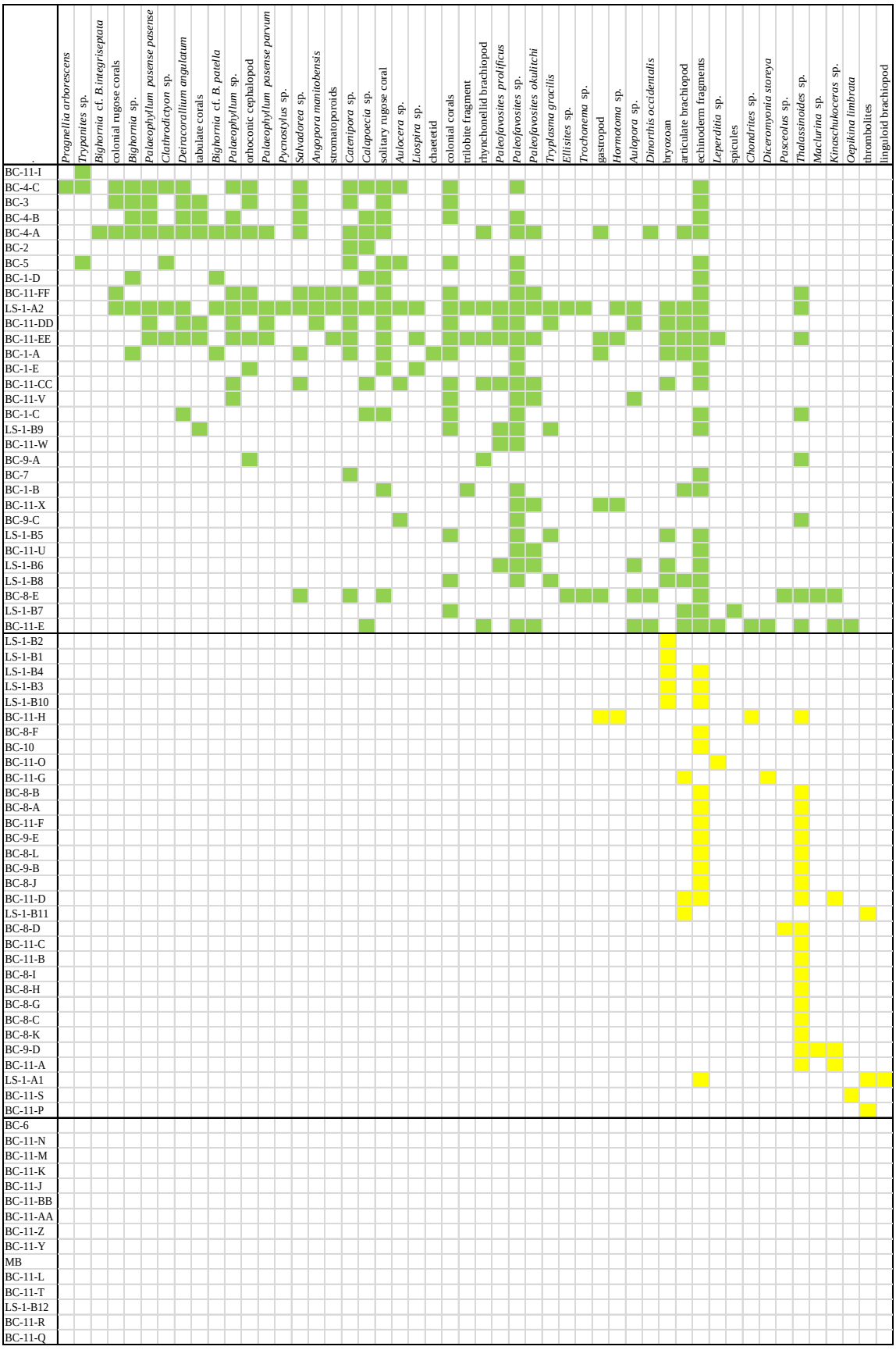
Pragnelia arborescens
Trypanites sp.
Bighornia cf. B.integriseptata
colonial rugose corals
Bighornia sp.
Palaeophyllum pasense pasense
Clathrodictyon sp.
Deiracorallium angulatum
tabulate corals
Bighornia cf. B. patella
Palaeophyllum sp.
orthoconic cephalopod
Palaeophyllum pasense parvum
Pycnostylus sp.
Salvadorea sp.
Angopora manitobensis
stromatoporoids
Catenipora sp.
Calapoecia sp.
solitary rugose coral
Aulocera sp.
Liospira sp.
chaetetid
colonial corals
trilobite fragment
rhynchonellid brachiopod
Paleofavosites prolificus
Paleofavosites sp.
Paleofavosites okulitchi
Tryplasma gracilis
Ellisites sp.
Trochonema sp.
gastropod
Hormotoma sp.
Aulopora sp.
Dinorthis occidentalis
bryozoan
articulate brachiopod
echinoderm fragments
Leperditia sp.
spicules
Chondrites sp.
Diceromyonia storeya
Pasceolus sp.
Thalassinoides sp.
Maclurina sp.
Kinaschukoceras sp.
Oepikina limbrata
thrombolites
linguloid brachiopod
BC-11-I
BC-4-C
BC-3
BC-4-B
BC-4-A
BC-2
BC-5
BC-1-D
BC-11-FF
LS-1-A2
BC-11-DD
BC-11-EE
BC-1-A
BC-1-E
BC-11-CC
BC-11-V
BC-1-C
LS-1-B9
BC-11-W
BC-9-A
BC-7
BC-1-B
BC-11-X
BC-9-C
LS-1-B5
BC-11-U
LS-1-B6
LS-1-B8
BC-8-E
LS-1-B7
BC-11-E
LS-1-B2
LS-1-B1
LS-1-B4
LS-1-B3
LS-1-B10
BC-11-H
BC-8-F
BC-10
BC-11-O
BC-11-G
BC-8-B
BC-8-A
BC-11-F
BC-9-E
BC-8-L
BC-9-B
BC-8-J
BC-11-D
LS-1-B11
BC-8-D
BC-11-C
BC-11-B
BC-8-I
BC-8-H
BC-8-G
BC-8-C
BC-8-K
BC-9-D
BC-11-A
LS-1-A1
BC-11-S
BC-11-P
BC-6
BC-11-N
BC-11-M
BC-11-K
BC-11-J
BC-11-BB
BC-11-AA
BC-11-Z
BC-11-Y
MB
BC-11-L
BC-11-T
LS-1-B12
BC-11-R
BC-11-Q

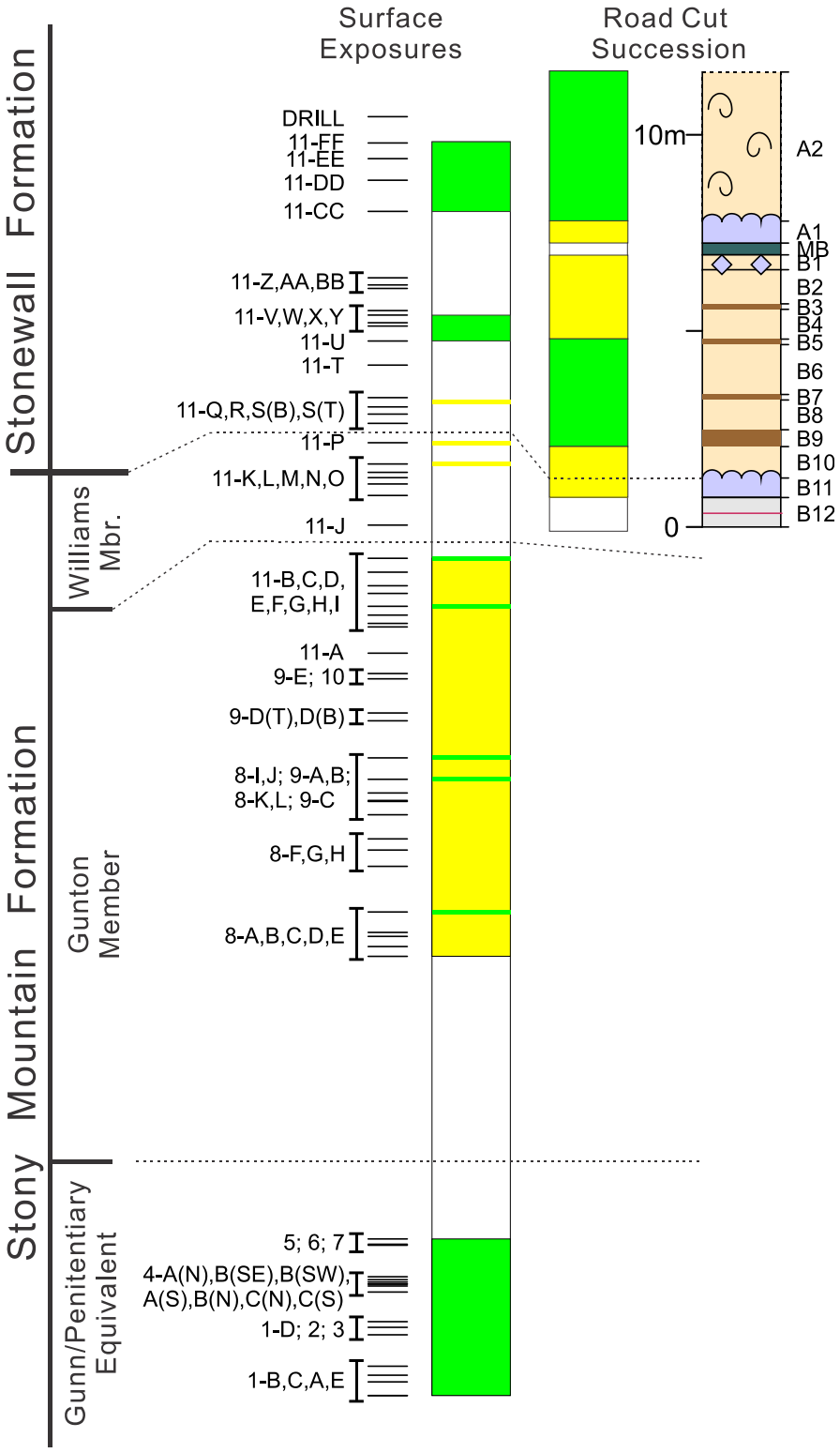

Figure 9.5: Stratigraphic section of surface exposures and road cut succession (for legend see Figure 5.8) showing the distribution of fossil clusters produced from seriation. Green indicates highly diverse assemblage, yellow indicates lower diversity assemblage, and white indicates unfossiliferous strata.

The information generated from the seriation statistical test is a valuable way of deciphering trends from large groups of data. The limitation of the test is that it uses only presence-absence data. In efforts to understand the biologic variance through the study section, the abundance of the major fossil groups categorized within the organized clusters was used to delineate further associations.

9.1.4 Relative Abundance

There is considerable variation in abundance of specimens between localities. Therefore, direct comparison of absolute abundances (number of individuals) amongst fossil groups is unsuitable for recognizing dominant species. Thus, a relative scale of abundance was utilized to recognize dominance. Groupings were formed where more than three stratigraphically adjacent localities were assigned to the same seriation assemblage, and were identified according to their stratigraphic position. Abundance classes were defined as rare (≤ 3 specimens), common (4-9 specimens), and abundant (≥ 10 specimens). The distribution and relative abundance of fossil material was considered in relation to the groupings. Figure 9.6 shows the distribution of the groupings with their relative abundances.

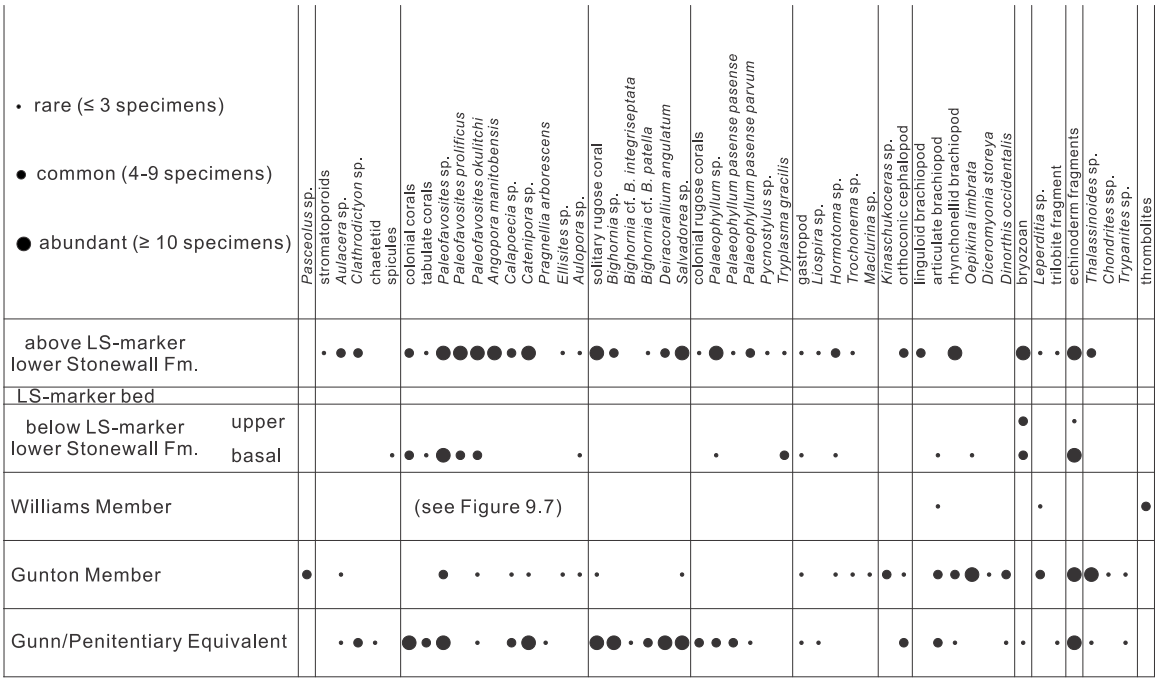

Figure 9.6: Distribution and relative abundance of identified fossil types from the William Lake study area.

The grouping from the Gunn/Penitentiary Equivalent is highly diverse. It is rich, with most major groups identified. Many of the groups are common or abundant, reflecting evenness through the interval. Solitary rugose corals are the most abundant fossils; most were not identifiable to the generic level, but all types of solitary rugosans are represented. The colonial rugosan *Palaeophyllum* sp. and tabulate corals are also relatively common. Echinoderm fragment material is abundant and occurs dispersed throughout the matrix. The only specimens of the chaetetid and the problematic coral *Pragnellia* sp. were identified within this assemblage. In addition, the trace fossil *Trypanites* sp. was identified in dense macrofossils. This grouping can be distinguished as a solitary rugose coral-dominated assemblage.

The grouping from the Gunton Member belongs to the lower diversity assemblage. It is fairly rich, with many types represented. Evenness is reduced, with rare occurrences of most of the groups that are present and a few groups occurring abundantly at isolated stratigraphic intervals. Echinoderm fragment material is abundant. In addition, specimens of the large gastropod *Maclurina* sp., the planispirally coiled *Kinaschukoceras* sp., and the trace fossil *Chondrites* sp. were identified only within this grouping. There are a few isolated surfaces that include a relatively higher richness than adjacent intervals. The isolated surface at BC-8-E contains most of the specimens of the problematic cyclocrinitid *Pasceolus* sp., as well as rare occurrences of other taxa as in the remainder of the grouping. The isolated surface at BC-11-E has locally abundant articulate brachiopods; all articulate brachiopod types are represented, though the strophomenid *Oepikina limbrata* occurs in greater abundance than the other species. This assemblage can be distinguished as being locally dominated by unique taxa.

Based on data in Figure 9.6, the Williams Member appears to be nearly devoid of fossils. In actuality, this grouping includes fossils of exceptionally preserved organisms exposed on discrete horizons. This represents a Konservat-Lagerstätte, characterized by *in situ* preservation of body fossils which include soft parts. It is rich, with fourteen groups identified within the unit, and abundance is highly variable (Figure 9.7). Linguloid brachiopods are the most abundant fossils; hydromedusae and conodont elements are common; and eurypterids, xiphosurids, dascycladacean algae, gastropods, cephalopods, and large chitinophosphatic problematic tubes are also present (Young et al., 2007). This grouping is distinguished as an exceptional preservation assemblage.

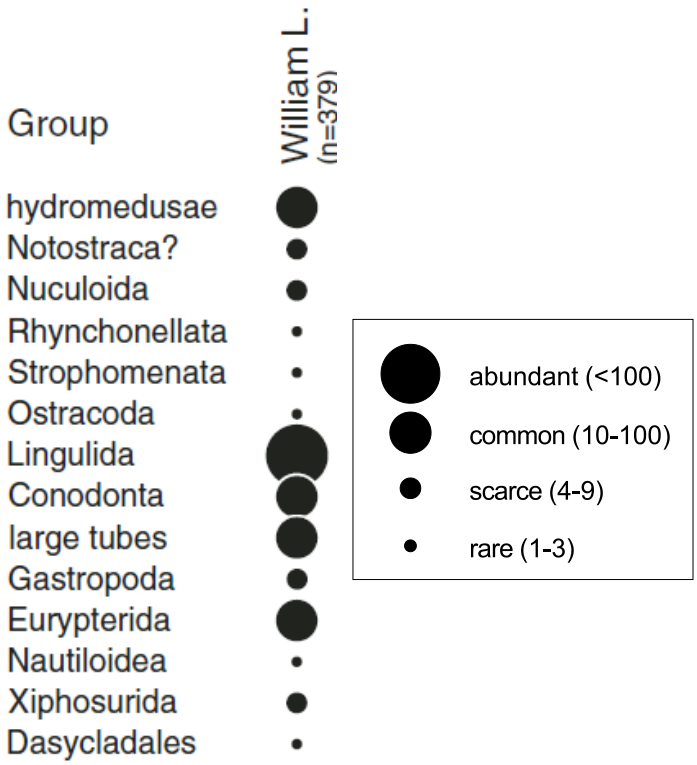

Figure 9.7: Distribution of major fossil groups at the William Lake site. Abundance classes are based on counts of all recognizable fossils on surfaces of slabs collected in 2004 and 2005. (Modified from Young et al., 2007, fig. 2)

The grouping from below the LS-marker bed interval in the lower Stonewall Formation includes both the higher and lower diversity assemblages. The higher diversity assemblage in the basal part of this interval is not as rich as the other diverse groupings, but many fossil groups from the tabulate coral major group are represented. Echinoderm fragment material is abundant and occurs dispersed throughout the matrix. The only other group in abundance is *Paleofavosites* sp., reflecting the low evenness of the interval. The first occurrence of *Tryplasma gracilis* was identified within this assemblage. Notably, common bryozoans occur in the basal and upper part of this interval. In the upper part, the only other represented group is echinoderm fragments. This grouping can be distinguished as a low diversity assemblage.

The grouping from above the LS-marker bed interval in the lower Stonewall Formation belongs to the higher diversity assemblage. It is the richest of the groupings, with nearly all major groups represented, and many occur in abundance reflecting an evenness in the interval. Colonial corals are the most abundant fossils. Of the corals, tabulate corals are most abundant; *Paleofavosites* sp., *P. prolificus*, *P. okulitchi*, and the superficially similar *Angopora manitobensis* dominate the grouping. All types of colonial rugose corals are represented, with *Palaeophyllum* sp. being abundant. Solitary rugose corals are common, with *Salvadorea* sp. being abundant. Stromatoporoids, molluscs, and brachiopods are also common through the assemblage. This grouping can be distinguished as the highest diversity assemblage.

9.2 MICROFOSSILS

Conodonts have been used extensively in paleontologic research, and as a result can be applied to understanding the ecologic framework of marine environments. Since many conodonts have been interpreted to be nektobenthic, the distribution of these forms can provide insight into the depositional conditions of the sediments they are found in. Some genera of conodonts have been used as paleobathymetric indicators, providing information on the environmental controls (Barnes and Fåhræus, 1975). The relative abundance of a genus that was confined to a particular depth zone in life can provide an estimate of the water depth at the deposition site. Therefore fluctuations in relative abundance can be used as a measure of changing water depth through the passage of time represented by the strata.

9.2.1 DISTRIBUTION

The conodont elements represent 15 named species and subspecies belonging to seven genera. The conodont elements are identified by locality within Appendix E and the results of Nowlan (2008; 2009) are summarized within Table 9.1. This diverse suite is indicative of the Late Ordovician (Maysvillian to Richmondian) age (Sweet, 1979) and is consistent with assemblages from other latest Ordovician strata of the Williston Basin reported from the subsurface of Saskatchewan (Esterhazy 16-26-20-33W1 well) and the surface and subsurface of Manitoba (Cormorant road cut and Cormorant Hill M-10-86, Warren M-1-86, and Sandridge M-23 and M-24 boreholes) by Norford et al. (1998). The suite is also consistent with previous work in the study area identifying the *Rhipidognathus* biofacies within the Williams Member of the Stony Mountain Formation (Young et al., 2007).

The faunal diversity of the conodont samples is fairly consistent and is of limited use for biostratigraphic zonation within the study area, but a few species are of interest in delimiting the age of the strata. In addition, a few species may be utilized to interpret paleoenvironmental conditions. Figure 9.8 shows the stratigraphic ranges of all conodonts through the section.

Table 9.1: Summary of microfossil data from the road cut succession. Data from Nowlan (2008; 2009).

Samples (in decending order)	**Identifiable Conodonts and Number of Elements**																							**Macrofossils** (identified in insoluble residue)
	Aphelognathus ? sp.	*Aphelognathus* aff. *A. divergens*	*Drepanoistodus* sp.	*Drepanoistodus suberectus*	*Oulodus* sp.	*Oulodus ulrichi*	*Panderodus* sp.	*Panderodus* cf. *P. liratus*	*Panderodus feulneri*	*Panderodus gibber*	*Panderodus gracilis*	*Panderodus panderi*	*Plegagnathus* sp.	*Plegagnathus nelsoni*	*Pseudobelodina* sp.	*Pseudobelodina adentata*	*Pseudobelodina inclinata*	*Pseudobelodina ? dispansa*	*Pseudobelodina vulgaris*	*Pseudobelodina vulgaris ultima*	*Rhipidognathus ?* sp.	*Rhipidognathus symmetricus*	trichonodelliform element indeterminate	
LS-1-A2 +380cm			1				1																	
LS-1-A2 +215cm						1					2		1						1					
LS-1-A2 +211cm	2																				1			
LS-1-A2 +146cm																								crinoid ossicles
LS-1-A2 +96cm	2			1							3	1		2										
LS-1-A2 base (non)				2	2				2		7												1	
LS-1-A2 base					2				3		6						1	1			1			
LS-1-A1 base		82						42	64	11	125					2			2	2				crinoid ossicles
LS-1-MB							1														4			
LS-1-B1 top		15																				35		
LS-1-B1 base		178									13	2										339		bryozoan
LS-1-B2		51	2		3			40			97								2			43		bryozoan
LS-1-B3		9	1				1															33		bryozoan
LS-1-B4		46						5			27				1					1		72		bryozoan, crinoid ossicles
LS-1-B5		27		12				42			51	2										10		bryozoan, crinoid ossicles
LS-1-B6				13					6		2									1				bryozoan, crinoid ossicles
LS-1-B7		22		4				11			33											14		sponge spicules, bryozoan
LS-1-B8	2			3				9			22											7		bryozoan, crinoid ossicles
LS-1-B9		16		22				1	4		14	2										10		
LS-1-B10 top	2																					16		
LS-1-B10 middle		56		37				41		3	88	3				2						85		bryozoan
LS-1-B10 base		48		11				12		1	19					2						60		bryozoan, crinoid ossicles
LS-1-B11 middle																						3		
LS-1-B12		10		5																		83		
TOTALS	8	560	4	110	7	1	3	203	79	15	509	10	1	2	1	6	1	1	5	4	6	810	1	

The most abundant and most common species is *Rhipidognathus symmetricus*, representing 34.5% of all conodont elements, and is found in all but ten of the 24 samples. This species is paleoenvironmentally significant as it is representative of the shallowest Late Ordovician biofacies, and is therefore regarded as an indicator of very shallow, possibly intertidal, conditions (Kohut and Sweet, 1968; Sweet, 1971). It is present at the top of the Ordovician sequence in several mid-continent sections (Sweet, 1979), and occurs close to stratigraphic discontinuities in Upper Ordovician strata (Nowlan, 2009).

The second most abundant species is *Aphelognathus* aff. *A. divergens*, representing 23.9% of all conodont elements, and is found in half of the samples. This species is paleoenvironmentally significant as it is considered an indicator of shallow subtidal environments, but had a deeper tolerance than *Rhipidognathus* (Sweet, 1971). This species is also useful biostratigraphically, indicating Richmondian age (Sweet, 1979).

The third most abundant species is *Panderodus gracilis,* representing 21.7% of all conodonts. Other species of this genus are also common, and collectively *Panderodus* is about as abundant as *Rhipidognathus*. The genus *Drepanoistodus* is also fairly common, extending through the sampled section. Both *Panderodus* and *Drepanoistodus* have long stratigraphic ranges and consequently are of limited use biostratigraphically (Sweet, 1979; Norford et al., 1998).

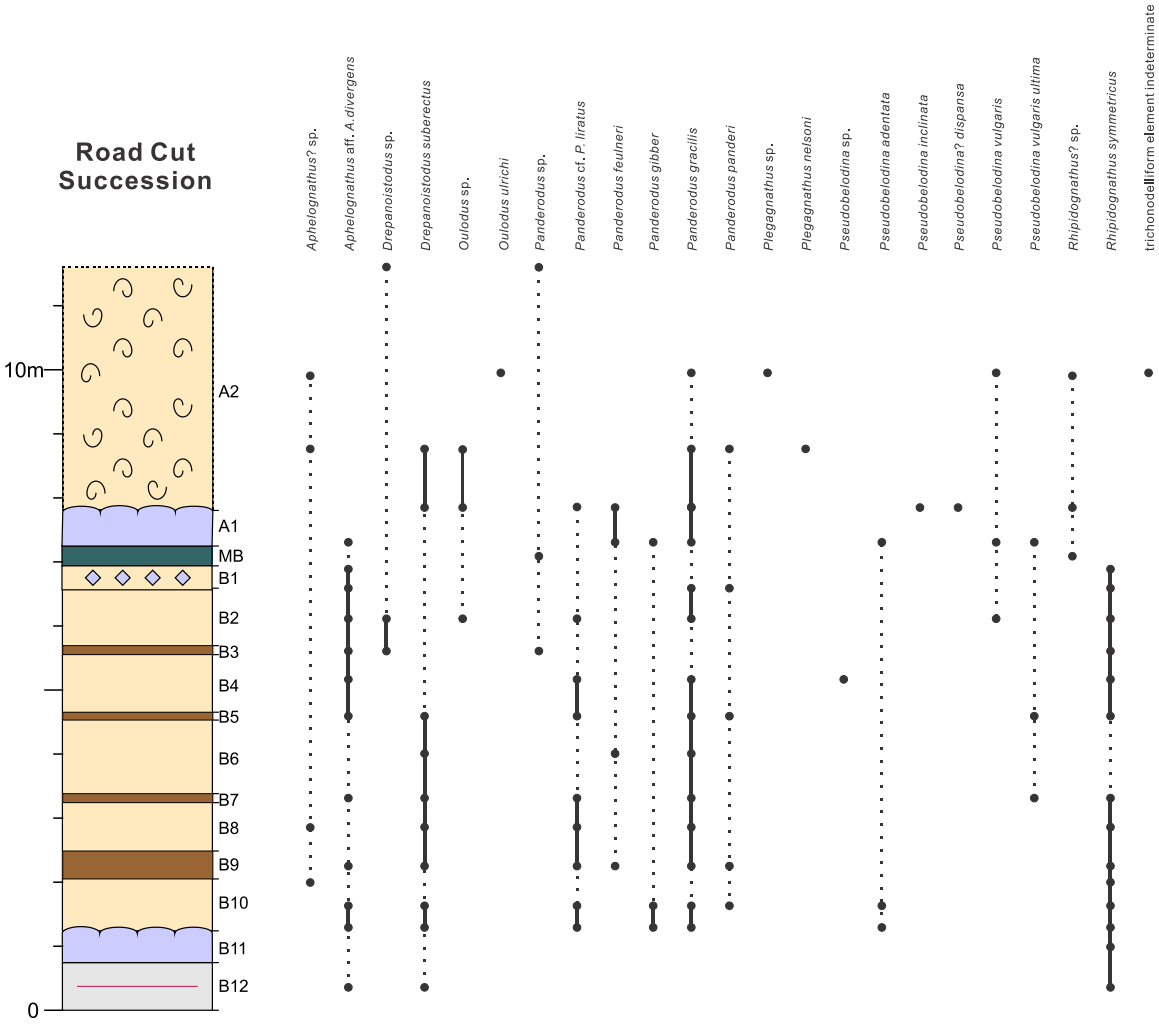

Figure 9.8: Lithologic section showing the stratigraphic ranges of conodonts identified from samples from the road cut succession at the William Lake study site. Data are from Nowlan (2008; 2009). For legend of lithofacies see Figure 5.8.

The presence of *Pseudobelodina vulgaris ultima* is biostratigraphically significant, as it is restricted to the latest Richmondian and into the Gamachian (Sweet, 1979). There is otherwise no evidence of a typical Gamachian fauna or an Early Llandovery fauna including *Ozarkodina hassi* or *O. oldhamensis* (Norford et al., 1998), therefore narrowing the age of the section to the latest Richmondian.

9.2.2 ABUNDANCE

The abundance of all conodonts (per kilogram) is shown in Figure 9.9. An average of about 50 conodonts/kg was extracted from the samples, but abundance fluctuates from a barren sample (LS-1-A2 +146 cm) to about 280 conodonts/kg. Large increases in abundance are recognized in intervals B10, B1, and A1 immediately above the LS-marker bed. In general, the abundance and diversity of conodonts in the sampled section is greater within the lower portion (average ~68/kg) and less (average ~4/kg) within the upper portion (LS-1-A2).

Relative abundance of *Aphelognathus* and *Rhipidognathus*

The conodont specimens identified within the study area are dominantly *Aphelognathus* and *Rhipidognathus*. Together these genera include almost 60% of the identified specimens. While both genera are indicative of shallow marine conditions, their slightly different tolerances make them useful in interpreting changes in water depth.

The relative abundances of these two genera were plotted against each other in an attempt to assess relative water depth conditions (Figure 9.9). Many samples include both genera in similar abundance, suggesting a close association within a shallow marine environment. While some intervals are dominated by one genus, relatively few include only one of the genera. The *Rhipidognathus* biofacies is considered to represent a period of relatively shallower water conditions, whereas the *Aphelognathus* biofacies represents a period of relatively deeper water conditions. The *Rhipidognathus* and *Aphelognathus*

biofacies are identified where there is a substantial dominance of one genus, or only one of the genera is present within the sample.

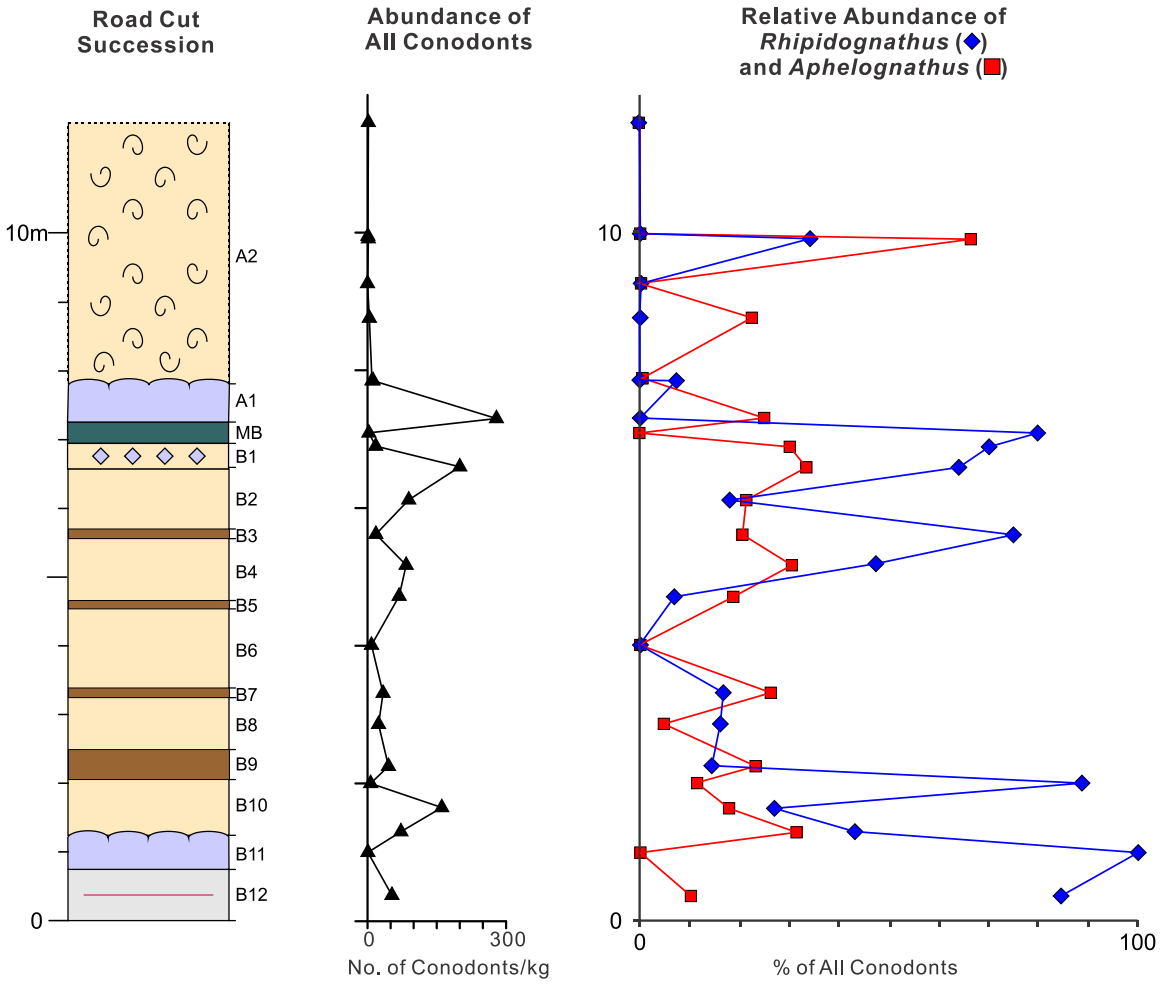

Figure 9.9: Lithologic section showing the total abundance of conodont elements (per kilogram) and the relative abundance of *Rhipidognathus* and *Aphelognathus*. For legend of lithofacies see Figure 5.8.

The *Rhipidognathus* biofacies is represented in interval LS-1-B12 and occurs without *Aphelognathus* in LS-1-B11, suggesting a shallowing episode. It is again represented in interval LS-1-B10-top and again in LS-1-B3, suggesting brief shallowing conditions.

Within the interval described as lithofacies 6 an interesting pattern is recognized. In most of the intervals identified as the thinner sublithographic mudstone (6a) the dominant genus is *Aphelognathus* (LS-B9, LS-B7, and LS-B5). In most of the intervals identified as the thicker nodular mudstone to wackestone (6b), the dominant genus is *Rhipidognathus* (LS-B10, LS-B8, and LS-B4). This alternation in dominance in the water-depth sensitive genera is reflected in the alternation in bedding within the lithofacies sediments.

The strata in the vicinity of the LS-marker bed are of particular interest. Below the LS-marker bed, the *Rhipidognathus* biofacies is represented in interval LS-1-B1-base and LS-1-B1-top and occurs without *Aphelognathus* in the LS-marker bed itself (LS-1-MB). The *Aphelognathus* biofacies occurs without *Rhipidognathus* in the interval LS-1-A1-base immediately above the LS-marker bed. This suggests a significant shallowing episode leading up to and concurrent with the LS-marker bed, which was then followed by a deepening episode.

9.2.3 TAPHONOMY

In addition to identification and occurrence, other aspects of conodonts are important in understanding environments. The condition in which conodonts are preserved can provide information about the nature of the environment in which they were deposited. Most of the conodont specimens were moderately well preserved with some interesting exceptions.

The specimens recovered from intervals LS-1-B10-base and LS-1-B10-middle are mostly moderately well preserved, but many unidentifiable fragmentary elements were

also noted. This suggests that there was sufficient deterioration of the material for the elements to become disconnected and in many cases broken. The specimens recovered from LS-1-B3 are mostly fragmentary, and some have a surface glaze, which is indicative of active abrasion suggesting transport or exposure.

The stratigraphic interval including the LS-marker bed is especially interesting. Below the LS-marker bed, the specimens recovered from interval LS-1-B1-base are moderately well preserved and there are also unidentifiable fragmentary elements. The specimens in the succeeding interval LS-1-B1-top are mostly fragmentary. Within the LS-marker bed LS-1-MB itself the specimens are fragmentary and all are abraded, suggesting re-working of the material. Above the LS-marker bed, specimens in the succeeding interval LS-1-A1 are moderately well preserved, but include additional unidentifiable fragmentary elements.

CHAPTER 10 - PALEOCURRENT ANALYSIS

Evidence of depositional environment is limited within the study area. The lithology is mostly mudstone, which is poor at preserving sedimentary characteristics. Many of the original features could have been disturbed by the bioturbation mottling which is present through much of the succession. The composition of the sediment has also been diagenetically altered to dolomite, obscuring original textural evidence.

The attitudinal and directional orientations of fossils can provide considerable insight into the conditions of the paleoenvironment. Upon death of an organism, the skeleton may become separated from the substrate, thereafter acting as a sedimentary particle influenced by the prevailing conditions. The preserved orientations of disoriented solitary rugose corals have been used to determine the hydrodynamic conditions for Late Ordovician paleoenvironments of North America, including from the Stony Mountain Formation in Manitoba (Elias, Zeilstra, et al., 1988). The recognition of common orientation among skeletons may be evidence of alignment with respect to prevailing directed water motion.

The calice of a solitary coral is directed upwards during life. During higher energy events, corals that lived unattached to the substrate were susceptible to reorientation. The resultant position of the disturbed individual would presumably be reoriented to a mechanically stable attitudinal position. For solitary corals, it is generally with the coral axis horizontal, but the side facing up was influenced by the cross-sectional shape of the corallum (Elias, 1982). The preferred directional orientation of corals has been related to their external form (Elias et al., 1987); slightly curved to straight forms were aligned parallel to currents with calice facing downstream and/or were rolled perpendicular with

calice facing slightly downstream, and greatly curved forms were oriented nearly perpendicular with convex side facing upstream (Figure 10.1).

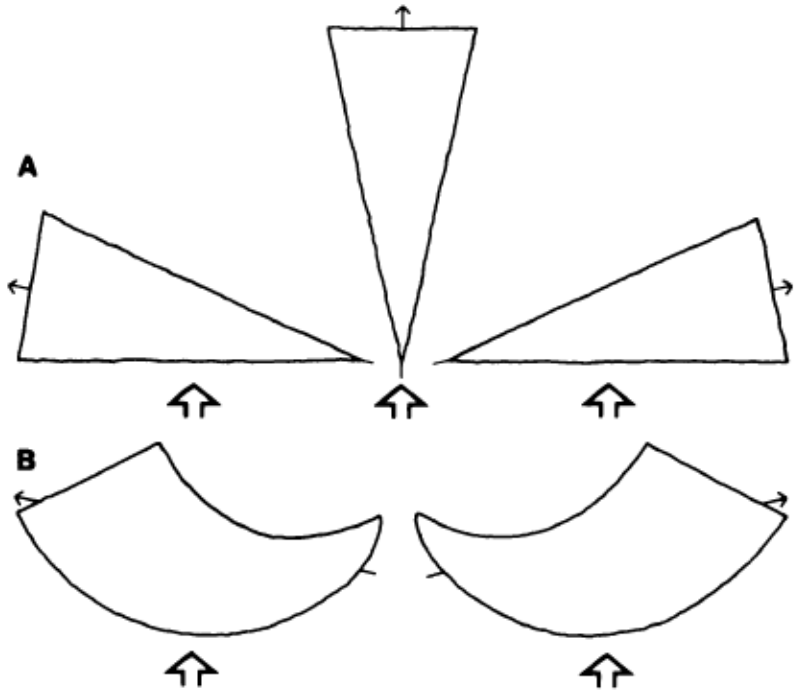

Figure 10.1: Plan view showing the orientation of coral axis and plane of curvature for the stable depositional orientations of unattached, straight (A) and curved (B) solitary rugose corals. The open arrows relate current direction to coral orientation. Small arrows indicate the calice direction. (Modified from Elias, Zeilstra, et al., 1988, fig. 1B)

For solitary corals, a general model was presented by Elias et al. (1987). The directional orientations may produce a unimodal distribution if the corals were aligned parallel to current with the apices pointing upstream. A bimodal distribution with slightly skewed equal opposite peaks may be produced if the corals were rolled perpendicular to the current, but with the apex directed slightly upstream. A trimodal distribution may be produced, formed from a combination of the previous effects. A random distribution does

not necessarily indicate low energy environments, as changes in flow or biologic interaction can produce such results.

Nine localities of weathered surface exposure were used to obtain measurements of fossil solitary rugose corals. They are all within the Gunn/Penitentiary Equivalent of the Stony Mountain Formation. They were chosen due to the sufficient abundance of measureable fossil specimens.

10.1 ATTITUDE ORIENTATION

The attitudinal orientation is presented in Table 10.1, and the azimuthal directional orientations of corals deposited with the axis horizontal are presented as rose diagrams in Figure 10.2. Statistical methods, such as the chi-square test, could not be conducted on most of the data set due to low counts for most localities. While these tests are useful for determining if the data distribution is random or preferred, they require sufficient data to account for the degrees of freedom. Alternatively, rose diagrams can be used as a qualitative assessment of trends in the hydraulic regime at the time of deposition.

Table 10.1: Attitudinal orientation of solitary corals, in stratigraphic order.

Locality	Horizontal		Upright		Upside Down		Totals
	#	%	#	%	#	%	
BC-4-C	55	72.4	21	27.6	0	0.0	76
BC-4-B	119	77.3	33	21.4	2	1.3	154
BC-4-A	109	64.9	58	34.5	1	0.6	168
BC-3	24	61.5	13	33.3	2	5.1	39
BC-1-D	26	50.0	22	42.3	4	7.7	52
BC-1-E	2	100.0	0	0.0	0	0.0	2
BC-1-A	10	55.6	8	44.4	0	0.0	18
BC-1-C	5	62.5	3	37.5	0	0.0	8
BC-1-B	2	50.0	2	50.0	0	0.0	4
Total	352	67.6	160	30.7	9	1.7	521

The attitudes of the solitary corals identified within the Gunn/Penitentiary Equivalent are similar from all localities. Very few corals were deposited upside down (2% of 521 specimens). These were undoubtedly transported before burial, as the coral calice is oriented up during life. A considerable proportion of corals are oriented with the calice upright (31%). While an upright orientation does not establish that the corals were preserved in life position, the high frequency of this orientation suggests that some may have retained this position during deposition and were not transported. The majority of corals (68%) were positioned sideways with the axis horizontal. This is the most stable depositional orientation, suggesting that there was influence of some hydrological regime.

10.2 DIRECTIONAL ORIENTATION

The azimuthal directional orientations of corals deposited with the axis horizontal are presented using rose diagrams in Figure 10.2 and the data are detailed in Appendix F. They are shown in typical geo-convention with a 360° range. In general, the data sets were limited by the low counts for individual localities. Consequently, the data for localities from site BC-1 (A, B, C, D, and E) were grouped together, as the counts were too small to assess individually, but are included in Appendix F.

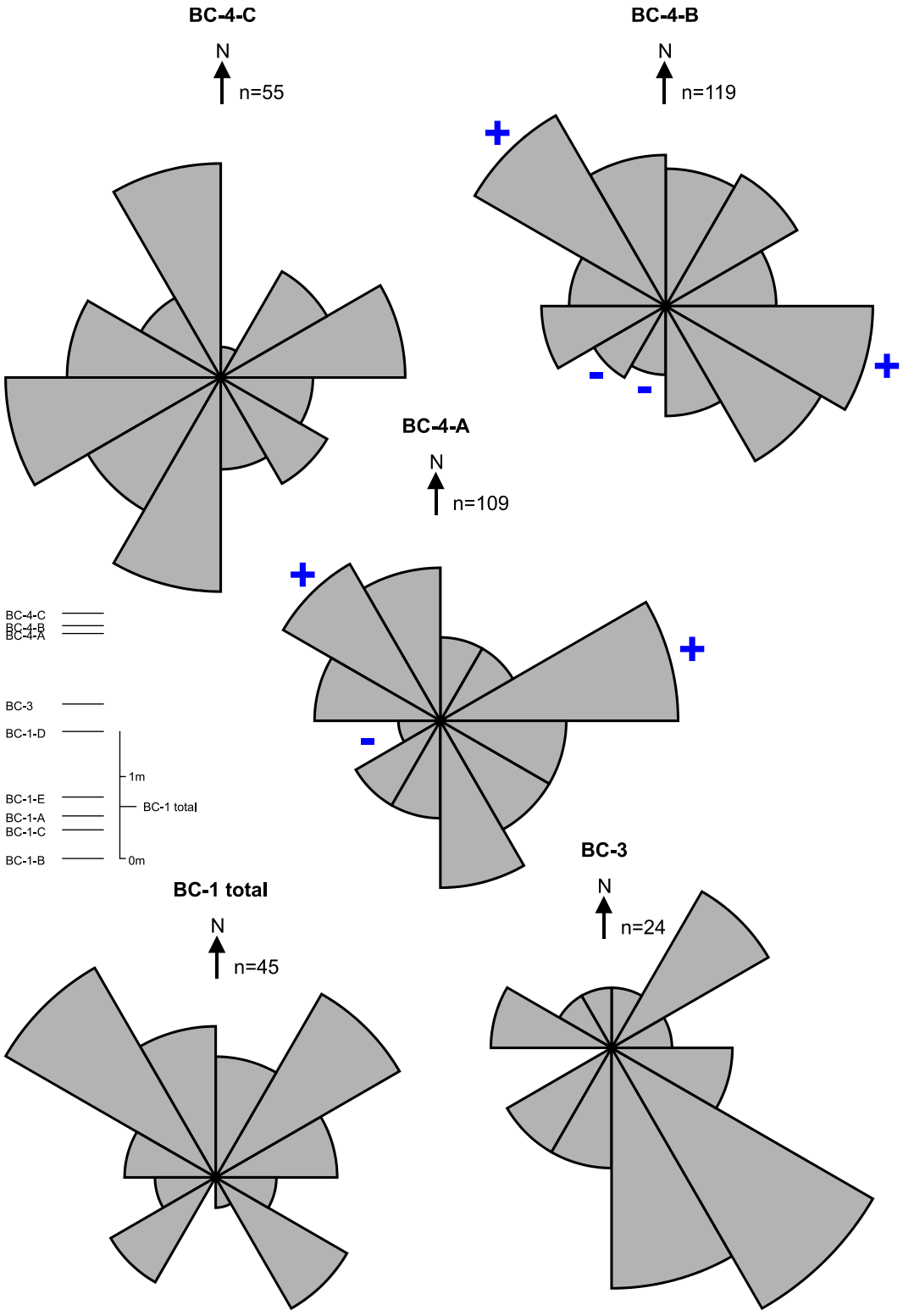

Figure 10.2: Rose diagrams showing the orientation of solitary rugose corals from surface exposures. Stratigraphic position of localities is shown at left. Blue + indicates anomalously high class, and blue – indicates anomalously low class.

The amount of data in most data sets was insufficient to run statistical tests. The chi-squared test is used to determine if the distribution of data is random or preferred. In order to apply this test, the average abundance for each class must maintain an average class frequency of five (Hammer, 2002). To reasonably assess the directionality of the paleocurrent data, a threshold of 12 classes was chosen to be used. Therefore, the minimum number of specimens for the test to be applied would be 60. Only two data sets have sufficient data to perform the chi-squared test (BC-4-A and BC-4-B). The rose diagrams, all plotted with 12 classes, are therefore used for a qualitative assessment of the distributions.

The chi-squared test evaluates the observed results in relation to the expected outcome to test for randomness of a data set. Expected values (E) are calculated based on the number of specimens (n) divided by the number of classes (*k*). The expected values are subtracted from the observed values (O) for each class, and the resultant is squared. The product is then divided by the expected value, and the sum total of these values represents the value for χ^2 (see following equation). The degrees of freedom (d.f.) is the number of classes minus one, which accounts for the inherent linear restriction in which sum of the values in all classes must equal the value n (Mendenhall et al., 2006). The calculated value for χ^2 is then compared with the tabulated critical value for $\chi^2_{0.05}$ for the calculated degrees of freedom (see Mendenhall et al., 2006, Appendix 1, Table 5). If the calculated value is greater than the critical value, a preferred orientation can be suggested for the data set.

$$\chi^2_{(calc.)} = \Sigma\,[(O - E)^2 / E]$$

The results of calculations are presented in Appendix F.2. A standard deviation (S.D.) was calculated as the square root of the sum total for the $(O-E)^2$ value for all classes. Classes where the observed value differed from the expected value by more than one standard deviation were considered to be anomalous.

The individual localities for BC-1 (BC-1-A to BC-1-E) did not have sufficient data to be considered individually. The combined distribution of specimens from BC-1-total shows a relatively large peak within the class between 300° and 330°, supported with a small peak opposite to it between 120° and 150°. There is also a generally perpendicular moderate sized peak within the class from 30° to 60°. This resembles a trimodal distribution weighted with a slight skew. The interpreted hydraulic condition orients the current flow toward a northeasterly direction, with a possible skew more towards the north.

The data from BC-3 are based on the fewest specimens. The distribution shows the majority of these corals oriented in a similar direction. There are two large peaks between 120° and 180°. There is a smaller peak within the class from 30° to 60°. This suggests a mostly unimodal distribution. The interpreted hydraulic condition orients the current flow toward a southeasterly direction. There is some influence in the northeasterly direction, supported by the smaller peak.

The data were abundant for the BC-4-A locality. This distribution shows a trend similar to that at BC-1. There is a large peak within the class from 60° to 90°. There are smaller peaks from 300° to 360° and from 150° to 180°, opposite to each other. This suggests a trimodal distribution. There were a sufficient number of values in this data set to conduct the chi-square test. While no preferred orientation was established,

anomalously high and low classes were identified. High values were recognized in the 61-90° and 301-330° classes, whereas low values were recognized in the 241-270° class. These results support the qualitative examination of the rose diagram. The interpreted hydraulic condition orients the current flow toward a northeasterly direction.

The data from BC-4-B were the most abundant. The distribution shows opposite peaks from 300° to 360° and from 90° to 150°. There is also a greater frequency on the northeastern side of these peaks than on the southwest side. This resembles a bimodal distribution, which is skewed to the northeast. There were a sufficient number of values in this data set to conduct the chi-square test. While no preferred orientation was established, anomalously high and low classes were identified. High values were recognized in the 91-120° and 301-330° classes, whereas low values were recognized in the 181-210° and 211-240° classes. These results support the qualitative examination of the rose diagram. The interpreted hydraulic condition orients the current flow toward a northeasterly direction.

The distribution of specimens from BC-4-C shows a trend different from the other localities. There are two sets of peaks. One set shows opposite peaks from 60° to 90° and 240° to 270°. The other set is slightly skewed, with peaks from 180° to 210° and 330° to 360°. The sets are approximately perpendicular to each other. This suggests that there are two bimodal distributions, with somewhat equal influence. The interpreted hydraulic condition orients the current flow from general north or south for the set of opposite peaks, and from the east for the slightly skewed set of peaks.

From the resultant rose diagrams, the general trend of interpreted current flow direction is toward the northeasterly direction, although there is some variance.

According to the model of Elias et al. (1987), a substantial proportion of corals were oriented perpendicular to current flow, interpreted from resultant bimodal distributions. However, there was also complexity of corals that were aligned with the prevailing current, interpreted from superimposed unimodal distributions. The result is trimodal distribution of varying strength.

To test the interpretation of the prevailing current, a rose diagram for the combined data from all nine locations was prepared, and is shown in Figure 10.3. The resultant diagram shows a weak trimodal distribution. There is a bimodal peak set from 120° to 150° and 300° to 330°, and a superimposed unimodal peak from 60° to 90°. The calculated mean for the 352 specimens is 40° (calculated to account for circularity of the rose diagram; for equation see Hammer, 2002). There was a sufficient number of values in the total data set to conduct the chi-square test. While no preferred orientation was established, anomalous high and low classes were identified. High values were recognized in the 61-90°, 121-150°, and 301-330° classes, whereas low values were recognized in the 181-210° and 241-270° classes. These results support the qualitative examination of the rose diagram. This supports the interpretation of the hydraulic conditions orienting the current flow toward the northeast.

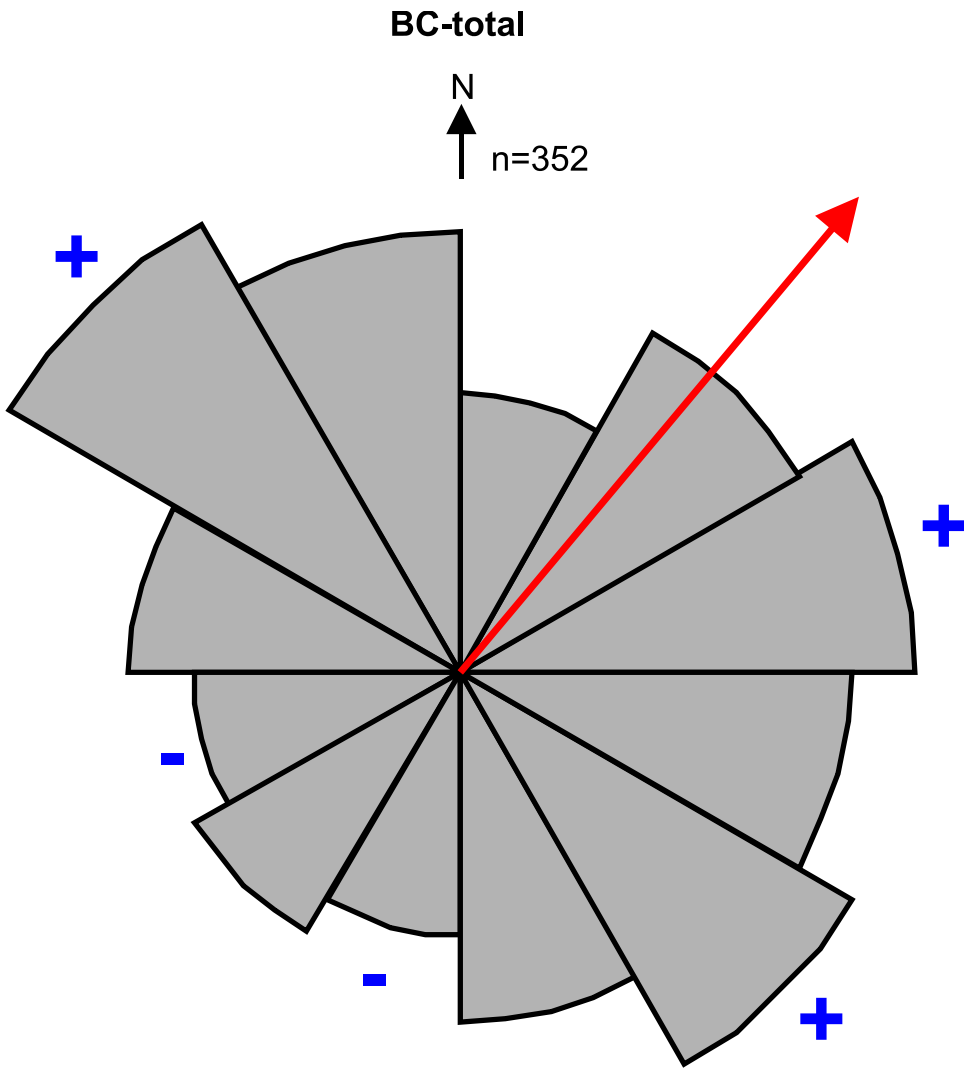

Figure 10.3: Rose diagram showing the orientation of combined data for all solitary rugose corals from the surface exposures. Red arrow shows location of calculated mean at 40°. Blue + indicates anomalously high class, and blue – indicates anomalously low class.

CHAPTER 11 – DISCUSSION AND INTERPRETATION

Information obtained through the study of the latest Ordovician succession exposed north of Grand Rapids allows for valuable interpretations to be made about its deposition. Details of the lithology may be used for paleoenvironmental reconstruction of the conditions existing at the time of deposition. The observed zonation of fauna may be used for paleoecological interpretation of communities and their changes leading up to the end-Ordovician mass extinction. Aspects concerning the stratigraphy of the Stony Mountain and Stonewall formations have historically been problematic; therefore continued study of this material yields a greater understanding of the stratigraphy of the Williston Basin. In addition, occurrence of key data can be used to explore the regional context of the basin.

11.1 GUNN/PENITENTIARY EQUIVALENT

The Gunn/Penitentiary Equivalent is interpreted to have been deposited in a low to moderate energy, shallow marine environment. The strata are identified as lithofacies 1, described as a highly fossiliferous bioturbated dolomitic mudstone. The abundance of micrite suggests low energy but the localized increase in bioclastic material indicates periods of deposition in a moderate energy environment. The presence of pervasive bioturbation and abundance of macrofauna suggest favorable conditions. Sedimentation rates were likely low, as macrofossils were exposed long enough to permit borers, which produced *Trypanites,* to capitalize on a hard dense substrate. The presence of very small halite molds suggests that there were periodic changes in salinity or water circulation.

The fauna of the Gunn/Penitentiary Equivalent is interpreted to be highly diverse. The assemblage is distinguished by the high abundance of solitary rugose corals. All groups of genera and species were represented, and there were sufficient measurable specimens to permit paleocurrent analyses to be performed on several surface exposures. Prior to burial, the corals were dislocated from their upright position, and were realigned with the prevailing current. The majority of the solitary corals were aligned in this fashion, although a substantial proportion remained in upright orientation. The paleocurrent direction is interpreted to have been flowing northeast, toward the interpreted edge of the Williston Basin.

The fauna included some unique occurrences. The only specimen of *Pragnellia arborescens* in the study area was identified herein. It has been interpreted to have been able to tolerate episodes of higher energy, as it could bend without breaking (Leith, 1952), supporting the interpretation of episodes of higher energy. The only specimen of a chaetetid was also identified. Its growth was comparable to other organisms that grew by accretion, such as stromatoporoids, which could modify their morphology in response to varying rates sedimentation (Kershaw and West, 1991).

The exposed portion of the Gunn/Penitentiary Equivalent in the William Lake study area is about 4 m thick, encompassing the upper portion of the member. In drill core it extends to about 13.75 m in thickness. The contact with the overlying Gunton Member was not identified in the field, but in core the contact is sharp, defined by a change in the character of bioturbation mottling. The contact between the members may be constrained to a narrow expanse along Highway #6 in the vicinity of 488500E/5987500N (NAD 27).

11.2 GUNTON MEMBER

The Gunton Member is interpreted to chronicle the initiation of less desirable conditions. The lower portion of the member is characterized by a densely *Thalassinoides*-bioturbated dolomitic mudstone, identified as lithofacies 2. The abundance of micrite and low proportion of bioclastic material suggest a low energy environment. The pervasive bioturbation suggests a favorable environment for biota, and the presence of *Thalassinoides* indicates an intertidal to shallow subtidal environment (Myrow, 1995). The lack of abundant and diversified fauna, however, is consistent with more restricted conditions. Toward the upper portion of the member, there is a gradational loss of the *Thalassinoides* bioturbation coincident with commencement of nodular bedding, identified as lithofacies 3. Evaporite molds resembling halite crystals occur near the top, signifying more restricted or possibly hypersaline conditions. The member is interpreted to have been deposited in low energy, shallow marine conditions that progressively became more restricted.

The fauna of the Gunton Member is interpreted to be of low diversity. There are discrete horizons with relative increases in richness, characterized by some unique occurrences. The only occurrence of the problematic alga *Pasceolus* is within the *Thalassinoides*-rich lower portion. This group has been interpreted to have occupied quiet water environments below wave base, or restricted pools or lagoons (Beadle, 1988). This supports the interpretation of more restricted conditions within the member. The large gastropod *Maclurina* and the planispirally coiled cephalopod *Kinaschukoceras* also occur only within the Gunton Member. The large gastropod has been interpreted to be robust enough to withstand higher energy, but would have had limited mobility, suggesting a

more sessile lifestyle (Linsley, 1977). The cephalopod would have had an active predatory lifestyle, but previous accounts of this group from the Hudson Bay Lowlands were from nearly unfossiliferous strata, consistent with the low diversity observed in the study site (Nelson, 1963). In the upper portion of the member, at horizon BC-11-E, there is the occurrence of the *Diceromyonia storeya* brachiopod community. The small size of the constituents of this community has been suggested to reflect increased environmental stress (Jin and Zhan, 2001).

The exposed portion of the Gunton Member in the study area is about 9.0 m thick. In drill core it extends about 14.4 m (average). The contact with the overlying Williams Member is not identified in the field, but in core it is relatively sharp, defined by a lithologic change from nodular bedded to laminated mudstones. The contact between the members may be constrained to a small gap between exposure surfaces BC-11-I and BC-11-J along Highway #6.

11.3 WILLIAMS MEMBER

The Williams Member is interpreted to have been deposited in a very low energy, very shallow water, possibly lagoonal environment. Most of the member is characterized by sublithographic mudstone with intervals of thin laminations, identified as lithofacies 4. This very fine mud suggests very low energy conditions. Superficially, this member appears to have few sedimentary structures. Upon further examination, it reveals very fine scale features recording a complex depositional history. The laminated intervals are interpreted to represent oscillating conditions, possibly related to changes in salinity, energy conditions, or sedimentation. The presence of evaporite molds suggests

hypersalinity, consistent with the interpreted restricted conditions. Symmetrical ripple marks indicate oscillating bi-directional water movement, suggesting a tidal influence. Crossbedding occurs in some intervals, and crosscutting channels have been documented suggesting fine scale changes in energy conditions. Dewatering structures have been identified on some horizons, suggesting instances of sufficiently rapid deposition to produce quick beds (Lowe and LoPiccolo, 1974). The occurrence of subrounded quartz grains within isolated intervals indicates incorporation of foreign terrigenous input. At the top of the Williams Member there is a thrombolitic dolomitic mudstone, identified as lithofacies 5. The presence of these biosedimentary structures suggests very shallow water conditions, but likely the return of normal marine conditions. The observed characteristics of this member detail an environment with a multitude of fine scale changes, within a backdrop of restricted conditions.

Although the Williams Member appears to be nearly barren of fossils from this study, within this member there is occurrence of exceptionally preserved fossils consistent with a Konservat-Lagerstätte (Young et al., 2007). The exceptional preservation suggests anoxic, quiet water conditions and a rapid rate of burial (Young et al., 2007). From a series of discrete horizons, a distinct suite of fauna has been identified, representing very shallow, restricted conditions. Of the fossils identified, linguloid brachiopods are the most abundant. They have been interpreted to occupy shallow water environments with sandy or muddy bottoms, and are resistant to osmotic stress (Paine, 1970). Xiphosurids and eurypterids have also been identified; these have been interpreted to occupy marginal marine, brackish, or possibly freshwater environments (Rudkin et al., 2008). Conodonts identified from this interval are from the

Rhipidognathus biofacies, which represent the shallowest conditions of the Late Ordovician of the Williston Basin (Nowlan and Haidl, 2001).

The exposed portion of the Williams Member in the study area is about 2.1 m thick. In drill core it extends 3.4 m (average). The contact with the overlying Stonewall Formation is observed in the road cut succession between LS-1-B11 and LS-1-B10. This contact is sharp but undulatory, reflecting the topography of the thrombolitic mudstone at the top of the Williams Member. It is similarly sharp when identified in the drill cores.

11.4 STONEWALL FORMATION

The Stonewall Formation is characterized by dolostones interbedded with thin argillaceous units, most notably the *t*-marker. Within the strata of the study area, another marker bed interval was recognized (LS-marker). In order to thoroughly explain this portion of formation, discussion will be separated into strata below the LS-marker interval, the LS-marker interval itself, and above the LS-marker interval.

Below the LS-marker interval

The portion of the Stonewall Formation below the LS-marker bed interval is interpreted to have been deposited in a series of shallowing cycles in a relatively shallow marine environment. The strata are characterized by massive bedded mudstone, with alternation of thick nodular mudstone to wackestone and thinner dense mudstone beds, identified as lithofacies 6. The repetition of units suggests oscillating conditions through the interval, which could be resultant from changes in relative sea-level, water energy, or water circulation. Through this interval there is the presence of water-depth sensitive

Rhipidognathus and *Aphelognathus* conodont microfossils. The relative abundance of these genera in this interval reveals an interesting pattern. The shallower tolerance *Rhipidognathus* dominates in the thicker nodular wackestone to mudstone units, and the deeper tolerance *Aphelognathus* dominates in the thinner dense mudstone units. This reciprocating pattern suggests that the oscillatory units were at least in part related to relative sea-level fluctuation influencing the fauna.

The top portion of this interval contains brecciated dolomitic mudstone, identified as lithofacies 7. This interval is interpreted as intraformational brecciation, since the composition of the clasts is similar to that of the surrounding material. The extent of this structure is limited to the immediate stratigraphic proximity below the LS-marker bed interval. It is delineated by bluish grey staining (similar colouring to the LS-marker bed interval) enveloping the clast material. This propinquity suggests formation associated with that of the LS-marker bed interval. Intraclasts, in modern and ancient examples, are interpreted to have been derived from subaerial exposure surfaces or submarine cemented hardgrounds (Demicco and Hardie, 1994). Shallow marine hydrodynamics of their transportation and deposition are generally poorly known (Demicco and Hardie, 1994). Therefore, the resultant fabrics and sedimentary structures of these processes involved with intraclasts are poorly understood.

The fauna of the Stonewall Formation below the LS-marker bed interval is diverse, suggesting more normal conditions. It is not as rich as some of the other strata within the study area, but contains many of the more normal marine faunal elements. It is abundant in echinoderm fragments and some tabulate corals. It marks the first appearance of *Tryplasma gracilis*, which is a characteristic fossil of the Stonewall Formation. There

is a high abundance of conodonts, suggesting that conditions were favorable, but possibly not stable enough for widespread benthic expansion. The conodonts are from the *Aphelognathus* and *Rhipidognathus* biofacies indicating shallow marine conditions (Nowlan and Haidl, 2001). The slightly shallower *Rhipidognathus* biofacies is present in strata immediately below the LS-marker bed interval, contributing to the interpretation of shallowing conditions approaching this interval.

The exposed portion of the Stonewall Formation below the LS-marker bed interval is 5.7 m thick. In drill core it extends 5.6 m. The contact of this portion of the formation with the LS-marker bed interval is observed in the road cut succession between LS-1-B1 and LS-1-MB. It is sharp, defined by a distinct change in lithology. It is similarly sharp when identified in the drill cores.

LS-marker bed interval

The LS-marker bed interval is interpreted to have been deposited under conditions of subaerial exposure. It is characterized by argillaceous fissile dolomitic mudstone, identified as lithofacies 8. This lithology contrasts strikingly from adjacent material, suggesting unusual deposition. The results of XRD identified quartz and possible phases of potassium aluminum silicate and/or glauconite in addition to the pervasive dolomite of the entire sequence. These additional phases are more concentrated near the base of the bed, decreasing toward the top, recognized by decreasing amounts of dissolution residue. The presence of these phases indicates that terrigenous material was incorporated, possibly from a source proximal to the Williston Basin.

The faunal component of the LS-marker bed interval is limited, represented by fragmentary and abraded conodont elements. The condition of these elements suggests re-working of the material, consistent with the interpretation of subaerial exposure. The unit is barren of macrofossils, indicating that the conditions were unfavorable for any invertebrate life.

The exposed portion of the LS-marker bed interval of the Stonewall Formation is 30 cm thick. In drill core it is 18 cm (average). The upper contact of the LS-marker bed interval is observed in the road cut succession between LS-1-MB and LS-1-A1. It is gradational into the thrombolitic mudstones above, accounting for the variation in thickness between the exposure and core.

Above LS-marker bed interval

The portion of the Stonewall Formation above the LS-marker bed interval is interpreted to chronicle the return of more normal marine conditions. Immediately above the LS-marker is the occurrence of thrombolitic dolomitic mudstone, identified as lithofacies 5. The thrombolites are similar to those described from the Williams Member, suggesting the return to very shallow, but likely marine conditions. The top of the thrombolites defines an undulatory sharp contact with the overlying lithology. The strata above are interpreted to have been deposited in a moderate energy, shallow marine environment. It is characterized by a highly bioturbated dolomitic wackestone, identified as lithofacies 9. The presence of wackestone to packstone suggests higher energy conditions than previously documented through the section. The pervasive bioturbation and abundance of macrofossils demonstrate a return to favorable normal marine

conditions. Sedimentation rates are interpreted to have been high, as portions of echinoderm stems are identified.

The fauna of the portion of the Stonewall Formation above the LS-marker bed interval is highly diverse. It encompasses the greatest richness and evenness of the studied strata. There is an abundance of tabulate, as well as solitary and colonial rugose corals, rhynchonellid brachiopods, bryozoans, and echinoderm fragments. Stromatoporoids, gastropods, and cephalopods are also common. This suite of fauna represents a wide variety of life forms and life habits, suggesting that there were sufficient favorable conditions for all to thrive. Within this interval, conodonts immediately above the LS-marker interval are abundant, representing the *Rhipidognathus* biofacies, indicating shallow marine conditions (Nowlan and Haidl, 2001). Above that initial abundance, there is a decrease in the abundance and diversity of the conodont elements.

The exposed portion of the Stonewall Formation above the LS-marker bed interval is 4.4 m thick. The upper extent of the material from the study site is within this unit, but in drill core it extends up to 6.3 m.

11.5 SUBAERIAL EXPOSURE SURFACES

Isotopic excursions have been used as a proxy for recognition of exposure surfaces (Theiling et al., 2007). The $\delta^{13}C$ signature in the vicinity of the intervals interpreted as representing subaerial exposure reveals characteristic patterns that may be related to exposure times and depths of truncation (Theiling et al., 2007). During subaerial exposure some of the altered sediment may be truncated then reworked and

incorporated into sediment above the surface of exposure (Theiling et al., 2007). Brief exposure would produce a thin zone of alteration, resulting in a negative excursion recognized above the exposure surface. Longer exposure would produce a greater proportion of alteration, resulting in a negative excursion recognized below the exposure surface.

In the Williams Member, a small -0.5‰ negative $\delta^{13}C$ excursion is identified within the thrombolitic interval. This segment of the $\delta^{13}C$ profile is interpreted to represent a brief subaerial exposure at the top of the thrombolites. This interpretation is supported by the occurrence of terrigenous quartz grains near the top of the member, and the sharp, irregular top of the thrombolites.

In the vicinity of the LS-marker bed interval, a small 0.3‰ positive $\delta^{13}C$ excursion immediately below the LS-marker is followed by a -1.3‰ negative $\delta^{13}C$ excursion through the marker into the thrombolites above. A minimum value occurs in the thrombolite interval. This segment of the $\delta^{13}C$ profile is interpreted to represent a subaerial exposure surface at the top of thrombolites above the LS-marker interval. The interpretation is supported by the sharp, irregular top of the thrombolites. The base of the LS-marker interval is defined by the sharp, irregular top of lithofacies 7 (LS-1-B1). Within the LS-marker bed, there is evidence of terrigenous material (quartz, and possibly glauconite and potassium aluminum silicate), which decreases in abundance upward from the base. This is interpreted to represent a brief subaerial exposure surface at the top of LS-1-B1, on which the LS-marker was deposited.

In drill core, there is a -0.8‰ negative $\delta^{13}C$ excursion below the *t*-marker followed by a substantial 1.4‰ positive excursion in the *t*-marker bed. A minimum value

occurs immediately below the base of the *t*-marker. This segment of the $\delta^{13}C$ profile is interpreted to represent another subaerial exposure surface of longer duration, on which the *t*-marker was deposited. These data are consistent with the profiles from other locations presented by Demski et al. (2011), which suggest the occurrence of the HICE in the upper Stonewall Formation.

In most cases (top of the Williams Member, top of the thrombolites above the LS-marker bed, and at the *t*-marker interval) there is a small negative excursion, followed by a return to background values. The interpretation of these profiles suggests that there were brief periods of subaerial exposure (Theiling et al., 2007). The length of exposure at the *t*-marker interval was likely greatest, since the magnitude of the negative excursion is recognized through a thicker interval of strata, and is preserved below the exposure surface. The exposures at the top of the Williams Member and top of the thrombolites above the LS-marker bed interval were likely short, as the negative excursion is through a thinner interval of strata and recovery to background values occurs within the deposits above the exposure surface (Theiling et al., 2007). While the exposure at the top of LS-1-B1 (on which the LS-marker bed was deposited) does not reveal a negative carbon isotope excursion, sedimentological evidence supports the interpretation of a subaerial exposure surface. Perhaps a negative excursion was removed by erosion of strata.

11.6 PALEOENVIRONMENT

During the latest Ordovician, the paleoenvironmental conditions in the vicinity of the William Lake study area were those of a shallow, open marine setting near the northern margin of the Williston Basin. Examination of the surface exposures, road cut

succession, and drill cores was used to describe nine lithofacies. Several transgression-regression cycles could be identified within the succession. Based on interpretations of the lithofacies, Figure 11.1 was constructed to visualize the changing conditions through the study area.

The Stony Mountain Formation chronicles a transgressive-regressive cycle. The gradual restriction of marine conditions is reflected in the change of lithologies from more normal marine bioturbated mudstones into restricted lagoonal laminated mudstones. This is echoed in a decrease in the diversity of faunal assemblages through the formation. The solitary rugose coral-dominated assemblage in the Gunn/Penitentiary Equivalent is succeeded in the Gunton Member by an assemblage distinguished by its punctuated occurrences of taxa that are otherwise absent. Contrary to this pattern of decreasing diversity, is the high diversity of the assemblage of exceptionally preserved fauna in the otherwise sparsely fossiliferous to unfossiliferous Williams Member. This reflects the ideal controls on preservation present in the Williams Member at certain times of deposition. A subaerial exposure surface is suggested at the top of the Williams Member, reflecting the maximum extent of the regression.

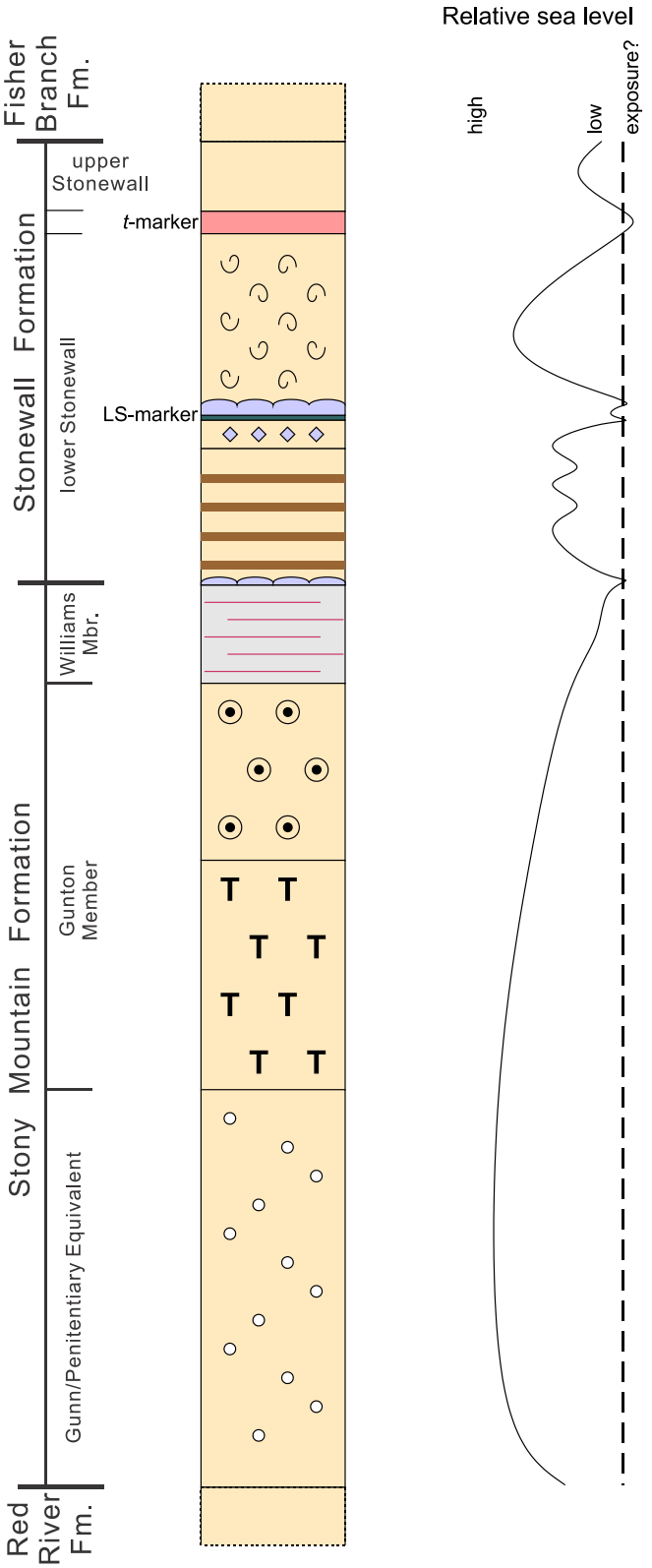

Figure 11.1. Idealized stratigraphic section of the William Lake study area showing interpreted sea level changes. For legend of lithofacies see Figure 5.8.

The Stonewall Formation chronicles environmental fluctuations within the basin. The recognition of multiple subaerial exposure surfaces suggests periodic emergence conditions within a very shallow marine environment. This relative sea level fluctuation in the environment is supported by the interbedded lithofacies below the LS-marker interval. The presence of terrigenous sediments within the LS-marker interval suggests that the paleo-shoreline was in proximate distance. Strata above the thrombolites above the LS-marker reveal a relative short lived return to more normal marine conditions, reflected in the occurrence of the most diverse faunal assemblage in the entire succession. The instability returned toward the top of the formation with the development of another subaerial exposure surface at the base of the *t*-marker.

The strata of the William Lake study area provide significant insight into the latest Ordovician of the Williston Basin. Fine-scale changes in environmental conditions are preserved, providing invaluable information about this critical time in Earth's history.

11.7 PALEOECOLOGY

The Ordovician radiation was one of the most significant events in Earth's history of life. It involved establishment of the Paleozoic Evolutionary Fauna, which would go on to dominate the marine environment for the remainder of the Paleozoic (Droser and Finnegan, 2003). Diversification included shifts in ecological dominance, increases in community complexity through development of adaptive strategies, and development of new communities (Bottjer et al., 2001).

The end-Ordovician was the first of the "big five" and the second largest mass extinction, with an estimated 85% of species loss (Sepkoski, 1996). Ecologically,

however, most changes occurred at the lower levels (Droser et al., 2000). Reef communities were strongly affected, but in the Silurian rebounded with subfamilies of rugose and tabulate corals, and stromatoporoids present in the Ordovician (Droser et al., 2000). In the pelagic realm, both graptolites and conodonts were reduced to few species, but diversified quickly after the extinction to regain their ecologic position (Droser et al., 2000). At the benthic level of the Ordovician, the dominant brachiopods were affected, but only mostly community based changes occurred, causing few severe alterations (Droser et al., 2000). Recovery from the mass extinction yielded ecologic patterns similar to those observed in the Ordovician, resulting in a less severe ecologic change (Sheehan, 2001).

Through detailed examination, tabulation, and statistical analysis, five faunal assemblages were recognized within the William Lake study area. Overall, the suite is diverse. A general evaluation of the different levels of diversity is presented. Diversity within the individual assemblages is varied, representing changes in diversity within the habitat, or alpha diversity. There is distinct variation in the richness and abundance of species between the identified assemblages. The assemblages were distinguished by the dominant fauna, such as the solitary rugose coral-dominated assemblage in the Gunn/Penitentiary Equivalent. Recognition of vastly different environments (shallow marine vs. restricted lagoonal) permits evaluation of the diversity between habitats, or beta diversity. In the study area there is distinctive variation identified within the Williams Member. This assemblage represents exceptional preservation of unusual fauna, distinguishing it from the more typical shallow marine fauna of the other assemblages.

11.8 WILLISTON BASIN

Many of the fossils identified within the William Lake study area were previously documented within the nearby region by Stearn (1956) and most fossils have been previously documented in southern Manitoba exposures (Young et al., 2008).

The Williston Basin and Hudson Bay Basin were situated within the Red River-Stony Mountain Province which occupied most of North America during the Late Ordovician (Elias, 1983; Elias, 1991; Webby et al., 2004). Overall this province is diverse, and diversity was highest in the Williston Basin (Webby et al., 2004). Corals show distinctive diversification patterns through the two major transgressive-regressive cycles of this province, of which the first was more diverse (Webby et al., 2004). In each cycle there was low to moderate diversity through the transgression to a maximum in the early regressive phase, followed by a decline to low levels at the extreme of regression (Webby et al., 2004). Solitary rugose corals *Bighornia patella* and *Deiracorallium angulatum* occur in both the Williston and Hudson Bay basins; *Salvadorea selecta* (=*Helicelasma selectum*) occurs in the Williston Basin and the similar species *Salvadorea distincta* (=*S. kingae*) occurs in the Hudson Bay Basin (Nelson, 1963; Elias, 1983; Elias, 1991). The solitary rugose coral species identified within the William Lake study site are consistent with those described from this biogeographic province, including *Bighornia* cf. *B. patella*, *Deiracorallium angulatum*, and *Salvadorea* sp. The specimens assigned to *Salvadorea* sp. are not identifiable to a species but have a greater affinity to the species described from the Hudson Bay Basin. The solitary rugose coral *Lobocorallium* and tabulate corals *Manipora*, *Trabeculites*, and *Protaraea* are included in the province

(Webby et al., 2004), but are not identified within the study site, suggesting that the range of these genera may not have extended to the northern edge of the basin.

The large planispirally coiled cephalopod *Kinaschukoceras churchillense* has been described and illustrated from within Member No. 4 of the Chasm Creek Formation of the Upper Ordovician of the Hudson Bay Lowlands (Nelson, 1963). This genus was previously unknown from the Ordovician within the Williston Basin. Specimens identified as *Kinaschukoceras* sp. were identified within the study site, but lacked the preservation necessary for identification to a higher level.

Salvadorea sp. of the William Lake study area shows greatest affinity to *Salvadorea kingae* of the Hudson Bay Basin. *Kinaschukoceras* is now known from the Hudson Bay Basin and the Williston Basin. These elements suggest that there could have been lateral connection between the Williston and Hudson Bay basins in the Late Ordovician.

The brachiopod assemblages from the Ordovician of southern Manitoba were recently reviewed by Jin and Zhan (2001). In the Selkirk Member of the Red River Formation, the brachiopods were assigned to the *Kjaerina hartae* Community (Jin and Zhan, 2001). The brachiopods in this member are less common than in other Ordovician rocks, and fossils were described as remarkably large. In the Gunn and Penitentiary members of the Stony Mountain Formation, the brachiopods are assigned to the *Diceromyonia storeya* Community (Jin and Zhan, 2001). Although they are diverse, they are numerically dominated by a few species. Jin and Zhan (2001) suggested that this dominance and comparable small size in these members was related to environmental stress, possibly attributable to the increased clastic input and turbidity of the Stony

Mountain seafloor. In the William Lake study area, the identifiable brachiopods are consistent with the *Diceromyonia storeya* Community, and reflect this change in community within the study area.

11.9 END-ORDOVICIAN MASS EXTINCTION

Evidence of the Ordovician radiation is readily observable in the strata of the Williston Basin. Diverse assemblages have been studied from sections in Manitoba recognizing diversification of faunas (Webby et al., 2004). Within the present study, there is identification of several diverse suites of fauna in the Stony Mountian and lower Stonewall formations and expansion into new complex environments, such as the interpreted lagoonal environment of the Williams Member. In this area of the Williston Basin, this succession represents the maximum extent of the Ordovician radiation before the end-Ordovician mass extinction.

Fossils are present through much of the studied sections. The highest position of identifiable macrofossil material from the studied material occurs within the road cut succession at approximately 2.75 m above the LS-marker, and at about 25 m depth of the M-06-79 Minago River Tower drill core (approximately 3.5 m above the LS-marker). The Stonewall Formation above this threshold contains only scattered unidentifiable bioclasts. Therefore, the maximum stratigraphic extent of the typical Ordovician fauna in the area of the Williston Basin can be constrained to the interval of the lower Stonewall Formation above the LS-marker, chronicling the first wave of the end-Ordovician mass extinction.

11.10 STRATIGRAPHY

The stratigraphy of the Ordovician within Manitoba has been debated among researchers for some time. New research developments have aided in delineating the placement of boundaries. Continued study of new exposures contributes to the global understanding of the latest Ordovician, and its stratigraphy.

The lithostratigraphic assignment of the Williams Member has been a subject of inconsistency among researchers. Some authors have placed it within the Stony Mountain Formation (Cowan, 1971; Young et al., 2008), whereas others have placed it within the Stonewall Formation (Bezys, 1995). The member is consistent with a continuation of the shallowing upward trend of the Gunn/Penitentiary Equivalent and Gunton Member of the Stony Mountain Formation, and is incongruous with the interbedded dolostones of the Stonewall Formation. This study retains placement of the Williams Member at the top of the Stony Mountain Formation.

The age of the Stonewall Formation has long been problematic for researchers. It was initially considered by Kindle (1914) to be Silurian, and this was supported by Baillie (1951). Other authors have suggested it to be Late Ordovician (Stearn, 1956; Porter and Fuller, 1959). Others still considered the formation to be both Ordovician and Silurian (Brindle, 1960; Cowan, 1971). Based on paleontologic data (conodonts) from drill cores in Saskatchewan, the Ordovician-Silurian boundary was defined within an eight-cm interval at the top of the upper *t*-marker interval (Norford et al., 1998). Recent re-examination of the upper Stonewall Formation within the Cormorant and Grand Rapids Uplands areas of Manitoba integrated stable isotope data with biostratigraphic data, suggesting the presence of the HICE (Hirnantian isotopic carbon excursion)

(Demski et al., 2011). The identification of subaerial exposure surfaces within the Stonewall Formation through the use of carbon isotope excursions will be useful in delineating the position of the Ordovician-Silurian boundary. The position of the boundary in the Williston Basin may be at the contact between the Stonewall and Fisher Branch formations. Constraint of the position is important to all areas of study of the Ordovician System.

CHAPTER 12 – CONCLUSIONS

The latest Ordovician succession exposed north of Grand Rapids, Manitoba represents distinct changes in environment and the ecologic succession of faunal assemblages, and chronicles the stratigraphy of the upper Stony Mountain and lower Stonewall formations. Study was completed on surface exposures, a road cut succession, and two drill cores. This succession had not been worked on in more than 55 years, and valuable information was gained from the application of modern concepts and approaches at previously undocumented sites.

The Stony Mountain Formation represents a shallowing upward succession, from a normal shallow marine environment of the Gunn/Penitentiary Equivalent, through increasingly restricted conditions of the Gunton Member, to extremely shallow, restricted, possibly lagoonal conditions of the Williams Member. Deposition within the Gunn/Penitentiary Equivalent was influenced by a prevailing current to the northeast, which oriented solitary rugose corals. The Stonewall Formation represents reciprocating conditions truncated by episodes of subaerial exposure.

The progression of assemblages through the succession mirrors the changing environmental conditions. The normal marine conditions of the Gunn/Penitentiary Equivalent supported a normal marine biota, dominated by solitary rugose corals. With increased stress leading into the more restricted conditions, the Gunton Member reveals low diversity, but includes some isolated occurrences of unusual taxa. The highly restricted conditions of the Williams Member allowed for exceptional preservation of a distinct suite of biota reflecting these conditions. The lower portion of the lower Stonewall Formation reveals a return to more normal marine conditions, but the

reciprocating conditions inhibited successful expansion of these faunas. The upper portion of the lower Stonewall Formation is associated with the return of a diverse normal marine fauna, represented by biota of varying lifestyles and trophic conditions.

The stratigraphy of the latest Ordovician to earliest Silurian has been problematic. Several authors have placed the Williams Member and Stonewall Formation at various positions with respect to formational and systemic boundaries. From examination of the succession in the William Lake area, it is suggested that the Williams Member be included at the top of the Stony Mountain Formation. Recent work on higher stratigraphic localities within the vicinity of the William Lake study area have suggested that the position of the Ordovician-Silurian boundary be placed at a higher stratigraphic position than previously thought, at the boundary between the Stonewall and Fisher Branch formations (Demski, 2011). The work includes integrating stable isotope data with biostratigraphic data, and the identification of subaerial exposure surfaces. The Stonewall Formation is punctuated by several ambiguous marker intervals, which make correlation of the formation difficult. The study site details a distinct marker interval, identified as LS-marker bed interval, which is interpreted to have been deposited on top of a subaerial exposure surface (top of LS-1-B1 interval). Above this marker is the development of an interval of thrombolitic mounds, the top of which is interpreted to be a subaerial exposure surface. The magnitude of this exposure is small in comparison to the identified exposure surface on which the *t*-marker was deposited (Demski, 2011). There is evidence of a possible exposure surface at the top of the Williams Member as well.

The Late Ordovician succession near William Lake chronicles a series of paleoenvironmental and paleoecological changes. The stratigraphy of the succession has

clarified some of the issues with placement of units and boundaries. This information contributes to the understanding of marine communities leading up to the latest Ordovician mass extinction. The studied succession chronicles the maximum extent of Ordovician radiation, as well as constrains the stratigraphic interval for the first wave of the end-Ordovician mass extinction.

REFERENCES

Aitken, J.D., 1967. Classification and environmental significance of crypt-algal limestones and dolomites, with illustrations from the Cambrian and Ordovician of southwestern Alberta. Journal of Sedimentary Petrology, **37**: 1163-1178.

Andrichuk, J.M., 1959. Ordovician and Silurian stratigraphy and sedimentation in southern Manitoba, Canada. American Association of Petroleum Geologists, Bulletin **43**: 2333-2398.

Baillie, A.D., 1951. Silurian geology of the Interlake area, Manitoba. Manitoba Mines Branch, Publication 50-1: 82 pp.

Baillie, A.D., 1952. Ordovician geology of Lake Winnipeg and adjacent areas. Manitoba Department of Mines and Natural Resources, Mines Branch, Publication 51-6, 82 pp.

Barnes, C.R., and Fåhræus, L.E., 1975. Provinces, communities, and the proposed nektobenthic habit of Ordovician conodontophorids. Lethaia, **8**: 133-149.

Baumiller, T.K., 2008. Crinoid ecological morphology. Annual Review of Earth and Planetary Sciences, **36**: 221-249.

Bayer, F.M., Boschema, H., Harrington, H.J., Hill, D., Hyman, L.H., Lecompte, M., Montanaro-Gallitelli, E., Moore, R.C., Stumm, E.C., and Wells., J.W., 1956. Part F: Coelenterata. *In*: Treatise on Invertebrate Paleontology, *Edited by*: R.C. Moore. Geological Society of America and University of Kansas, 358 pp.

Beadle, S.C., 1988. Dasyclads, cyclocrinitids and receptaculitids: comparative morphology and paleoecology. Lethaia, **21**: 1-12.

Beadle, S.C., and Johnson, M.E., 1986. Palaeoecology of Silurian cyclocrinitid algae. Palaeontology, **29**: 585-601.

Beaver, H.H., Caster, K.E., Durham, J.W., Fay, R.O., Fell, H.B., Kesling, R.V., Macurda, D.B., Jr., Moore, R.C., Ubaghs, G., and Wanner, J., 1967. Part S: Echinodermata 1, Volumes 1-2. *In*: Treatise on Invertebrate Paleontology, *Edited by*: R.C. Moore. Geological Society of America and University of Kansas, 650 pp.

Benson, R.H., Berdan, J.M., Van den Bold, W.A., Hanai, T., Hessland, I., Howe, H.V., Kesling, R.V., Levinson, S.A., Reyment, R.A., Moore, R.C., Scott, H.W., Shaver, R.H., Sohn, I.G., Stover, L.E., Swain, F.M., Sylvester-Bradley, P.C., and Wainwright, J., 1961. Part Q: Arthropoda 3. *In*: Treatise on Invertebrate Paleontology, *Edited by*: R.C. Moore and C.W. Pitrat. Geological Society of America and University of Kansas, 442 pp.

Bezys, R.K., 1995. Stratigraphic mapping (NTS 62I and 63G) and corehole program 1995. *In*: Manitoba Energy and Mines, Mineral Division, Report on Activities 1995: 99-108.

Bezys, R.K., 1998. P-1 Paleozoic Erosion Surface: Subcrop-Outcrop and Structure Contour Map. *In*: Manitoba Stratigraphic Database and the Manitoba Stratigraphic Map Series, Open File Report OF98-7, *Digitized by:* M.E. McFarlane. Government of Manitoba, Department of Innovation, Energy, and Mines, Mineral Resources Division.

Bezys, R.K., 2006. Summary of investigations for the sedimentary and industrial minerals section, Manitoba Geological Survey. Report on Activities 2006, Manitoba Science, Technology, Energy and Mines, Manitoba Geological Survey: 240-245.

Bezys, R.K., and Bamburak, J.D., 2004. Lower to Middle Paleozoic stratigraphy of southwestern Manitoba. Manitoba Geological Survey, Industry, Economic Development and Mines, WCSB/TGI II Field Trip guidebook, 72 pp.

Bezys, R. K., and McCabe, H. R., 1996. Lower to Middle Paleozoic stratigraphy of southwestern Manitoba – Field Trip Guide Book B4. Geological Association of Canada/Mineralogical Association of Canada Annual Meeting, Winnipeg, Manitoba, May 27-29, 1996, 92 pp.

Blakey, R.C., 2008. Gondwana paleogeography from assembly to breakup - A 500 m.y. odyssey. *In*: Resolving the Late Paleozoic Ice Age in Time and Space, *Edited by*: C.R. Fielding, T.D. Frank, and J.L. Isbell. Geological Society of America Special Paper 441, pp. 1-28.

Boardman, R.S., Cheetham, A.H., Blake, D.B., Utgaard, J., Karklins, O.L., Cook, P.L., Sandberg, P.A., Lutaud, G., and Wood, T.S., 1983. Part G: Bryozoa (revised), Volume 1. *In*: Treatise on Invertebrate Paleontology, *Edited by*: R.A. Robison. Geological Society of America and University of Kansas, 626 pp.

Bottjer, D.J., Droser, M.L., Sheehan, P.M., and McGhee, G.R., Jr., 2001. The ecological architecture of major events in the Phanerozoic history of marine invertebrate life. *In*: Evolutionary Paleoecology: The Ecological Context of Macroevolutionary Change. *Edited by*: W.D. Allmon and D.J. Bottjer. Columbia University Press, pp. 35-61.

Briggs, D.E.G., 1992. Conodonts: a major extinct group added to the vertebrates. Science, **256**: 1285-1286.

Brindle, J.E., 1960. The faunas of the Lower Palaeozoic carbonate rocks in the subsurface of Saskatchewan. Saskatchewan Department of Mineral Resources, **52**, 45 pp.

Bromley, R.G., 1972. On some ichnotaxa in hard substrates, with a redefinition of *Trypanites* Magdefrau. Paläontologische Zeitschrift, **46**: 93-99.

Brower, J.C., and Kile, K.M., 1988. Seriation of an original data matrix as applied to paleoecology. Lethaia, **21**: 79-93.

Choquette, P.W., and Pray, L.C., 1970. Geologic nomenclature and classification of porosity in sedimentary carbonates. Bulletin of the American Association of Petroleum Geologists, **54**: 207-250.

Cowan, J., 1971. Ordovician and Silurian stratigraphy of the Interlake area, Manitoba. *In*: Geoscience Studies in Manitoba, *Edited by*: A.C. Turnock, Geological Association of Canada, Special Paper 9, pp. 235-241.

Cowan, J., 1977. Ordovician and Silurian stratigraphy of the Interlake area, Manitoba. M.Sc. Thesis, University of Manitoba, Winnipeg, Manitoba, 73 pp.

Cuffey, R.J., 1972. The roles of bryozoans in modern coral reefs. Geologische Rundschau, **61**: 542-550.

Demicco, R.V., and Hardie, L.A., 1994. Sedimentary structures and early diagenetic features of shallow marine carbonate deposits. Society for Sedimentary Geology (SEPM), Atlas Series Number 1, 265 pp.

Demski, M.W., Wheadon, B.J., Stewart, L.A., Elias, R.J., Young, G.A., Nowlan, G.S., and Dobrzanski, E.P., 2011. Ordovician-Silurian boundary interval in the Williston and Hudson Bay basins, Manitoba: isotopic carbon excursion and conodont turnover. GAC/AGC-MAC/AMC-SEG-SGA Joint Annual Meeting, University of Ottawa, May 25-27, Abstracts, **34**: 50-51.

Dickson, J.A.D., 1966. Carbonate identification and genesis as revealed by staining. Journal of Sedimentary Research, **36**: 491-505.

Dowling, D.B., 1900. Report on the geology of the west shore and islands of Lake Winnipeg. Geological Survey of Canada, Annual Report 1898, Part F, 100 pp.

Droser, M.L., Bottjer, D.J., Sheehan, P.M., and McGhee, G.R., Jr., 2000. Decoupling of taxonomic and ecologic severity of Phanerozoic marine mass extinctions. Geology, **28**: 675-678.

Droser, M.L., and Finnegan, S., 2003.The Ordovician Radiation: a follow-up to the Cambrian Explosion? Integrative and Comparative Biology, **43**: 178-184.

Droser, M.L., and Sheehan, P.M., 1997. Palaeoecology of the Ordovician radiation; resolution of large-scale patterns with individual clade histories, palaeogeography and environments. Geobios, **20**: 221-229.

Duncan, H., 1957. *Bighornia*, a new Ordovician coral genus. Journal of Paleontology, **31**: 607-615.

Dunham, R.J., 1962. Classification of carbonate rocks according to depositional texture. American Association of Petroleum Geologists Memoir 1, pp. 108-121.

Ekdale, A.A., Bromley, R.G., and Pemberton, S.G., 1984. Ichnology: trace fossils in sedimentology and stratigraphy. Society of Economic Paleontologists and Mineralogists, Short Course No. 15, 317 pp.

Elias, R.J., 1980. Borings in solitary rugose corals of the Selkirk Member, Red River Formation (late Middle or Upper Ordovician), southern Manitoba. Canadian Journal of Earth Sciences, **17**: 272-277.

Elias, R.J., 1982. Paleoecology and biostratinomy of solitary rugose corals in the Stony Mountain Formation (Upper Ordovician), Stony Mountain, Manitoba. Canadian Journal of Earth Sciences, **19**: 1582-1598.

Elias, R.J., 1983. Late Ordovician solitary rugose corals of the Stony Mountain Formation, southern Manitoba, and its equivalents. Journal of Paleontology, **57**: 924-956.

Elias, R.J., 1991. Environmental cycles and bioevents in the Upper Ordovician Red River-Stony Mountain solitary rugose coral province of North America. *In*: Advances in Ordovician Geology. *Edited by*: C.R. Barnes and S.H. Williams. Geological Survey of Canada, Paper 90-9, pp. 205-211.

Elias, R.J., 2010. Stability strategies and hydrodynamic behavior of liberosessile solitary rugose corals (Ordovician; Red River-Stony Mountain Province, North America). Palaeoworld, **19**: 368-373.

Elias, R.J., McAuley, R.J., and Mattison, B.W., 1987. Directional orientations of solitary rugose corals. Canadian Journal of Earth Sciences, **24**: 806-812.

Elias, R.J., Nowlan, G.S., and Bolton, T.E., 1988. Paleontology of the type section, Fort Garry Member, Red River Formation (Upper Ordovician), southern Manitoba. New Mexico Bureau of Mines and Mineral Resources Memoir 44, pp. 341-359.

Elias, R.J., and Young, G.A., 2000. Enigmatic fossil encrusting an Upper Ordovician rocky shore on Hudson Bay, Canada, is a coral. Journal of Paleontology, **74**: 179-180.

Elias, R.J., Zeilstra, R.G., and Bayer, T.N., 1988. Paleoenvironmental reconstruction based on horn corals, with an example from the Late Ordovician of North America. Palaios, **3**: 22-34.

Embry, A.F., III, and Klovan, J.E., 1972. Absolute water depth limits of Late Devonian paleoecological zones. Geologische Rundschau, **61**: 672-686.

Gensmer, R.P., and Weiss, M.P., 1980. Accuracy of calcite/dolomite ratios by X-ray diffraction and comparison with results from staining techniques. Journal of Sedimentary Research, **50**: 626-629.

Goddard, E.N., Trask, P.D., DeFord, R.K., Rove, O.N, Singewald, J.T., Jr., and Overbeck, R.M., 1970. Rock-Color Chart. Geological Society of America, Boulder.

Google (2012): Google Maps Canada, URL <http://maps.google.ca/maps>, February 15, 2012.

Hammer, O., 2002. Palaeontological community and diversity analysis-brief notes. Reference Manual for PAST (PAlaeontological Statistics), URL <http://nhm2.uio.no/norlex/past/doc1.html>, April 1, 2012: 226 pp.

Harper, D.A.T., 2006: The Ordovician biodiversification: Setting an agenda for marine life. Palaeogeography, Palaeoclimatology, Palaeoecology, **232**: 148-166.

Harrington, H.J., Henningsmoen, G., Howell, B.F., Jaanusson, V., Lochman-Balk, C., Moore, R.C., Poulsen, C., Rasetti, F., Richter, E., Schmidt, H., Sdzuy, K., Struve, W., Størmer, L., Stubblefield, C.J., Tripp, R., Weller, J.M., and Whittington, H.B., 1959. Part O: Arthropoda 1. *In*: Treatise on Invertebrate Paleontology, *Edited by*: R.C. Moore. Geological Society of America and University of Kansas, 560 pp.

Hass, W.H., Häntzschel, W., Fisher, D.W., Howell, B.F., Rhodes, F.H.T., Müller, K.J., and Moore, R.C., 1962. Part W: Miscellanea, Conodonts, conoidal shells of uncertain affinities, worms, trace fossils and problematica. *In*: Treatise on Invertebrate Paleontology, *Edited by*: R.C. Moore. Geological Society of America and University of Kansas, 259 pp.

Hill, D., 1981. Part F: Coelenterata, Supplement 1: Rugosa and Tabulata, Volumes 1-2. *In*: Treatise on Invertebrate Paleontology, *Edited by*: C. Teichert. Geological Society of America and University of Kansas, 762 pp.

Jin, J., and Zhan, R., 2001. Late Ordovician articulate brachiopods from the Red River and Stony Mountain formations, southern Manitoba. National Research Council Press, Ottawa, 117 pp.

Johnson, M.E., and Lescinsky, H.L., 1986. Depositional dynamics of cyclic carbonates from the Interlake Group (Lower Silurian) of the Williston Basin. Palaios, **1**: 111-121.

Kendall, A.C., 1976. The Ordovician carbonate succession (Bighorn Group) of southwestern Saskatchewan. Department of Mineral Resources, Saskatchewan Geological Survey, Sedimentary Geology Division, Report No. 180, 186 pp.

Kendall, A.C., 1977. Origin of dolomite mottling in Ordovician limestones from Saskatchewan and Manitoba. Bulletin of Canadian Petroleum Geology, **25**: 480-504.

Kennard, J.M., and James, N.P., 1986. Thrombolites and stromatolites: two distinct types of microbial structures. Palaios, **1**: 492-503.

Kershaw, S., 1998. The applications of stromatoporoid palaeobiology in palaeoenvironmental analysis. Palaeontology, **41**: 509-544.

Kershaw, S., and West, R.R., 1991. Chaetetid growth form and its controlling factors. Lethaia, **24**: 333-346.

Kindle, E.M.,1914. The Silurian and Devonian section of western Manitoba. Geological Survey of Canada, Summary Report 1912, pp. 247-261.

Knight, J.B., Cox, L.R., Keen, A.M., Smith, A.G., Batten, R.L., Yochelson, E.L. Ludbrook, N.H., Robertson, R., Yonge, C.M., and Moore, R.C., 1960. Part I: Mollusca 1. *In*: Treatise on Invertebrate Paleontology, *Edited by*: R.C. Moore and C.W. Pitrat. Geological Society of America and University of Kansas, 351 pp.

Kohut, J.J., and Sweet, W.C., 1968. The American Upper Ordovician standard. X. Upper Maysville and Richmond conodonts from the Cincinnati region of Ohio, Indiana, and Kentucky. Journal of Paleontology, **42**: 1456-1477.

Koleff, P., Gaston, K.J., and Lennon, J.J., 2003. Measuring beta diversity for presence-absence data. Journal of Animal Ecology, **72**: 367-382.

Landing, E., English, A., and Keppie, J.D., 2010. Cambrian origin of all skeletalized metazoan phyla – discovery of Earth's oldest bryozoans (Upper Cambrian, southern Mexico). Geology, **38**: 547-550.

Lee, D., and Elias, R.J., 1991. Mode of growth and life-history strategies of a Late Ordovician halysitid coral. Journal of Paleontology, **65**: 191-199.

Leith, E.I., 1952. Schizocoralla from the Ordovician of Manitoba. Journal of Paleontology, **26**: 789-796.

Linsley, R.M., 1977. “Laws” of gastropod shell form. Paleobiology, **3**: 196-206.

Lobdell, F.K., 1992. Arthrostylidae (Bryozoa: Cryptostomata) from the Gunn Member, Stony Mountain Formation (Upper Ordovician), North Dakota and Manitoba. *In*: Proceedings of the F.D. Holland Jr., Geological Symposium, *Edited by*: J.M. Erikson and J.W. Hoganson. North Dakota Geological Survey, Miscellaneous Series 76, pp. 99-115.

Lowe, D.R., and LoPiccolo, R.D., 1974. The characteristics and origins of dish and pillar structures. Journal of Sedimentary Petrology, **44**: 484-501.

McCabe, H.R., 1971. Stratigraphy of Manitoba, an introduction and review. *In*: Geoscience Studies in Manitoba, *Edited by*: A.C. Turnock. Geological Association of Canada Special Paper No. 9, pp. 167-187.

McCabe, H.R., 1979. Stratigraphic mapping program. Report on Field Activities 1979, Manitoba Department of Mines, Natural Resources and Environment, Mineral Resources Division, pp. 72-75.

McCabe, H.R., and Barchyn, D., 1982. Paleozoic stratigraphy of southwestern Manitoba. Geological Association of Canada and Mineralogical Association of Canada, Joint Annual Meeting, Winnipeg, Manitoba, Field Trip Guidebook, Trip 10, 47 pp.

McInnes, W., 1913. The basins of the Nelson and Churchill rivers. Geological Survey of Canada, Memoir No. 30, 146 pp.

Mendenhall, W., Beaver, R.J., and Beaver, B.M., 2006. Introduction to Probability and Statistics. Thomson Learning Inc., Belmont, California, 746 pp.

Myrow, P.M., 1995. *Thalassinoides* and the enigma of Early Paleozoic open-framework burrow systems. Palaios, **10**: 58-74.

Natural Resources Canada, 2012. The Atlas of Canada – Toporama, URL <http://atlas.nrcan.gc.ca/site/english/maps/topo/map>, June 23, 2012.

Nelson, S.J., 1963. Ordovician paleontology of the northern Hudson Bay Lowland. Geological Society of America, Memoir 90, 152 pp.

Nelson, S.J., 1981. Solitary streptelasmatid corals, Ordovician of northern Hudson Bay Lowland, Manitoba, Canada. Palaeontographica, Abteilung A, **172**: 1-71.

Nitecki, M.H., Webby, B.D., Spjeldnaes, N., and Yong-Yi, Z., 2004. Receptaculitids and algae. *In:* The Great Ordovician Biodiversification Event, *Edited by:* B.D. Webby, F. Paris, M.L. Droser, and I.G. Percival. Columbia University Press, New York., pp. 336-347.

Norford, B.S., Nowlan, G.S., Haidl, F.M., and Bezys, R.K., 1998. The Ordovician-Silurian boundary interval in Saskatchewan and Manitoba. *In*: Eighth International Williston Basin Symposium, *Edited by*: J.E. Christopher, C.F. Gilboy, D.F. Paterson, and S.L. Bend. Saskatchewan Geological Society Special Publication Number 13, pp. 27-45.

Nowlan, G.S., 2008. Paleontological Report 004-GSN-2008. Geological Survey of Canada (Calgary), 4 pp.

Nowlan, G.S., 2009. Paleontological Report 002-GSN-2009. Geological Survey of Canada (Calgary), 13 pp.

Nowlan, G.S., and Haidl, F.M., 2001. Biostratigraphy and paleoecology of Late Ordovician conodonts from a composite section in the subsurface of Saskatchewan. Saskatchewan Energy and Mines Miscellaneous Report 2001-4.1, pp. 14-31.

Okulitch, V.J., 1943. The Stony Mountain Formation of Manitoba. Transactions of the Royal Society of Canada, Section IV, **37**: 59-73.

Paine, R.T., 1970. The sediment occupied by Recent lingulid brachiopods and some paleoecological implications. Palaeogeography, Palaeoclimatology, Palaeoecology, **7**: 21-31.

Plotnick, R.E., 1985. Lift based mechanisms for swimming in eurypterids and potunid crabs. Transactions of the Royal Society of Edinburgh: Earth Sciences, **76**: 325-337.

Porter, J.W., and Fuller, J.G.C.M., 1959. Lower Paleozoic rocks of northern Williston Basin and adjacent areas. Bulletin of the American Association of Petroleum Geologists, **43**: 124-189.

Riding, R., 2000. Microbial carbonates: the geologic record of calcified bacterial-algal mats and biofilms. Sedimentology, **47**: 179-214.

Rigby, J.K., 1971. Sponges of the Ordovician Cat Head Member, Lake Winnipeg, Manitoba. *In*: Contributions to Canadian Paleontology: Fossils of the Ordovician Red River Formation (Cat Head Member), Manitoba. Geological Survey of Canada, Bulletin 202, pp. 35-79.

Rigby, J.K. (coordinating author), Finks, R.M., Reid, R.E.H., and Rigby, J.K. (authors), 2003. Part E: Porifera (revised), Volume 2. *In*: Treatise on Invertebrate Paleontology, *Edited by*: R.L. Kaesler. Geological Society of America and University of Kansas, 349 pp.

Rudkin, D.M., Young, G.A., and Nowlan, G.S., 2008. The oldest horseshoe crab: a new xiphosurid from Late Ordovician Konservat-Lagerstatten deposits, Manitoba, Canada. Palaeontology, **51**: 1-9.

Schopf, J.M., 1969. Paleoecology of Ectoprocts (Bryozoans). Journal of Paleontology, **43**: 234-244.

Scrutton, C.T., 1997. The Paleozoic corals, I: origins and relationships. Proceedings of the Yorkshire Geological Society, **51**: 177-208.

Scrutton, C.T., 1998. The Paleozoic corals, II: structure, variation and palaeoecology. Proceedings of the Yorkshire Geological Society, **52**: 1-57.

Scrutton, C., 1999. Paleozoic corals: their evolution and palaeoecology. Geology Today, **15**: 184-193.

Sepkoski, J.J., Jr., 1996. Patterns of Phanerozoic extinction: a perspective from global databases. *In*: Global Events and Event Stratigraphy, *Edited by*: O.H. Walliser. Berlin, Springer, pp. 35-51.

Servais, T., Harper, D.A.T., Li, J., Munnecke, A., Owen, A.W., and Sheehan, P.M., 2009. Understanding the Great Ordovician Biodiversification Event (GOBE): influences of paleogeography, paleoclimate, or paleoecology? GSA Today, **19**: 4-10.

Servais, T., Owen, A.W., Harper, D.A.T., Kröger, B., and Munnecke, A., 2010. The Great Ordovician Biodiversification Event (GOBE): the palaeoecological dimension. Palaeogeography, Palaeoclimatology, Palaeoecology, **294**: 99-119.

Sheehan, P., 2001. The Late Ordovician mass extinction. Annual Review of Earth and Planetary Sciences, **29**: 331-364.

Shimer, H.W., and Shrock, R.R., 1944. Index Fossils of North America. The Massachusetts Institute of Technology Press, Cambridge, Massachusetts, 837 pp.

Sinclair, G.W., and Leith, E.I., 1958. New name for an Ordovician shale in Manitoba. Journal of Paleontology, **32**: 243-244.

Smith, D.L., 1963. A lithologic study of the Stony Mountain and Stonewall formations in southern Manitoba. M.Sc. Thesis, University of Manitoba, Winnipeg, 219 pp.

Stearn, C.W., 1956. Stratigraphy and palaeontology of the Interlake Group and Stonewall Formation of southern Manitoba. Geological Survey of Canada, Memoir 281, 162 pp.

Stearn, C.W., Webby, B.D., Nestor, H., and Stock, C.W., 1999. Revised classification and terminology of Paleozoic stromatoporoids. Acta Palaeontologica Polonica, **44**: 1-70.

Stirling, G., and Wilsey, B., 2001. Empirical relationships between species richness, evenness, and proportional diversity. The American Naturalist, **158**: 286-299.

Sweet, W., 1971. An ecologic model for conodonts. Journal of Paleontology, **45**: 869-880.

Sweet, W.C., 1979. Late Ordovician conodonts and biostratigraphy of the western Midcontinent Province. *In*: Conodont Biostratigraphy of the Great Basin and Rocky Mountains, *Edited by*: C.A. Sandberg and D.L. Clark. Bringham Young University, Geology Studies 26, pp. 45-85.

Sweet, W.C., 1982. Conodonts from the Winnipeg Formation (Middle Ordovician) of northern Black Hills, South Dakota. Journal of Paleontology, **56**: 1029-1049.

Sweet, W.C., 1988. The Conodonta: morphology, taxonomy, paleoecology, and evolutionary history of a long-extinct animal phylum. Oxford University Press, 212 pp.

Sweet, W.C., and Donoghue, P.C.J., 2001. Conodonts: past, present, future. Journal of Paleontology, **75**: 1174.

Taylor, P.D., and Ernst, A., 2004. Bryozoans. *In*: The Great Ordovician Biodiversification Event, *Edited by*: B.D. Webby, F. Paris, M.L. Droser, and I.G. Percival. Columbia University Press, New York, pp. 147-156.

Teichert, C., Kummel, B., Sweet, W.C., Stenzel, H.B., Furnish, W.M., Glenister, B.F., Erben, H.K., Moore, R.C., and Nodine Zeller, D.E., 1964. Part K: Mollusca 3. *In*: Treatise on Invertebrate Paleontology, *Edited by*: R.C. Moore. Geological Society of America and University of Kansas, 519 pp.

Theiling, B.P., Railsback, L.B., Holland, S.M., and Crowe, D.E., 2007. Heterogeneity in geochemical expression of subaerial exposure in limestones, and its implications for sampling to detect exposure surfaces. Journal of Sedimentary Research, **77**: 159-169.

Tyrrell, J.B., 1892. Report on north-western Manitoba with portions of the adjacent districts of Assiniboia and Saskatchewan. Geological Survey of Canada, Annual Report 1890-91, Part E, 240 pp.

Ulrich, E.O., 1889. On some Polyzoa (Bryozoa) and Ostracoda from the Cambro-Silurian rocks of Canada, part 2. Contributions to the Micro-Palaeontology of the Cambro-

Silurian Rocks of Canada, Geological and Natural History Survey of Canada, pp. 27-57.

Webby, B.D., 2004. Stromatoporoids. *In*: The Great Ordovician Biodiversification Event, *Edited by*: B.D. Webby, F. Paris, M.L. Droser, and I.G. Percival. Columbia University Press, New York, pp. 112-118.

Webby, B.D., Elias, R.J., Young, G.A., Neuman, B.E.E., and Kaljo, D., 2004. Corals. *In*: The Great Ordovician Biodiversification Event, *Edited by*: B.D. Webby, F. Paris, M.L. Droser, and I.G. Percival. Columbia University Press, New York, pp. 124-146.

Weber, J.N., and Smith, F.G., 1961. Rapid determination of calcite-dolomite ratios in sedimentary rocks. Journal of Sedimentary Petrology, **31**: 130-132.

Westrop, S.R., and Ludvigsen, R., 1983. Systematics and paleoecology of Upper Ordovician trilobites from the Selkirk Member of the Red River Formation, southern Manitoba. Manitoba Department of Energy and Mines, Mineral Resources Division, Geological Report GR 82-2, 51 pp.

Whiteaves, J.F., 1897. The fossils of the Galena-Trenton and Black River formations of Lake Winnipeg and its vicinity. Geologic Survey of Canada, Paleozoic Fossils, vol. 3, pt. 3, pp. 129-242.

Williams, A., Brunton, C.H.C., Carlson, S.J., Alvarez, F., Ansell, A.D., Baker, P.G., Bassett, M.G., Blodgett, R.G., Boucot, A.J., Carter, J.L., Cocks, L.R.M., Cohen, B.L., Copper, P., Curry, G.B., Cusack, M., Dagys, A.S., Emig, C.C., Gawthrop, A.B., Gourvennec, R., Grant, R.E., Harper, D.A.T., Holmer, L.E., Hou, H., James, M.A., Jin, Y., Johnson, J.G., Laurie, J.R., Lazarev, S., Lee, D.E., Mackay, S., MacKinnon, D.I., Manceñido, M.O., Mergl, M., Owen, E.F., Peck, L.S., Popov, L.E., Racheboeuf, P.R., Rhodes, M.C., Richardson, J.R., Rong J., Rubel, M., Savage, N.M., Smirnova, T.N., Sun, D., Walton, D., Wardlaw, B., and Wright, A.D., 1997. Part H: Brachiopoda, Volume 1. *In*: Treatise on Invertebrate Paleontology, *Edited by*: R.L. Kaesler. Geological Society of America and University of Kansas, 525 pp.

Wong, S., 2002. Paleoenvironmental and paleoecological reconstruction of the Tyndall Stone, Selkirk Member, Red River Formation (Late Ordovician), southern Manitoba. M.Sc. Thesis, University of Manitoba, Winnipeg, 343 pp.

Young, G.A., and Elias, R.J., 1999A. Relationships between internal and external morphology in *Paleofavosites* (Tabulata): the unity of growth and growth form. Journal of Paleontology, **73**: 580-597.

Young, G.A., and Elias, R.J., 1999B. Coral distribution and association in the Upper Ordovician Stony Mountain Formation of Manitoba. Acta Universitatis Carolinae, Geologica, **43**: 429-432.

Young, G.A., Elias, R.J., Wong, S., and Dobrzanski, E.P., 2008. Upper Ordovician rocks and fossils in southern Manitoba. Canadian Paleontology Conference, Winnipeg, Manitoba, Field Trip Guidebook No. 13, 97 pp.

Young, G.A., and Hagadorn, J.W., 2010. The fossil record of cnidarian medusae. Palaeoworld, **19**: 212-221.

Young, G.A., Rudkin, D.M., Dobrzanski, E.P., Robson, S.P., and Nowlan, G.S., 2007. Exceptionally preserved Late Ordovician biotas from Manitoba, Canada. Geology, **35**: 883-886.

APPENDIX A: LOCATION DATA

Details of the geographic coordinates, stratigraphic heights of the localities measured above the lowest surface exposure and above base of road cut succession, and length of drill holes used for the study.

APPENDIX A.1 – Surface exposures.

APPENDIX A.2 – Road cut succession.

APPENDIX A.3 – Drill cores.

APPENDIX A.1 – SURFACE EXPOSURES

Surface Exposures

POSITION	UTM		GEOGRAPHIC		HEIGHT
	NAD 27 N	NAD 27 E	Latitude	Longitude	(m)
BC-1-A	5990164	489251	54° 03' 41.5"	99° 09' 51.2"	0.52
BC-1-B	5990193	489286	54° 03' 42.5"	99° 09' 49.3"	0.00
BC-1-C	5990172	489283	54° 03' 41.8"	99° 09' 49.4"	0.35
BC-1-D	5990111	489240	54° 03' 39.8"	99° 09' 51.8"	1.16
BC-1-E	5990074	489239	54° 03' 38.6"	99° 10' 00.7"	0.75
BC-2	5989444	489076	54° 03' 18.2"	99° 10' 01.8"	1.74
BC-3	5989354	489056	54° 03' 15.3"	99° 10' 07.1"	1.89
BC-4-A	5989030	488959	54° 03' 04.8"	99° 10' 08.7"	2.64
BC-4-B	5988965	488930	54° 03' 02.7"	99° 10' 04.9"	2.90
BC-4-C	5988896	488999	54° 03' 00.5"	99° 10' 26.8"	2.96
BC-5	5987777	488598	54° 02' 24.2"	99° 10' 28.1"	3.84
BC-6	5987719	488574	54° 02' 22.4"	99° 10' 27.4"	3.86
BC-7	5987586	488587	54° 02' 18.0"	99° 10' 42.8"	4.00
BC-8-A	5986509	488304	54° 01' 43.2"	99° 10' 42.5"	11.20
BC-8-B	5986504	488309	54° 01' 43.0"	99° 10' 42.4"	11.45
BC-8-C	5986502	488310	54° 01' 43.0"	99° 10' 42.4"	11.71
BC-8-D	5986502	488310	54° 01' 43.0"	99° 10' 42.4"	11.81
BC-8-E	5986498	488280	54° 01' 42.8"	99° 10' 44.1"	12.33
BC-8-F	5986451	488301	54° 01' 41.3"	99° 10' 42.8"	13.50
BC-8-G	5986421	488280	54° 01' 40.3"	99° 10' 44.1"	13.91
BC-8-H	5986426	488206	54° 01' 40.5"	99° 10' 48.1"	14.20
BC-8-I	5986397	488198	54° 01' 39.6"	99° 10' 48.6"	14.81
BC-8-J	5986381	488193	54° 01' 39.0"	99° 10' 48.9"	15.15
BC-8-K	5986368	488197	54° 01' 38.6"	99° 10' 48.6"	15.39
BC-8-L	5986358	488195	54° 01' 38.3"	99° 10' 48.7"	15.72
BC-9-A	5986106	488163	54° 01' 30.1"	99° 10' 50.5"	15.18
BC-9-B	5986111	488184	54° 01' 30.3"	99° 10' 49.3"	15.37
BC-9-C	5986106	488191	54° 01' 30.1"	99° 10' 48.9"	16.26
BC-9-D	5986080	488212	54° 01' 29.3"	99° 10' 47.8"	17.41
BC-9-E	5985925	488227	54° 01' 24.3"	99° 10' 48.9"	18.28
BC-10	5985839	488040	54° 01' 21.5"	99° 10' 57.2"	18.41

BC-11-A	5985685	488033	54° 01' 16.5"	99° 10' 57.5"	18.93
BC-11-B	5985648	488028	54° 01' 15.3"	99° 10' 57.8"	19.60
BC-11-C	5985646	488031	54° 01' 15.2"	99° 10' 57.6"	19.69
BC-11-D	5985643	488030	54° 01' 15.1"	99° 10' 57.7"	19.90
BC-11-E	5985625	488031	54° 01' 14.6"	99° 10' 57.6"	20.13
BC-11-F	5985588	488027	54° 01' 13.4"	99° 10' 57.9"	20.46
BC-11-G	5985567	488030	54° 01' 12.7"	99° 10' 57.7"	20.65
BC-11-H	5985555	488030	54° 01' 12.3"	99° 10' 57.7"	21.00
BC-11-I	5985544	488027	54° 01' 11.9"	99° 10' 57.9"	21.35
BC-11-J	5985528	488026	54° 01' 11.4"	99° 10' 57.9"	22.20
BC-11-EU	5985520	488025	54° 01' 11.2"	99° 10' 58.0"	22.52
BC-11-K	5985511	488020	54° 01' 10.9"	99° 10' 58.2"	22.95
BC-11-L	5985506	488017	54° 01' 10.7"	99° 10' 58.4"	23.25
BC-11-M	5985503	488017	54° 01' 10.6"	99° 10' 58.4"	23.41
BC-11-N	5985499	488014	54° 01' 10.5"	99° 10' 58.5"	23.54
BC-11-O	5985493	488013	54° 01' 10.3"	99° 10' 58.6"	23.76
BC-11-P	5985486	488009	54° 01' 10.1"	99° 10' 58.8"	24.30
BC-11-Q	5985405	488030	54° 01' 07.4"	99° 10' 57.7"	24.79
BC-11-R	5985397	488030	54° 01' 07.2"	99° 10' 57.7"	25.03
BC-11-S	5985391	488026	54° 01' 07.0"	99° 10' 57.9"	25.45
BC-11-T	5985375	488018	54° 01' 06.5"	99° 10' 58.3"	26.28
BC-11-U	5985361	488019	54° 01' 06.0"	99° 10' 58.3"	26.89
BC-11-V	5985355	488017	54° 01' 05.8"	99° 10' 58.4"	27.27
BC-11-W	5985354	488017	54° 01' 05.8"	99° 10' 58.1"	27.36
BC-11-X	5985345	488022	54° 01' 05.5"	99° 10' 58.4"	27.55
BC-11-Y	5985339	488023	54° 01' 05.3"	99° 10' 58.0"	27.67
BC-11-Z	5985335	488021	54° 01' 05.2"	99° 10' 58.1"	28.23
BC-11-AA	5985334	488021	54° 01' 05.1"	99° 10' 58.1"	28.32
BC-11-BB	5985320	488026	54° 01' 04.7"	99° 10' 57.9"	28.50
BC-11-CC	5985311	488020	54° 01' 04.4"	99° 10' 58.2"	30.20
BC-11-DD	5985300	488018	54° 01' 04.0"	99° 10' 58.3"	30.99
BC-11-EE	5985291	488018	54° 01' 03.7"	99° 10' 58.3"	31.54
BC-11-FF	5985273	488013	54° 01' 03.2"	99° 10' 58.6"	31.94
DRILL	5985262	488007	54° 01' 02.8"	99° 10' 58.9"	32.61

APPENDIX A.2 – ROAD CUT SUCCESSION

Road Cut Succession					
POSITION	UTM		GEOGRAPHIC		HEIGHT
	NAD 27 N	NAD 27E	Latitude	Longitude	(m)
LS-1 (North)	5985502	487925	54° 01' 10.6"	99° 11' 03.5"	
LS-1 (South)	5985082	487805	54° 00' 57.0"	99° 11' 10.0"	
LS-1-B12					0.75
LS-1-B11					1.25
LS-1-B10					2.05
LS-1-B9					2.48
LS-1-B8					3.24
LS-1-B7					3.38
LS-1-B6					4.65
LS-1-B5					4.79
LS-1-B4					5.55
LS-1-B3					5.69
LS-1-B2					6.56
LS-1-B1					6.94
LS-1-MB					7.24
LS-1-A1					7.80
LS-1-A2					11.60
LS-2 (North)	5985547	487897	54° 01' 12.0"	99° 11' 05.0"	
LS-2 (South)	5985139	487777	54° 00' 58.8"	99° 11' 11.5"	

APPENDIX A.3 – DRILL CORES

Drill Cores					
POSITION	UTM		GEOGRAPHIC		LENGTH
	NAD 27 N	NAD 27E	Latitude	Longitude	(m)
M-2-05	5985262	488007	54° 01' 02.8"	99° 10' 58.9"	90.6
M-6-79	5980034	486200	53° 58' 13.5"	99° 12' 37.3"	111.9

APPENDIX B – LITHOFACIES DESCRIPTION

Detailed descriptions that were used to identify lithofacies for the study site localities. Sedimentologic characteristics were utilized for identification of lithofacies. Mineralogy, lithologic characteristics, and sedimentary features are summarized.

Classification of carbonate rocks follows Dunham (1962) as modified by Embry and Klovan (1972). Porosity classification follows Choquette and Pray (1970). Colour descriptions are derived from the "Geological Society of America Rock-Color Chart" (Goddard et al., 1970).

Bioturbation
x = bioturbation mottling that is unidentifiable to an ichnogenus
x_T = bioturbation mottling that is identifiable as *Thalassinoides*

APPENDIX B.1 – lithofacies descriptions for surface exposures.

APPENDIX B.2 – lithofacies descriptions for road cut succession.

APPENDIX B.1 - Lithofacies descriptions for surface exposures.

Location	Comp.		Lithology			Porosity					Sedimentary features												Colour		Comments	
	dolomite	silicification	mudstone	wackestone	packstone	%	vuggy	interparticle	moldic	fracture	massive	bedded	nodular	bioturbation	thrombolites	laminations	brecciation	evaporite molds	iron oxides	chert	% bioclasts	fresh	weathered		Lithofacies
BC-1-A	×		×			1-2		×			×							×	×		10	v.p. orange - p. yellowish brown	v.l. gray - white	1-2 mm evaporite molds, echinoderms	1
BC-1-B	×	×	×			3-5	×	×			×								×		5	v.p. orange - p. yellowish brown	v.l. gray - white	echinoderms	1
BC-1-C	×	×	×	×		5	×	×	×		×			$×_T$					×		10-20	v.p. orange - p. yellowish brown	v.l. gray - white	bioclast concentration in burrows	1
BC-1-D	×		×			3-5	×	×			×			×				×	×		10	v.p. orange - p. yellowish brown	v.l. gray - white	fossil dissolution, bioclasts in burrows	1
BC-1-E	×	×	×			5	×	×			×		×	×					×	×	5	v.p. orange - p. yellowish brown	v.l. gray - white	nodes 15 mm diameter, silicified fossils	1
BC-2	×	×	×			3-5	×	×		×	×								×		5	v.p. orange - p. yellowish brown	v.l. gray - white		1
BC-3	×	×	×			1-2	×	×			×							×	×	×	5	v.p. orange - p. yellowish brown	v.l. gray - white	silicified fossils and patches; corals	1
BC-4-A	×		×			3-5	×	×			×							×	×	×	5	v.p. orange - p. yellowish brown	v.l. gray - white		1
BC-4-B	×		×			3-5	×	×			×			×				×	×	×		v.p. orange - p. yellowish brown	v.l. gray - white		1
BC-4-C	×	×	×			5	×	×	×		×							×	×	×	5	p. - dk yellowish brown	v.l. gray - white	silicified fossils, 2-3 mm evaporite molds	1
BC-5	×		×			3-5	×	×			×								×		5	v.p. orange - p. yellowish brown	v.l. gray - white		1
BC-6	×		×			1-2	×	×			×			×					×		5	v.p. orange - p. yellowish brown	v.l. gray - white		1
BC-7	×		×			1-2	×	×		×	×			×					×		5	v.p. orange - p. yellowish brown	v.l. gray - white		1
BC-8-A	×		×			3-5		×			×			$×_T$							<5	v.p. orange	v.l. gray - white	*Thalassinoides* prominent; white whisps	2
BC-8-B	×		×			3-5		×		×	×			$×_T$							<5	v.p. orange	v.l. gray - white	*Thalassinoides* prominent, bioclast in burrows	2
BC-8-C	×		×			1-2		×			×			$×_T$							<5	v.p. orange	v.l. gray - white	*Thalassinoides* prominent, dissolution	2
BC-8-D	×		×			3-5		×	×		×			$×_T$							<5	v.p. orange	v.l. gray - white	*Thalassinoides* prominent	2
BC-8-E	×		×			1-2		×			×			$×_T$							<5	v.p. orange	v.l. gray - white	*Thalassinoides* prominent	2

Location	Comp.		Lithology			Porosity					Sedimentary features											Colour		Comments	
	dolomite	silicification	mudstone	wackestone	packstone	%	vuggy	interparticle	moldic	fracture	massive	bedded	nodular	bioturbation	thrombolites	laminations	brecciation	evaporite molds	iron oxides	chert	% bioclasts	fresh	weathered		Lithofacies
BC-8-G	×		×			1-2		×			×			$\times_T$							<5	v.p. grey - white	v.l. gray - white	bioclast concentration in burrows	3
BC-8-H	×		×			1-2		×			×			$\times_T$							<5	v.p. grey - white	v.l. gray - white		3
BC-8-I	×		×			1-2		×			×			$\times_T$							<5	v.p. grey - white	v.l. gray - white	clotted appearance	3
BC-8-J	×		×			1-2		×			×			$\times_T$							<5	v.p. grey - white	v.l. gray - white	decrease bioturbation	3
BC-8-K	×		×			1-2		×			×			$\times_T$							<5	p. grey - white	v.l. gray - white		3
BC-8-L	×		×			1-2		×			×			$\times_T$							<5	v.p. orange - white	v.l. gray - white		3
BC-9-A	×		×			1-2		×			×			$\times_T$							<5	p. grey - white	v.l. gray - white		3
BC-9-B	×		×			1-2		×			×			$\times_T$							<5	p. grey - white	v.l. gray - white		3
BC-9-C	×		×			1-2		×			×			$\times_T$							<5	p. grey - white	v.l. gray - white	bioclast concentration in burrows	3
BC-9-D	×		×			5		×			×		×	×							<5	p. grey - white	v.l. gray - white		3
BC-9-E	×		×			3-5		×			×		×	×							<5	p. grey - white	v.l. gray - white		3
BC-10	×		×			1-2		×			×		×	×							<5	p. grey - white	v.l. gray - white	small patches of bioclasts	3
BC-11-A	×		×			1-2		×			×		×	×								v.p. orange - white	v.l. gray - white		3
BC-11-B	×		×			1-2		×			×		×	×								v.p. orange - white	v.l. gray - white	irregular bedding	3
BC-11-C	×		×	×		1-2		×			×		×	×								v.p. orange - white	v.l. gray - white		3
BC-11-D	×		×			1-2		×			×		×	×								v.p. orange - white	v.l. gray - white		3
BC-11-E	×		×			1-2	×	×			×		×	×				×				v.p. orange - white	v.l. gray - white	2-3mm evaporites	3
BC-11-F	×		×			3-5		×			×		×	×								v.p. orange - white	v.l. gray - white		3
BC-11-G	×		×			1-2		×			×		×	×								v.p. orange - white	v.l. gray - white		3
BC-11-H	×		×			1-2		×			×		×	×				×				v.p. orange - white	v.l. gray - white		3
BC-11-I	×		×			1-2		×			×		×	×				×				v.p. orange - white	v.l. gray - white		3

Location	Comp.		Lithology			Porosity					Sedimentary features											Colour		Comments	
	dolomite	silicification	mudstone	wackestone	packstone	%	vuggy	interparticle	moldic	fracture	massive	bedded	nodular	bioturbation	thrombolites	laminations	brecciation	evaporite molds	iron oxides	chert	% bioclasts	fresh	weathered		Lithofacies
BC-11-J	×		×			1-2		×			×					×		×				v.l. gray - white	v.l. gray - white	ripple laminations	4
BC-11-K	×		×			1-2		×			×					×						v.l. gray - white	v.l. gray - white		4
BC-11-L	×		×			1-2		×			×					×	×	×				v.l. gray - white	v.l. gray - white	disturbed white whisps	4
BC-11-M	×		×			1-2		×			×					×						v.l. gray - white	v.l. gray - white	clastic material	4
BC-11-N	×		×			1-2		×			×					×						v.l. gray - white	v.l. gray - white		4
BC-11-O	×		×			1-2		×				×				×						v.l. gray - white	v.l. gray - white	greyish red purple cross laminations	4
BC-11-P	×		×			3-5	×	×							×							gray - l. bluish grey	v.l. gray - white		5
BC-11-Q	×		×			3-5		×			×			×		×						v.p. orange - p. yellowish brown	v.l. gray - white	remnant pockets of disturbed sediment	6
BC-11-R	×		×			5	×	×			×			×								v.p. orange - p. yellowish brown	v.l. gray - white	white whisps, dissolution	6
BC-11-S	×		×	×		5	×	×			×										10	v.p. orange - p. yellowish brown	v.l. gray - white	echinoderms	6
BC-11-T	×		×			5	×	×		×	×			×							<5	v.p. orange - p. yellowish brown	v.l. gray - white	dense	6
BC-11-U	×		×	×		5-7	×	×			×		×	×							5-10	v.p. orange - p. yellowish brown	v.l. gray - white	knobbly appearance	6
BC-11-V	×		×			5	×	×		×	×										<5	v.p. orange - p. yellowish brown	v.l. gray - white	dense	6
BC-11-W	×		×			1-2	×	×			×		×	×							5	v.p. orange - p. yellowish brown	v.l. gray - white		6
BC-11-X	×		×			1-2	×	×			×		×	×							5	v.p. orange - p. yellowish brown	v.l. gray - white		6
BC-11-Y	×		×			5	×	×			×		×	×							5	v.p. orange - p. yellowish brown	v.l. gray - white	knobbly appearance	6
BC-11-Z	×		×			1-2	×	×			×			×							<5	v.p. orange - p. yellowish brown	v.l. gray - white		6
BC-11-AA	×		×			3-5	×	×		×	×			×							<5	v.p. orange - p. yellowish brown	v.l. gray - white	dense	6
BC-11-BB	×		×			1-2	×	×			×			×							<5	v.p. orange - p. yellowish brown	v.l. gray - white		6

Location	Comp.		Lithology			Porosity					Sedimentary features												Colour		Comments	
	dolomite	silicification	mudstone	wackestone	packstone	%	vuggy	interparticle	moldic	fracture	massive	bedded	nodular	bioturbation	thrombolites	laminations	brecciation	evaporite molds	iron oxides	chert	% bioclasts	fresh	weathered		Lithofacies
BC-11-CC	×			×	×	15-20	×	×	×		×			×							40	p. yellowish brown	v.l. gray - white	dissolution of fossil fragments	9
BC-11-DD	×			×		10	×	×		×	×			×						×	20	p. yellowish brown	v.l. gray - white		9
BC-11-EE	×			×	×	10	×	×	×		×			$\times_T$							30	p. yellowish brown	v.l. gray - white		9
BC-11-FF	×		×	×		5	×	×			×			$\times_T$							10	p. yellowish brown	v.l. gray - white		9

APPENDIX B.2 - Lithofacies descriptions for road cut succession.

Location	Mineral		Lithology				Porosity					Sedimentary features											Colour		Comments	
	dolomite	silicification	mudstone	wackestone	packstone	grainstone	%	vuggy	interparticle	moldic	fracture	massive	bedded	nodular	bioturbation	thrombolites	laminations	brecciation	evaporite molds	iron oxides	chert	% bioclasts	fresh	weathered		Lithofacies
LS-1-B12	×		×				1-2		×			×	×				×						v.l. gray		scour and fill, weathers platy	4
LS-1-B11	×		×				1-2	×	×			×				×							v.l. gray			5
LS-1-B10	×		×	×			5	×	×	×		×	×	×								10	v.p. orange			6
LS-1-B9	×		×	×			5	×	×			×	×								×	10	v.p. orange			6
LS-1-B8	×		×				5-10	×	×			×	×	×	×							10	white		weathers to mud	6
LS-1-B7	×		×				3-5		×		×	×	×								×	5	v.p. orange		white whisps	6
LS-1-B6	×			×			5	×	×			×	×	×	×							20	white			6
LS-1-B5	×		×				5		×		×	×	×									5	v.p. orange		white whisps	6
LS-1-B4	×		×	×			5	×	×			×	×	×	×							10	white			6
LS-1-B3	×		×				3-5		×		×	×	×									<5	v.p. orange			6
LS-1-B2	×		×				3-5	×	×			×										<5	v.p. orange			6
LS-1-B1	×		×				3-5		×			×						×					v.p. orange			7
LS-1-MB	×		×				10	×	×								×						bluish gray		argillaceous	8
LS-1-A1	×		×				10	×	×			×				×							l. bluish gray			5
LS-1-A2	×			×	×		10	×	×	×		×	×	×	$\times_T$							40	v.p. orange			9

APPENDIX C – CORE DESCRIPTIONS

Core descriptions for William Tower (M-2-05) and Minago River Microwave Tower (M-06-79).

Core analysis for this study was conducted at the Manitoba Department of Innovation, Energy, and Mines Core Storage Facility in Winnipeg Manitoba. Colour descriptions are derived from the "Geological Society of America Rock-Color Chart" (Goddard et al., 1970). Classification of carbonate rocks follows Dunham (1962) as modified by Embry and Klovan (1972), and porosity classification follows Choquette and Pray (1970).

APPENDIX C.1 – M-2-05 William Tower Drill core.

The core was drilled by the Government of Manitoba, Mineral Resources Division, in the summer of 2005. It was initially logged by R.K. Bezys of the Manitoba Geological Survey, which was used as a guide (Bezys, 2006). Detailed examination and description for the upper portion of the core from 0 m to 40.8 m was used for this study.

APPENDIX C.2 – M-06-79 Minago River Microwave Tower Drill core.

The core was drilled by the Government of Manitoba, Mineral Resources Division, in 1979. It was initially logged by H.R. McCabe of the Manitoba Geological Survey, which was used as a guide (McCabe, 1979). Detailed examination and description for the upper portion of the core from 0.0 m to 65.7 m, but only interval from 19.0 to 65.7 m was used for this study.

APPENDIX C.1

M-2-05 William Tower
14-16-58-12 WPM
5985262N 488007E

Metres	Description
0.00-9.10	**Lower Stonewall Formation**
0.00-3.02	Very pale orange to pale yellowish brown, mottled mudstone to wackestone; 5-10% bioclastic material; porosity 15-20% of total volume (small <1-2 mm); significant bioturbation (40-80%) (*Thalassinoides*); Fossils: Corals – solitary rugose, *Catenipora*; disarticulated echinoderm columnals
3.02-3.31	Light gray to light bluish gray, thrombolitic dolomitic mudstone; porosity 0-5% of rock volume, vuggy (small <1 mm) and interstitial; clotted appearance with microbial? lamination; minor bioturbation (10-15%)
3.31-3.52	**LS-marker interval** – Medium light gray to greenish gray, argillaceous, fissile, dolomitic mudstone; porosity 0-5% of rock volume, vuggy (small <1 mm) to fracture
3.52-4.30	Very pale orange to light grayish orange, dolomitic mudstone; porosity 0-5% of total volume, vuggy (small <1 mm); intervals of brecciation recognized where there is darkening of matrix material, clasts are 1-4 mm and composed of surrounding lithology; devoid of fossils
4.30-4.51	Very pale orange to white, chalky, nodular, dolomitic mudstone; 5% poorly preserved small bioclastic material; porosity 20-25% of total volume, vuggy (medium 1-6 mm), fracture, and interstitial; Fossils: disarticulated echinoderm columnals and coral pieces
4.51-4.67	Pale yellowish brown, massive, dense, sublithographic dolomitic mudstone; porosity 5% of total volume, mainly fracture and vuggy (small <1 mm); thin light coloured whispy material along cracks; devoid of fossils
4.67-5.67	Very pale orange to white, chalky, nodular, dolomitic mudstone; 5% poorly preserved small bioclastic material; porosity 20-25% of total volume, vuggy (1-5 mm) and fracture; Fossils: Corals – *Paleofavosites*, colonial corals; disarticulated echinoderm columnals

5.67-8.10	Very pale orange to white with pale yellowish brown, chalky, dolomitic mudstone to wackestone; 5-10% poorly preserved bioclastic material; porosity 10-20% of total volume, vuggy (medium 1-10 mm) and interstitial; minor bioturbation (<10%); isolated areas of more dense, massive material; Fossils: Corals – *Paleofavosites*, *Tryplasma gracilis*, colonial corals; disarticulated echinoderm columnals
8.10-8.62	Very pale orange to light grayish orange, massive, dolomitic mudstone to wackestone; 5-10% bioclastic material; porosity 0-5% of total volume, vuggy (small <2 mm) and interstitial; Fossils: disarticulated echinoderm columnals
8.62-9.10	Pale yellowish brown to very pale orange, dolomitic mudstone; 0-5% bioclastic material; porosity 0-5% of total volume, vuggy (small <1 mm); minor lamination; Fossils: disarticulated echinoderm columnals
	Stony Mountain Formation
9.10-12.40	**Williams Member**
9.10-9.24	Light gray to light bluish gray, thrombolitic dolomitic mudstone; porosity 0-5% of total volume, vuggy (small <1 mm); clotted appearance due to microbial? thrombolites
9.24-10.45	Light to medium gray thinly laminated, sublithographic dolomitic mudstone; tight porosity; laminae are grayish red purple, 0.5-1.0 mm thick, and spaced 1-10 mm apart, possibly microbially mediated; dendrites present; devoid of fossils
10.45-12.40	Light gray to very pale orange, massive sublithographic dolomitic mudstone; tight porosity; few ripples; devoid of fossils
12.40-27.10	**Gunton Member**
12.40-21.22	Very pale orange to very pale yellowish brown, mottled dolomitic mudstone to wackestone; 5-15% bioclastic material; porosity 5-10% of total volume, vuggy (small <2 mm) and interstitial; evaporite molds; bioturbation (20-30%); Fossils: Corals – colonial; stromatoporoid; disarticulated echinoderm columnals
21.22-27.10	Very pale orange, mottled dolomitic mudstone to wackestone; 5-8% bioclastic material; porosity 10-15% of total volume, vuggy (small 1-2 mm) and interstitial; pervasive bioturbation (70-100%) with yellowish brown along mottles; Fossils: Corals – colonial; disarticulated echinoderm columnals

27.10-40.80	**Gunn/Penitentiary Equivalent**
27.10-28.30	Light to medium gray to pale yellowish brown mottled dolomitic mudstone to wackestone; 5-10% bioclastic material; porosity 5-10% of total volume, vuggy (small <2 mm) and interstitial; dendrites; moderate bioturbation (30-50%); Fossils: Corals – solitary and colonial; disarticulated echinoderm columnals
28.30-40.80	Pale yellowish brown to medium gray, mottled dolomitic mudstone to wackestone; 5-10% bioclastic material; porosity 5-10% of total volume, vuggy (small <2 mm) and interstitial; pyrite crystals; dendrites; pervasive bioturbation (80-100%); Fossils: Corals – colonial and solitary; disarticulated echinoderm columnals
	[Remainder as logged by Bezys (2006)*]*
40.80-84.40	**Red River Formation**
40.80-51.00	**Upper Red River (Fort Garry)** – Mainly grey, mottled, dolomudstone
51.00-83.20	**Lower Red River** – Tan dolowackestone
83.20-84.40	**(Hecla Beds)** – Very sandy dolomite, mottled, pyritized
84.40-90.60	**Winnipeg Formation** Dark mottled brown sandstone, no shale

END OF HOLE

APPENDIX C.2

M-06-79 Minago River Microwave Tower
14-16-58-12 WPM
5985262N 488007E

Metres	Description
0.00-3.40	**Atikameg Formation** Pale yellowish orange to very pale orange, dolomitic wackestone; porosity 20-25% of rock volume, predominantly vuggy (medium, up to 10 mm) and interstitial; devoid of fossils
3.40-10.50	**Moose Lake Formation** Very light gray, dolomitic mudstone; porosity 5-7% of total volume, vuggy (very small <2 mm) and interskeletal; stromatolitic; Fossils: Stromatolites <5% rock volume, tabular to domical, up to 3 cm high
10.50-10.90	**U_1 Marker** Very light greenish gray to pale yellowish brown, brecciated fine to medium grained sandy dolomitic wackestone with grayish yellow green clay partings; clasts are very light gray to light pink dolomitic mudstone, 3-10 mm in diameter; porosity 0-5% of total volume, vuggy (small <2 mm); devoid of fossils
10.90-19.00	**Fisher Branch Formation** Very pale orange to very light gray, dolomitic mudstone; 0-5% mostly unidentifiable bioclastic material; porosity 20-25% of total volume, vuggy (medium <8 mm) and interstitial; Fossils: Corals – solitary rugose
19.00-21.42	**Upper Stonewall Formation (Silurian?)**
19.00-19.60	Light gray, massive dolomitic mudstone; <5% bioclastic material; porosity 0-5% of total volume, vuggy (small <2 mm); Fossils: disarticulated echinoderm columnals
19.60-20.54	Pale yellowish brown, lightly mottled dolomitic mudstone; porosity 0-5% of total volume, vuggy (small <2 mm); 20-25% bioturbated
20.54-21.08	Pale yellowish orange to very pale orange (within vugs), dolomitic mudstone; porosity 20-25% of total volume, vuggy (medium, up to 5 mm); devoid of fossils
21.08-21.42	Light gray to pale yellowish brown, dolomitic mudstone; few thin pale reddish brown laminae; porosity 0-5% of total volume,

	vuggy (small <2 mm); minor bioturbation (<10%); devoid of fossils
21.42-22.20	***t*-marker** Mostly pale reddish brown to grayish red, argillaceous dolomitic mudstone; porosity 0-5% of total volume, vuggy (small <2 mm) and interstitial; bioturbation (50-60%); devoid of fossils 21.42-21.55 and 22.14-22.20: similar lithology but does not show red colouring; medium to light gray, argillaceous dolomitic mudstone
22.20-34.30	**Lower Stonewall Formation (Ordovician)**
22.20-22.72	Light gray to grayish orange, dolomitic mudstone; porosity 0-5% of total volume, vuggy (small <2 mm); dendrites as fracture fill (manganese/pyrite); minor bioturbation (~10%)
22.72-22.83	Medium light gray to pale olive gray, dolomitic mudstone; porosity 0-5% of total volume, vuggy (small <2 mm); dendrites as fracture fill; wavy laminations; devoid of fossils
22.83-22.97	Very pale orange, dolomitic mudstone; porosity 0-5% of total volume, vuggy (small <2 mm); dendrites as fracture fill; devoid of fossils
22.97-23.45	Medium light gray to very pale orange, brecciated dolomitic mudstone; clasts 5-10 mm in diameter composed of pale orange dolomitic mudstone; porosity 5-10% of total volume, vuggy (small 1-2 mm) and interstitial; dendrites as fracture fill; devoid of fossils
23.45-24.15	Very pale orange, massive dolomitic mudstone; minor laminations of darker material; porosity 0-5% of total volume, vuggy (small <2 mm); devoid of fossils 23.67: horizon of brecciated material within grayish red matrix
24.15-25.03	Very pale orange to pale yellowish brown, massive dolomitic mudstone to wackestone; 5-10% very poorly preserved small bioclastic material; porosity 5-10% of total volume, vuggy (small 1-2 mm); minor bioturbation (5-10%)
25.03-28.15	Very pale orange to pale yellowish brown, mottled dolomitic wackestone; 10-15% poorly preserved bioclastic material; porosity 20-25% of total volume, vuggy (medium 1-8 mm) stained darker yellowish orange and interstitial; dendrites as fracture fill; significant bioturbation (mainly about 50-60% but contains intervals approaching 100%); Fossils: Corals – colonial

	(5%), *Paleofavosites*, *Catenipora*; disarticulated echinoderm columnals (5-10%)
28.15-28.50	Pale yellowish brown to light gray, thrombolitic dolomitic mudstone; porosity 0-5% of total volume, vuggy (small <1 mm) and interstitial; clotted appearance with microbial? laminations; minor bioturbation (10%); devoid of fossils
28.50-28.65	**LS-marker interval -** Medium light gray to light bluish gray, argillaceous, irregularly laminated, fissile dolomitic mudstone; laminae are thin (1-2 mm) and vary from dark gray to dark yellowish orange to dark greenish gray; porosity 0-5% of total volume, vuggy (small <1 mm) and interstitial; devoid of fossils
28.65-29.66	Very pale orange, dolomitic mudstone; porosity 0-5% of total volume, vuggy (small <1mm); minor lamination; intervals of brecciation recognized where there is darkening of matrix material, clasts are 1-3 mm in diameter and are composed of the surrounding lithology; devoid of fossils
29.66-30.30	Very pale orange to white, chalky, dolomitic mudstone to wackestone; 5-8% poorly preserved unidentifiable small bioclastic material; porosity 20-25% of total volume, vuggy (medium 1-10 mm), fracture, and interstitial; slightly nodular
30.30-30.51	Medium yellowish brown, massive, dense, sublithographic dolomitic mudstone; porosity 5-8% of total volume, vuggy to fracture; thin light-coloured whispy material along cracks
30.51-31.11	Very pale orange to white, chalky, nodular, dolomitic wackestone; 5-8% poorly preserved bioclastic material; porosity 20-25% of total volume, mainly vuggy (1-8 mm) and fracture, but interstitial and interskeletal; Fossils: Corals – colonial (few small unidentifiable pieces); disarticulated echinoderm columnals (5%)
31.11-31.26	Medium yellowish brown, massive, dense, sublithographic dolomitic mudstone; porosity 5-10% of total volume, mainly fracture; thin light-coloured whispy material along cracks
31.26-31.39	Very pale orange to white, chalky, nodular, dolomitic mudstone; sparse small bioclastic material; porosity 15-20% of total volume, vuggy (small <2 mm); Fossils: Corals – colonial; disarticulated echinoderm columnals
31.39-32.75	Pale orange to white to medium yellowish brown, dense to slightly chalky, dolomitic mudstone; sparse small bioclastic

material; porosity 10-15% of total volume, mainly fracture and vuggy (small 1-2 mm); Fossils: Corals – colonial; disarticulated echinoderm columnals

32.75-33.69 Very pale orange to light gray, chalky, nodular, dolomitic wackestone; 8-10% mostly poorly preserved bioclastic material; porosity 20-25% of total volume, mainly vuggy (medium 1-8 mm) and interstitial; Fossils: Corals – colonial (5%), *Paleofavosites*, *Tryplasma gracilis*; brachiopod pieces; disarticulated echinoderm columnals (5%)

33.69-34.30 Very pale orange to pale yellowish brown, dolomitic wackestone; 5-10% poorly preserved unidentifiable small bioclastic material; porosity 5-10% of total volume, vuggy (small <1 mm); minor light coloured laminae; minor bioturbation (10-15%)

Stony Mountain Formation

34.30-37.80 **Williams Member**

34.30-34.39 Light gray to medium dark gray, thrombolitic dolomitic mudstone; porosity 0-5% of total volume, vuggy (small <1 mm); clotted appearance with microbial? laminations

34.39-35.70 Light gray, thinly laminated sublithographic dolomitic mudstone; tight porosity; laminae are grayish red, 0.5-1.0 mm thick, and spaced 1-15 mm apart with increase in abundance up core, possibly microbially mediated; ripples present with height of 10-15 mm; dendrites present; devoid of fossils

35.70-36.39 Very pale orange, massive sublithographic dolomitic mudstone; tight porosity; devoid of fossils

36.39-37.80 Very pale orange, massive sublithographic dolomitic mudstone; tight porosity; few ripples and areas of cross-lamination; minor bioturbation present near base (10%); devoid of fossils

37.80-51.90 **Gunton Member**

37.80-43.94 Very pale orange to very pale yellowish brown, mottled dolomitic mudstone to wackestone; 5-10% small bioclastic material; porosity 5-10% of total volume, vuggy (mainly small <2 mm, with few large holes 10-15 mm) and interstitial; dendrites present; moderate bioturbation (10-20%); Fossils: Corals – solitary rugose and colonial (3-5%); disarticulated echinoderm columnals (5%)
39.25-39.35: relative increase in porosity to 15-20%

43.94-51.90 Very pale yellowish orange to light gray, heavily mottled dolomitic wackestone, with dark yellowish brown along edges of

	mottling; 5-10% small bioclastic material; porosity 10-15% of total volume, vuggy (small <2 mm) and interstitial; some pyrite crystals; pervasive bioturbation (80-100%); Fossils: Corals – solitary rugose and colonial (3-5%); disarticulated echinoderm columnals (3-5%)
51.90-65.70	**Gunn/Penitentiary Equivalent**
51.90-52.91	Pale yellowish brown to light gray, mottled dolomitic mudstone to wackestone; 5-8% bioclastic material; porosity 5-10% of total volume, vuggy (small <2 mm); moderate bioturbation (30-40%); Fossils: Corals – solitary rugose and colonial; disarticulated echinoderm columnals
52.91-65.70	Pale yellowish brown to light gray and medium yellowish brown, mottled dolomitic mudstone to wackestone; 5-15% bioclastic material; porosity 5-10% of total volume, vuggy (small <1 mm) and interstitial; moderate bioturbation (30-40%); Fossils: Corals – solitary rugose and colonial; shelly material; disarticulated echinoderm columnals
	[Remainder as logged by McCabe (1979)*]*
65.70-109.9	**Red River Formation**
65.70-75.50	**Fort Garry Member** – Dolomite, dense, shaly interbeds
75.50-109.9	**Selkirk Member** (etc.) – Dolomite, mottled
109.9-111.9	**Winnipeg Formation** Sandstone

END OF HOLE

APPENDIX D – MACROFOSSILS, TRACE FOSSILS, AND BIOSEDIMENTARY STRUCTURES DATA

Identification of macrofossils, trace fossils, and biosedimentary structures from the study area.

Explanation of rows
Top row – column headings

Groupings of rows contain information on fossils identified on individual samples. The groupings are separated by horizontal lines.
1st row – identification of location from which sample was obtained.
Remaining rows – identification of fossils for the sample

BLUE shaded rows indicate identifications obtained from the conodont analysis (Nowlan, 2008; 2009).
GRAY shaded rows indicate field identifications.
UNSHADED rows indicate identifications made from field and laboratory examination.

Explanation of columns
Locality = site name/stratigraphic position from which the sample was obtained
e.g. **BC-1-A-4**
BC = surface exposure
1 = site identification
A = locality of collection
4 = sample number
e.g. **LS-1-B6 (+45cm)**
LS = roadcut succession
1 = site identification
B6 = stratigraphic unit
(+45cm) = stratigraphic position above base of unit

N = identification was completed in the field, but not collected
C = identification included in conodont analysis (Nowlan, 2008; 2009)

Fossil Identification = identification of all macrofossils and trace fossils recognized on sample. Blank cell indicates that no fossils were identified within sample

Comments = any extraneous information relevant to fossil identification

Description = measurable information and orientation data relevant to the individual fossils; D=diameter, W=width

APPENDIX D.1 – Macrofossils, trace fossils, and biosedimentary structures identified from surface exposures.

APPENDIX D.2 – Macrofossils, trace fossils, and biosedimentary structures identified from road cut succession.

APPENDIX D.3 – Summary table of abundances of identified fossils.

APPENDIX D .1 – SURFACE EXPOSURES

Locality	Fossil Identification	Comments	Description
BC-1			
BC-1-A			
N	corals		
N	*Catenipora* sp.		
N	*Paleofavosites* sp.		
N	colonial coral		
N	solitary rugose coral	(see paleocurrent data)	
N	gastropod		
N	bryozoan		
N	echinoderm fragments		
BC-1-A-1	*Bighornia* cf. *B. patella*	oblique	D=15 mm, triangulate
	solitary rugose coral		
	echinoderm fragments		
BC-1-A-2	*Bighornia* sp.		D=20 mm, circular
	echinoderm fragments		
BC-1-A-3	*Bighornia* sp.		
	solitary rugose coral		fragment
BC-1-A-4	solitary rugose coral		fragment
	brachiopod		fragment
BC-1-A-5	*Bighornia* sp.		D=4 mm, triangulate
	colonial coral fragment		
	echinoderm fragments		
BC-1-A-6	solitary rugose coral	silicified	D=9 mm, triangulate
BC-1-A-7	solitary rugose coral	oblique	
BC-1-A-8	solitary rugose coral		D= 6 mm, round
BC-1-A-9	*Catenipora* sp.	silicified	
BC-1-A-10	*Paleofavosites* sp.	silicified	
	echinoderm fragments		
BC-1-A-11	*Salvadorea* sp.		D=7 mm, circular
	solitary rugose coral		
	solitary rugose coral		
	solitary rugose coral		
	coral fragments		
	echinoderm fragments		
BC-1-A-12	chaetetid		
	solitary rugose coral	oblique	
	echinoderm fragments		
BC-1-A-13			
BC-1-A-14	solitary rugose coral		
BC-1-A-15	*Bighornia* cf. *B. patella*		D=5 mm, triangulate
BC-1-B			
N	*Paleofavosites* sp.		
N	solitary rugose coral	(see paleocurrent data)	
N	brachiopod		
N	echinoderm fragments		
BC-1-B-1	*Paleofavosites* sp.		
	trilobite fragment		
	echinoderm fragments		
BC-1-B-2	solitary rugose coral		D=9 mm
BC-1-B-3	brachiopod	incomplete	

Locality	Fossil Identification	Comments	Description
	BC-1-C		
N	*Calapoecia* sp.		
N	solitary rugose coral	(see paleocurrent data)	
N	echinoderm fragments		
N	*Thalassinoides* sp.		
BC-1-C-1	*Paleofavosites* sp.	silicified	D=2 mm
	solitary rugose coral	oblique	
	echinoderm fragments		
BC-1-C-2	*Deiracorallium angulatum*		D=13 mm, oval
	solitary rugose coral		D=2 mm, oval
BC-1-C-3	solitary rugose coral	oblique	
	BC-1-D		
N	colonial coral		
N	*Calapoecia* sp.		
N	*Bighornia* sp.		
N	solitary rugose coral	(see paleocurrent data)	
N	solitary rugose coral		
N	echinoderm fragments		
BC-1-D-1	solitary rugose coral		D=16 mm, circular
BC-1-D-2	*Bighornia* sp.		D=11 mm
	coral fragments		
	echinoderm fragments		
BC-1-D-3	*Bighornia* sp.		
	echinoderm fragments		
BC-1-D-4	solitary rugose coral		D=25 mm
BC-1-D-5	*Calapoecia* sp.		
	echinoderm fragments		
BC-1-D-6	*Paleofavosites* sp.	silicified	D=2 mm
BC-1-D-7	echinoderm fragments		
BC-1-D-8	*Paleofavosites* sp.	silicified	D=2-3 mm
BC-1-D-9	solitary rugose coral	oblique	
	solitary rugose coral	oblique	
	solitary rugose coral		triangulate
	echinoderm fragments		
BC-1-D-L1	solitary rugose coral		
	Bighornia cf. *B. patella*		D=12 mm
	solitary rugose coral		triangulate
	solitary rugose coral	oblique	
	echinoderm fragments		
BC-1-D-L2	*Bighornia* sp.		D=9 mm, triangulate
	solitary rugose coral		
	echinoderm fragments		
	BC-1-E		
N	*Paleofavosites* sp. fragments		
N	solitary rugose coral	(see paleocurrent data)	
N	orthoconic cephalopod	Az 300°	
BC-1-E-1	orthoconic cephalopod		
	echinoderm fragments		
BC-1-E-2	solitary rugose coral		
	solitary rugose coral		D=21 mm
	echinoderm fragments		
Locality	Fossil Identification	Comments	Description
BC-1-E-3	solitary rugose coral	oblique	
	solitary rugose coral		
	Liospira sp.		

Locality	Fossil Identification	Comments	Description
	echinoderm fragments		
	BC-2		
N	*Catenipora* sp.		
N	*Catenipora* sp.		
N	*Calapoecia* sp.		
BC-2	*Catenipora* sp.		
	BC-3		
N	colonial coral		
N	tabulate coral		
N	solitary rugose coral	(see paleocurent data)	
N	colonial rugosan		
N	orthoconic cephalopod	Az 236°	
N	echinoderm fragments		
BC-3-1	*Bighornia* sp.		D=22 mm, triangulate
	solitary rugose coral		
	solitary rugose coral		
BC-3-2	*Bighornia* sp.		D=13 mm, oval
BC-3-3	solitary rugose coral		D=25 mm, irregular
BC-3-4	solitary rugose coral		D=14 mm
BC-3-5	solitary rugose coral		
BC-3-6	*Deiracorallium angulatum*		D=5 mm, triangulate
	solitary rugose coral		fragment
BC-3-7	*Salvadorea* sp.		D=13 mm, circular
	solitary rugose coral	oblique	
	solitary rugose coral		D=10 mm, triangulate
	Catenipora sp.		
	Palaeophyllum pasense pasense		D=4 mm, separated
BC-3-8	orthoconic cephalopod		
BC-3-9			
	BC-4		
	BC-4-A		
N	*Paleofavosites* sp.		
N	*Calapoecia* sp.		
N	*Catenipora* sp.	30 x 18 cm	
N	solitary rugose coral	(see paleocurrent data)	
N	solitary rugose coral		
N	rugose colonial		
N	gastropod	Az 133°	
N	orthoconic cephalopod	Az 180°	
N	echinoderm fragments		
BC-4-A-1	*Deiracorallium angulatum*		D=6 mm, triangulate
	Deiracorallium angulatum		
	Deiracorallium angulatum		
	Salvadorea sp.		
	Salvadorea sp.		D=2 mm, round
	solitary rugose coral		
	solitary rugose coral		
	solitary rugose coral		
	solitary rugose coral		
	solitary rugose coral		
	solitary rugose coral fragments		

Locality	Fossil Identification	Comments	Description
	Palaeophyllum pasense parvum		
	Catenipora sp.		
	rhynchonellid brachiopod		
	echinoderm fragments		
BC-4-A-2	*Bighornia* sp.		D=11 mm, oval
BC-4-A-3	*Salvadorea* sp.		D=20 mm, circular
BC-4-A-4	*Deiracorallium angulatum*		D=6 mm, triangulate
	echinoderm fragments		
BC-4-A-5	tabulate coral fragments		
	Deiracorallium angulatum		D=6 mm, triangulate
	echinoderm fragments		
BC-4-A-6	*Bighornia* cf. *B. patella*		D=14 mm, oval
BC-4-A-7	*Deiracorallium angulatum*		D=7 mm, triangulate
	rhynchonellid brachiopod		
BC-4-A-8	*Deiracorallium angulatum*		D=4 mm, triangulate
BC-4-A-9	*Deiracorallium angulatum*		triangulate
	solitary rugose coral	oblique	D=12 mm
	solitary rugose coral		
	echinoderm fragments		
BC-4-A-10	tabulate coral fragments		
	Salvadorea sp.		D=20 mm, circular
	solitary rugose coral	oblique	
	solitary rugose coral	oblique	
	solitary rugose coral	oblique	
	solitary rugose coral fragments		
BC-4-A-11	*Salvadorea* sp.		D=16 mm, circular
	solitary rugose coral		
BC-4-A-12	*Bighornia* cf. *B. integriseptata*		D=20 mm, circular
BC-4-A-13	*Deiracorallium angulatum*		D=9 mm, triangulate
BC-4-A-14	*Deiracorallium angulatum*		D=8 mm, triangulate
	Bighornia sp.		D=10 mm, oval
	Bighornia sp.		D=5 mm, oval
	Bighornia sp.		D=3 mm
	solitary rugose coral	oblique	
	solitary rugose coral		
	solitary rugose coral	oblique	
	solitary rugose coral		
	solitary rugose coral		
	solitary rugose coral		
	solitary rugose coral		
	solitary rugose coral fragments		
BC-4-A-15	*Salvadorea* sp.		D=32 mm, circular
	echinoderm fragments		
BC-4-A-16	*Bighornia* sp.		D=9 mm, circular
	Bighornia sp.		
	Deiracorallium angulatum		D=2 mm
	Deiracorallium angulatum	oblique	
	solitary rugose coral	oblique	
	solitary rugose coral		
	solitary rugose coral		
	solitary rugose coral		
	solitary rugose coral		
	solitary rugose coral		
	solitary rugose coral		
	brachiopod		fragment
	echinoderm fragments		

Locality	Fossil Identification	Comments	Description
BC-4-A-17	*Clathrodictyon* sp.		
BC-4-A-18	*Catenipora* sp.		
	echinoderm fragments		
BC-4-A-19	orthoconic cephalopod		
BC-4-A-20	*Palaeophyllum pasense pasense*		D=3 mm
	Deiracorallium angulatum		triangulate
BC-4-A-21	*Catenipora* sp.	silicified	
	Paleofavosites sp.	silicified	D=3 mm
	solitary rugose coral		
	echinoderm fragments		
BC-4-A-22	solitary rugose coral fragments		
	solitary rugose coral		
BC-4-A-23	*Catenipora* sp.		
BC-4-A-24	*Paleofavosites* sp.		D=2 mm
BC-4-A-25	*Palaeophyllum pasense pasense*		D=3-4 mm
	echinoderm fragments		
BC-4-A-26	*Catenipora* sp.		
	Deiracorallium angulatum		D=10 mm, triangulate
	Palaeophyllum sp.		
	echinoderm fragments		
BC-4-A-27	solitary rugose coral	oblique	
	Palaeophyllum sp.		
BC-4-A-28	*Paleofavosites* sp.		
	solitary rugose coral	oblique	
	echinoderm fragments		
BC-4-A-29	*Paleofavosites* sp.	silicified	
BC-4-A-30	solitary rugose coral	oblique	
BC-4-A-31	*Paleofavosites okulitchi*	silicified	
BC-4-A-32	*Paleofavosites okulitchi*		D=3 mm
BC-4-A-33			
BC-4-A-34	*Paleofavosites* sp.	silicified	
BC-4-A-35	echinoderm fragments		
BC-4-A-36	*Dinorthis occidentalis*		
BC-4-A-37	echinoderm fragments		
BC-4-B			
N N N	*Calapoecia* sp. solitary rugose coral large corals	38 cm x 31 cm (see paleocurrent data)	
BC-4-B-1	solitary rugose coral		triangulate to oval
BC-4-B-2	*Bighornia* sp.		D=15 mm, triangulate
	solitary rugose coral fragments		
BC-4-B-3	*Bighornia* sp.		triangulate
	Bighornia sp.		
	solitary rugose coral		
	solitary rugose coral	oblique	
	solitary rugose coral	oblique	
	solitary rugose coral		
	echinoderm fragments		
BC-4-B-4	*Deiracorallium angulatum*		D=6 mm, triangulate
	solitary rugose coral		triangulate to trilobate
	echinoderm fragments		
BC-4-B-5	*Paleofavosites* sp.		
	Salvadorea sp.		D=30 mm, circular
	solitary rugose coral fragments		
	echinoderm fragments		
BC-4-B-6	*Deiracorallium angulatum*		triangulate

Locality	Fossil Identification	Comments	Description
	tabulate coral fragments		
BC-4-B-7	*Bighornia* sp.		oval
	solitary rugose coral	oblique	
	echinoderm fragments		
BC-4-B-8	*Salvadorea* sp.	oblique	
BC-4-B-9	*Salvadorea* sp.		circular
	solitary rugose coral fragments		
BC-4-B-10	*Salvadorea* sp.		
	Palaeophyllum pasense pasense		
	echinoderm fragments		
BC-4-B-11	*Paleofavosites* sp.		
	echinoderm fragments		
BC-4-B-12	*Palaeophyllum* sp.	oblique	
BC-4-B-13	*Bighornia* sp.		oval
	solitary rugose coral	oblique	
	echinoderm fragments		
BC-4-B-14	*Palaeophyllum pasense pasense*		
BC-4-B-15	solitary rugose coral		
	solitary rugose coral		
	solitary rugose coral		
	solitary rugose coral		
	solitary rugose coral fragments		
	echinoderm fragments		
BC-4-C			
N	*Paleofavosites* sp.		
N	*Paleofavosites* sp.	16 x 18 cm	
N	*Catenipora* sp.		
N	*Catenipora* sp.	>30 cm wide	
N	*Calapoecia* sp.	>33 x >25 cm	
N	*Pragnellia* sp.	Az 276°	276°
N	solitary rugose coral	(see paleocurrent data)	
N	*Palaeophyllum* sp.	14 x 6 cm	
N	*Palaeophyllum* sp.		D=6 mm
N	*Palaeophyllum* sp.	>40 cm	
N	colonial rugose coral		
N	colonial rugose coral		
N	orthoconic cephalopods	Az 84°, 120°, 170°, 55°	
BC-4-C-1	*Catenipora* sp.		
	solitary rugose coral	oblique	
BC-4-C-2	*Catenipora* sp.	oblique	
BC-4-C-3	*Catenipora* sp.		
	Paleofavosites sp.		
	Paleofavosites sp.		
	echinoderm fragments		
BC-4-C-4	*Palaeophyllum pasense pasense*		D=2-3 mm
BC-4-C-5	*Deiracorallium angulatum*		D=7 mm, triangulate
	solitary rugose coral fragments		
BC-4-C-6	*Palaeophyllum* sp.	oblique	
BC-4-C-7	*Paleofavosites* sp.	silicified	D=3 mm
BC-4-C-8	*Clathrodictyon* sp.		
	Paleofavosites sp.	silicified	
	solitary rugose coral		
	Trypanites sp.		
	echinoderm fragments		
BC-4-C-9	orthoconic cephalopod		
BC-4-C-10	*Salvadorea* sp.		fragment

Locality	Fossil Identification	Comments	Description
BC-4-C-11	*Calapoecia* sp.	silicified	
	solitary rugose coral	oblique	
BC-4-C-12	*Bighornia* sp.		D=14 mm
	colonial coral fragments		
BC-4-C-13	*Aulacera* sp.		
	solitary rugose coral		fragment
	echinoderm fragments		
BC-4-C-14	*Clathrodictyon* sp.		
BC-4-C-15	*Clathrodictyon* sp.	silicified	
	solitary rugose coral	oblique	
	echinoderm fragments		
	Trypanites sp.		
I-3918	*Pragnellia arborescens*	Manitoba Museum	
BC-5			
N	stromatoporoid		
N	*Paleofavosites* sp.		
N	*Catenipora* sp.		
N	solitary rugose coral		
BC-5-1	*Aulacera* sp.		cross-section
	echinoderm fragments		
BC-5-2	*Clathrodictyon* sp.		
	Trypanites sp.		
BC-6			
BC-6			
BC-7			
N	*Catenipora* sp.		
BC-7-1	*Catenipora* sp.	silicified	
	echinoderm fragments		
BC-7-2	echinoderm fragments		
BC-8			
BC-8-A			
N	echinoderm fragments		
N	*Thalassinoides* sp.	prominent	
BC-8-A	echinoderm fragments		
BC-8-B			
N	*Thalassinoides* sp.	prominent	
BC-8-C			
N	*Thalassinoides* sp.	prominent	
BC-8-D			
N	*Pasceolus* sp.		
N	*Thalassinoides* sp.	prominent	
BC-8-D			
BC-8-E			
N	*Catenipora* sp.		
N	*Aulopora* sp.		

Locality	Fossil Identification	Comments	Description
N	solitary rugose coral		
N	*Maclurina* sp.	9 x 7 cm	
N	gastropods		
N	echinoderm fragments		
N	*Thalassinoides* sp.	prominent	
BC-8-E-1	*Ellisites* sp.		
BC-8-E-2	*Salvadorea* sp.	oblique	
BC-8-E-3	*Dinorthis occidentalis*		
	Dinorthis occidentalis		
	Dinorthis occidentalis		
	echinoderm fragments		
BC-8-E-4	*Pasceolus* sp.		
	Pasceolus sp.		
	Pasceolus sp.		
	Pasceolus sp.		
	Pasceolus sp.		
	Pasceolus sp.		
	echinoderm fragments		
BC-8-E-5	*Kinaschukoceras* sp.		
BC-8-E-6	*Trochonema* sp.		
	echinoderm fragments		
BC-8-E-7	*Kinaschukoceras* sp.		
BC-8-F			
BC-8-F	echinoderm fragments		
BC-8-G			
N	*Thalassinoides* sp.		
BC-8-G			
BC-8-H			
N	*Thalassinoides* sp.		
BC-8-H			
BC-8-I			
N	*Thalassinoides* sp.		
BC-8-I			
BC-8-J			
N	*Thalassinoides* sp.		
BC-8-J	echinoderm fragments		
BC-8-K			
BC-8-K			
BC-8-L			
BC-8-L	echinoderm fragments		
BC-9			
BC-9-A			
N	orthoconic cephalopod		
N	*Thalassinoides* sp.		
BC-9-A-1			
BC-9-A-2	orthoconic cephalopod		
	rhynchonellid brachiopod		fragment

Locality	Fossil Identification	Comments	Description
	BC-9-B		
N	*Thalassinoides* sp.		
BC-9-B	echinoderm fragments		
	BC-9-C		
N	*Paleofavosites* sp.		
N	*Thalassinoides* sp.		
BC-9-C-1			
BC-9-C-2	*Paleofavosites* sp.		
BC-9-C-t	*Aulacera* sp.		fragment
	BC-9-D		
N	*Maclurina* sp.		
N	*Kinaschukoceras* sp.	18 cm across	
N	*Thalassinoides* sp.		
BC-9-D			
	BC-9-E		
N	*Thalassinoides* sp.		
BC-9-E-1			
BC-9-E-2	echinoderm fragments		
BC-9-E-3	echinoderm fragments		
	BC-10		
BC-10-1	echinoderm fragments		
BC-10-2			
	BC-11		
	BC-11-A		
N	*Kinaschukoceras* sp.		
N	*Thalassinoides* sp.		
BC-11-A-1			
BC-11-A-2			
	BC-11-B		
N	*Thalassinoides* sp.		
BC-11-B			
	BC-11-C		
N	*Thalassinoides* sp.		
BC-11-C			
	BC-11-D		
	Kinaschukoceras sp.		
BC-11-D-1	brachiopod		fragment
BC-11-D-2	*Chondrites* sp.		
	BC-11-E		
N	*Kinaschukoceras* sp.		
N	brachiopod bed		
N	*Thalassinoides* sp.		
BC-11-E-1	*Paleofavosites* sp.		
	Aulopora sp.		
BC-11-E-2	*Paleofavosites* sp.		
BC-11-E-3	*Paleofavosites okulitchi*		

Locality	Fossil Identification	Comments	Description
BC-11-E-4	*Oepikina limbrata*	many	W=10-20 mm
	Chondrites sp.		
BC-11-E-5	rhynchonellid brachiopod		W=12 mm
	Oepikina limbrata		W=10 mm
	Leperditia sp.		W=10 mm
BC-11-E-6	*Oepikina limbrata*		W=16 mm
BC-11-E-7	*Oepikina limbrata*		fragments
BC-11-E-8	*Oepikina limbrata*		
	Oepikina limbrata		
	Leperditia sp.		
BC-11-E-9	*Oepikina limbrata*	several	
BC-11-E-10	*Oepikina limbrata*	few	
	Leperditia sp.		
BC-11-E-11	*Oepikina limbrata*	few	
	Leperditia sp.		W=1-2 mm
BC-11-E-12	*Dinorthis occidentalis*		
BC-11-E-13	*Oepikina limbrata*	few	
BC-11-E-14			
BC-11-E-15	*Oepikina limbrata*		
BC-11-E-16	brachiopod fragments		
BC-11-E-17	*Oepikina limbrata*	few	
BC-11-E-18	*Oepikina limbrata*	few	
BC-11-E-19	*Oepikina limbrata*		
BC-11-E-20	*Calapoecia* sp.		
	Oepikina limbrata		
	brachiopod fragments		
BC-11-E-21	*Oepikina limbrata*		
BC-11-E-22	*Oepikina limbrata*		
BC-11-E-23	*Oepikina limbrata*		
BC-11-E-24	*Oepikina limbrata*		
BC-11-E-25	*Oepikina limbrata*		
BC-11-E-26	*Oepikina limbrata*		
BC-11-E-27	*Oepikina limbrata*		
BC-11-E-28	*Oepikina limbrata*		
BC-11-E-29	*Oepikina limbrata*	few	
BC-11-E-30	*Oepikina limbrata*	many	
	Diceromyonia storeya		
BC-11-E-31	*Oepikina limbrata*		
	Leperditia sp.		
BC-11-E-32	rhynchonellid brachiopod		
	Oepikina limbrata		
BC-11-E-33	*Oepikina limbrata*	many	
	Diceromyonia storeya		
BC-11-E-34	*Oepikina limbrata*		
BC-11-F			
N	*Chondrites* sp.		
N	*Thalassinoides* sp.		
BC-11-F-1			
BC-11-F-2	*Chondrites*		
BC-11-G			
N	brachiopods		
BC-11-G-1	*Diceromyonia storeya*		
BC-11-G-2			

Locality	Fossil Identification	Comments	Description
BC-11-H			
N	gastropod		
N	*Thalassinoides* sp.		
BC-11-H-1	*Hormotoma* sp.		
	Hormotoma sp.		
BC-11-H-2			
BC-11-H-3			
BC-11-H-4			
BC-11-I			
N	*Chondrites* sp.		
BC-11-I-1	*Chondrites* sp.		
BC-11-I-2			
BC-11-I-Eurypt			
BC-11-J			
N	Graham's eurypterid bed		
BC-11-J-1			
BC-11-J-2			
BC-11-K			
BC-11-K			
BC-11-L			
BC-11-L			
BC-11-M			
BC-11-M			
BC-11-N			
N	Graham arthropod		
BC-11-N-1			
BC-11-N-2			
BC-11-N-3			
BC-11-N-4			
BC-11-N-5			
BC-11-N-6			
BC-11-N-7			
BC-11-O			
BC-11-O-1			
BC-11-O-2			
BC-11-O-3			
BC-11-O-4			
BC-11-O-5	*Leperditia* sp.		
BC-11-O-6			
BC-11-P			
N	thrombolites		
BC-11-P-th-1	thrombolites		
BC-11-P-th-2	thrombolites		
BC-11-P-th-3	thrombolites		
BC-11-P-th	thrombolites		
BC-11-P-non			
BC-11-Q			
BC-11-Q			

Locality	Fossil Identification	Comments	Description
	BC-11-R		
BC-11-R			
	BC-11-S		
BC-11-S-1	*Oepikina limbrata*		
BC-11-S-2			
	BC-11-T		
BC-11-T			
	BC-11-U		
N	*Paleofavosites* sp.		
BC-11-U-1	*Paleofavosites okulitchi*		
	echinoderm fragments		
BC-11-U-2	*Paleofavosites* sp.		
BC-11-U-3	*Paleofavosites* sp.		
BC-11-U-4	echinoderm fragments		
	BC-11-V		
N	corals		
N	*Paleofavosites* sp.		
N	*Aulopora* sp.		
BC-11-V-1	*Paleofavosites okulitchi*		
BC-11-V-2	*Palaeophyllum* sp.		
BC-11-V-3	*Paleofavosites okulitchi*		
	BC-11-W		
N	*Paleofavosites* sp.		
BC-11-W	*Paleofavosites prolificus*		
	Paleofavosites sp.		
	BC-11-X		
N	*Paleofavosites* sp.		
N	gastropod		
BC-11-X-1			
BC-11-X-2	*Hormotoma* sp.		
BC-11-X-3	*Paleofavosites okulitchi*		
	BC-11-Y		
BC-11-Y			
	BC-11-Z		
BC-11-Z			
	BC-11-AA		
BC-11-AA			
	BC-11-BB		
BC-11-BB			
	BC-11-CC		
N	*Calapoecia* sp.		
N	*Paleofavosites* sp.	2 species	
N	*Paleofavosites* sp.		
BC-11-CC-1	*Paleofavosites prolificus*		
	Paleofavosites sp.		
	Paleofavosites sp.		

Locality	Fossil Identification	Comments	Description
	rhynchonellid brachiopod		
	bryozoan		
	echinoderm fragments		
BC-11-CC-2	*Paleofavosites prolificus*		
	colonial coral fragments		
	echinoderm fragments		
BC-11-CC-3	*Paleofavosites* sp.		
	Calapoecia sp.		
	Palaeopyllum sp.		
	echinoderm fragments		
BC-11-CC-4	*Paleofavosites* sp.		
	Palaeopyllum sp.		
	echinoderm fragments		
BC-11-CC-5	*Paleofavosites* sp.		
	Salvadorea sp.		D=20 mm, circular
BC-11-CC-6	*Aulacera* sp.		
	Calapoecia sp.		
	Paleofavosites okulitchi		
	colonial coral fragments		
	echinoderm fragments		
	BC-11-DD		
N	*Paleofavosites* sp.		numerous fragmentary
N	*Paleofavosites* sp.		
N	*Paleofavosites* sp.		
N	*Catenipora* sp.		
N	*Aulopora* sp.		
N	*Deiracorallium angulatum*		
N	solitary rugose coral		
N	colonial rugose coral		
N	*Palaeophyllum* sp.		
N	*Palaeophyllum sp.*		
N	*Tryplasma gracilis*		
N	brachiopods		
N	echinoderm fragments		
BC-11-DD-1	*Catenipora* sp.		
	Paleofavosites sp.		
	colonial coral fragments		
	bryozoan		
	echinoderm fragments		
BC-11-DD-2	*Angopora manitobensis*		
	Palaeophyllum sp.		
	echinoderm fragments		
BC-11-DD-3	*Catenipora* sp.		
	Palaeophyllum sp.		
	echinoderm fragments		
BC-11-DD-4	*Paleofavosites* sp.		
	echinoderm fragments		
BC-11-DD-5	*Paleofavosites* sp.		
	Palaeophyllum sp.		
	echinoderm fragments		
BC-11-DD-6	*Paleofavosites* sp.		
	Angopora manitobensis		
	echinoderm fragments		
BC-11-DD-7	*Palaeophyllum pasense pasense*		
	echinoderm fragments		
BC-11-DD-8	*Palaeophyllum* sp.		

Locality	Fossil Identification	Comments	Description
	echinoderm fragments		
BC-11-DD-9	*Palaeophyllum* sp.		
	echinoderm fragments		
BC-11-DD-10	*Aulopora* sp.		
	tabulate coral		
	Palaeophyllum sp.		
	echinoderm fragments		
BC-11-DD-11	*Deiracorallium angulatum*		D=10 mm, triangulate
	echinoderm fragments		
BC-11-DD-12	solitary rugose coral	oblique	
	echinoderm fragments		
BC-11-DD-13	solitary rugose coral		
BC-11-DD-14	solitary rugose coral	oblique	
	solitary rugose coral		
	Palaeophyllum pasense parvum		
	echinoderm fragments		
BC-11-DD-15	*Catenipora* sp.		
	Paleofavosites prolificus		
BC-11-EE			
N	stromatoporoid		
N	*Paleofavosites* sp.		
N	*Catenipora* sp.		
N	solitary rugose coral		
N	solitary rugose coral		
N	tabulate coral fragments		
N	*Palaeophyllum* sp.		
N	*Palaeophyllum* sp.		
N	*Palaeophyllum* sp.		
N	rhynchonellid brachiopods		
N	gastropod		
N	orthoconic cephalopod		
N	echinoderm stem segment		
N	rhombiferan cystoid		echinoderm plate
N	echinoderm calyx		
N	echinoderm fragments		
N	*Thalassinoides* sp.		
BC-11-EE-1	*Paleofavosites okulitchi*		
BC-11-EE-2	*Paleofavosites* sp.		
	solitary rugose coral		
	colonial coral fragments		
	echinoderm fragments		
BC-11-EE-3	*Deiracorallium angulatum*		D=12 mm, triangulate
	solitary rugose coral	oblique	
	echinoderm fragments		
BC-11-EE-4	*Palaeophyllum* sp.		
	Leperditia sp.		
	echinoderm fragments		
BC-11-EE-5	*Paleofavosites okulitchi*		
	solitary rugose coral		
	brachiopod		
	Hormotoma sp.		
	echinoderm fragments		
BC-11-EE-6	*Palaeophyllum* sp.		
	solitary rugose coral		
	echinoderm fragments		
BC-11-EE-7	*Clathrodictyon* sp.		

Locality	Fossil Identification	Comments	Description
	echinoderm fragments		
BC-11-EE-8	*Paleofavosites* sp.		
	colonial coral fragments		
	brachiopod		
	bryozoan		
	echinoderm fragments		
BC-11-EE-9	*Palaeophyllum* sp.		
	solitary rugose coral	oblique	
BC-11-EE-10	*Paleofavosites okulitchi*		
	solitary rugose coral		
	Palaeophyllum sp.		
	brachiopod		
	echinoderm fragments		
BC-11-EE-11	echinoderm fragments	stem	
BC-11-EE-12	*Palaeophyllum pasense pasense*		
	echinoderm fragments		
BC-11-EE-13	*Paleofavosites* sp.		
	echinoderm fragments		
BC-11-EE-14	*Catenipora* sp.		
	Paleofavosites prolificus		
	Palaeophyllum sp.		
	echinoderm fragments		
BC-11-EE-15	*Paleofavosites okulitchi*		
	Paleofavosites sp.		
BC-11-EE-16	*Paleofavosites prolificus*		
	Catenipora sp.		
	solitary rugose coral		
	orthoconic cephalopod		
	bryozoan		
	echinoderm fragments		
BC-11-EE-17	*Paleofavosites okulitchi*		
	brachiopod		
	bryozoan		
BC-11-EE-18	*Catenipora* sp.		
	solitary rugose coral		
	Palaeophyllum pasense parvum		
	Liospira sp.		
	echinoderm fragments		
BC-11-EE-19	rhombiferan cystoid		
	echinoderm fragments		
BC-11-EE-20	*Paleofavosites* sp.		
	Leperditia sp.		
	echinoderm fragments		
BC-11-EE-21	*Paleofavosites* sp.		
	Palaeophyllum sp.		
	rhynchonellid brachiopod		
	echinoderm fragments		
BC-11-EE-22	*Palaeophyllum* sp.		
	orthoconic cephalopod		
BC-11-EE-23	*Paleofavosites prolificus*		
BC-11-EE-24	*Paleofavosites* sp.		
	Palaeophyllum pasense parvum		
	brachiopod		
	echinoderm fragments		
BC-11-EE-25	*Paleofavosites* sp.		
	solitary rugose coral		
	Palaeophyllum sp.		

Locality	Fossil Identification	Comments	Description
	Leperditia sp.		
	trilobite fragment		
	echinoderm fragments		calyx
	echinoderm fragments		
BC-11-FF			
N	stromatoporoid		
N	*Paleofavosites* sp.		
N	*Paleofavosites* sp.		
N	*Paleofavosites* sp.		
N	*Catenipora* sp.		
N	*Catenipora* sp.		
N	solitary rugose coral		
N	solitary rugose coral		
N	solitary rugose coral		
N	colonial rugose coral		
N	colonial rugose coral		
N	colonial coral fragments		
N	orthoconic cephalopod		
N	*Thalassinoides* sp.		
BC-11-FF-1	*Palaeophyllum* sp.		
	solitary rugose coral	oblique	
	echinoderm fragments		
BC-11-FF-2	*Angopora manitobensis*		
BC-11-FF-3	*Paleofavosites okulitchi*		
	echinoderm fragments		
BC-11-FF-4	*Salvadorea* sp.		circular
BC-11-FF-5	solitary rugose coral	oblique	
BC-11-FF-6	*Angopora manitobensis*		
BC-11-FF-7	*Salvadorea* sp.		D=9 mm, circular
	Paleofavosites sp.		
	echinoderm fragments		

APPENDIX D.2 - ROAD CUT SUCCESSION

Locality	Fossil Identification	Comments	Measurement
	LS-1-B12		
LS-1-B12 +25 cm			
LS-1-B12 near top			
LS-1-B12 top			
	LS-1-B11		
N	thrombolites		
LS-1-B11 bottom			
LS-1-B11 middle			
LS-1-B11 top non-th	thrombolites		
LS-1-B11 top th high	brachiopod		
	thrombolites		
LS-1-B11 top th	thrombolites		
	LS-1-B10		
C	bryozoan		fragments
C	crinoid ossicles		
N	echinoderm fragments		
LS-1-B10 +10cm			
LS-1-B10 +35cm			
LS-1-B10 +70cm			
	LS-1-B9		
N	colonial coral fragments		fragments
N	*Tryplasma gracilis*		fragments
LS-1-B9 lith	echinoderm fragments		
LS-1-B9 conodonts	*Paleofavosites prolificus*		D=1-2 mm
	Paleofavosites prolificus		
	Paleofavosites sp.		fragments
	tabulate coral fragments		
	echinoderm fragments		
LS-1-B9-1	*Paleofavosites* sp.		
	Paleofavosites sp.		
	Tryplasma gracilis		D=4 mm
	echinoderm fragments		
LS-1-B9-2	*Paleofavosites* sp.		
	Paleofavosites sp.		
	Paleofavosites sp.		
	Paleofavosites sp.		
	Paleofavosites sp.		
	Paleofavosites sp.		
	Tryplasma gracilis		fragments
	echinoderm fragments		
	LS-1-B8		
C	bryozoan		fragments
C	crinoid ossicles		
N	colonial coral fragments		fragments
N	brachiopod fragments		fragments
LS-1-B8 +25 cm	*Tryplasma gracilis*		
LS-1-B8 +46 cm	*Paleofavosites* sp.		
	Tryplasma gracilis		
	echinoderm fragments		

Locality	Fossil Identification	Comments	Measurement
	LS-1-B7		
C	sponge spicules		
C	crinoid ossicles		
N	colonial coral fragments		fragments
N	brachiopod fragments		fragments
LS-1-B7	brachiopod		
	LS-1-B6		
C	bryozoan		fragments
C	crinoid ossicles		
N	*Paleofavosites* sp.		fragments
LS-1-B6 +15 cm	*Paleofavosites* sp.		
LS-1-B6 +45 cm	*Paleofavosites* sp.		
LS-1-B6 +60 cm	*Paleofavosites* sp.		
LS-1-B6 +70 cm	echinoderm fragments		
LS-1-B6 +77 cm	*Paleofavosites* sp.		D=2 mm
LS-1-B6 +87 cm			
LS-1-B6 +102 cm	*Paleofavosites* sp.		
LS-1-B6 +112 cm	*Paleofavosites okulitchi*		D=3 mm
LS-1-B6 +117 cm-1	*Paleofavosites* sp.		D=3 mm
LS-1-B6 +117 cm-2	*Paleofavosites* sp.		
LS-1-B6 top-1	*Paleofavosites* sp.		
LS-1-B6 top-2	*Aulopora* sp.		
LS-2-B6			
LS-2-B6 +11 cm	*Paleofavosites prolificus*		
LS-2-B6 +114 cm	*Paleofavosites* sp.		
	LS-1-B5		
C	bryozoan		fragments
C	crinoid ossicles		
LS-1-B5 lith	*Tryplasma gracilis*		
	colonial coral fragments		
LS-1-B5 top	*Paleofavosites* sp.		D=1-3 mm
	LS-1-B4		
C	bryozoan		fragments
C	crinoid ossicles		
LS-1-B4 +10 cm			
LS-1-B4 +51 cm			
	LS-1-B3		
C	bryozoan		fragments
LS-1-B3			
	LS-1-B2		
C	bryozoan		fragments
LS-1-B2 +17 cm			
LS-1-B2 +67 cm			
	LS-1-B1		
C	bryozoan		fragments
LS-1-B1 +8 cm			
LS-1-B1 +13 cm			
LS-1-B1 top-1			
LS-1-B1 top-2			
LS-2-B1 +13 cm			

Locality	Fossil Identification	Comments	Measurement
LS-1-MB			
LS-1-MB			
LS-1-MB-0			
LS-1-MB-1			
LS-1-MB-2			
LS-1-A1			
C	crinoid ossicles		
N	thrombolites		
LS-1-A1 base of th-1	thrombolites		
LS-1-A1 base of th-2			
LS-1-A1 top of th	thrombolites		
LS-1-A1 top	thrombolites		
LS-1-A1-1	linguloid brachiopod	Obolidae	
LS-1-A2			
C (+146)	crinoid ossicles		
N (+40)	rhynchonellid brachiopod		
N (+80)	orthoconic cephalopod		
N (+78)	*Paleofavosites* sp.		
N (+90)	*Palaeophyllum* sp.		
N (+85)	*Paleofavosites* sp.		
N (+45)	*Paleofavosites* sp.		
N (+100)	*Paleofavosites* sp.		
N (+80)	*Paleofavosites* sp.		
N (+80)	*Paleofavosites* sp.		
N (+75)	*Paleofavosites* sp.		
N (+145)	*Paleofavosites* sp.		
N (+85)	*Pycnostylus* sp.		
N (+72)	*Paleofavosites* sp.		
N (+65)	*Paleofavosites* sp.		
N (+65)	*Paleofavosites* sp.		
N (+15)	rhynchonellid brachiopod		
N (+178)	*Paleofavosites* sp.		
N (+54)	*Paleofavosites* sp.		
N (+113)	*Palaeophyllum* sp.		
N (+165)	colonial rugose coral		
N (+90)	*Palaeophyllum* sp.		
N (+70)	*Palaeophyllum* sp.		
N (+170)	*Palaeophyllum* sp.		
N (+210)	solitary rugose coral		
N (+225)	solitary rugose coral		
N (+225)	solitary rugose coral		
N (+208)	stromatoporoid		
N (+205)	*Paleofavosites* sp.		
N (+80)	*Paleofavosites* sp.		
LS-1-A2 base th low			
LS-1-A2 base th high			
LS-1-A2 +40cm	*Thalassinoides* sp.		
	echinoderm fragments		
LS-1-A2 +90 cm	*Paleofavosites* sp.		
	echinoderm fragments		
	Thalassinoides		
LS-1-A2 +155 cm	*Clathrodictyon* sp.		
	Paleofavosites sp.		
	Paleofavosites sp.		
	Ellisites sp.		

Locality	Fossil Identification	Comments	Measurement
	echinoderm fragments		
	Thalassinoides sp.		
LS-1-A2 +230 cm	echinoderm fragments		
LS-1-A2 top	echinoderm fragments		
LS-1-A2-1 (+30 cm)	*Paleofavosites* sp.		D=1-2 mm
	rhynchonellid brachiopod		
LS-1-A2-2 (+85 cm)	*Clathrodictyon* sp.		
	Trochonema sp.		
	echinoderm fragments		
LS-1-A2-3 (+75cm)	*Paleofavosites prolificus*		D=2 mm
LS-1-A2-4 (+70cm)	*Paleofavosites okulitchi*		D=3 mm
LS-1-A2-5 (+75cm)	*Angopora manitobensis*		D=1 mm
LS-1-A2-6 (+80cm)	*Palaeophyllum* sp.		
	echinoderm fragments		
LS-1-A2-7 (+83cm)	*Angopora manitobensis*		D=1-2 mm
	Tryplasma gracilis		
	Hormotoma sp.		
	echinoderm fragments		
LS-1-A2-8 (+88cm)	*Angopora manitobensis*		D=2 mm
LS-1-A2-9 (+110cm)	*Bighornia* cf. *B. patella*		
	Paleofavosites sp.		
	echinoderm fragments		
LS-1-A2-10 (+60cm)	*Paleofavosites prolificus*		D=1 mm
	rhynchonellid brachiopod		
	rhynchonellid brachiopod		
LS-1-A2-11 (+112cm)	*Catenipora* sp.		
	echinoderm fragments		
LS-1-A2-12 (+97cm)	*Pycnostylus* sp.		
LS-1-A2-13 (+133cm)	*Catenipora* sp.		
	rhynchonellid brachiopod		
	echinoderm fragments		stem
LS-1-A2-14 (+84cm)	solitary rugose coral		
	Tryplasma gracilis		
	Liospira sp.		
	echinoderm fragments		
LS-1-A2-15 (+120cm)	*Aulopora*		
	echinoderm fragments		
LS-1-A2-16 (+89cm)	*Angopora manitobensis*		
	Pycnostylus sp.		
	bryozoan		
	echinoderm fragments		
LS-1-A2-17 (+75cm)	*Paleofavosites okulitchi*		D=2-4 mm
	Paleofavosites sp.		
	Hormotoma sp.		
LS-1-A2-18 (+138cm)	echinoderm fragments		stem
	echinoderm fragments		
LS-1-A2-19 (+107cm)	*Paleofavosites prolificus*		
	Catenipora sp.		
	Bighornia sp.		D=15 mm
	echinoderm fragments		
LS-1-A2-20 (+55cm)	*Angopora manitobensis*		D=1 mm
LS-1-A2-21 (+84cm)	orthoconic cephalopod		
LS-1-A2-22 (+160cm)	*Pycnostylus* sp.		fragments
LS-1-A2-23 (+180cm)	solitary rugose coral		D=26 mm
	echinoderm fragments		
LS-1-A2-24 (+135cm)	*Catenipora* sp.		fragments
	solitary rugose coral		

Locality	Fossil Identification	Comments	Measurement
	echinoderm fragments		
LS-1-A2-25 (+210cm)	*Bighornia* sp.		D=15 mm
	Bighornia sp.		D=15 mm
	Paleofavosites sp.		
	Paleofavosites prolificus		
	Paleofavosites sp.		
	echinoderm fragments		
LS-1-A2-26 (+140cm)	*Catenipora* sp.		
	Palaeophyllum pasense parvum		D=1-2 mm
	echinoderm fragments		
LS-2-A2-27 (+20cm)	*Aulacera* sp.		D=1 mm
LS-2-A2-28 (+20cm)	rhynchonellid brachiopod		
LS-2-A2-29 (+60cm)	rhynchonellid brachiopod		
	Hormotoma sp.		
	echinoderm fragments		
LS-2-A2-30 (+65cm)	*Palaeophyllum pasense pasense*		
	echinoderm fragments		
LS-2-A2-31 (+65cm)	*Angopora manitobensis*		
LS-2-A2-32 (+63cm)	*Paleofavosites okulitchi*		D=4 mm
	echinoderm fragments		
LS-2-A2-33 (+58cm)	*Paleofavosites okulitchi*		D=2 mm
	echinoderm fragments		
LS-2-A2-34 (+75cm)	*Paleofavosites okulitchi*		D=2 mm
	echinoderm fragments		
	orthoconic cephalopod		
LS-2-A2-35 (+120cm)	*Salvadorea* sp.		D=10 mm
	solitary rugose coral		
	echinoderm fragments		
LS-2-A2-36 (+64cm)	*Angopora manitobensis*		D=1 mm
	orthoconic cephalopod		
	echinoderm fragments		
LS-2-A2-37 (+68cm)	*Paleofavosites prolificus*		D=1-2 mm
LS-2-A2-38 (+82cm)	*Aulacera* sp.		
	echinoderm fragments		
LS-2-A2-39 (+208cm)	solitary rugose coral		fragments
LS-2-A2-40 (+225cm)	solitary rugose coral		
	echinoderm fragments		
LS-2-A2-41 (+185cm)	trilobite fragment		
LS-2-A2-42 (+215cm)	*Paleofavosites* sp.		
	solitary rugose coral	oblique	
	solitary rugose coral	oblique	
	solitary rugose coral		
	solitary rugose coral	oval	
	solitary rugose coral		fragments
	solitary rugose coral	oval	
	echinoderm fragments		
LS-2-A2-43 (+185cm)	*Tryplasma gracilis*		
	Angopora manitobensis		
	echinoderm fragments		
LS-2-A2-44 (+207cm)	solitary rugose coral	circular	
	solitary rugose coral	oblique	
	solitary rugose coral	oblique	
	echinoderm fragments		
LS-2-A2-45-1 (+215cm)	*Paleofavosites okulitchi*		
	Salvadorea sp.	broken	
	solitary rugose coral	oblique	
LS-2-A2-45-2 (+215cm)	*Salvadorea* sp.		

Locality	Fossil Identification	Comments	Measurement
	solitary rugose coral		
	echinoderm fragments		
LS-2-A2-46-1 (+200cm)	solitary rugose coral	triangulate	D=9 mm
	echinoderm fragments		
LS-2-A2-46-2 (+200cm)	*Paleofavosites* sp.		
	Salvadorea sp.		D=25 mm
	solitary rugose coral	oblique	D=30 mm
	echinoderm fragments		
LS-2-A2-46-3 (+200cm)	*Paleofavosites* sp.		
	solitary rugose coral		
	solitary rugose coral	circular	
	echinoderm fragments		
LS-2-A2-46-4 (+200cm)	*Clathrodictyon* sp.		
	Paleofavosites okulitchi		
	Paleofavosites sp.		
	Paleofavosites sp.		
	Paleofavosites sp.		
	colonial coral fragments		
	solitary rugose coral	triangulate	
	echinoderm fragments		
LS-2-A2-47 (+200cm)	*Bighornia* sp.		D=10 mm
LS-2-A2-48 (+200cm)	*Clathrodictyon* sp.		
	Paleofavosites sp.		
	Paleofavosites sp.		
	Salvadorea sp.		
	solitary rugose coral		
	solitary rugose coral		
	solitary rugose coral		
	Tryplasma gracilis	circular	fragments
	bryozoan		
	echinoderm fragments		
LS-2-A2-49 (+215cm)	*Aulacera* sp.		
	Paleofavosites okulitchi		
	Paleofavosites sp.		
	Salvadorea sp.		
	solitary rugose coral		
	brachiopod	circular	
	bryozoan		
	echinoderm fragments		
LS-2-A2-50 (+200cm)	solitary rugose coral	oblique	
LS-2-A2-51 (+200cm)	*Catenipora* sp.		
	echinoderm fragments		
LS-2-A2-52 (+200cm)	*Palaeophyllum pasense parvum*		
	Angopora manitobensis		
	echinoderm fragments		
LS-2-A2-53 (+200cm)	*Angopora manitobensis*		
	Tryplasma gracilis		fragments
	echinoderm fragments		
LS-2-A2-54 (+200cm)	*Salvadorea* sp.		D=8 mm
	echinoderm fragments		
LS-1-A2 +115cm	*Deiracorallium angulatum*		
LS-1-A2 loose-1	*Aulacera* sp.		D=5 mm
LS-1-A2 loose-2	*Calapoecia* sp.		
	solitary rugose coral		
	echinoderm fragments		
LS-1-A2 loose-3	*Paleofavosites okulitchi*		D=3 mm
	orthoconic cephalopod		

Locality	Fossil Identification	Comments	Measurement
	bryozoan		
	echinoderm fragments		
LS-1-A2 loose-4	*Catenipora* sp.		
	Liospira sp.		
	echinoderm fragments		
LS-1-A2 loose-5	*Angopora manitobensis*		
	brachiopod		
	Hormotoma sp.		
	bryozoan		
	echinoderm fragments		
LS-1-A2 loose-6	*Paleofavosites* sp.		
	Calapoecia sp.		
	Catenipora sp.		
	echinoderm fragments		
LS-1-A2 loose-7	*Aulacera* sp.		D=5 mm
	echinoderm fragments		

APPENDIX D.3 - SUMMARY TABLE

	Paseeolus sp.	stromatoporoids	*Aulocera* sp.	*Clathrodictyon* sp.	chaetetid	spicules	colonial corals	tabulate corals	*Paleofavosites* sp.	*Paleofavosites prolificus*	*Paleofavosites okulitchi*	*Angopora manitobensis*	*Calapoecia* sp.	*Catenipora* sp.	*Pragnellia* sp.	*Ellisites* sp.	*Aulopora* sp.	solitary rugose coral	*Bighornia* sp.	*Bighornia* cf. *B.integriseptata*	*Bighornia* cf. *B. patella*	*Deiracorallium angulatum*	*Salvadorea* sp.	colonial rugose corals	*Palaeophyllum* sp.	*Palaeophyllum pasense pasense*	*Palaeophyllum pasense parvum*	*Pycnostylus* sp.	*Tryplasma gracilis*	gastropod	*Liospira* sp.	*Hormotoma* sp.	*Trochonema* sp.	*Maclurina* sp.	*Kinaschukoceras* sp.	orthoconic cephalopod	linguloid brachiopod	articulate brachiopod	Rhynchonellid brachiopod	*Oepikina limbrata*	*Diceromyonia storeya*	*Dinorthis occidentalis*	bryozoan	*Leperditia* sp.	trilobite fragment	echinoderm fragments	*Thalassinoides* sp.	*Chondrites* sp.	*Trypanites* sp.	thrombolites	**total of localities**
LS-1-A2		1	5	4			1		33	5	9	11	2	8		1	1	31	4		1	1	7	1	6	1	2	5	4		2	4	1		5		2	8					5		1	51	3				**226**
LS-1-A1																																				1									1				4	**6**
MB																																																		**0**
LS-1-B1																																												1						**1**
LS-1-B2																																												1						**1**
LS-1-B3																																												1		1				**2**
LS-1-B4																																												1		1				**2**
LS-1-B5							1		1																			1															1		1				**5**
LS-1-B6									10	1	1						1																										1		2				**16**
LS-1-B7						1	1																														2									1					**5**
LS-1-B8							1		1																			2									1						1		2				**8**
LS-1-B9							1	1	9	2																		3																	4					**20**
LS-1-B10																																												1		2				**3**
LS-1-B11																																				1													4	**5**
LS-1-B12																																																		**0**
DRILL																																																			**0**
BC-11-FF		1					1		4		1	2		2				5					2	2	1										1									3	1				**26**
BC-11-EE		1		1			2	1	9	3	5			4				11				1			11	1	2			1	1	1			3		5	2					3	3	1	25	1				**98**
BC-11-DD							1	1	7	1		2		4			2	6				2			7	1	1	1									1							1		14				**52**
BC-11-CC			1				2		7	2	1		3										1		2													1						1		5				**26**
BC-11-BB																																																		**0**
BC-11-AA																																																		**0**
BC-11-Z																																																		**0**
BC-11-Y																																																		**0**
BC-11-X									1		1																			1		1																	**4**
BC-11-W									2	1																																								**3**
BC-11-V							1		1		2						1								1																									**6**
BC-11-U									3		1																																			2					**6**
BC-11-T																																																		**0**
BC-11-S																																						1													**1**
BC-11-R																																																		**0**
BC-11-Q																																																		**0**
BC-11-P																																																	5	**5**
BC-11-O																																												1						**1**
BC-11-N																																																		**0**
BC-11-M																																																		**0**
BC-11-L																																																		**0**
BC-11-K																																																		**0**
BC-11-J																																																		**0**
BC-11-I																																																2		**2**
BC-11-H																														1		2														1	1			**5**
BC-11-G																																						1			1									**2**
BC-11-F																																														1	2				**3**
BC-11-E									2		1		1				1																	1			3	2	29	2	1		5		1	1	1			**51**
BC-11-D																																		1			1								1	1				**4**
BC-11-C																																														1					**1**
BC-11-B																																														1					**1**
BC-11-A																																		1												1					**2**
BC-10																																														1					**1**
BC-9-E																																														2	1				**3**
BC-9-D																																		1	1												1					**3**
BC-9-C			1						2																																						1					**4**
BC-8-L																																														1	1				**2**
BC-8-K																																															1					**1**
BC-9-B																																														1	1				**2**
BC-8-J																																														1	1				**2**
BC-9-A																																				2			1								1					**4**
BC-8-I																																															1					**1**
BC-8-H																																															1					**1**
BC-8-G																																															1					**1**
BC-8-F																																														1					**1**
BC-8-E	6													1		1	1	1					1						1			1	1	2						3				4	1				**24**
BC-8-D	1																																														1					**2**
BC-8-C																																															1					**1**
BC-8-B																																														1	1				**2**
BC-8-A																																														2	1				**3**
BC-7														2																																	2					**4**
BC-6																																																			**0**
BC-5			1	1			1		1					1				1																											1			1		**8**
BC-4-C			1	3			1		6				2	5	2			7	1			1	1	2	4	1									2									4			2		**45**
BC-4-B							1	1	2				1					17	5			2	4		1	2																		8					**44**
BC-4-A				1				2	6		2		1	6				37	6	1	1	14	6	1	2	2	1		1						2		1	2		1				14					**110**
BC-3							1	1					1					9	2			1	1	1		1									2									1					**21**
BC-2													1	3																																						**4**
BC-1-D									2				2					11	4		1																							8					**28**
BC-1-E									1									5												1					2									3					**12**
BC-1-A					1		4		2					2				12	3		2		1							1							1						1		7					**37**
BC-1-C							2		1				1					4				1																							2	1				**12**
BC-1-B									2									2																			2							1	2				**9**
totals	**7**	**3**	**9**	**10**	**1**	**1**	**22**	**7**	**115**	**15**	**24**	**15**	**14**	**39**	**2**	**2**	**7**	**159**	**25**	**1**	**5**	**23**	**24**	**7**	**35**	**9**	**6**	**5**	**11**	**6**	**4**	**8**	**2**	**2**	**6**	**19**	**1**	**21**	**16**	**30**	**3**	**5**	**19**	**9**	**3**	**184**	**30**	**2**	**5**	**13**	**991**

APPENDIX E – MICROFOSSILS

Summaries of microfossil data from the road cut succession at the William Lake study site, based on reports by Nowlan (2008; 2009) resulting from analysis at the Geological Survey of Canada Calgary Conodont Laboratory.

Identification of material from individual samples described in descending stratigraphic order by location.

Explanation of rows:
Top row – column headings

Groupings of rows contain information on conodont elements resultant from analysis of individual samples. Groupings are separated by bold lines.
1st row – identification of location from which sample was obtained, mass of sample for analysis, and total number of conodont elements (#)
Remaining rows – identification of conodont elements and individual abundances

Explanation of columns:
Location – site name and stratigraphic position from which the sample was obtained
e.g. LS-1-A2 +380cm
LS = roadcut succession
1 = site identification
A2 = stratigraphic unit of collection
+380cm = stratigraphic position above base of unit
Conodonts – identifiable conodont elements within sample
- number of identifiable conodont elements
Comments – description of the nature of preservation of conodont elements, and identification of macrofossils where present

Location	Mass (kg)	Conodonts	#	Comments
LS-1-A2 +380cm	2.470	total	2	poorly preserved
		Drepanoistodus sp.	1	
		Panderodus sp.	1	
LS-1-A2 +215cm	2.644	total	5	moderately well preserved
		Oulodus ulrichi	1	
		Panderodus gracilis	2	
		Plegagnathus sp.	1	
		Pseudobelodina vulgaris	1	
LS-1-A2 +211cm	1.605	total	3	fragmentary
		Aphelognathus? sp.	2	
		Rhipidognathus? sp.	1	
LS-1-A2 +146cm	1.587	total	0	crinoid ossicles
LS-1-A2 +96cm	2.144	total	9	moderately well preserved
		Aphelognathus? sp.	2	
		Drepanoistodus suberectus	1	
		Panderodus gracilis	3	
		Panderodus panderi	1	
		Plegagnathus nelsoni	2	
LS-1-A2 base (non)	1.340	total	14	mostly fragmentary
		Drepanoistodus suberectus	2	
		Oulodus sp.	2	
		Panderodus feulneri	2	
		Panderodus gracilis	7	
		trichonodelliform element indeterminate	1	
LS-1-A2 base	1.146	total	14	mostly fragmentary
		Oulodus sp.	2	
		Panderodus feulneri	3	
		Panderodus gracilis	6	
		Pseudobelodina inclinata	1	
		Pseudobelodina? *dispansa*	1	
		Rhipidognathus? sp.	1	
LS-1-A1 base	1.181	total	330	moderately well preserved and many unidentifiable fragments; crinoid ossicles
		Aphelognathus aff. *A. divergens*	82	
		Panderodus cf. *P. liratus*	42	
		Panderodus feulneri	64	
		Panderodus gibber	11	
		Panderodus gracilis	125	
		Pseudobelodina adentata	2	
		Pseudobelodina vulgaris	2	
		Pseudobelodina vulgaris ultima	2	

LS-1-MB	1.685	total	5	fragmentary and many unidentifiable fragments; all specimens are abraded
		Panderodus sp.	1	
		Rhipidognathus? sp.	4	
LS-1-B1 top	2.777	total	50	mostly fragmentary
		Aphelognathus aff. *A. divergens*	15	
		Rhipidognathus symmetricus	35	
LS-1-B1 base	2.662	total	532	moderately well preserved and many unidentifiable fragments; fragments of dolomitized? bryozoan colonies
		Aphelognathus aff. *A. divergens*	178	
		Panderodus gracilis	13	
		Panderodus panderi	2	
		Rhipidognathus symmetricus	339	
LS-1-B2	2.659	total	238	moderately well preserved; fragments of bryozoans
		Aphelognathus aff. *A. divergens*	51	
		Drepanoistodus sp.	2	
		Oulodus sp.	3	
		Panderodus cf. *P. liratus*	40	
		Panderodus gracilis	97	
		Pseudobelodina vulgaris	2	
		Rhipidognathus symmetricus	43	
LS-1-B3	2.421	total	44	mostly fragmentary with surface glaze; fragments of dolomitized? bryozoan colonies
		Aphelognathus aff. *A. divergens*	9	
		Drepanoistodus sp.	1	
		Panderodus sp.	1	
		Rhipidognathus symmetricus	33	
LS-1-B4	1.812	total	152	moderately well preserved; fragments of dolomitized? bryozoan colonies and crinoid ossicles
		Aphelognathus aff. *A. divergens*	46	
		Panderodus cf. *P. liratus*	5	
		Panderodus gracilis	27	
		Pseudobelodina sp.	1	
		Pseudobelodina vulgaris ultima	1	
		Rhipidognathus symmetricus	72	
LS-1-B5	2.098	total	144	moderately well preserved; fragments of dolomitized? bryozoan colonies and crinoid ossicles
		Aphelognathus aff. *A. divergens*	27	
		Drepanoistodus suberectus	12	
		Panderodus cf. *P. liratus*	42	
		Panderodus gracilis	51	
		Panderodus panderi	2	
		Rhipidognathus symmetricus	10	
LS-1-B6	2.508	total	22	moderately well preserved; fragments of bryozoan colonies and crinoid ossicles
		Drepanoistodus suberectus	13	
		Panderodus feulneri	6	
		Panderodus gracilis	2	
		Pseudobelodina vulgaris ultima	1	

LS-1-B7	2.489	total	84	moderately well preserved; fragments of sponge spicules and bryozoan fragments
		Aphelognathus aff. *A. divergens*	22	
		Drepanoistodus suberectus	4	
		Panderodus cf. *P. liratus*	11	
		Panderodus gracilis	33	
		Rhipidognathus symmetricus	14	
LS-1-B8	1.797	total	43	moderately well preserved; fragments of dolomitic? bryozoan colonies and crinoid ossicles
		Aphelognathus? sp.	2	
		Drepanoistodus suberectus	3	
		Panderodus cf. *P. liratus*	9	
		Panderodus gracilis	22	
		Rhipidognathus symmetricus	7	
LS-1-B9	1.513	total	69	moderately well preserved
		Aphelognathus aff. *A. divergens*	16	
		Drepanoistodus suberectus	22	
		Panderodus cf. *P. liratus*	1	
		Panderodus feulneri	4	
		Panderodus gracilis	14	
		Panderodus panderi	2	
		Rhipidognathus symmetricus	10	
LS-1-B10 top	2.610	total	18	well preserved
		Aphelognathus? sp.	2	
		Rhipidognathus symmetricus	16	
LS-1-B10 middle	1.958	total	315	moderately well preserved and many unidentifiable fragments; fragments of dolomitic? bryozoan colonies
		Aphelognathus aff. *A. divergens*	56	
		Drepanoistodus suberectus	37	
		Panderodus cf. *P. liratus*	41	
		Panderodus gibber	3	
		Panderodus gracilis	88	
		Panderodus panderi	3	
		Pseudobelodina adentata	2	
		Rhipidognathus symmetricus	85	
LS-1-B10 base	2.111	total	153	moderately well preserved with many unidentifiable fragments; fragments of dolomitic? bryozoan colonies and crinoid ossicles
		Aphelognathus aff. *A. divergens*	48	
		Drepanoistodus suberectus	11	
		Panderodus cf. *P. liratus*	12	
		Panderodus gibber	1	
		Panderodus gracilis	19	
		Pseudobelodina adentata	2	
		Rhipidognathus symmetricus	60	
LS-1-B11 middle	3.485	total	3	well preserved
		Rhipidognathus symmetricus	3	
LS-1-B12	1.855	total	98	moderately well preserved

		Aphelognathus aff. *A. divergens*	10	
		Drepanoistodus suberectus	5	
		Rhipidognathus symmetricus	83	

APPENDIX F: PALEOCURRENT DATA

APPENDIX F.1 – Raw Data.

The compiled tables of azimuthal directional orientation measurements collected from the exposed bedrock along the surface exposures succession. Nine areas were selected for analysis, and are identified by the locality.

All measurements are unidirectional (recorded as azimuths in range 1°-360° to the nearest degree). The measurements were taken parallel to the long axis of solitary coral fossils from the apical end toward the calicular end, or in the direction of corallum expansion where the position of the calice could not be determined.

APPENDIX F.2 – Chi-square data.

Chi-square tests (χ^2) were generated in order to test for randomness of directional data. Analyses were conducted on data of solitary rugose corals for which there were at least 60 observed values, so that the Expected number in each of the 12 classes would be at least five.

O = number of Observed values
E = Expected numbers per cell
d.f. = degrees of freedom (#classes-1)
S.D. = standard deviation
$\chi^2_{0.05}$ = critical value of Chi-square at α=0.05 (see Mendenhall et al., 2006, Appendix 1, Table 5)
$\chi^2_{(calc.)}$ = calculated value of Chi-square (sum of $(O-E)^2/E$ for all classes)

APPENDIX F.1 – RAW DATA

BC-1-A							
270	148	323	326	306	332	226	320
19	55						

BC-1-B							
142	341						

BC-1-C							
61	100	60	284	82			

BC-1-D							
329	351	59	122	235	320	226	20
224	33	115	62	271	82	252	55
332	56	273	132	13	151	52	30
356	324						

BC-1-E							
131	327						

BC-3							
147	28	147	145	167	114	181	33
57	218	139	91	135	156	279	315
35	220	173	155	209	344	70	300

BC-4-A							
223	125	63	162	170	70	341	200
169	164	195	167	11	95	164	274
31	160	311	282	165	9	75	79
103	98	251	64	65	298	235	86
45	64	240	142	329	80	31	38
180	215	240	129	123	33	126	170
91	339	311	85	311	279	315	202
330	314	344	81	130	106	143	3
263	222	280	355	342	306	6	91
200	354	81	195	214	333	280	73
357	290	293	85	150	192	284	109
121	158	12	75	61	76	165	301
312	322	351	241	110	345	303	325
346	100	204	42	1			

BC-4-B							
230	324	308	85	80	11	359	89
93	5	118	141	302	83	24	299
253	118	228	119	311	9	355	62
51	0	84	129	247	341	226	201
132	330	297	305	106	9	309	135
125	282	305	159	149	112	178	300
321	315	275	34	130	174	159	254
133	316	125	91	347	306	210	312
311	324	263	131	171	298	253	232
71	340	18	68	290	113	205	92
241	3	8	21	110	150	213	93
41	301	262	54	41	336	171	101
111	45	38	195	215	33	161	335
268	59	133	354	177	93	349	250
331	54	126	182	50	94	9	

BC-4-C							
234	163	259	211	244	161	183	242
341	293	53	69	160	196	65	187
301	62	139	131	103	352	242	24
86	194	233	69	305	134	278	104
356	340	72	43	217	262	258	110
335	32	38	297	331	355	233	

APPENDIX F.2 – CHI-SQUARE DATA

BC-4-A (n = 109)

Classes	O	E	$(O-E)^2/E$	$(O-E)^2$	
1-30°	6	9.08	1.05	9.50	
31-60°	6	9.08	1.05	9.50	
61-90°	17	9.08	6.90	62.68	
91-120°	9	9.08	0.00	0.01	
121-150°	9	9.08	0.00	0.01	
151-180°	12	9.08	0.94	8.51	
181-210°	7	9.08	0.48	4.34	
211-240°	7	9.08	0.48	4.34	
241-270°	3	9.08	4.07	37.00	
271-300°	9	9.08	0.00	0.01	
301-330°	13	9.08	1.69	15.34	
331-360°	11	9.08	0.40	3.67	
d.f. = 11			χ^2 = 17.06	12.91	[sum/#classes]
$\chi^2_{0.05}$ = 19.68				S.D. = 3.59	$[\sqrt{(O-E)^2}]$

Anomalously HIGH E + S.D. = 12.67
Anomalously LOW E – S.D. = 5.49

$\chi^2_{(calc.)} < \chi^2_{0.05}$ **No preferred orientation**

BC-4-B (n = 119)

Classes	O	E	$(O-E)^2/E$	$(O-E)^2$	
1-30°	11	9.92	0.12	1.17	
31-60°	11	9.92	0.12	1.17	
61-90°	8	9.92	0.37	3.67	
91-120°	15	9.92	2.61	25.84	
121-150°	13	9.92	0.96	9.51	
151-180°	8	9.92	0.37	3.67	
181-210°	5	9.92	2.44	24.17	
211-240°	6	9.92	1.55	15.34	
241-270°	9	9.92	0.08	0.84	
271-300°	7	9.92	0.86	8.51	
301-330°	16	9.92	3.73	37.01	
331-360°	10	9.92	0.00	0.01	
d.f. = 11			χ^2 = 13.20	10.91	[sum/#classes]
$\chi^2_{0.05}$ = 19.68				S.D. = 3.30	$[\sqrt{(O-E)^2}]$

Anomalously HIGH E + S.D. = 13.21
Anomalously LOW E – S.D. = 6.61

$\chi^2_{(calc.)} < \chi^2_{0.05}$ **No preferred orientation**

BC-total (n = 352)

Classes	O	E	$(O-E)^2/E$	$(O-E)^2$	
1-30°	23	29.33	1.37	40.11	
31-60°	31	29.33	0.09	2.78	
61-90°	36	29.33	1.52	44.45	
91-120°	31	29.33	0.09	2.78	
121-150°	36	29.33	1.52	44.45	
151-180°	28	29.33	0.06	1.78	
181-210°	21	29.33	2.37	69.44	
211-240°	24	29.33	0.97	28.44	
241-270°	21	29.33	2.37	69.44	
271-300°	26	29.33	0.38	11.11	
301-330°	41	29.33	4.64	136.12	
331-360°	34	29.33	0.74	21.78	
d.f. = 11			χ^2 = 16.11	39.39	[sum/#classes]
$\chi^2_{0.05}$ = 19.68				S.D. = 6.28	$[\sqrt{(O-E)^2}]$

Anomalously HIGH E + S.D. = 35.61
Anomalously LOW E – S.D. = 23.05

$\chi^2_{(calc.)} < \chi^2_{0.05}$ **No preferred orientation**